Geochemical and Isotopic Studies of sub-surface sediments from Cauvery Delta, South India

Thesis submitted to

PONDICHERRY UNIVERSITY

for the award of the degree of

DOCTOR OF PHILOSOPHY

in

EARTH SCIENCES

by

MALIK ZUBAIR AHMAD

DEPARTMENT OF EARTH SCIENCES
SCHOOL OF PHYSICAL, CHEMICAL & APPLIED SCIENCES
PONDICHERRY UNIVERSITY, PUDUCHERRY - 605 014
INDIA

APRIL 2013

PONDICHERRY UNIVERSITY
School of Physical, Chemical & Applied Sciences
Department of Earth Sciences
PONDICHERRY 605 014 India

Dr. Pramod Singh
Reader

Tel.: +91-413-265 4489
+91 - 9442625562
Fax:+91-413-2655211
Email:pramods@yahoo.com

CERTIFICATE

It is certified that the thesis entitled **"Geochemical and Isotopic Studies of sub-surface sediments from Cauvery Delta, South India"** submitted to Pondicherry University for the award of the degree of Doctor of Philosophy in Earth Sciences is a bonafide record of research work carried out by Mr. Malik Zubair Ahmad, in the Department of Earth Sciences, Pondicherry University, Puducherry, India, during the period October 2007 to April 2013 under my supervision. It is also certified that the thesis represents his independent, original investigation without forming previously part of the material for the award of any Degree, Diploma or any other similar title in any University.

Date:

(PRAMOD SINGH)

(Supervisor)

PONDICHERRY UNIVERSITY
School of Physical, Chemical & Applied Sciences
Department of Earth Sciences
PONDICHERRY, 605 014 India

Malik Zubair Ahmad
Research Scholar

Tel.: +91-9500642358
Email:malikzubair.amu@gmail.com

DECLARATION

It is hereby declared that the thesis entitled **"Geochemical and Isotopic Studies of sub-surface sediments from Cauvery Delta, South India"** submitted to Pondicherry University for the award of the degree of Doctor of Philosophy in Earth Sciences is a bonafide record of research work carried out by me, during the period October 2007 to April 2013 under the supervision of Dr. Pramod Singh, Reader, Department of Earth Sciences.

I also declare that the thesis represents my independent, original investigation without forming previously part of the material for the award of any Degree, Diploma or any other similar title in any University. Keeping with the general practice in reporting scientific observation, due acknowledgements have been made for technical services and laboratory facilities availed during the course of this study.

Date: (MALIK ZUBAIR AHMAD)

Dedicated

to

my parents

&

Sisters

Acknowledgement

In the name of Allah without his blessing and mercy I would not have been able to successfully accomplish this work. With great amount of pleasure I take this opportunity to express my gratitude to the people who have been instrumental in the completion of this thesis. First among all I would like to show my greatest appreciation to my Supervisor Dr Pramod Singh. Reader, Department of Earth Sciences, Pondicherry University. This work would not have come to a logical end without his enthusiastic and invaluable assistance, support and supervision. His analytical approach and attention towards minor details are a quality to be imbibed. I hope that I could be as lively, enthusiastic, and energetic as him. I always tried to learn (however small) from his in-depth knowledge– through every discussion we had. I am also thankful to him to teach me the nuances of sediment geochemistry. It is through his teachings, encouragement and support that I have gained and grown. I thank him from the bottom of my heart for all his help towards the successful completion of this work.

I am thankful to my doctoral committee members Prof. S. Balakrishnan, Head, Dept. of Earth Sciences, Pondicherry University and Associate Prof. Dr.Bala Manimaran, Dept. chemical Sciences, Pondicherry University for their valuable feedback, suggestions and constructive comments that initiated me to improvise the quality of this work. I would like to extend my sincere thanks to Dr. Rajneesh Bhutani Dr Nurul Absar Dr. S. Bhadra, and Dr H.H Khan Dept. of Earth Sciences who were kind enough to provide me selfless support and encouragement. I am also thankful to Prof. M. S. Pandian, Dr. D. Senthilnathan, Dr. Srinivas Moorthy, Dr. Sreyas Managave, Dr. Manisha Kumari, Dr. Lasitha and Dr. Kusuma, Dept. of Earth Sciences for their constant encouragement, valuable suggestions and support during the course of this work and for their positive response whenever I approached them in person for any academic matter work.

My humble thanks to Prof. V. Rajamani, Jawaharlal Nehru University, for his stimulating encouragement, incredible and innovative suggestions every time we met. Attending his lectures has always brought curiosity; I wish that someday be able to command an audience as well as he does.

I gratefully acknowledge the help and co-operation of Balamurugan, Karunakaran Jayanti Madam, Nirmala Madam, Mr. Vaithianathan (Late), Mr. Sarvanan, Shankar, Vetriselvam, Govindan, Arunachalam and other non-teaching staff of the department. To my fellow geology majors, thank you for making this experience worthwhile. I really couldn't image a better group of people to work with and made my lab and department atmosphere equally pleasant and enthusiastic. I am highly thankful to all of them. A brief list of the name includes, Bapi bhai, Anand G, Jitubhai, were among those who kept me going at the beginning Deepthy Didi,Manish chata, Arun chata, Smitha, Laxmi Soumya Perumal, Kamal, Vijayanand, Sureshraja, Kambatan, ,Raja Manikam, Chandru, Dame, Binu, Manil, , Shalini, Amjaid, Milton, Dr. Zeena, Jugina, Simla, Vidya, Tabita, Lalitha, Bijilal, Sarvanav, Pawan Manil Murli Arun chand,Treesa, Arunima, Irshad Kaleem, Ibrahim, Sambith and others for their great company and support. Special thanks to Jitubhai for his help throughout the course of this work especially helping me in various laboratory activities. I also feel pleasure to mention my good friends, *Pragyan(ppm), Srikant, Sujeet bahi and Maya.J.M…..xyz, for their care, support and creating a pleasant atmosphere in lab and helping me throughout my research work.*

The stay in Pondicherry has been less homesick just bcoz of some good friends I got here A brief list of them is Javid Naeem Ishtiaq Qadir Sartaj, Khursheid Aarif Ashraf & Imtiyaz . I also extend my thanks to Azhar, Gowher, Shahid, Aamir, Naseer, Aasif Sikander, Samiullha, Safeer, Muneer, Mudasir, Munazir, Venki, Aazad, Kailash bahi, Biswa bahi,bhagiraj Anna, Rajesh, Rao, Murthy, Ramakrishnann, Ramesh, Ghoshel, Praveen, Sonali, Arundhati and Rasmi for their love and support.

It's my pleasure to gratefully acknowledge the support of some special friends like Yousuf, Saadat Showkat Zameer Majid Fayaz, Aabid, Primrose, Anzar Aamir Yasir, Imran, Hamid,Masood Mujeeb, Baseer, Haris, Hilal bahi Shafiq Faraz and Nehal .

No one walks alone on the journey of life. just where do you start to thank those that joined you, walked beside you, and helped you along the way continuously support through your thick and thin days. I feel blessed to have dear friends Zahoor Suhail and Zahid in my life. I have shared some most memorable moments of life with them. Thank you doesn't seem sufficient, but I say it with appreciation and respect for their support, encouragement, care, understanding and precious friendship.

Words fail me to express my appreciation to Anita Mam for her, generous care when I was ill for weeks. A special note of thanks to little Shambavi for bringing cheer, whenever she visited lab and teaching me many riddles.

I greatly acknowledge the love and support from my Aunts, Uncles and all my cousin sisters and cousin brothers since childhood. I also wholeheartedly thank Ashiq Sahib for his encouragement & support.

I am highly thankful to Ambreen and her family for their constant encouragement, love & support during the final stage of thesis which kept me motivating.

To dearest Shezain who never fails to bring a smile on my face whenever I hold him. I have missed him most during the last three years.

Last but not the least to my parents and sisters who gave me their unequivocal support throughout, as always, for which my mere expression of thanks likewise does not suffice. I doubt that I will ever be able to convey my appreciation fully, to them, but I owe my eternal gratitude to them. I will be contented & happy if my work in any form can bring smile on their faces & benefit them.

I also acknowledge the financial support from Department of Science and Technology (DST, India) in the form of Junior Research Fellowship and Senior Research Fellowship and also University Grant Commission in the form Junior Research Fellowship (UGC-JRF).

Finally I thank one and all knowingly or unknowingly who have supported me at different phases of my journey.

Place: Puducherry
Date:

(MALIK ZUBAIR AHAMAD)

Table of Contents

List of Figures

.

List of tables

Abstract

The primary control on the composition of detrital sediments is the nature of source rock from which it has been derived. Other factors such as weathering, sorting and diagenesis have the modifying effect on the composition of sediments. Chemical weathering of silicate rocks plays an important role in modifying the earth climate by affecting the global atmospheric CO_2 budget. CO_2 a major green house gas is consumed during the weathering of silicate rocks. Therefore the continued increase in chemical weathering of silicate rocks over a period of time may result in reduction of atmospheric CO_2 and global fall in atmospheric temperature. Although the above in turn may lead to decrease in weathering rate and again result in buildup of atmospheric CO_2 and thus warming. Chemical weathering is thus believed to buffer atmospheric CO_2 and moderate the global temperature over geological time scales. The chemistry of sediments records in them the variation in weathering during different periods. Thus the sediment chemistry has been widely used to decipher the weathering changes that have occurred in their source that may help to reconstruct the past climate changes. Weathering also affects the mobility of different elements and therefore their enrichment or depletion. This has further been used to understand the behavior of element under different extent of weathering.

In spite of the above modifying effects the sediment chemistry is known to preserve in them certain chemical signatures that do not get affected by secondary processes. The signatures preserved in the immobile elements such as Al, Fe, Ti and REE are generally believed to provide valuable information about nature of source rocks and the tectonic setting of their emplacement. In addition to the above major and trace elements, the isotopic signature of the heavier radiogenic isotopes such as Sr and Nd, that do not get fractionated by sedimentary processes, have proved to be more robust tools for identification of the source, particularly where the sediments have been modified after their deposition.

Two sediment core, one from the distal (Uttrangudi location) and other from the central axial coastal part (Porayar Location), from the Cauvery Delta region has been studied for their textural, geochemical and Sr-Nd isotopic composition. The Cauvery River originates in the Western Ghat region of south India and on its way to Bay of Bengal drains through various lithologies of Archean and Early Proterozoic

age. In its upper catchment region the exposed rocks chiefly comprise of Archaean tonalitic-trondhjemitic-granodioritic gneisses (TTG) known as Peninsular Gneiss that are metamorphosed up to amphibolites grade along with minor amount of metavolcanics. The catchment rocks of Late Archaean to Neoproterozoic high grade granulite terrain drained by several tributaries in the middle reaches are comprised mainly of charnockites forming highland massifs and retrogressed migmatitic gneisses as forming part of several regional scale shear zones. The climate along the drainage basin of the Cauvery River changes from humid to sub humid to arid climate and experiences bimodal rainfall pattern from south west monsoon (SWM) and northeast monsoon (NEM) with major part of its annual rainfall occurring during NEM season (the three month period from October to December). The coastal part receives about 60% of its annual rainfall, while the interior part receives about 40-50% of annual rainfall during NEM.

The sediment in the 28 m core from the Uttrangudi location are of upper Mid-Pleistocene to Holocene in age with a large unconformity marked by absence of almost entire Upper Pleistocene record. Similarly of the 24 m sediment core from Porayar location the top 18 m is Holocene in age and a marked unconformity is present at ~20 m depth below which lies the rock of Tertiary or Cretaceous period. The sediments from Uttrangudi core comprising of cyclic channel and flood plain sequence are moderately to poorly sorted with their mean size ranging between medium sand to fine silt. The sediments from Porayar location are also poorly sorted and their mean size ranges between fine sand and silt. Almost the entire Holocene sediments from this location got deposited under water in an estuarine or Bay setting as indicated by the presence of Foraminifera tests in them.

The depth wise variation in concentration of silca in both the studied core show trend opposite to that of Al, Fe, Mg, Mn and Ti which implies that the variation in the concentration of later elements is primarily due to the dilution effect of quartz. Further on comparison with texture, it is also observed to have exerted its control on the chemistry. The zone having higher sand percentage and, lower silt and clay, show higher abundance of Si and lower abundance of above elements. On the contrary the zones having higher percentage of silt and clay, and lower sand percentage, show higher concentration of above elements (Al, Fe, Mg, Mn and Ti) except silica. The

observed correlation of silica with sand percentage, and of Al, Fe, Mg, Mn and Ti with silt and clay would indicate that the sand is having higher percentage of quartz, whereas the mafic minerals such as pyroxene and amphibole and their weathering product (clay) dominate the finer fraction. Thus the first order control over the concentration of Si, Al, Fe, Mg, Mn and Ti is probably due to variation in texture because of selective sorting of mafic minerals and quartz in finer and coarser size fractions respectively. In Porayar core and Pleistocene section of Uttrangudi core Na_2O, CaO and to a great extent K_2O show behavior similar to SiO_2 suggesting that feldspar are also mostly hosted in sand i.e. they constitute the coarser fraction. Unlike the above in the Holocene sediments of Uttrangudi borehole Na_2O, CaO and K_2O exhibit positive correlation with Al and negative with Si suggesting that in this part major feldspar population resides in fines or these elements have got attached to clays. Among the trace elements the variation trend in Ni, Cr and Y correspond to the variation pattern of Al, Fe, Mg, Mn and Ti, indicating that these elements are held in mafic and clay minerals. Ba and Sr are observed to exhibit similar variation pattern and their similarity with the variation pattern of Na, Ca and K suggests that these elements are also held in feldspar.

The total range of Chemical Index of Alteration (CIA) values, corrected for secondary Ca from carbonate, are 52 to 97 for Pleistocene sediments of Uttrangudi core, 67 to 84 for Holocene sediments from Uttrangudi and 50 to 80 for Holocene sediments from Porayar core. higher CIA values, in conjunction with low absolute contents of Sr, Ca and Na in Pleistocene sediments, reflect an intensely weathered provenance and indicate wetter climate during upper mid Pleistocene. The relatively lower CIA values with higher Sr, Ca and Na in Holocene sediments indicate relatively lower weathering and overall reduced rainfall during Holocene compared to Pleistocene period.

REE analysis of sediments was carried out on selected samples from both the cores. Good correlation of REE's and their chondrite normalized ratios with Ti, Th and Y in both the cores suggest control of Allanite, Titanite and Monazite among heavy minerals on the REE distribution in sediments. Further the good to strong positive correlation among REE and Al, Fe, Mg, Ni, Cr, Sc and Co in both the cores suggest, to some extent, the control of mafic minerals and clay. It is observed that in

both the cores Eu/Eu* values show a significant anti correlation with the CIA values, particularly in Uttrangudi sediments. This would suggest that the Eu in sediments have been modified to different extent by the process of weathering effecting its loss and lowering of Eu/Eu* values.

To infer the provenance the chemistry of sediments from both the cores was compared with major rock types from different areas of catchment comprising mainly of (i) Archean Gneisses from Dharwar Craton (DC) and (ii) granulite facies rocks from Southern Granulite Terrain (SGT) comprising of late Archean to Proterozoic Charnokites and Migamatic gnessis. The bi-variant plot of the immobile major element ratios (Fe/Ti vs Ti*100/Al) suggest that the Porayar core sediments and the Holocene sediments from Uttrangudi core have been derived from the mix of various lithologies exposed in the SGT whereas in the above plot gneisses from Dharwar Craton (DC) fall outside the field of sediments. Unlike above the Pleistocene sediments from Uttrangudi core do not show much overlap with SGT and plot away from DC gneisses. On further comparison it is observed that these sediments (Uttrangudi Pleistocene) plot with Tertiary rocks exposed towards the west of the core location. It was inferred that the shift in the plot of Uttrangudi sediments in the above plot may be due to the variable enrichment of Fe, Al and Ti during the laterization process that has occurred in the Tertiary rocks. Further the REE chemistry of sediments (that is considered more robust) was compared with the above catchment rocks. The chondrite normalized plots of REE in sediments from both the core are almost parallel to each other and exhibit similarly fractionated patterns with the $(Ce/Yb)_N$ ratio of ~8.2 although with large variations in their abundance. The more fractionated nature of LREE and flatter HREE along with slight negative to positive Eu anomaly, suggests that the sediments have been derived from a rock of intermediate composition. Comparison of the chondrite normalized plot of the sediments with that of various catchment rocks lead to infer that the SGT has acted as the source to the sediments including the Pleistocene sediments from Uttrangudi core. Further comparison of Sr and Nd isotopic composition of sediments with above rock types corroborate the inference made based upon REE although with help of the isotopic composition some inferences could be made about the temporal variability in erosion within the SGT.

Further study was carried out on the Sr isotope composition of the exchangeable phases associated with the sediments to determine the temporal variability in the isotopic composition of ground water. The isotopic composition of the leachate fractions (Carbonate, Fe-Mn and organic phase) that are supposed to act as the proxy for ground water indicate that the ground water during Pleistocene resembled the mix of fresh water (taken as present day River composition) and sea water in equal proportion. In contrast the Sr isotopic composition in Uttrangudi core for the Holocene period shows a shift towards River water composition, whereas in the Porayar sediments it shows greater affinity to sea water composition which is expected as these sediments are inferred to have been deposited in an estuarine environment.

Chapter 1

INTRODUCTION

INTRODUCTION

Weathering is an important component of many basic geochemical processes on Earth's surface that helps in reshaping the earth's surface and maintaining balance. It is the process behind simple dissolved ions and secondary clay minerals that are released from primary minerals and ultimately transported to ocean by Rivers. The term 'Weathering' may be defined as a combination of complex suite of chemical, biological and physical processes that transforms bedrock into soils (Anderson et al., 2004). Erosion is considered as one of the drivers of chemical erosion by continuously removing the weathered materials and exposing the fresh bedrock to the weathering front. The proportion of various elements in the dissolved phase is a complex interplay of their relative abundances in minerals and of the mode and rate of their weathering. (Campos Alvarez and Roser 2007; Bhatia, 1983; Condie et al., 1995; Cullers, 1987, 1994, 2000; Huntsman-Mapila et al., 2009; Hurowitz and McLennan, 2005; McLennan et al., 1990, 1993).

Chemical weathering of silicate rocks have significant control on the CO_2 budget of the atmosphere and hence moderates the Earth's climate. According to Chamberlin, (1899), the enhanced rates of chemical weathering coupled with major mountain building episodes in Earth's history resulted in a large scale drawdown of atmospheric CO_2 that subsequently led to periods of global cooling. The demanding interest in past as well as present global climate change has renewed the efforts to quantitatively understand the feedback mechanisms between climate and chemical weathering. On longer timescales, atmospheric CO_2 levels is believed to have been primarily controlled by the balance between the rate of volcanic inputs from the Earth's interior and the rate of uptake through chemical weathering of silicates at the Earth's surface (Ruddiman., 1997). Weathering is widely accepted as the principal moderator in controlling large increases and decreases in global temperature along with precipitation through the greenhouse effects of CO_2 over geologic time (Berner and Berner., 1997).

Weathering apart from its modifying effect on climate also results in modification of the chemical and physical properties of soil. This ultimately controls the nature of sediments formed by their transport and deposition. Weathering and erosion also plays a dominant role in shaping the landscape of the Earth. Physical and

chemical erosion of rocks on continents determines the exogenic cycles of elements and material transfer within and among surface reservoirs (Raymo et al., 1988; Drever and Zobrist., 1992; Stallard and Edmond., 1983, 1987; Bluth and Kump., 1994; Roy et al 2010). These erosive processes also play an important role in the biogeochemical cycles of elements by supplying nutrients and solutes to surface reservoirs such as soil, atmosphere, oceans and sediments. The signatures of the intensity and nature of weathering and erosion, contained in the abundance and composition of dissolved and particulate phases of rivers, are in turn transferred into the sediments. Several studies carried on weathering profiles have provided insights into the behavior of various elements. Nesbitt et a1 (1980, 1989) in their study of weathering profile developed over granodiorite have discussed the behavior of alkalis and alkaline earth elements and developed the parameter called chemical index of alteration (CIA) to quantify the degree of weathering. These and other workers have later tried to relate the response of other elements with varying weathering intensity. In their study it was observed that several elements including the rare earth elements, that are generally considered to be immobile, get mobilized to different extent under the influence of weathering (Nesbitt, 1979; Condie., 1991; Sharma and Rajamani, 2000a). Therefore it is important to understand the processes of rock weathering and its effect on sediment chemistry before applying it for making inferences related to their provenance. We as part of the first objective in the present study have tried to understand the weathering variability in sediments and the associated chemical changes, and have tried to relate it with the surface geological processes and depositional environment. As sediments are transported long distances from the source area further changes take place in them due to the operational hydrodynamic conditions that results in sorting of the sediments, both textural and mineralogical. Coarse sediments enriched in quartz are separated from the fine and the lithics are further physically and chemically broken down. This results in quartz-rich sandstones that are characteristic of continental interiors and passive margin platform settings and massive mud-rich deltas and passive continental margin slope settings (Bhatia., 1983; Condie et al., 1995; Cullers, 1987, 1994, 2000; McLennan et al., 1990, 1993; Roser and Korsch., 1986, 1988; Ryan and Williams., 2007). Thus the chemical and mineralogical compositions of clastic sedimentary rocks is the manifestation of composite interaction of various variables including source rock composition, weathering, erosion, transportation and

sedimentation processes such as mechanical sorting, decomposition and diagenesis (McLennan et al., 1993). Even though the exposed rocks in the catchment regions are altered into soil and finally into the sediments by the combined effect of several factors mentioned above, the sediments preserve in them the original signature of their source rocks. In view of this, geochemical composition of clastic rock has been widely used to decipher the composition of source area (Wronkievicz and Condie., 1987, 1990; Naqvi et al., 1988, 2002; McLennan et al., 1995; Cullers., 2000; Cullers and Podkovyrov., 2000; Condie et al., 2001; Singh and Rajamani, 2001 a,b; Singh, 2009, 2010) and to evaluate the composition and evolution of continental crust (Taylor and McLennan, 1985, 1995; McLennan and Taylor., 1991; Condie, 1993; Lahtinen., 2000). It is particularly found to be useful in inferring the nature of Precambrian crust, where either the source rock has been destroyed by erosion or exhumed by subduction processes (Feng and Kerrich., 1990; Hofmann., 2005; Hofmann et al., 2003; Holland., 1984; Johnson., 1993). The geochemistry and mineralogy of sediments has also been used to evaluate weathering history and paleoclimate (Fedo et al., 1995, 1996; Nesbitt and Young., 1982) of the region. Bhatia (1983), Bhatia and Crook (1986) and Roser and Korsch (1986 and 1988) have used the chemistry of sediments to reconstruct the tectonic setting of depositional basin.

The sediment chemistry, in particular the immobile major and trace elements, such as Al, Fe, Ti, Th, Sc, Co, Zr and the rare earth elements (REE's) have been found to be useful indicators of the source (Taylor and McLennan., 1985). These elements are thought to be negligible in the dissolved load and carried primarily in the particulate load. They are found to exhibit similar behavior during the process of weathering, erosion and transportation. Due to the similar hydrodynamic behavior of the mineral phases holding them, the ratios of these elements are believed to be similar to their parent rocks and therefore they serve as excellent tracer of their source.The effect of diagenesis is also believed to have minor effects on these elements except in some anoxic environments (Milodowski and Zalasiewicz., 1991; Bock et al., 1994; Lev et al., 1998). Among these elements the REE, Th, Sc and Co are generally considered to be the most useful for inferring source rock composition because their distribution is less affected by secondary processes such as diagenesis and metamorphism and by heavy mineral fractionation (Bhatia and Crook, 1986; Floyd and Stiven et al, 1991; McLennan and Taylor., 1991; Cullers., 1994). These are

considered to be immobile under surface conditions and thus inherit the characteristic of the source rock (Floyd and Stiven et al, 1991; Amorosi et al, 2002; Zimmermann and Bahlburg., 2003, Roy et al., 2012). The immobile elements such as Th, Zr and REEs are generally enriched in felsic rather than mafic rocks, because they are highly incompatible during most igneous melting and fractionation processes, while input from mafic and ultramafic source areas would result in enrichment of Sc, Cr and Co (Bhatia and Crook, 1986; McLennan et al, 1993; Cullers and Berendsen., 1998). Thus the ratios of these groups of compatible and incompatible elements are highly useful in distinguishing mafic from felsic source. Higher ratios of Th/Sc, Th/Co, La/Sc suggest towards felsic source, whereas their lower ratios indicate mafic source. Similarly higher concentrations of trace elements such as Ni and Cr also indicate derivation of sediments from mafic and ultramafic sources (McLennan et al., 1983, Taylor and McLennan., 1985; Wronkiewicz and Condie., 1989; Cox et al., 1995., Bock et al., 1998., Garver et al. (1996., Jaques et al., 1983).

In addition to above rare earth elements (REE) in sediments have been widely used to probe the chemical evolution of continental crust (Taylor and McLennan, 1985; Condie, 1991) chemical weathering in drainage basins (Nesbit., 1979), sediment provenance and tectonic setting (Taylor and McLennan., 1985; Cullers et al., 1987). They undergo limited fractionation by sedimentary processes and low grade metamorphism and are comparatively insoluble and present in very low concentrations in sea and river water. Therefore, the provenance of sediments is considered to be the single most important factor contributing to the REE content of clastic sediments (Fleet., 1984; McLennan., 1989). Thus the REE pattern of fine-grained siliciclastic sediments and some elemental ratios, especially Eu/Eu*, are assumed to reflect the exposed crustal abundances (McLennann et al., 1993; Mongelli., G. et al., 1996; Fedo et al., 1996; Hassan et al., 1999; Bauluz et al., 2000; Cullers., 2000; Condie et al., 2001; Mongelli., 2004) and are useful indicators of source rock chemistry (Taylor and McLennan., 1985, 1995; McLennan., 1989). However, it has been observed in several studies that the process of weathering, hydraulic sorting and diagenesis alter the chemical signatures of the sediments that are considered to be carrier of the source signature (Cullers et al. 1987; Banfield and Eggelton., 1989; Milodowski and Zalasevicz., 1991; Bock et al. 1994; Condieet al. 1995). Trace elements including the REE have been reported to get mobilized during

the chemical weathering and redistribute itself within the weathering profile by getting absorbed by the secondary phases. Several studies have shown that although REE can get mobilized and redistributed within a weathering profile, there is no net losses or gains of specific REEs, that is, they do not leave the system (Nesbitt, 1979; Duddy., 1980; Banfield and Eggleton., 1989, and Sharma and Rajamani.,2000a, 2000b). Subsequent erosion and transportation lead to re-homogenisation of REE chemistry there by giving source rock REE pattern (Nesbitt, 1979; Martin and Meybek., 1979; Goldstein and Jacobson., 1988; and Condie., 1991). Contrary to above, Sholkovitz (1988) observed that REE of river-borne sediments, particularly the suspended load have REE patterns that are strongly depleted in HREE relative to shale. Studies carried out by Cullers et al. (1987, 1988) on riverbed sediments produced in different climatic conditions suggests that silt and clay size fractions most closely resemble their source REE patterns but with higher abundance. They also observed the differences in Eu anomaly between sediments derived from an intensely weathered source and unweathered source. Their study suggest that all the size fractions have negative Eu anomaly in case of extremely weathered sediments, whereas only the sand fractions shows apositive Eu anomaly in moderately weathered sediments. Thus more studies needs to be carried out on modern clastic sediments originating from diverse lithologies under different climatic conditions and depositional environment.

In the context of Nd isotopes, the melting of mantle to form the evolved plutonic and volcanic rocks that are exposed within the continental crust is the most important process for fractionation of Sm-Nd, and thus provides the conditions necessary for significant isotope variation with time. Sm and Nd are comparatively immobile REEs and while significant parent-daughter fractionation occurs during mantle-crust differentiation (O‟Nions et al., 1983; Chaudhuri and Clauer., 1992). Sm-Nd are believed to be transported together without significant fractionation during sedimentary processes (McCulloch and Wasserburg, 1978). As such they can retain isotope ratios that reflect those of the source area (Nelson and DePaolo, 1988), which when coupled with other trace element data can provide significant information on sediment provenance. Neodymium isotopes have been used to study sedimentary rocks primarily focusing on issues like evolution of continental crust (McCulloch and Wasserburg, 1978; Taylor et al, 1983) and also in predicting the tectonic setting

(Nelson and DePaolo, 1988; McLennan et al., 1990; McLennan and Hemming., 1992). McLennan et al (1990) examined the isotopic character of sediments from a variety of tectonic settings to test the relationship between tectonic setting and provenance. Several other studies have employed the Nd isotopes to constrain basin evolution (e.g., Gleason et al., 1995; Garzione et al., 1997; Ball and Farmer., 1998; Patchett et al., 1999b, 2004; Dickinson et al., 2003). The Nd model age of sedimentary rocks has been used or generally interpreted as to reflect mean age of mantle extraction of various provenance components (McCulloch and Wasserburg., 1978). Therefore the application of radiogenic isotope techniques in sedimentary provenance studies is useful, as it provides a fundamentally different perspective of time. The main advantage of Sr and Nd isotopes is that they act as fingerprints for provenance and transport pathways of detrital sediments (Innocent et al., 2000; Rutberg et al., 2005). Isotopic ratios of Sr and Nd vary according to the age and geological history of crustal rocks which leads in an inverse relationship between $^{87}Sr/^{86}Sr$ and εNd_0 (Goldstein and Jacobsen., 1987). Sediments of rivers draining older crust have high radiogenic Sr and non-radiogenic Nd contrary to the rivers draining the younger crust. Depleted mantle Nd model ages (T_{DM}) add a temporal dimension to the provenance study of sediments by providing extraction ages of the sediment sources from the depleted mantle. Thus Nd isotope study on the sediments along with the geochemical studies has also been successfully used for provenance and tectonic setting. Radiogenic isotopic compositions of sediments reflect their continental source, which in turn provides very useful information about their provenance (Goldstein et al., 1984; Revel et al.,1996). Further Sm–Nd analyses of fine-grained clastic sediments are also a potent sedimentological tool to expound paleogeography, sediment recycling and maturity as well as different aspects of sediment transport (Miller and O'Nions., 1984).

In addition to Sm-Nd, Sr isotope has also been found to be an important tracer of weathering and provenance. The four naturally occurring stable isotopes of Strontium are ^{84}Sr (0.56%), ^{86}Sr (9.87%), ^{87}Sr (7.04%) and ^{88}Sr (82.53%). ^{87}Sr results from the decay of ^{87}Rb, which substitutes for potassium in feldspars, micas, K-bearing clays and other minerals. Strontium is also present as a trace element in major fluid reservoirs such as seawater and groundwater (Lerouge et al., 2009). Ca^{2+} and Sr^{2+} actively participates in fluid–rock interactions. The Sr isotopic composition found in

streams and groundwater has been found to vary depending upon the chemical weathering of different types of bed rocks (Faure et al., 1963). Due to these characteristics, strontium isotopes act as good tracers of strontium sources (solid and fluid) and a powerful tool for fluid–rock interactions and hydro geological investigations (Pace et al., 2007). Thus Sr isotopic concentration has been found useful as a natural tracer to study the streams that drain through different kind of rock types and to recognize the subsurface movement and chemical evolution of groundwater (Eastin and Faure 1970; Steuber et al., 1984, 1993; Fisher and Stuber., 1976; Franklyn et al., 1991; Armstrong et al., 1998).

The need to understand the distribution, mobility, ecotoxicity and phytoavailability of heavy metals in contaminated sediments and soils led to the establishment of sequential extraction techniques (Gupta and Chen., 1975; Agemian and Chau, 1976; Stover and Sommers., 1976; Gibbs., 1977; Malo., 1977; Tessier et al., 1979). Lately sequential extraction techniques have been expanded to the understanding of the distribution, mobility and possible uptake of radionuclides by plants (Bunzel et al., 1995, 1996; Rigol et al., 1999; Morton et al., 2001; Pett-Ridge et al., 2007; Galindo et al., 2007. The Sr isotope in river, ocean and ground water equilibrate with the secondary phases precipitating out of it. According to Jenne (1977), the ‘matrix vehicle' or residual fraction is associated with more labile and thermodynamically unstable components such as carbonates, amorphous aluminosilicates, organic matter, etc. These fractions are usually coated with Fe- and Mn-oxides and organic material (both living and non-living). It is therefore desirable to discriminate between the different locations of the elements including the Sr isotope in the sediments to assess the contribution of ground water and the provenance to the bulk composition of the sediments. We in the present study have tried to measure the Sr isotope composition of the secondary phases and the residual detrital phase to make assessment of the provenance to ground water and the clastic component.

The catchment area of the Cauvery river includes the two major Terrains, 1)the northern greenstone granite terrain of Dharwar craton (DC) consisting predominantly the gneisses and 2) the Southern Granulite Terrain (SGT) comprising of charnockites and migmatitic gneisses transected by several shear zones. The river

draining through these rocks has bulid up a vast delta east of Tiruchirappalli. Out of the two monsoon system i.e southwest (Indian summer monsoon) and northeast (winter) monsoons, the Northeast monsoon dominates the studied region.

Quaternary environmental paleo-environmental studies in south India has rarely been carried out thus far despite the important role that the coastal area plays as the direct link between the marginal seas and the continent. Consequently, there is insufficient information to better understand palaeo-environmental problems including the paleo-climate and the sediment-to-source process during the Quaternary.In the present study geochemical and isotopic study of the core sediments from the Cauvery delta region representing late Pleistocene and Holocene were analysed and investigated to understand the nature of weathering, climate and provenance to the sediments.

In the present study attempt has been made to highlight the importance of relief and spatial variability of rainfall on provenance studies. The significant differences in characteristics such as rainfall, rocktype and relief within the basins provide an opportunity to evaluate their role in influencing weathering processes. The present study also involves determination of $^{87}Sr/ ^{86}Sr$ ratio on several leached fractions in order to better constrain the origin of the secondary components. The method has also been used to understand the interaction of groundwater with the sediments that has led to variation in $^{87}Sr/ ^{86}Sr$ ratio of different phases.

Objectives:

The objective of the present study includes textural, mineralogical and geochemical including REE and isotopic (Sr and Nd) characterization of the sediment cores obtained from two distinct locations from the Cauvery delta region, with the following objectives:

(A) To study the spatial and temporal change in the texture and weathering intensity as recorded in the sediments and in turn infer their influence on the behavior and distribution of elements.

(B) To determine the source of the sediments and its variation with time using Major, Trace, Rare Earth elements (REE) and Sr-Nd Isotope.

(C) To study the influence of relief and spatial variation in rainfall distribution pattern in determining the supply of sediments from different catchment lithologies.

(D) Measurement of $^{87}Sr/^{86}Sr$ ratio in different leachates (exchangeable, carbonate, Fe-Mn oxide and organic) and residual phase of the core sediments to infer the variation in composition of ground water and effect of sediment pore water interaction.

Chapter 2

Geology of the Cauvery River Basin

2.1 The River Cauvery:

The River Cauvery flows for about 800 km before it joins Bay of Bengal and drains a total area of around 81,155 km^2 of which 34,273 km^2 lies in Karnataka, 43,856 km^2 in Tamil Nadu and 2,866 km^2 in Kerala (*Int. Hyd. Data Book.*, CWC, 2007). The catchment area of Cauvery River lies between 10°7'N and 13°28'N latitudes, 75°28'E and 79°52'E longitudes. The Cauvery River originates from the Brahmagiri ranges of Western Ghats near Talakaveri, Kodagu district of Karnataka. In its initial stretch the River flows eastward over the Mysore plateau and is joined by several tributaries from north and south. The major tributary Hemavati River joins the main channel at Krishna Raja Sagar. Other tributaries joining from north are Shimsha and Akravathy Rivers. Over the Mysore plateau the main channel is joined from south by tributaries namely Kabini and Kapila Rivers. After flowing through Mysore Plateau the River while passing through Biligirirangan hills form falls through height of 100 m in a series of water falls and rapids at Shivasamudram before taking a southerly bend at Hogenekal where again through series of waterfalls and rapids it enters into the state of Tamil Nadu. Flowing south it enters into the Plains after Mettur and between this stretches it is joined by tributaries draining Biligirirangan hills namely Palar River from west and Chennar River from North east. The main River continues flowing southward till it takes an easterly bend after Erode. Between Mettur and Erode it is joined from west by River Bhavani formed by confluence of Moyar and Bhavani Rivers draining the Niligiri hills. In its final eastward course it is joined by a major tributary from south draining the Palani and Kodaikanal hills and its adjoining areas. From here it continues flowing east and before meeting Bay of Bengal it forms a vast delta after Tiruchirrapalli.

2.2 Climate:

The Cauvery basin receives variable rainfall during both south west monsoon also known as Indian summer monsoon and north east (winter) monsoons. The total average annual rainfall in the basin is ~1092 mm. The annual mean temperature of the basin is ~26 °C, however, in the temperature in summer may reach maximum upto 41°C and during winter a minimum of ~14 °C. Precipitation varies considerably across the basin. The Western Ghats act as an orographic barrier and shelter the Cauvery catchment region from the high intensity rain bearing winds of south west

(SW) monsoon, which leads to less rainfall during south west monsoon (Balachadran et al., 2006). More than 50% rainfall in the Cauvery catchment and basin takes place during the north east (NE) monsoon period. The effect of SW monsoon decreases on moving from west to east while, the NE monsoon influence increases. The coastal part receives about 60% of its rainfall during the NE monsoon period, while in western part it receives 40-50% rainfall during this season. The overall basin experiences humid to sub humid climatic conditions. The drainage basin in north-western part has a humid climate while on eastwards it is sub-humid.

2.3 The Geology:

The catchment area of the Cauvery River includes the two major terrains, the northern green stone granite terrain of Dharwar craton and the southern granulite terrain (Fig 2.1). These terrains constitute mosaic of several Precambrian terrains separated by several N-S and E-W trending major shear zones (Swami Nath and Ramakrishnan., 1981, Harris et al., 1994; Bhaskar Rao et a1., 1996; Valdiya., 1998; Chadwick et al., 2000; Jayananda et al., 2000; Meissner et al., 2001). The major shear zones comprises of Moyar, Bhavani, Palghat, Cauvery and Attur shear zones (Harris et al., 1994; Bhaskar Rao et a1., 1996; Raith et al., 1990; 1999., Valdiya., 1998; Chadwick et al., 2000; Meisner et al., 2001). These shear zones play a key role in reconstructing the Precambrian evolution of South India (Meissner et al., 2001). The subsequent reactivation of these shear zones during later periods is believed to have resulted in the upliftment and formation of several block mountains, dominantly made up of granulites such as the Nilgiri hills, Biligirirangan Hills and the Palani-Kodaikanal hills (Raith et al., 1990, 1999; Harris et al., 1994, Valdiya.,1998).

The upliftment of these rocks is believed to have occurred during the late Mesozoic period. Further the break up of Madagascar led to the upliftment of peninsulalar India which subsequently resulted in the formation of Sahydri range (Western Ghat) along the west coast of peninsula (Gunnnel, 1998). According to Vaidyanathan (1964), this upliftment resulted in the eastward tilt of peninsular India and initiation of the east flowing Rivers including the Cauvery River.

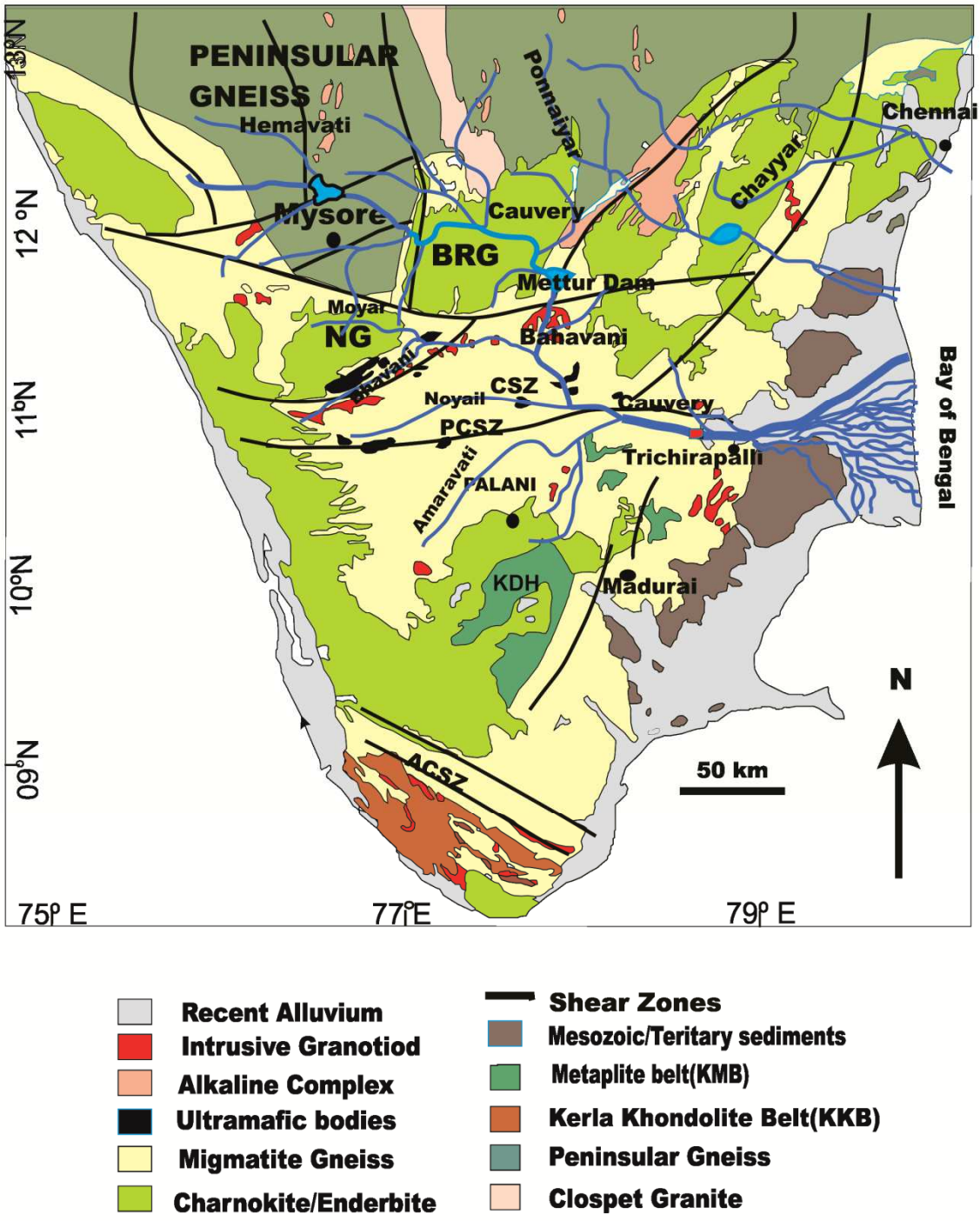

Figure 2.1: Geological map of Cauvery Basin modified after Santosh et al., 2009.

In its upper reaches the Cauvery River flows through Archean granitoid gneiss, intrusive granites and supracrustal rocks of Dharwar Craton which have been metamorphosed to amphibolite grade. The Dharwar craton comprises vast areas of Tonalite Trondzehmite gneisses (TTG-commonly known as Peninsular gneisses) which is further subdivided into the western (WDC) and eastern blocks (EDC) based on the nature and abundance of greenstone belts, degree of regional metamorphism and melting as well as the nature and age of their gneissic basement rocks (Swaminath et al., 1976, Chadwick et a1., 1981, 2000; Swaminath and Ramakrishnan, 1981, Rollinson et al., 1981., Radhakrishna, 1983,; Jayananda et al., 2000) and according to Chadwick et al. (1992) are separated by Mylonitic zone along the eastern margin of the Chitradurgah schist belt. Earlier Viswanatha and Ramakrishnan (1981) placed the boundry between eastern Dharwar Craton (EDC) and a western Dharwar Craton (WDC) with reference to N-S trending belt of granitoid intrusives known as "Closepet Granites". The western Dharwar craton is dominated by TTG Peninsular gneisses and volcano-sedimentary greenstone belts, whereas, the EDC is dominated by late Archaean granitic rocks with minor TTG and thin narrow elongated greenstone belts. (Swaminath and Ramakrishnan, 1981, Chadwick et al., 2000; Jayananda et al., 2000). The suite of rocks forming the gneisses comprises of banded migmatitic gneiss, boitite-gneiss and light grey feldspathic gneisses formed by migmatisation of supracrustals in different phases at different stratigraphic levels Naha et al., 1993. The most dominant variety of Peninsular Gneiss consists of leucocratic and melanocratic bands. The leucocratic bands consist of quartz, microcline and oligoclase with traces of muscovite, apatite and zircon and the melanocratic bands are composed of biotite, hornblende and epidote. The TTG type Peninsular gneisses of western Dharwar craton (WDC) are as old as 3.4 Ga (Beckinsale et al., 1980, Taylor et al., 1984, Meen et al., 1992, Peucat et al., 1993). Further, Jayananda and Peucat., (1996) isotopic age data shows that the protoliths of peninsular gneisses accreted during three main crust forming events viz. 3.4 Ga, 3.3-3.2 Ga and 3.0-2.9 Ga. The highly deformed and metamorphosed 3.6-3.23 Ga. Sargur Group forming greenstone belts of WDC (Jayananda et al., 2008; Kumar et al., 1996; Nutman et al., 1992, Peucat et al., 1995) formed at mid to deep crustal levels in the WDC (Swaminath et al., 1976; Bouhallier et al., 1993, 1995, Janardhan et al., 1979) is unconformably overlain by 3.0–2.6 Ga supracrustals of Dharwar Supergroup (Kumar et al., 1996; Nutman et al., 1996,

Taylor et al.,1984., Trendall et al., 1997a,b). It is a volcanic sequence made up of ultramafic komatiite and tholeiitic rocks containing subordinate felsic lava flows and is metamorphosed up to amphibolite-facies in the northern part, and reaches granulite facies in the southern part of the Mysore area. The EDC is characterizd by the presence of TTG that are younger (2.7 Ga) than the TTG basement of WDC and also contains calc alkaline to high pottasic intrusions (Balakrishnan et al, 1990, 1999; Krogstad et al., 1991; Chadwick et al., 2000). The EDC is characterizd by the presence of TTG that are younger (2.7 Ga) than the TTG basement of WDC and also contains calc alkaline to high pottasic intrusions (Balakrishnan et al, 1990, 1999; Krogstad et al., 1991; Chadwick et al., 2000). Widespread plutonisim took place in the EDC between 2.56 and 2.51 Ga and by contrast in WDC plutonisim ceased by 2.61 Ga (Jayananda et al ., 2006).

The outstanding characteristics of the Archaean terrain in southern India is progressive transition from low to medium grade TTG-greenstone terrains in the north to high grade granulite massifs in the south (Pichamuthu., l965). The extension of the South India Shield south of Dharwar Craton is known as Southern Indian granulite province or Southern Granulite terrain (SGT). The boundary between the granite Gneiss and granulite terrain was first demarcated by Fremor (1936) as ortho-pyroxene isograd. The origin of Granulite formation has been discussed by several workers. The Granulitization was explained due to mantle or lower crustal CO_2 rich fluid streaming (Janardhan et al., 1979, 1982; Hansen et al., 1984). According to Stahle et al (1987) granulite development took place by internal fluid buffering whilst Santosh et al (1991) invoke a magmatic source of heat and fluids for the transformation of the magmatic gneisses into charnokites. The SGT forming part of Cauvery catchment is delineated by the crustal scale shear zones that subdivided it into two major blocks, the Northern Granulite Block (NGB) occupying the area between Dharwar and the Palghat-Cauvery shear zone (PCSZ) and the Southern Granulite Block (SGB) between two major shear zones viz., Palaghat-Cauvery and Achankovil shear zones. The northern part of SGT in the Cauvery catchment area consists of Meso- to Neo Archean charnockite massifs forming Nilgiri hills massif, Biligirirangan hills massif and the Shevroy hills massif (Rajesh., 2012) whereas the SGB consists of Palani-Kodaikanal massif of Madurai Block (MB). Cauvery Shear Zone is believed to be a deep dissected section of an ancient orogenic belt (Ramakrishnan., l993) and is

regarded as a zone of Neoproterozoic reworking of the Archaean crust (Bhaskar Rao et al.,1996). Sm-Nd garnet-whole rock isochrones of layered complexes along the northern boundary of the PCZ indicate 2935 ± 60 Ma for emplacement of their protoliths, whilst Sm-Nd mineral isochron (gt-plag-hbl-WR) define an age of 726±9 Ma (Bhaskar Rao et al., 1996). The CSZ predominantly consists of deformed Neoarchaean variably retrograded charnockitic gneisses associated with biotite and hornblende bearing migmatite gneisses. Similar zircon U–Pb age for same unit has been found by (Ghosh et al., 2004) indicate that the predominant supracrustal gneiss association of the CSZ is at least ca. 3.0 Ga old. Geochronological data (Bhaskar Rao et al., 2003, Chetty et al., 2003) suggests that the CSZ has experienced at least two major tectonothermal events that culminated during the Neoarchaean (ca. 2.5 Ga, D1) and during the Neoproterozoic (ca. 0.8–0.5 Ga, D2). According to Gopalakrishnan, (1994) the dominant rock types along the CSZ include supracrustal sequences metamorphosed to granulite facies, migmatized orthogneisses showing varying degree of retrogression, charnockites, granites, banded iron formations, and several dismembered suites of mafic–ultramafic complexes with varying lithological association including dunite, peridotite–websterite and garnet-bearing gabbro–anorthosite complexes. Further John et al. (2005) stated that the CSZ marked the presence of 2–3 km wide E–W trending mylonitic (augen) gneisses, that composed of augen shaped quartz and feldspar grains and also consists of mica and hornblende, situated on the northern bank of the Cauvery River. Mafic granulite and granite migmatites occur on the northern part of the CSZ while granitic gneisses constitute the southern part. These mafic granulites usually occur as variably sized enclaves within the granitic gneisses in the south. Hornblende biotite gneiss occurs as a thin band sub-parallel to CSZ in the northern part.

The Moyar shear zone (MSZ), separates the Nilgiri hills from the Dharwar Craton and the Biligirirangan hills. The regional extend of the Dharwar Craton is truncated by the E–W trending structures of the Moyar share zone (Fig 1). The Nilgiri highland massif exposes a strongly tilted section of granulite grade lower crust. The entire crustal section is essentially composed of garnetiferous enderbitic granulites, which have been subjected to polyphase deformation and dehydration processes (Raith et al., 1990, 1999; Srikantappa., 1996). The northern part of it is intruded by intermediate and basic magmatic rocks, represented mainly by non-garnetiferous

enderbites, garnetiferous basic granulites, gabbroic to anorthositic two-pyroxene granulites and pyroxenites. The calculated age for garnetiferous enderbites arrays reported in the Rb–Sr and Sm–Nd evolution diagrams is 2460±81 Ma and 2506±70 Ma respectively (Raith et al., 1999).

The Bhavani Shear Zone traverses through the southern margin of the Nilgiri Hills and trending ENE unite with MSZ (Fig 1). Retrograde biotite within the gneiss in the shear zone yield Rb – Sr ages of 521 to 472 Ma and some of the coronitic garnet in a meta-dolerite yield an age of 552 Ma, indicating, Pan African tectonothermal events in the Moyar – Bhavani Shear Zones (Srikantappa, 2001). Occurrence of pseudotachylite along the shear zone, indicates frictional heating. The Bhavani Shear Zone, according to Naha and Srinivasan (1996) is upto 2 km wide south of Mettupalaiyam (GSI ., 2006).

To the south of the PCSZ directly lies the Madurai Block (MB). It is separated from the Trivandrum Block (TB) further south by the Achankovil Shear Zone (ASZ) (Drury and Holt, 1980). Madurai block (MB), largest crustal block in southern India is composed mainly of biotite-hornblende gneiss and massive charnockite with minor supracrustal rocks such as pelitic granulites and quartzite (Toshiaki and Santosh., 2003). The Madurai block comprises the largest highland granulite massifs in southern India, which includes the Palani, Anaimalai and Cardamom hills located in the Kodaikanal region. The charnokites from uplifted areas (e.g. the Palani Hills) are surrounded by supracrustals in tectonically complicated swathes forming the lower ground. Nd model ages of Madurai block indicates that differentiation of crustal protoliths from depleted mantle occurred during 3.2-2.0 Ga (Harris et al., 1994, Brandon and Meen., 1995). On the contrary, single zircon evaporation ages together with U-Pb zircon concordia define ages ranging from 2.5-2.1 Ga for the magmatic crystallization of protoliths (Bartlett et al., 1995, Jayananda et al., 1995a, Ghosh., 1997).

The Cauvery River drains through the above described lithologies and starts forming the delta east of Tiruchirrapalli. The exposed older rocks mainly of sedimentary origin border the present day Cauvery delta. Towards the north it is bordered by Cretaceous sediments consisting of conglomeratic sandstone, fossiliferous limestone and shale and the Tertiary formations of Mio-Pliocene age

mainly consisting of argillaceous and ferruginous sandstone and clay stones (Subramanian and Selvan., 2001). The Tertiary formations of Mio-Pliocene age also border the delta towards the south west. The Creataceous sediments found along the east coast were laid down during the phase of marine transgression which was followed by sedimentation in a platform carbonate environment in Miocene.

2.4 Cauvery Delta:

The present Cauvery River delta has formed by erosion and later deposition over the older sedimentary rocks of Cauvery Basin. The underlying older sediments of Cretaceous and Tertiary age were deposited in the intra-cratonic rift basin that was further divided into a number of sub-parallel horsts and grabens, trending in a general NE-SW direction. The basin is believed to have come into existence due to divergent tensional block faulting of continental crust and subsidence during Late Jurassic age and records a sedimentation history till recent with alternative transgressive and regressive cycles (Radhakrishna.,1993). The basin is charcterised by features of block faulting, subsidence and sedimentation. The basin is divided into number of sub-basins separated by ridges. According to Sastri and Raviverman (1968) the main blocks of early subsidence run NE-SW and were formed along the western part of the basin. The horst and graben formed by the above activity got filled and leveled by Oligocene. The present day delta has formed over the erosional surface developed over the Tertiary sedimentary rocks.

The Cauvery River forms a moderate sized delta that commences at Tiruchirapalli. The apex of the Cauvery Delta is about 30 km west of Thanjavur and the area of the deltaic plain is often called *the garden of southern India.* The radiocarbon dates obtained from the borehole peat from 20 m depth in delta, suggested that the Holocene sediments are 3 m thick about 50 km inland and about 30 m thick near the present shoreline (Sadakata.,1980). Meijrink (1971) and Sambasiva Rao (1982) based on the number of abandoned distributary channels stated that the Holocene maximum transgression was in the southeastern side of the delta and that there was a continuous counterclockwise shift in the delta lobes towards the northeast. Based on Remote-sensing and geomorphologic studies Mitra and Agarwal (1991) stated that Cauvery delta lacks the protuberance which is regarded as one of the most essential elements of a delta. They further inferred that the recent longshore

wave action has made its coastline smooth and straight fringed by beach ridges and occasional swales. There is a view that cretaceous sediments found along the east coast were laid down during the phase of marine transgression which was followed by sedimentation in a platform carbonate environment in Miocene (Subaramanian and Selvan., 2001). The Quaternary sediments in the coastal tract are deltaic littoral sands and muds (Mitra and Agarwal., 1991). On the basis of morphology the Cauvery delta has been divided into an upland plain, a deltic plain and a coastal plain (Subaramanian and Selvan, 2001).

Chapter 3

Methodology

3.1 Introduction:

To address the stated objectives, conventional methods of sample processing for geochemical and isotopic studies were employed. Core drilling, core cutting and preservation of cores formed the preliminary part of the work. Sub sampling of the cores were carried out and representative samples were subjected to chemical procedures required for Major, trace element (including REE) and isotope analyses. Sequential extraction procedures were followed to extract leachates for isotope studies. Calibration of ion-exchange columns (liquid-chromatography) was carried out for effective separation of elements. The elemental abundances and isotopic ratios were determined using the Inductively Coupled Plasma – Atomic Emission Spectrometer (ICP-AES), Inductively Coupled Plasma–Mass Spectrometer (ICP-MS) and Thermal Ionization Mass Spectrometer (TIMS) respectively with the facilities at the Department of Earth Sciences, Pondicherry University. The identification of minerals has been carried out using X-Ray Diffractometer (XRD). The detailed procedures involved with the analysis of the samples are discussed below.

3.2 Core Drilling and Core Preservation:

The core drilling was done in two phases, carried out as a part of shallow subsurface studies (SSS) project sponsored by DST, India. M/s. Hydro-Geosurvey Consultants Pvt. Ltd., Jodhpur, was hired for drilling and retrieving cores from the selected sites in the Cauvery delta (Fig 3.1). Drilling employed a diamond/Tungsten core drilling bit involving a double barrel core tube. A PVC pipe was inserted within the core tube to retrieve the cored sediments. A slow direct circulation rotary method was used for the muddy formation with almost 100% core recovery. In sandy strata, a combination of rotary and percussion methods was used to arrest the core with slightly lesser core recovery (70–80%) including a slight compaction due to percussion. The sediment compaction and expansion was measured within the drilling interval as the difference between the drilling depth and the actual core retrieved. During the first phase, drilling was carried out (during April and May 2007) at five locations [Uttrangudi (UG), Valangaiman (VM), Kadlangudi (KG), Nanillam (NM) and Karikal (KK)] situated in the southern and central part of the delta (Fig 3.2). After studying the sub-basin structure, lithological and textural variations of the cored sediments, further four new sites were selected in order to understand the Quaternary

buildup of Cauvery delta in detail. Thus in the second phase further cores were retrieved from the delta during the months of March and April months 2009.

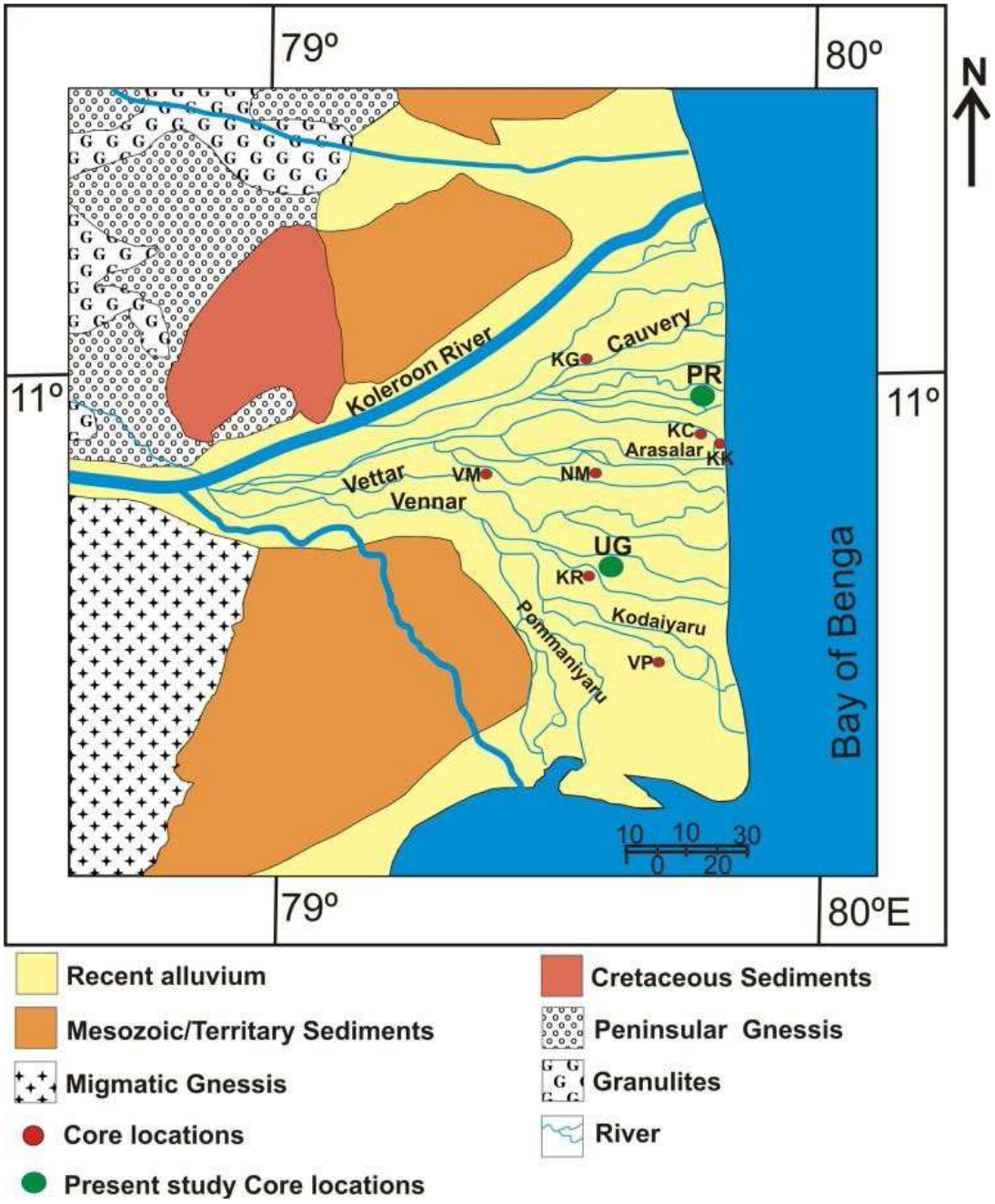

Figure 3.1: Map of Cauvery Delta showing core locations on Cauvery River delta. UG- Uttarangudi, PR- Porayar, VP- Vadapadi, VM-Valangaiman, NM-Nannilam, KK-Karaikal, KC-Kottucheri west, KR-Keeralthur, KG_ Kadalangudi.

The new drilling locations were taken from the south and central parts of the delta more towards the present day sea coast. These sites include Porayar (PR), Kattucherry (KC), Vadapadi (VP) and Kerralthur (KR). All the collected cores were

stored in a refrigerated room maintained at a temperature of -4° C. The refrigerated room was designed with PUF panels along with PPGI inside and outside to achieve complete insulation. Refrigeration Instrument BR101 (Condensing unit-BR101C and Evaporators BCU-10) were installed for temperature monitoring.

For the present study two cores Uttrangudi (UG) and Porayar (PR) from distinct delta geomorphic setting were analyzed for geochemical and isotopic work.The core from Uttarangudi (UG) was collected around 25 km inland from the Bay of Bengal coast near Tiruvarur area (N 10^{o} 39’17.7”, E 79^{o} 39’42.2’’). At Porayar (PR), core sediment was collected from around 2 km inland from Bay of Bengal, located north of Karaikal region (N 11^{o} 01’17.8’’, E 79^{o} 50’42.6’’). The local elevation of this site is 2 m above mean sea level (amsl).

The core sections were split on opposite sides in the laboratory using the circular saw. After cutting the plastic pipe, a nylon string was passed down the core section to yield two halves (Fig 3.2a). Any smeared sediment was carefully scraped off the exposed sediment surface in a horizontal fashion using a plastic spatula. Subsequently the core lithologies were visually described and plastic U-channels were covered with transparent plastic bags and stored in the stainless steel core racks specifically designed for the cores.

(a) (b)

Figure 3.2: (a) Representative Core sections (b) Core Sample storage

Next, the cores were sub sampled at 10 cm interval and labeled according to depth and stored in plastic bags. The remaining part of the core was once again cold stored as repository for future analysis (Fig 3.2b).

3.3 Lab ware cleaning:

The lab ware cleaning is essential for the geochemical studies in order to avoid foreign contaminations. Brief descriptions of cleaning different types of lab ware adopted during the present study are given below.

Teflon® crucible cleaning:

The Teflon crucibles were pre-cleaned by filling about 30 ml of 6 N HCl and kept on hot plate for 6 hours. The beakers were then cleaned three times with single distilled water (SDW) and rinsed thrice with Triple distilled water (TDW). Further the Teflon® beakers were air dried in a hot oven at ~ 60° C.

Nickel Crucible cleaning:

25 ml Nickel crucibles were used for fusion of REE and silca analysis. The Nickel crucibles were kept in 1N HNO_3 for 15-20 minutes. After this Nickel crucibles were repeatedly washed with tap water and diluted Extran® MA 02 (Neutral) cleaning solution. Finally Nickel crucibles were cleaned by SDW and TDW and dried in a hot air oven.

Glassware cleaning.

The glassware's were kept in 35% Nitric Acid overnight. The glassware were taken out the next day and washed with diluted Extran® MA 02 (Neutral) and three times with TDW dried and kept in oven.

3.4 Sample Processing:

The subsamples were dried in an oven at 50 to 70º C for one day to remove moisture. After drying the samples were powdered to ~ 60 mesh size with the help of hardened steel mortar specially designed for geochemical analysis. About 40 g of representative sample powder was taken (after coning and quartering) and further size was reduced by using agate-lined vibrating cup mill (Pulvarisette-9, Fritsch, Germany of 75 ml capacity) at 750 rotation per minute (RPM). After this the samples were finally powdered to < 200 mesh (0.075 mm) size in agate mortar and stored in air tight plastic boxes for geochemical analysis. At every step utmost care was taken to avoid contamination. Based on the color and textural variations around 180 samples

were selected for detail major and trace element studies from both cores (UG & PR). After analyzing the major and trace elemental behavior, (60) samples were taken for Rare earth element (REE) studies from both sites. Out of these 30 samples were selected for phase extraction and subsequently the residue left was taken for Rb-Sr and Sm-Nd isotope analysis.

3.5 Texture Analysis:

. Grain size analysis is an important descriptive measure to understand the mechanisms operative during transportation, deposition as well as the distance of sediment transport. The grain size of core sediments was measured by laser particle size analyzer (Cillas 1190). The basic principle of Laser diffraction method (LDM) is that particles of a given size diffract light through a given angle. The angle of diffraction is correlated inversely proportional to particle size, and thus the intensity of the diffracted beam at any angle measures the number of particles with a specific cross-sectional area coming in the optical path. The parallel beam of monochromatic light passing through a suspension enclosed in a sample cell, and the diffracted light is focused onto detectors.

About 0.2 g subsample was taken with 30 % Hydrogen peroxide (H_2O_2) and 0.1 M HCL to remove organic matter and carbonates, respectively. Further the samples were added with 20 ml of TDW and 10 % Sodium hexamataphosphate [$Na_3(PO_3)_6$] stirred properly, till the sample was in suspension. Sample was then poured into the sample cell for analysis. Each sample was analyzed twice with three repetitions. Each time sample cell was rinsed three times before moving to next sample.

3.6 Bulk Mineralogy:

The powdered bulk samples were used for mineralogical analysis by using PANalytical X'pert PRO X-ray Diffractometer (XRD) equipped with θ-θ type goniometer. The samples were scanned between 2θ values of 2º and 50º with scan speed of 2.4° 2θ/min and 40 kV acceleration voltage. The Cu $K_\alpha$wavelength for the X-Ray generated was 1.54 Å. The minerals were identified by standard procedures (Dixon et al., 1977; Brindley and Brown., 1980, Nesse., 2000).

3.7 Geochemical analysis:

3.7.1 Major and Trace analysis:

For major and trace element determination standard B-solution procedure of Shapiro and Brannock (1962) was followed. About 0.5 gm of -200 mesh size (0.075 mm) sample powder was transferred into 60 ml Teflon® crucibles. 10ml conc. HF, 5ml conc. HNO_3 and 2.5 ml concentrated $HClO_4$ was added to the crucible containing sample and digested 8 to 10 hours at 90° C with lid on over a hot plate. After digestion the crucible contents were evaporated to complete dryness. After this 5 ml HF, 10 ml HNO_3 and 2 ml $HClO_4$ were added to the crucible and evaporated to complete dryness at 120º C. 5 ml HNO_3 was added twice to the crucible each after drying to remove the traces of fluorides. The dried crucible contents were dissolved in dilute HCl and transferred into pre-cleaned calibrated 100 ml volumetric glass flask and volume was made up to 100 ml volume. The crucibles were cleaned repeatedly with dilute HCl and TDW. This formed 200 times diluted solution for trace elements. For major element analysis 5 ml from this solution was taken and volume of 100 ml was made (4000 times dilution). The digested solution was taken for determination of trace and major elements by ICP-AES. This method was preferred since the nitric acid used dissolves carbonates and sulphides and takes many elements including the iron into higher valency states. The $HClO_4$ used oxidizes the organic matter.

3.7.2. Silca Analysis:

Silica content of samples was done by Solution A method of Shapiro and Brannock, (1962). 60 ml Nickel crucible were cleaned with 1:1 HCl and washed with water. 10 ml of 15% NaOH was placed and evaporated to dryness under an infrared lamp. About 0.05 g of – 200 mesh samples were loaded in crucibles and fused by Maker Burner at Red hot condition for 12-15 min. The crucibles were left to be cooled and 2/3rd of each was filled with Milli Q® water and kept covered and left overnight. The contents of crucible were transferred to 500 ml plastic beakers containing about 300 ml of Milli Q® and 10ml of concentrated HCl. The contents in the beaker were quantitatively transferred to a series of 1000 ml flasks. Finally the volume was made up on cooling and 100 ml of each was further transferred to plastic bottles and taken for SiO_2 determination.

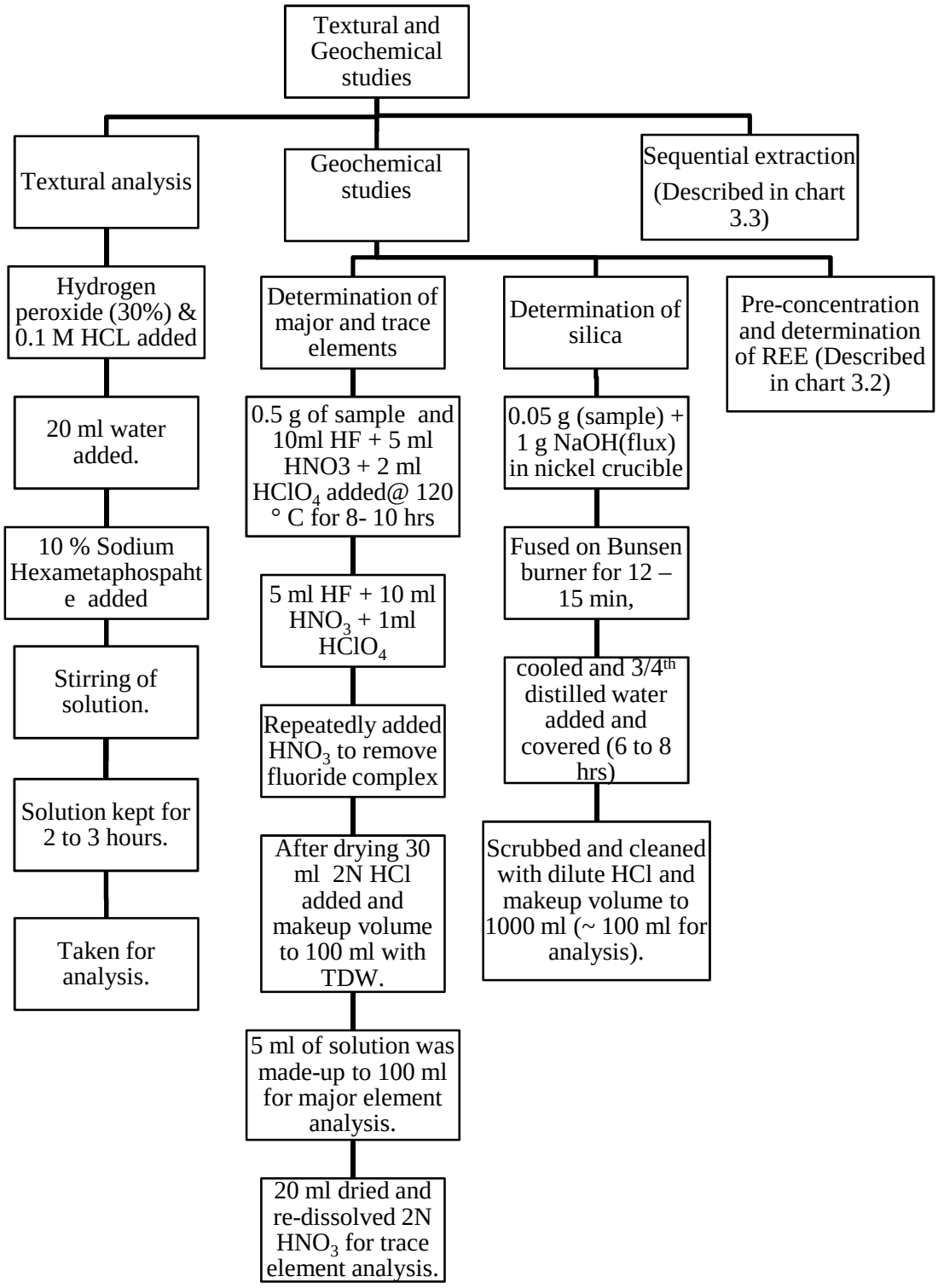

Chart 3.1: *Flowchart showing chemical procedure for geochemical and Textural studies.*

Reagents Used:

Ammonium Molybdate Solution 7.5% : This was prepared by dissolving 7.5 g of Merck® GR grade Ammonium. Molybdate in 75 ml of Milli Q® in 100 ml volumetric flask. Then subsequently 10 ml of 1:1 H_2SO_4 is added and volume is made up to 100 ml. The solution made was stored in a plastic bottle.

Tartaric acid solution of 8%: It was prepared by dissolving 40 gm of reagent grade tartaric acid in Milli Q® and volume was made to 500 ml and stored in plastic bottle.

Reducing solution: The preparation of reducing solution requires three reagents. The solution forms of 0.5 g of reagent grade anhydrous Sodium Sulfite and 0.15 g of 1Amino-2Napthol-4 Sulphonic acid in 10 ml of distilled water in a 100 ml volumetric flask. Separately 9 gm of anhydrous Sodium bi/disulphide are dissolved in 70 ml Milli Q®**.** Both solutions are taken in 100 ml volumetric flask and transferred to 100 ml plastic bottle and covered with aluminum foil.

Determination of Silica:

10 ml aliquot of each sample solution A was pipetted out and transferred to a series of 100 ml volumetric flasks to which 1 ml of Ammonium Molybdate was added and stirred. The solution becomes yellowish and is allowed to stand for 10 min. 5 ml of Tartaric acid was added to this solution and mixed thoroughly. Further 1 ml of reducing solution was also added and stirred properly. The volume was made up to 100 ml and allowed to stand for 30 min. The absorbance of each solution was measured at 650 nm. With respect to "blank solution – A" used as a reference blank which was compared with absorbance of "Solution – A" of rock standards. The factor for each of two standard solutions is computed and average has taken:

$$\textbf{Factor} = \frac{\%\ \textbf{SiO2 of standard}}{\textbf{Absorbance of standard}}$$

Now percentage of SiO_2 of each sample is computed by using the formula Percentage of SiO_2 = average factor x absorbance of sample solution

For major and trace element determination standard B-solution procedure of Shapiro and Brannock (1962) was followed. About 0.5 gm of < 200 mesh size (0.075

mm) sample powder was transferred into 60 ml Teflon® crucibles. 10ml conc. HF, 5ml conc. HNO_3 and 2.5 ml conc. $HClO_4$ were added to the crucible containing sample and kept 8 to 10 hours at 90º C with lid on over a hot plate. After digestion the crucible contents were evaporated to complete dryness and 5 ml HF, 10 ml HNO_3 and 2 ml $HClO_4$ were added to the crucible and again evaporated to complete dryness at 120º C. About 5 ml HNO_3 was added twice to the crucible each after drying to remove the traces of fluorides. The dried crucible contents were dissolved in dilute HCl and transferred into pre-cleaned calibrated 100 ml volumetric glass flask and volume was made up to 100 ml volume. The crucibles were cleaned repeatedly with dilute HCl and TDW. This formed 200 times diluted solution for trace element analysis. For major element analysis 5 ml from this solution was taken and volume of 100 ml was made (4000 times dilution). The digested solution was taken for determination of trace and major elements by ICP-AES. This method was preferred since the nitric acid used dissolves carbonates and sulphides and takes many elements including the iron into higher valency states. The $HClO_4$ used oxidizes the organic matter.

3.7.3. Preparation of NaOH-Na_2O_2 fused solution for Rare earth elements (REE):

The NaOH-Na_2O_2 fused solution was used for determination of Rare earth elements (REE). 1 gm NaOH pellets and 1.25 gm Na_2O_2 granules were taken in 25 ml nickel crucible. 0.5 g of sample powder <200 mesh size (0.075 mm) was added carefully so that it does not touch the wall of the crucible and the lid was put on. The sample and the flux were then fused by heating on the Bunsen burner with continuously swirling. The crucible was heated for 12-15 minutes continuously. The crucible was then left to cool down. On cooling the nickel crucible was filled with $3/4^{th}$ volume by TDW and left overnight with lid on. After around 12 hours the digested sample was scraped with the help of clean Teflon® rod and transferred into 500 ml beakers. The nickel crucibles were further scrapped and cleaned with the help of 6 N HCl and the contents were transferred into the beaker. The beaker was then kept on a hot plate at 70- 80º C to evaporate the acids till the H_4SiO_4 gel forms. The silica gel precipitate was filtered by using 41-42 Whatman filter paper and subsequently cleaned with 6 N HCl followed by TDW till no traces of acid remains

(till the Filter paper becomes completely white). The filtrate from the flask was transferred into the beaker and kept once again for drying. The flask was repeatedly cleaned till no trace of filtrate remains inside the flask.

After the filtrate was completely dried 30 ml 1 N HCl was added and then the solution was transferred into centrifuge bottle by repeated washing by 2 N HCl and TDW. 12-14 drops of phenol red indicator were added to solution and the color of solution becomes orange. 1:1 Ammonia solution is added in drops to the solution till the color of the solution changes from orange to pink and a brown color precipitate starts forming. The pH of the solution at this point is about 8. The ammonia step is used to precipitate the tri- and tetravalent cations leaving the mono- and divalent cations in solution, which come in the decant.

The above solution with its precipitate is centrifuged at 6000 RPM at a temperature of around 4º C for 30 minutes. The centrifuged solution is then decanted. The precipitate formed is then taken repeatedly with the help of 6 N HCl and transferred to a 250 ml PFA beaker. The solution was then kept on hot plate at 80º C for complete drying. If any trace of silica was left, 5-10 ml HF and HNO_3 was added to it and dried. Further 10 ml HNO_3 was added so to remove any trace of HF and the solution was once again completely dried. The dried residue left was picked by 30 ml 1 N HNO_3 and warmed on hot plate so as the residue dissolves and becomes completely transparent. Now the solution is ready for loading on to the column.

Two types of column were used: HNO_3 and HCl acid cation exchange columns for group separation of REE from the other elements. AG 50W –X8 of 100-200 mesh size cation exchange resin was used in both the columns. 10 ml of 1N HNO_3 was added to column for resin equilibration. The solution was then loaded onto the HNO_3 column. Once the loaded 30 ml sample solution had passed through the column, 70 ml of 1.74 N HNO_3 was eluted. Then 180 ml of 6 N HNO_3 was passed through the column and collected in 500 ml Teflon® beakers. The solution was once again dried on hot plate. After drying the contents were re-dissolved in 30 ml 1N HCl and loaded onto the HCl column after equilibrating it with 10 ml 1 N HCl. After the 30 ml 1 N HCl was passed through the column followed by 70 ml 1.7 N HCl and discarded. Then 140 ml of 6 N HCl was passed through the column and collected. The collected solution was dried and dissolved in 10 ml 1 N HNO_3 and taken for analysis.

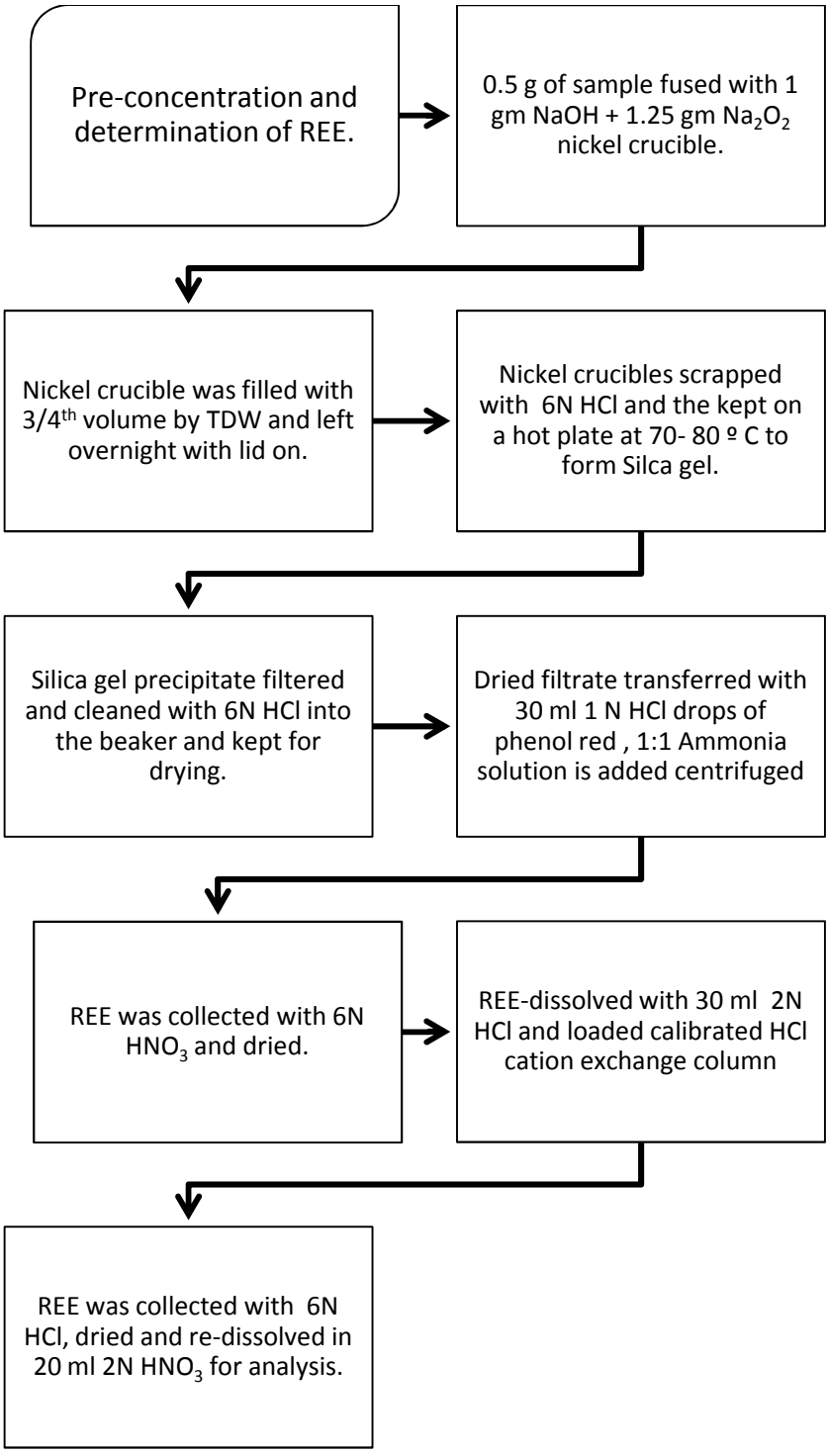

Chart 3.2: *Flowchart showing Pre-concentration of REE in cation exchange columns.*

3.8 Elemental analysis using ICP-AES and ICP-MS:

The Trace element, including REE, analysis of all the studied samples was carried out using an Inductively Coupled Plasma Atomic Emission Spectrometer (ICP-AES) (Model: Jobin Yvon Ultima 2) and Inductively Coupled Plasma- Mass Spectrometer (ICP-MS)-X-Series. The B-solutions prepared as described in section (3.7.1) were analyzed in (ICP-AES) for determination of major elements and trace elements, such as Ba, Cr, Ni, Sr, Zr and Y. Rock standards. AMH and DGH supplied by the Wadia institute of Himalaya Geology Dehradun (Saini et al., 1998) and internal rock standards 21-6, 22-22, 22-7 and VM-9 were calibrated using the USGS rock standards BHVO-1, RGM-1, BCR-2 and STM-1 for calibration of ICP-AES for major and trace element analysis. Trace elements Sc, Co, U, Th and Rb were analyzed by (Thermo scientific, Xseries-2), ICP-MS. The element analysis in (ICP-MS) was carried by using international USGS standards AGV-2, SCO-1, GSP-2, W-2a, SDC-1, and BHVO-2 were used for calibration.

Rare Earth Elements were determined on pre-concentrated solutions after calibrating the ICP-AES with the standards AMH, DGH, 86-89 and 90-57. REE values of the internal rock standards were previously determined using isotope dilution technique at Stony Brook, New York, USA (Krogstad, et al., 1995). And these values were checked by analyzing the standards AMH and DGH as unknowns. The precision of major, trace and REE were checked by replicate analysis of samples. Both precision and accuracy for major elements are better than 2% and for trace elements and REE, precision and accuracy are better than 2 % and 5 % respectively. For low REE samples (<5× chondrite) the precision was 5–10 % for Ce and Nd. The precision on repeat measurement for Th, Sc, Co, U Ta and, Nb is <3%. The accuracy of measurement is better than 10%. Blank levels measured for various major and trace elements are shown in (Table 3.1**)**

Table 3.1: Blank concentration of Major, Trace and Rare earth elements (REE) were anaylsed using ICP – AES.

Element	**Blank concentration**
SiO_2 Al_2O_3 Fe_2O_3, MgO, CaO P_2O_5, , K_2O and Na_2O	< 0.01 (wt %)
MnO and TiO_2	> 0.01 (wt %)
Ni and Cr	1.5 ppm
Ba	<0.5 ppm
Sr and Y. For La, Ce, Nd and Sm	0.03 ppm
Eu, Gd, Dy, Yb and Lu	≤0.007 ppm

3.9 Sequential extraction procedure:

The Leleyter and Probst, (1999) sequential extraction scheme was followed with these exceptions:

(1) Instead of 1 gm of sample 3 gm was taken and subsequently the reagent was increased in same proportion.
(2) The water soluble step was not followed
(3) In the exchangeable step magnesium nitrate ($MgNO_3$) was replaced by magnesium chloride ($MgCl_2$).

First step: Exchangeable fraction (Exch):

(i) 30 ml of 1 M magnesium chloride ($MgCl_2$) solution adjusted to pH 7.0 was added to each centrifuge tube containing sample, closed tightly and shaken vigorously for mixing. Then the tubes were placed in a mechanical water bath shaker with continuous agitation at room temperature for 1 hour. (Chart 3.3)

(ii) The centrifuge tubes were kept for centrifugation at 7000 RPM for 2-5 minutes.

(iii) The Supernatants were filtered through 0.45 µm filter paper (Whatman ®) and stored in previously labeled polypropylene bottles. The residue on the filter paper in case left, was returned to the residue remaining in the tube to minimize the loss.

(iv) Before moving to the next step, the residue was washed with 10 ml of Milli Q® ultra pure water and centrifuged for 5 minutes. The supernatants were transferred and added to the previously labeled flat bottom Tarson® polypropylene bottle. This procedure was applied to all the following steps.

Second step: Carbonate (Carb)

(v) 30 ml of 1 M sodium acetate (CH_3COONa) that has been adjusted to pH of 5.0 with acetic acid (CH_3COOH) was added to the residue from step one and the centrifuge tubes closed tightly and shaken vigorously for mixing. Then they were subjected to continuous agitation in a mechanical water shaker for 5 hours at room temperature.

(vi) Steps ii, iii and iv were repeated.

Third step: Bound to Mn oxides (MnO)

(vii) 30 ml of 0.1 M hydroxyl ammonium hydrochloride (NH_2.OH HCl) in 25 % (v/v) acetic acid (CH_3COOH) was added to the residues from the second step accompanied with agitation for 30 minutes.

(viii) Steps ii, iii and iv were repeated.

Fourth step: Bound to amorphous iron oxide (AFe Ox):

(ix) 30 ml 0.2 M Ammonium Oxalate + 0.2 M Oxalic acid was added to the residues from the third step and kept for 4 hours at room temperature.

(x) Steps ii, iii and iv were repeated.

Fifth step: Bound to crystalline iron oxides (Cfe Ox):

(xi) 30 ml (0.2 M Ammonium Oxalate + 0.2 M oxalic acid + 0.1 M Ascorbic acid was added to the residues from the fourth step and kept for 30minutes at 80°C.

(xii) Steps ii, iii and iv were repeated.

Sixth step: Bound to organic matter (Org):

(xiii) 48 ml [{9ml of 0.02 M HNO_3 (20%(v/v)} +(15ml 30% H_2O_2) +(9ml H_2O_2)+(15ml NH_4OAc)] for 3hr at 80 °C was added to the residues from the fifth step.

(xiv) Steps ii, iii and iv were repeated.

Seventh Step: Residual fraction:

(xv) The leftover residue from the sixth step was dried and powdered to -200 mesh (0.075 mm) size and taken for Rb-Sr and Sm-Nd analysis.(Details in Section 3.9)

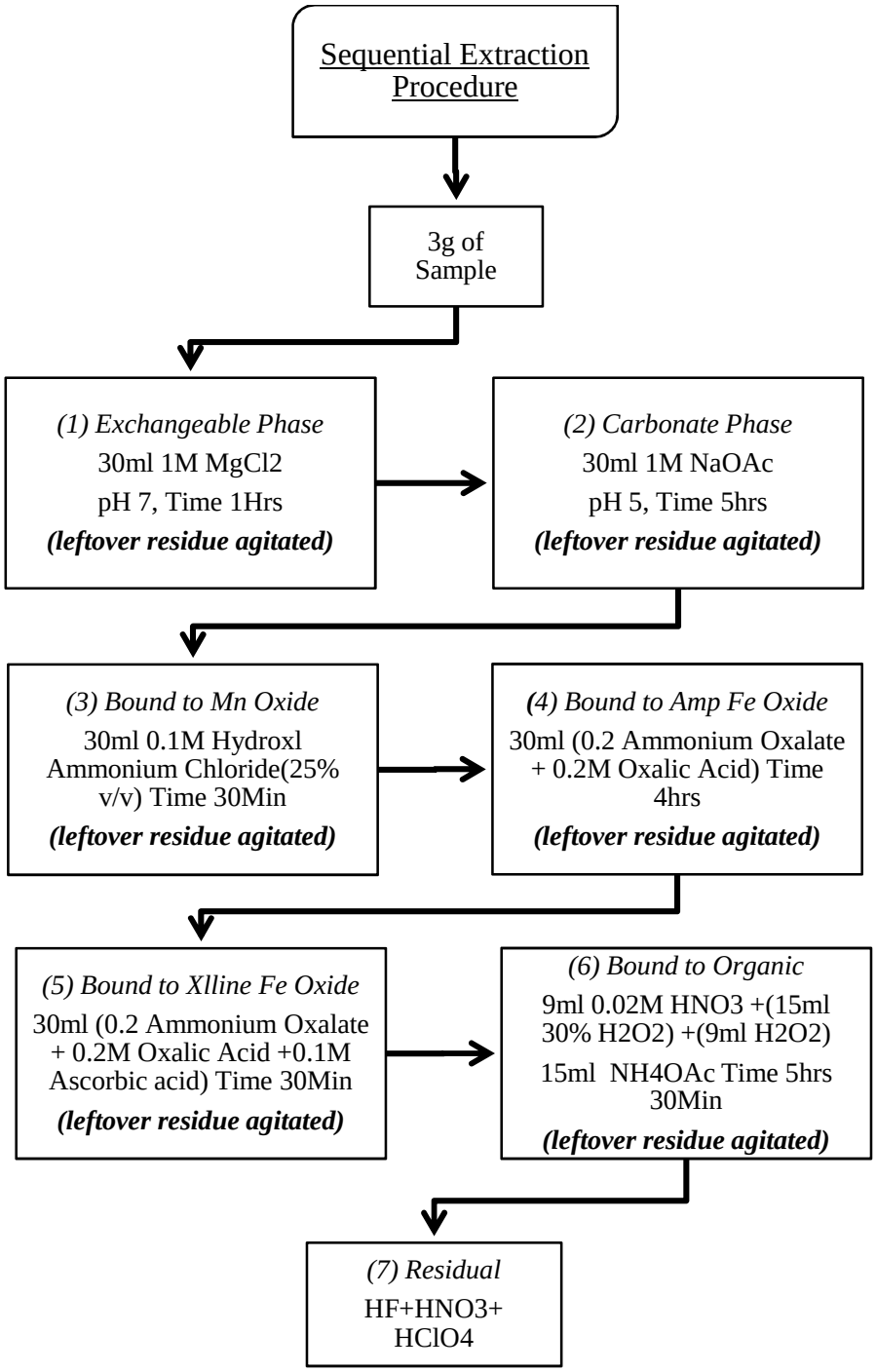

Chart 3.3: *Flowchart showing the sequential extraction procedure modified after (Leleyter and Probst., 1999). After each step sample were stored in bottles and taken for analysis in TIMS.*

3.10 Sr concentration in sequentially extracted phases:

From the Uttrangudi samples exchangeable, carbonate, Fe-MnO and organic phases were extracted while from Porayar samples only three phases were were used for Sr isotope analysis i.e. carbonate, Fe-MnO and organic. 2 ml of (Exch), 10 ml of (Carb) and 10 ml of (Org) were taken in 25 ml Teflon beaker. For Uttrangudi site in addition of these phases 15 ml of Fe-MnO combined phase was taken by mixing 5ml each from (MnO), (AFe Ox) and (CFe Ox) phases. The Teflon® beakers were kept for drying on hot plate at 70-80 °C followed by drying with 5 ml of concentrated HNO_3 (2 to 3 times) in order to reduce the matrix level. After this the sample was dissolved with 2 ml 2 N HCl and transferred into the column filled with Bio-Rad AG50-WX8 (200-400 mesh) cation exchange resin. Sr was collected with 2 N HCl and dried and cleaned through the clean-up column (Chart 3.2). Sr was dissolved in 1 µl of concentrated HNO_3 and loaded on degassed Tungsten (W) filament kept preheated at 1A current. Around 0.1 to 0.5 µl of TaO was loaded on its top. The Tungsten (W) filament was dried at 1 A current. Further the filament was kept at 2 A current for 1 minute to fume off un-dried acids. The filament was then glowed to dull red for about 20 seconds and loaded on the turret for analysis in Thermal Ionization Mass Spectrometer (TIMS).

The blank level for each phase was determined by spiking the each phase with the previously calibrated mixed isotope tracer solution for Rb-Sr (Anand., 2007). The blank levels were found to be minimal. The blank level of Sr for exchangeable phase was 33.03 ng/g, 2.14 ng/g for carbonate, 1.22 ng/g for MnO and 5 ng/g for Organic.

3.11 Rb-Sr and Sm-Nd Isotope Analysis:

Rb-Sr and Sm-Nd isotope studies were carried on residual phase. The residual portion left after the sequential extraction procedure was dried and powdered to -200 mesh (0.075 mm) size in agate mortar. About 100 mg of sample was weighed accurately using a high precision analytical balance and transferred to a 7 ml Savillex® vials. The digestion was carried out using double distilled HF-HNO_3-HCl acids in Teflon®-lined stainless steel bomb at 200° C for 3 days in order to dissolve any refractory phases such as zircon,. After the sample was completely digested, the

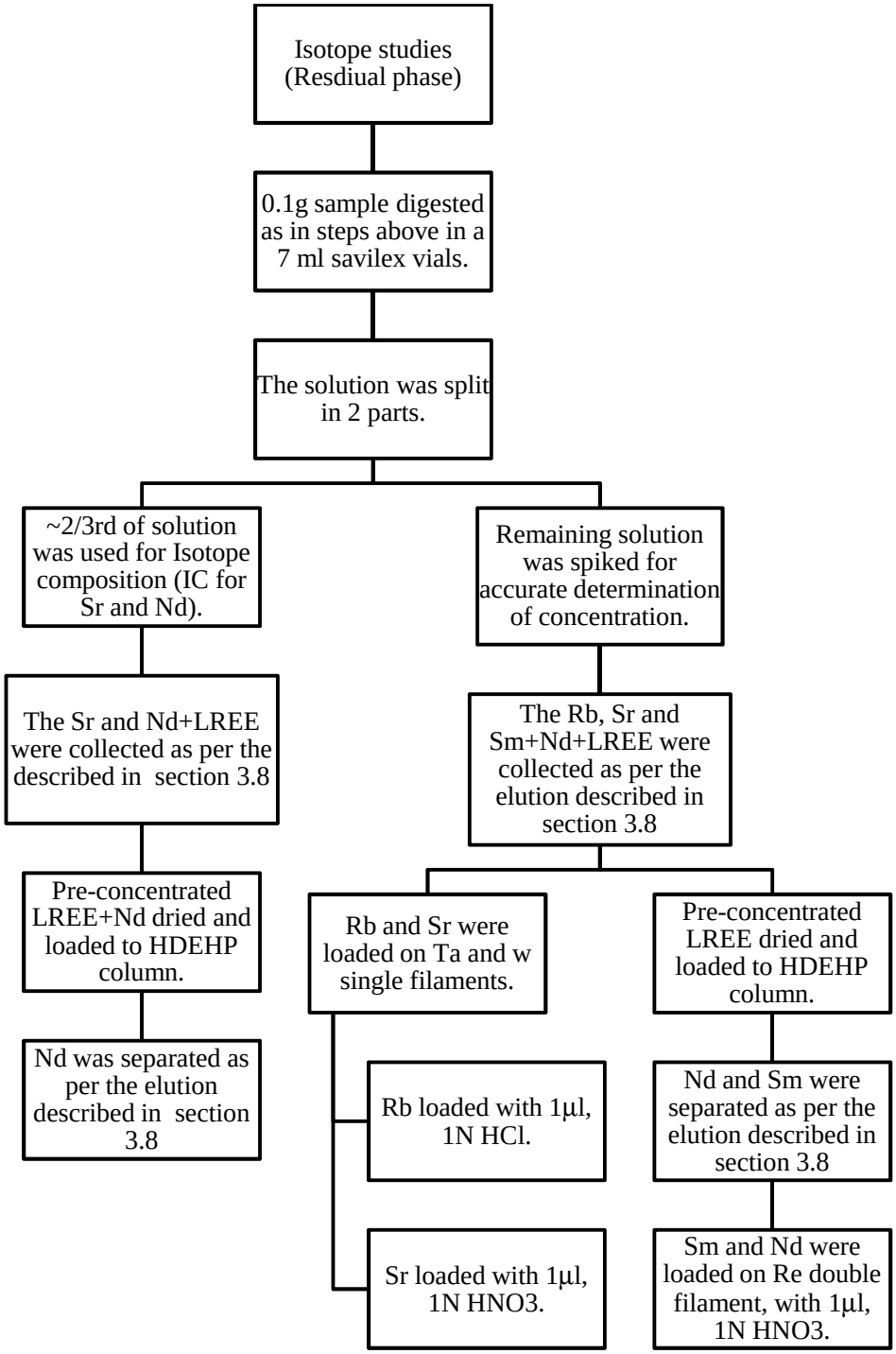

Chart 3.4: *Flowchart showing the procedure for separation of Rb, Sr, Sm and Nd in residual phase for isotope studies*.

ml of $HClO_4$ was added and the sample was dried again. The sample was further treated with concentrated HCl and HNO_3 and dried completely, so that remaining traces of HF were evaporated. The beaker contents were dissolved in 2 N HCl and split into two fractions. Out of the two fractions one was used for the determination of

isotopic composition (IC) of Sr and Nd, while the other fraction was spiked to the determination of Rb, Sr, Sm, and Nd concentration by isotope dilution (ID). The tracer solutions (spike) were used for Isotopic Dilution (ID) analyses for the precise determination of concentrations of elements.

Isotope dilution analysis involves addition of a known amount of isotope tracer solution to a precisely weighed sample solution. For this purpose, the calibrated Rb, Sr, Sm and Nd mixed isotope tracer solution was added to the fraction to be used for ID analysis. Electronic balance (Sartorius ME 235S model) was used for weighing the amount of tracer solution was accurately determined by weighing the bottle containing the tracer solution before and after dispensing (Anand and Balakrishnan, 2010).The procedural blank associated with the Rb, Sr, Sm, and Nd isotopic studies are 55.75, 0.4020, 0.2467, and 0.0557 ng, respectively and are <1000 times the concentration in the samples taken for determination of isotopic composition.

The IC and ID fractions were passed through 4.5 ml quartz columns filled with Bio-Rad AG50-WX8 (200-400 mesh) cation exchange resin calibrated for separation ofRb, Sr, and REE (Sm and Nd) (Anand., 2007). Rb and Sr were pre-concentrated with 2 N HCl and isolated from the matrix elements to a large extent, while the LREE as a group was collected with 6 N HCl. Rb and Sr fractions thus separated were purified further by passing through a set of secondary 2 ml polypropylene Bio-Rad columns filled with AG50-WX8 (200-400 mesh) cation exchange resin and calibrated for the above mentioned elements. Rb and Sr were collected from this column with 2 N HCl and were dried.

Sm and Nd were separated from the REE collected as group from HCl column using HDEHP (2-ethyl hexyl hydrogen phosphate) coated Teflon resin (procedure modified from Richard et al, 1976 and Gioia and Pimentel, 2000). The REE fraction was dried and dissolved in 300 µl of 0.18 N HCl for loading into the column. These columns consist of HDEHP resin-coated Teflon® powder in 1 ml quartz column sandwiched with about 0.5 cm with Bio-Rad AG1-WX8 anion-exchange resin and each column was calibrated separately to determine the elution required for collection of Nd and Sm. Nd was collected with 0.3N HCl and Sm was collected with 0.4N HCl. (Chart 3.3). Few drops of<0.5M H_3PO_4 was added to the collected Nd and Sm cuts and dried to ensure visibility while loading onto the filaments. Double distilled (using

sub-boiling quartz still) EMerck GR grade hydrochloric acid and Milli Q® ultra pure water were used for digestion of samples, tracer solutions and calibrating solutions.

3.12 Mass Spectrometry:

Rb and Sr were loaded by following procedure for mass spectrometry:

1 µl of Tantalum oxide (TaO) activator was loaded on a pre-warmed rhenium (Re) single filament and dried at 0.5 A current. Rb was dissolved in 1 to 2 µl of 1N HCl and loaded on top of TaO on the filament and dried at 0.5 A current. 1 µl of Tantalum oxide (TaO) activator was again loaded on top of the sample making a sandwich of sample between layers of TaO. The filament was then glowed to dull red for about 10 seconds and loaded on the turret of the TIMS for analysis. The samples with less Sr concentrations were loaded on W filament. Sr was dissolved in 1 µl of 10N $HNO_3$and loaded on Tungsten (W) filament. Around 0.1 to 0.5 µl of TaO was loaded on its top. The Tungsten (W) filament and dried at 1 A current. Further the filament was kept at 2 A current for 1 minute. The filament was then heated to dull red colour for about 20 seconds and loaded on the turret of the TIMS for analysis.

Data acquisition for Sr IC carried out in 20 blocks and 11 cycles (220 measurements) in the static mode. During measurement, cup rotation, baseline calibration and auto focusing were performed at fixed intervals of four blocks. Sr isotope analysis of international standard SRM 987 was carried out repeatedly during the course of analysis of samples to check the accuracy and precision of the analysis. The mean value of $^{87}Sr/^{86}Sr$ ratio of 0.710259 with an external precision of 0.000004 (1 s.d.) was obtained from 40 number of standard measurements. The recommended $^{87}Sr/^{86}Sr$ ratio for SRM 987 is 0.710240. Instrumental mass fractionation during the determination of Sr isotopic compositions in standards and samples was corrected by internally normalizing the measured ratios by the ratios $^{86}Sr/^{88}Sr = 0.1194$ for Sr using exponential fractionation law. The mass fractionation for the ID samples was determined through multiple measurements of isotopic standards and factors were assigned externally A double filament assembly includes two filaments of which one is used as sample evaporation filament and the other is used as ionization filament for Sm and Nd analysis. Nd and Sm were dissolved separately in 1 µl of 1N $HNO_3$and were loaded on pre-warmed rhenium (Re) double filaments for mass spectrometry.

The sample was loaded on the filament at 0.5 A current and allowed to dry. Then the current was increased to 1.2 A for 1min in order to fume-off, followed by individually heating the filament to dull red for about 20 seconds ensuring sample fusing to the filament until all the H_3PO_4 evaporated and were loaded in the turret of the TIMS for analysis. The mean value obtained on 30 analyses of AMES for Nd is 0.511968 ± 3 (Fig. 3.3) (recommended value of AMES for Nd 0.511968 ± 4.Govindaraju., 1994).

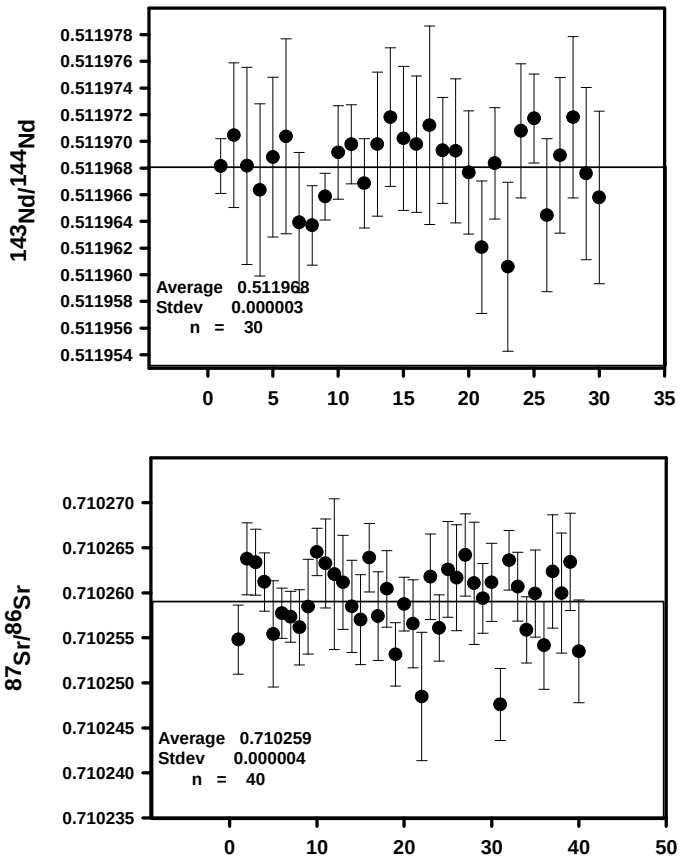

Figure 3.3: The Sr and Nd values of standards AMES and SRM987 measured in TIMS during the period of measurements of the sediment samples.

Chapter 4

Geochemical studies on the Core sediments from Cauvery delta.

4.1 Introduction:

Weathering is an important component of many basic geochemical processes on Earth's surface (Gunnel et al., 1997, 2007; Louvat and Allegre., 1997; Dessert et al., 2001). It is the process behind the generation of simple dissolved ions and secondary clay minerals that are released from primary minerals and ultimately transported to ocean by Rivers, and therefore act as primary agents for erosion. The term 'Weathering' may be defined as a combination of complex suite of chemical, biological and physical processes that transforms bedrock into soils (Anderson et al., 2004). Physical erosion is considered as one of the drivers of chemical erosion. The proportion of various elements in the dissolved phase is governed by variety of complex phenomena but is primarily dependent on their relative abundances in minerals and on the mode and rate of their weathering. Chemical weathering of silicate rocks also exerts significant control on the CO_2 budget of the atmosphere and hence moderates the Earth's climate (Berner, 1995, Gaillardet et al., 1999; Dupré et al., 2003). The demanding interest in present and past global climate change studies has significantly contributed towards better quantitative understanding of the feedback mechanisms between climate and chemical weathering.

Further the sediments and sedimentary rocks are fundamental in reconstructing the tectonic, climate and paleo-geography of the concerned sedimentary basin. The most important controls on sediment composition are characteristic (composition, grain-size, texture) of the source rocks, relief, climate, transport and/or depositional mechanisms (McLennan et al., 1990, 1993; Singh and Rajamani, 2001). The provenance of sediments from ancient and modern successions can be inferred by elemental geochemistry, especially trace elements and radiogenic isotopes. The chemical signatures in spite of various intermediate processes are eventually transferred in sedimentary records and provide a useful tool for deciphering the nature and extent of weathering suffered, and the changes brought in the original composition of the source rocks. Therefore the quantitative estimation of the chemical weathering of silicates through indices such as the calculated values of chemical index of alteration (CIA), plagioclase index of alteration (PIA) and chemical index of weathering (CIW) are helpful in understanding the weathering history of sediments (Nesbitt and Young., 1982; Harnois., 1988; Fedo et al., 1995). The above needs to be understood to further apply the sediment chemistry for provenance studies

In the present chapter are presented the results of textural, mineralogical and geochemical compositions of sediments obtained from two cores retrieved from the Cauvery River Delta developed along the east coast of southern India. In earlier work carried out on Cauvery River, Singh and Rajamani (2001) have studied the surface sediment from the middle reaches mainly to understand the present day weathering and provenance of sediments. In later work Srikanth (2012) has studied the surface sediments from the delta region to understand the changes that has taken place in this region. Here as a part of the major project in the present study I have tried to understandthe spatial and temporal change in the texture and weathering intensity as recorded in the sediment cores from above two locations, one situated in the distal part and the other in coastalpart along the central axis of the delta. The other objective is to infer the post depositional changes in sediment as recorded in their chemistry. Finally an attempt has been made to infer the provenance using major element chemistry of the sediments.

4.2 Results:

4.2.1 Borehole Lithology:

Two drill core sediments were retrieved one from the Uttrangudi location and the other from the Porayar location (Fig 4.1 and Fig 4.2). The Uttrangudi bore hole consist sediments of middle to late Pleistocene and Holocene age and the Porayar bore hole consists of sediments mostly of Holocene age resting unconforamably over older Tertiary/Cretaceous sedimentary rocks. The lithostratigraphic boundaries are recognized by change of lithology and physical characteristics of sediments, such as color and texture. Both Pleistocene and Holocene sediments are composed of clayey silt, silty, sandy silt and silty sand, gravely to pebbly sand units. The sediments range in color from light brown, dark brown, grayish, greenish gray, grayish brown, grayish black to red. In some places dispersed mottling is present, whereas some bands are completely mottled. Rootlets and traces of rootlets are present along with decomposed vegetal matter and plant fragments in the entire depth in Porayar sediments except at depth greater than 20 m, whereas in Uttrangudi sediments it is limited to around top 7 m. Foraminiferal tests and fragments of molluscan shells are present in the Porayar sediments, whereas the Uttrangudi sediments are devoid of fossil. Quartz and feldspar constitutes the major primary minerals, whereas smectite, kaolinite and illite constitute the clay minerals. Illite is present in the entire depth in Porayar location,

whereas it is restricted to Holocene in Uttrangudi sediments and is absent in Pleistocene sediments.

4.2.1.1 Uttrangudi Borehole:

Based upon the texture the 31.5 m core obtained from Uttrangudi location has been divided into eight fluvial units. The bottom Six units (unit VIII to III) from 30.75 m to 7.5 m depth comprise the Pleistocene deposits and the top 2 units i.e. 7 m upward constitutes Holocene deposits. (Fig 4.1)

Unit I: The bottom unit I between 31.75 m and 28.2 m depth contains a channel fill and flood plain facies. It starts with a basal pebbly horizon which grades upward into fine to very fine sand and the flood plain mud.

Unit II: The interval 28.2 m to 22.4 m constitutes Unit II which is normally graded and exhibit a fining upward sequence similar to unit I and changes from bottom channel to top flood plain sequence. Silt forms the dominant composition followed by sand and subordinate clay. In various subunits the silt ranges between 48 and 76%, followed by sand ranging between 21 and 49% and less than 10% clay (1.5% - 10%) (Table 4.1, given at the end of chapter). The bottom of the units also contains pebbles upto 5 mm in diameter. Towards the bottom from 28 m to 24.9 m depth the sediment shows gradation in texture and is greenish to grey in colour. The sand percentage decrease upward and silt and clay show an upwardincrease. This is overlain by flood plain mud (24.9-22.4 m) of which 24.9 to 23 m is grey colored and contains two 1cm band of calcrete. It is in turn capped by 60 cm yellow colored sediment, bottom of which is sandy silt and contains two thin layer of frerrugenous concretions/pebbles. The silty sand unit may be crevase splay which had remained exposed for long and undergone pedogenesis.

Unit III: The unit III ranges from 22.4- 18.7 m. This zone dominantly consists of silt (38 to 88%), whereas sand shows wide range varying from 8 to 58% and clay ranges between 1 to 14%. The bottom part upto 20.7 m is grey in color with mottling and consist dominantly sand followed by silt and clay. This is overlain by grey mud with dispersed ferruginous nodule/concretions and is laminated near bottom showing dark grey to black colour thin layers. The mud is mottled at places and contains one ferruginous concretion upto 3 cm in diameter.

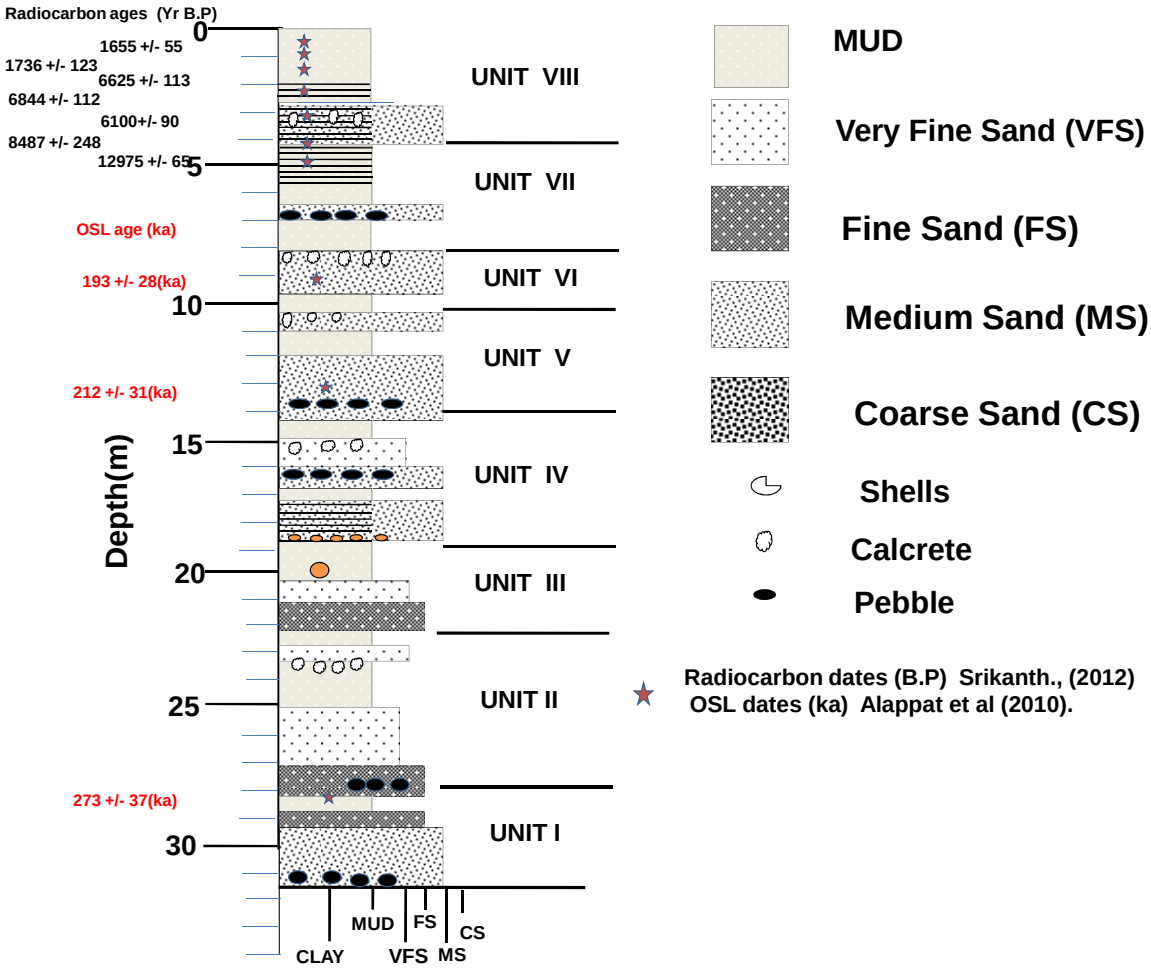

Figure 4.1 Bore hole lithology and stratigraphic position of radiocarbon dated levels for Uttrangudi (UG) core from distal part of Cauvery delta.

Unit IV: ranges from 18.7- 14.3 m. This unit consists of ~3.6 m thick bottom massive sand body which sandwitch a mud layer in between. This sand body show normal fining upward sequence upto sandwitched mud and at bottom is is overlain by lateritic and quartz pebble. Another quartz pebble layer of 26 cm thickness overlying the thin mud is present at ~16.5 m depth and is overlain by normal graded fine to very fine sand. The sand body contains dark band towards bottom and is light brown in lower half and becomes grey towards top. The top mud layer overlying the sand unit is grey in color and contains dispersed calcrete one of which is 3 cm in diameter. A sand lense with rootlets is also present in mud. The presence of calcrete indicates prolonged exposure.

Unit V: The unit V ranges from 14.3 - 10.1 m. This unit also shows a bottom ~2.2 m thick light brown medium grained sand body which contains ripples. It contains pebbly bed at bottom which contains pebbles upto 5 cm in diameter. It is overlain by ~1.5 m thick fine sand that is light brown in color and contains black/red spots. Near top it contains a layer with calcretes up to 2 cm in diameter. The above fine sandy bed probably is part of the levee. The sand is overlain by mud sequence probably marking the flood plain deposit.

Unit VI: The depth of unit VI ranges from 10.1–8.0 m depth. From bottom up to 8.3 m this unit is comprised of fine sand body that contains ripples separated by thin black micaceous layers. Near top it is overlain by brownish mud that containis black spots and small dispersed calcretes.

Unit VII: The unit VII ranges from ~ 8 m to 4.2 m depth. The bottom of this unit up to 6.3 m depth is sandy in nature and contains pebbles. It is grey in colour and contains black organic dispersed material. It is capped by ~ 40 cm layer between 6.3 to 5.9 m depth by reddish grey mud with pebbles that changes to light brown in color near the top and also contains one black concretions measuring upto 2 cm in diameter. From ~5 m to 5.9 m this unit comprise of grey colored well laminated mud with reddish orange layers. ~5 m upward up to 4.2 m depth the sediments constitute alternating layers of sandy and clayey silt which is grey in colour and contains dispersed organic material. The sandy silt layers are of ~1cm thickness and are separated by ~1-2 mm clayey silt layers.

Unit VIII: This unit ranges from ~ 4.2 m depth up to top. The bottom of this unit from 4.2 m to 2.95 m depth has no internal structure preserved in it and is grey in colour. The bottom 50 cm contains dispersed calcretes. This part of Unit VIII represents an overall coarsening upward sequence starting at bottom with mud containing ~ 30% fine to coarse sand. Moving upward the percentage sand show a gradual increase reaching upto 80% at 2.95 m depth. The top 2.95 m to 0 m depth of this unit is made up of fines, predominantly silt (70% - 91%) and sand is almost absent (< 5%). The bottom ~1.5 m of this part is dark brown in color and its lower 50 cm is laminated. The top 1.5 m is massive mud layer without any internal structure and is light yellowish brown in colour. The texture of this part is similar to underlying sediments and it contains visible organic matter with rootlets dispersed within it.

4.2.1.2 Mineralogy:

The dominant minerals that are present in the sediments of Uttrangudi core are quartz and feldspar. The other minerals that have been identified by X-ray diffraction include micas/clay minerals (muscovite-illite) with occasional occurrence of hornblende and pyroxene. The clay minerals present are Smectite, Illite and Kaolinite in varying proportions.

4.2.1.3 Chemistry:

The major and trace element composition is shown in (Table 4.2). The overall range of SiO_2 in core samples range from 52.36% to 89.29 % at an average of 75.33%. The Al_2O_3 ranges from 5.55% to 24.85%, at an average of 13.51% being lowest in the high silica sample and highest in silica deficient samples. The other major oxides like CaO* ranges from 0.03 - 2.93 % at an average of 0.88 %, Feo(T) concentration ranges from 2.10 – 11.7 % at an average of 5.86 %, MgO ranges from 0.26 – 2.74 % at an average of 1.25 %, MnO ranges 0.01 – 0.36 at an average of 0.11. P_2O_5 ranges from 0.01- 0.2 % at an average of 0.05%, TiO_2 ranges from 0.47 – 1.42 %, at an average 0.87 %, K_2O ranges 0.12 – 2.11% at an average of 0.89% and Na_2O ranges from 0.02- 3.36 % at an average of 0.92 %.

Similarly among trace elements Ba shows a large range from 40 – 2394 ppm at an average 601 ppm, Cr ranges from 53 – 783 ppm at an average of 211 ppm, Ni shows range of 28-120 ppm at an average of 93 ppm, Sr concentration ranges from 19 – 449 ppm at an average of 205 ppm, Y ranges from 9 – 48 ppm at an average of 26 ppm and Zr ranges from 43 to 409 ppm at an average of 154 ppm. (Table 4.2).

4.2.1.4 Down core variation of Chemistry in Uttrangudi core:

The vertical down core distribution characteristics of major elements are shown in (Fig 4.2).The chemistry is described from bottom up of the lithology i.e. II to VIII. The SiO_2 shows variable concentration with depth and in general is higher in the lower part of the core in depth range of 28.0 m to 12.3 m (Unit II to bottom half of Unit V) and thereafter show a general decrease upward except in bottom of Unit VIII, where it is highest.

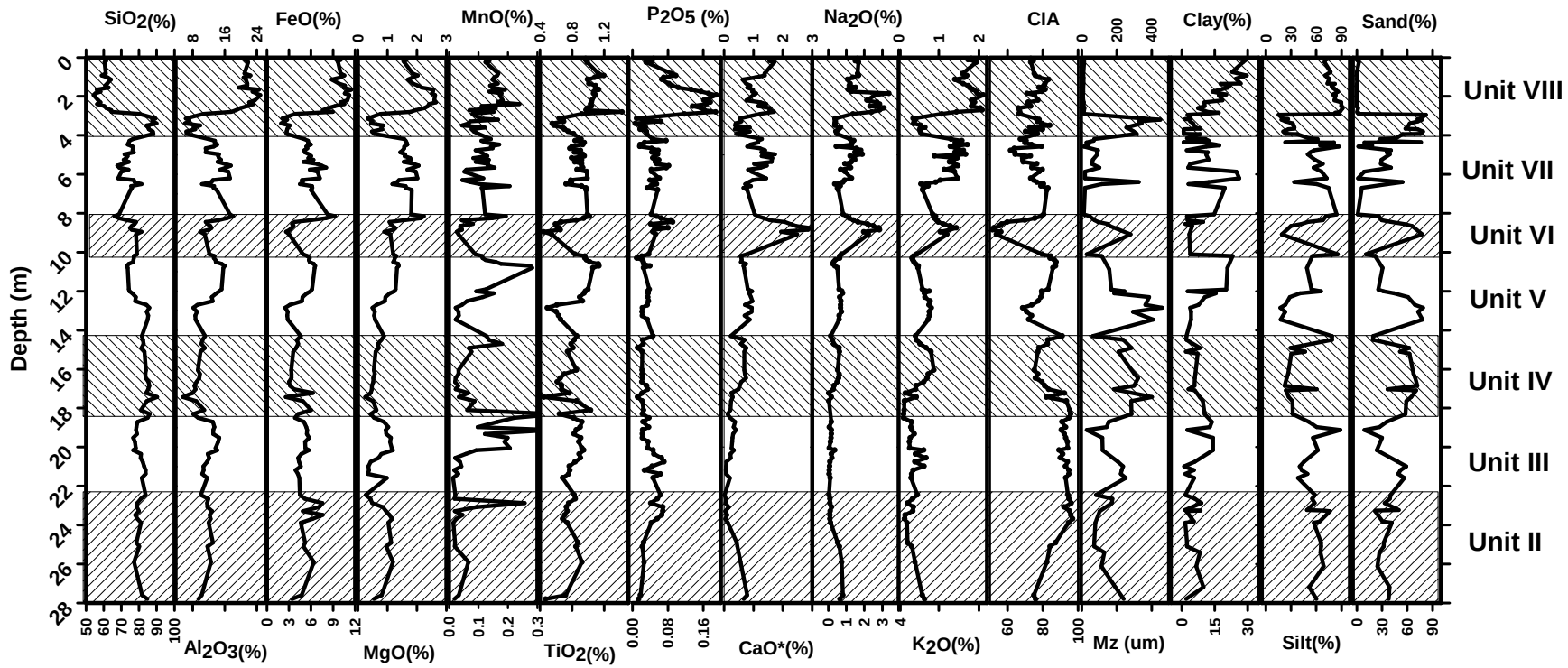

Figure 4.2: Depth wise variation in concentration of Major element oxides (%), Clay (%), Silt (%), Sand (%) and Mean grain size(Mz) (μm) along with values of CIA in core sediments from Uttrangudi borehole.

Table 4.2: Major (%) and trace (ppm) element concentrations of Uttrangudi Borehole sediments from Cauvery delta.

Sample	Depth	SiO_2	Al_2O_3	TiO_2	Fe_2O_3	MgO	MnO	Ca*O	$Na*_2O$	K_2O	P_2O_5	Ba	Cr	Ni	Sr	Y	CIA	LOI
UG 4	**6**	61.79	20.91	0.97	9.46	1.62	0.12	1.65	1.62	1.81	0.06	668	304	214	252	45	73	12
UG 10	**12**	61.25	21.08	0.97	10.01	1.65	0.13	1.55	1.59	1.73	0.04	745	289	198	239	46	74	12
UG 17	**20**	61.20	21.54	0.99	9.60	1.54	0.14	1.54	1.50	1.90	0.05	771	311	214	234	46	75	11
UG 20	**25**	60.45	21.85	0.99	9.66	1.57	0.12	1.71	1.67	1.93	0.04	658	321	214	261	47	73	12
UG 83	**83**	61.01	21.02	1.13	10.10	1.86	0.17	1.39	1.63	1.59	0.09	797	427	194	240	41	75	14
UG 93	**93**	58.84	22.37	1.20	10.55	2.03	0.16	1.39	1.68	1.70	0.10	756	425	180	257	42	76	15
UG 103	**103**	60.93	21.38	1.12	10.32	1.92	0.16	1.09	1.36	1.64	0.07	766	418	172	245	42	78	15
UG 113	**113**	62.01	22.46	1.05	9.32	1.80	0.16	0.67	1.06	1.40	0.07	745	353	156	239	41	83	16
UG 135	**135**	60.80	22.29	1.04	10.10	1.92	0.17	0.78	1.21	1.60	0.09	647	307	206	255	42	81	16
UG 145	**145**	57.29	23.56	1.19	11.60	2.22	0.15	0.98	1.17	1.73	0.10	854	428	188	261	47	81	17
UG 155	**155**	59.89	20.95	1.18	11.23	2.34	0.16	0.85	1.52	1.77	0.11	690	402	220	229	43	78	17
UG 165	**165**	56.04	24.52	1.13	11.49	2.56	0.19	0.98	1.10	1.85	0.13	919	456	212	245	46	81	18
UG 175	**175**	58.16	22.98	1.07	10.79	2.55	0.14	0.96	1.26	1.93	0.16	827	446	190	251	43	80	17
UG 185	**185**	55.26	23.81	1.07	10.58	2.52	0.18	1.09	3.36	1.96	0.17	909	446	178	260	43	71	17
UG 193	**193**	52.36	25.94	1.14	11.70	2.74	0.18	1.04	2.61	2.11	0.20	669	455	184	223	43	75	18
UG 220	**220**	56.89	23.48	1.05	10.92	2.60	0.18	0.76	2.15	1.82	0.16	770	446	178	232	45	77	17
UG 230	**230**	57.51	22.38	1.06	10.16	2.69	0.17	1.26	2.70	1.89	0.18	834	419	159	307	41	72	18
UG 240	**240**	56.29	23.17	1.03	10.55	2.41	0.24	1.44	2.85	1.85	0.17	880	357	172	255	42	71	16
UG 250	**250**	60.18	21.59	1.04	9.27	2.39	0.11	1.17	2.31	1.81	0.14	644	421	152	262	39	73	15
UG 260	**260**	61.54	19.90	1.00	8.28	2.26	0.16	1.58	3.09	2.04	0.16	887	364	125	327	36	66	12
UG 270	**270**	61.90	20.05	1.04	8.11	2.08	0.07	1.64	2.85	2.08	0.17	651	364	125	317	40	67	11
UG 280	**280**	64.36	17.56	1.42	8.98	1.79	0.15	1.70	2.41	1.44	0.19	626	377	139	249	37	67	12
UG 290	**290**	78.24	11.69	1.01	4.21	0.84	0.09	1.35	1.37	1.07	0.13	522	185	53	240	20	67	5
UG 313	**313**	89.31	6.25	0.64	2.10	0.33	0.11	0.53	0.38	0.36	0.01	400	61	28	122	13	76	4
UG 319	**319**	85.72	8.14	0.79	3.19	0.47	0.19	0.65	0.39	0.42	0.04	546	111	44	147	19	78	5
UG 329	**329**	87.70	7.15	0.70	2.45	0.49	0.07	0.59	0.39	0.39	0.06	297	108	30	127	18	77	5
UG 339	**339**	87.63	7.44	0.68	2.39	0.54	0.08	0.49	0.37	0.37	0.01	362	78	31	141	22	80	7
UG 349	**349**	84.22	9.86	0.57	3.14	0.86	0.04	0.38	0.36	0.54	0.02	284	75	43	179	28	84	7
UG 359	**359**	81.80	10.20	0.84	3.56	0.98	0.15	1.09	0.69	0.66	0.04	704	102	47	221	28	73	8
UG 369	**369**	85.48	8.64	0.70	2.79	0.82	0.08	0.36	0.57	0.53	0.02	662	79	35	207	19	80	8
UG 380	**380**	86.10	7.32	0.86	3.09	0.54	0.10	1.00	0.42	0.54	0.04	407	95	36	153	16	70	5
UG 392	**392**	85.73	7.71	0.98	3.23	0.66	0.12	0.49	0.48	0.56	0.04	565	83	39	158	21	77	6

Sample	Depth	SiO_2	Al_2O_3	TiO_2	Fe_2O_3	MgO	MnO	Ca*O	$Na*_2O$	K_2O	P_2O_5	Ba	Cr	Ni	Sr	Y	CIA	LOI
UG 419	**419**	76.57	11.87	0.91	5.08	1.57	0.14	1.29	1.21	1.30	0.05	1096	204	67	282	35	67	11
UG 427	**427**	70.74	15.50	0.96	6.41	1.86	0.13	1.33	1.42	1.57	0.09	968	188	82	310	24	71	12
UG 437	**437**	74.31	13.45	0.95	5.60	1.65	0.12	1.16	1.31	1.41	0.03	953	243	77	280	21	70	10
UG 447	**447**	69.25	16.46	1.09	6.98	1.95	0.20	1.05	1.29	1.71	0.02	1561	260	86	301	21	74	11
UG 457	**457**	74.81	14.17	0.85	5.74	1.67	0.15	0.85	0.45	1.29	0.02	625	167	73	254	23	79	11
UG 467	**467**	76.48	11.25	0.77	5.52	1.58	0.15	1.22	1.56	1.44	0.04	773	181	78	256	21	64	9
UG 477	**477**	74.94	12.02	0.96	5.40	1.62	0.10	1.48	1.81	1.61	0.06	632	253	77	289	22	62	9
UG 487	**487**	77.04	11.22	0.83	5.17	1.44	0.11	1.27	1.48	1.40	0.04	1320	188	71	299	23	64	9
UG 497	**497**	71.71	14.53	0.93	5.76	1.61	0.12	1.73	1.89	1.67	0.06	759	182	74	322	23	64	9
UG 506	**506**	73.52	14.36	0.95	6.03	1.58	0.13	1.28	1.21	0.89	0.05	641	145	107	328	26	73	9
UG 516	**516**	70.46	15.79	0.86	6.12	1.93	0.09	1.78	1.45	1.46	0.05	709	205	94	1335	30	69	12
UG 526	**526**	71.23	15.07	0.92	6.33	1.80	0.14	1.62	1.47	1.36	0.06	593	213	130	319	26	69	10
UG 536	**536**	74.14	14.22	0.83	4.97	1.55	0.09	1.62	1.27	1.26	0.05	746	110	79	331	18	69	12
UG 546	**546**	70.76	16.07	0.92	6.84	1.90	0.13	1.02	0.92	1.40	0.05	555	197	99	269	24	77	12
UG 556	**556**	67.73	17.53	0.92	7.44	2.06	0.13	1.46	1.17	1.47	0.08	527	178	121	303	28	74	12
UG 566	**566**	68.77	16.27	0.93	8.08	1.89	0.16	1.25	1.24	1.33	0.08	552	196	140	301	33	74	12
UG 576	**576**	72.92	15.52	0.90	6.11	1.76	0.06	0.86	0.69	1.14	0.04	448	162	119	246	25	80	14
UG 586	**586**	69.96	16.84	0.98	6.90	1.96	0.05	0.94	0.92	1.39	0.04	509	157	141	261	23	78	13
UG 620	**620**	68.16	17.26	0.99	7.19	2.02	0.12	1.44	1.29	1.47	0.06	675	193	124	381	27	73	12
UG 630	**630**	76.99	13.06	0.78	4.76	1.39	0.05	0.98	0.91	1.04	0.04	457	103	60	248	18	75	10
UG 640	**640**	77.57	12.70	0.79	4.91	1.33	0.07	0.85	0.81	0.92	0.05	476	102	125	237	21	77	10
UG 650	**650**	81.51	10.30	0.72	4.50	1.17	0.11	0.72	0.36	0.55	0.05	535	95	82	195	28	80	10
UG 660	**660**	75.45	13.31	0.92	6.14	1.62	0.21	0.91	0.66	0.74	0.04	783	203	104	261	28	79	11
UG 670	**670**	76.08	13.19	0.97	6.21	1.62	0.11	0.66	0.50	0.61	0.03	658	162	99	230	24	83	12
UG 680	**680**	75.15	13.96	0.97	5.98	1.82	0.11	0.79	0.56	0.60	0.06	952	182	121	263	23	82	12
UG 795	**805**	68.75	17.30	0.99	8.27	1.81	0.12	1.04	0.83	0.85	0.04	919	173	131	314	27	81	14
UG 815	**815**	66.09	18.07	1.01	9.25	2.24	0.19	1.14	1.01	0.92	0.05	803	245	179	300	29	79	14
UG 825	**825**	68.73	16.51	0.94	8.04	2.14	0.15	1.36	1.17	0.90	0.06	1810	188	148	367	33	75	14
UG 835	**835**	73.33	14.32	0.85	5.92	1.56	0.04	1.56	1.39	0.94	0.09	461	156	105	348	26	70	9
UG 845	**845**	78.35	11.26	0.67	3.81	1.07	0.06	2.06	1.65	0.98	0.09	637	80	67	371	19	60	5
UG 855	**855**	77.53	11.65	0.59	3.45	1.11	0.08	2.25	2.18	1.11	0.04	648	109	49	442	18	57	5
UG 865	**865**	75.88	12.39	0.60	3.62	1.17	0.04	2.45	2.50	1.28	0.05	639	95	59	419	18	55	4
UG 875	**875**	74.80	12.64	0.64	3.35	1.27	0.04	2.93	2.81	1.44	0.08	701	125	51	450	16	52	3
UG 885	**885**	75.94	12.01	0.65	3.13	1.21	0.04	2.86	2.84	1.27	0.05	653	102	79	408	17	52	3

Sample	Depth	SiO_2	Al_2O_3	TiO_2	Fe_2O_3	MgO	MnO	Ca*O	$Na*_2O$	K_2O	P_2O_5	Ba	Cr	Ni	Sr	Y	CIA	LOI
UG 895	**895**	80.27	10.43	0.47	2.76	0.95	0.03	2.05	1.96	1.04	0.05	584	53	42	337	15	56	4
UG 908	**908**	78.26	11.04	0.55	3.04	1.10	0.03	2.49	2.23	1.20	0.05	632	81	52	365	19	54	3
UG 1005	**1010**	78.78	12.18	0.83	4.93	1.20	0.09	0.77	0.74	0.45	0.04	368	144	88	191	29	80	10
UG 1020	**1020**	77.09	13.42	0.96	5.54	1.31	0.11	0.56	0.63	0.37	0.02	346	163	151	148	27	85	12
UG 1030	**1030**	77.04	13.23	0.96	5.83	1.25	0.11	0.59	0.64	0.33	0.01	509	162	98	153	29	84	11
UG 1040	**1040**	76.86	13.70	0.98	5.73	1.24	0.13	0.60	0.40	0.35	0.02	336	224	97	157	32	87	10
UG 1050	**1050**	76.73	13.78	1.02	5.82	1.20	0.16	0.57	0.30	0.38	0.02	802	238	92	172	31	88	11
UG1060	**1060**	74.32	15.19	1.13	6.37	1.37	0.18	0.75	0.26	0.42	0.03	1022	263	112	207	46	87	15
UG 1070	**1070**	73.06	16.02	1.13	6.57	1.38	0.28	0.66	0.37	0.49	0.04	1600	218	102	213	48	87	15
UG 1080	**1080**	73.52	15.62	1.06	6.50	1.33	0.28	0.68	0.50	0.48	0.02	2394	248	105	207	36	86	13
UG1190	**1190**	74.24	15.18	1.00	6.14	1.27	0.13	0.81	0.60	0.59	0.04	807	232	91	257	31	83	12
UG1200	**1200**	74.58	14.66	0.97	5.96	1.24	0.09	0.96	0.75	0.76	0.03	832	225	85	281	30	79	10
UG1210	**1210**	76.18	13.90	0.95	5.42	1.08	0.15	0.85	0.80	0.64	0.04	726	209	86	219	27	80	9
UG1230	**1230**	78.21	12.77	0.89	4.84	0.94	0.11	0.92	0.63	0.65	0.03	431	149	76	223	26	79	8
UG1250	**1250**	77.86	12.96	0.93	4.78	0.92	0.06	0.97	0.70	0.78	0.04	439	215	63	234	23	77	8
UG 1270	**1270**	84.28	9.13	0.61	3.12	0.63	0.04	0.71	0.68	0.75	0.03	461	118	42	221	16	74	6
UG1285	**1285**	85.84	8.18	0.49	2.51	0.49	0.02	0.95	0.68	0.81	0.02	459	116	34	215	14	69	5
UG 1305	**1305**	84.38	9.10	0.60	2.86	0.57	0.03	0.94	0.73	0.76	0.02	437	118	37	210	14	71	6
UG1325	**1325**	85.23	8.68	0.63	2.78	0.55	0.03	0.70	0.60	0.76	0.02	405	124	64	199	14	74	7
UG 1345	**1345**	84.92	8.72	0.66	2.85	0.58	0.02	0.88	0.60	0.74	0.03	414	107	35	230	16	72	6
UG 1430	**1430**	81.60	11.09	0.86	4.61	0.88	0.13	0.23	0.13	0.42	0.05	661	171	67	161	25	91	12
UG 1450	**1450**	82.27	10.45	0.83	4.12	0.79	0.14	0.70	0.24	0.44	0.02	596	161	59	151	23	83	10
UG 1470	**1470**	82.50	10.15	0.78	4.27	0.68	0.18	0.58	0.30	0.53	0.02	568	144	59	163	18	83	9
UG1490	**1490**	81.37	11.00	0.81	3.99	0.71	0.07	0.76	0.60	0.69	0.01	387	136	55	193	17	78	9
UG 1510	**1510**	80.72	11.35	0.84	4.07	0.68	0.09	0.79	0.62	0.81	0.02	501	181	57	203	15	77	7
UG1605	**1605**	83.84	9.30	0.85	3.33	0.54	0.03	0.69	0.52	0.88	0.02	400	114	50	179	15	75	8
UG1625	**1625**	81.68	10.97	0.78	3.74	0.64	0.04	0.80	0.60	0.74	0.02	378	164	54	193	15	77	7
UG 1645	**1645**	83.76	9.63	0.65	3.37	0.52	0.02	0.75	0.57	0.71	0.02	366	152	71	191	14	76	8
UG1665	**1665**	82.40	10.77	0.74	3.60	0.63	0.03	0.70	0.49	0.63	0.03	541	196	49	187	14	80	8
UG1685	**1685**	85.85	8.47	0.67	3.18	0.48	0.03	0.54	0.31	0.43	0.03	271	141	50	137	14	81	8
UG 1703	**1703**	83.76	9.58	0.74	4.08	0.52	0.02	0.55	0.28	0.42	0.04	266	153	45	140	16	83	7
UG 1723	**1723**	83.99	8.03	0.77	6.26	0.44	0.07	0.25	0.02	0.16	0.02	1289	214	75	87	23	92	9
UG 1743	**1743**	89.07	6.25	0.50	2.90	0.28	0.04	0.34	0.17	0.44	0.01	411	131	37	144	17	82	6
UG 1763	**1763**	84.31	8.90	0.85	4.91	0.51	0.09	0.23	0.03	0.14	0.02	250	181	64	76	21	93	8

Sample	Depth	SiO_2	Al_2O_3	TiO_2	Fe_2O_3	MgO	MnO	Ca*O	$Na*_2O$	K_2O	P_2O_5	Ba	Cr	Ni	Sr	Y	CIA	LOI
UG 1810	**1810**	81.06	10.84	1.03	6.02	0.63	0.06	0.22	b.d	0.14	0.02	187	244	70	70	30	95	10
UG1830	**1830**	85.99	8.17	0.64	4.21	0.44	0.36	0.13	b.d	0.12	0.02	852	165	61	64	39	96	9
UG 1850	**1850**	84.87	9.40	0.81	3.83	0.55	0.22	0.21	b.d	0.12	0.04	948	158	60	81	29	95	10
UG1870	**1870**	79.06	13.04	0.92	5.04	0.89	0.17	0.38	0.16	0.32	0.02	614	226	82	126	30	91	12
UG 1897	**1897**	78.53	13.36	0.90	5.36	1.03	0.10	0.33	0.06	0.30	0.04	332	264	75	110	21	93	13
UG1912	**1912**	78.30	13.15	0.85	5.47	0.94	0.35	0.41	0.16	0.33	0.02	917	235	84	136	25	91	12
UG 1932	**1932**	72.63	16.93	1.06	7.00	1.24	0.16	0.40	0.16	0.39	0.03	420	254	93	131	25	92	12
UG 1952	**1952**	76.63	14.63	0.91	5.76	1.12	0.20	0.29	0.15	0.29	0.02	549	286	87	108	23	93	12
UG1972	**1972**	74.67	16.26	1.00	5.88	1.24	0.21	0.31	0.12	0.27	0.04	526	272	97	121	28	94	14
UG2005	**2005**	78.12	13.72	0.92	5.24	1.15	0.21	0.26	0.06	0.28	0.03	238	190	107	134	41	94	13
UG 2015	**2015**	73.10	16.30	1.09	6.60	1.37	0.11	0.39	0.36	0.62	0.05	4752	241	89	176	32	89	14
UG 2035	**2035**	81.02	11.71	0.89	4.68	0.80	0.06	0.22	0.17	0.41	0.05	146	163	60	68	25	91	10
UG 2055	**2055**	78.00	13.98	1.05	4.91	0.81	0.02	0.27	0.20	0.68	0.08	564	196	67	79	24	90	10
UG 2075	**2075**	82.05	11.63	0.84	4.36	0.44	0.04	0.09	0.09	0.40	0.07	121	190	76	46	30	94	8
UG 2098	**2098**	79.85	12.53	0.90	5.42	0.42	0.05	0.09	0.07	0.63	0.05	96	112	78	46	33	93	8
UG 2118	**2118**	83.69	10.74	0.77	3.91	0.37	0.02	0.06	0.06	0.36	0.03	638	192	68	47	26	95	9
UG 2138	**2138**	83.80	10.35	0.76	4.22	0.34	0.03	0.07	0.05	0.32	0.06	101	171	65	45	28	95	8
UG 2158	**2158**	81.64	11.60	0.68	4.42	0.98	0.01	0.20	0.10	0.31	0.05	40	146	45	20	13	93	7
UG 2245	**2245**	83.76	10.05	0.83	4.48	0.26	0.02	0.03	0.04	0.47	0.06	54	783	106	100	21	94	8
UG 2265	**2265**	81.10	11.90	0.84	5.16	0.43	0.02	0.06	0.10	0.35	0.06	53	174	57	32	16	95	9
UG 2287	**2287**	78.92	11.63	0.76	7.55	0.49	0.26	0.05	0.08	0.22	0.04	714	247	78	46	26	96	10
UG 2307	**2307**	78.76	11.68	0.73	7.11	0.84	0.09	0.16	0.19	0.37	0.07	249	272	60	62	16	92	11
UG 2328	**2328**	80.02	12.81	0.74	4.90	0.95	0.02	0.04	0.11	0.35	0.07	59	150	53	38	9	95	12
UG 2348	**2348**	77.90	12.25	0.71	7.61	1.07	0.05	0.11	0.09	0.16	0.07	421	179	65	49	14	96	13
UG 2368	**2368**	79.11	12.48	0.68	6.20	1.16	0.02	0.04	0.10	0.15	0.06	60	125	58	44	9	97	13
UG 2388	**2388**	81.11	11.99	0.74	4.61	1.03	0.01	0.13	0.13	0.21	0.04	100	215	80	67	13	95	12
UG 2490	**2490**	78.48	13.06	0.87	5.22	1.13	0.02	0.44	0.53	0.22	0.02	108	237	83	54	13	87	ND
UG 2510	**2510**	80.12	11.67	0.85	4.95	0.96	0.02	0.46	0.62	0.33	0.02	100	212	68	67	16	84	ND
UG 2590	**2590**	77.15	12.56	0.92	6.37	1.19	0.07	0.56	0.74	0.41	0.03	226	212	94	85	23	82	ND
UG 2760	**2760**	81.77	10.25	0.72	4.74	0.81	0.03	0.80	0.80	0.59	0.02	313	149	49	155	29	75	ND
UG 2780	**2780**	84.68	9.45	0.47	3.43	0.55	0.02	0.67	0.65	0.65	0.01	329	138	43	138	15	76	ND

In Unit II to III it varies within a narrow range of 77 and 85 %. In Unit IV and bottom half of Unit V it shows an increase in maximum value with ranges from 81 to 89% and 78% to 86%respectively. Above this in top half of Unit VI and in Unit VII it shows a decrease with range from 66% to 73% and 68% to 81% respectively. In bottom half of zone VIII it shows a sudden increase with values reaching as high as 89% .and ranging between 82% and 88%. On closer examination it is observed that Si variation show a cyclic nature with higher values near the lower part of each Unit that shows a decrease upward on moving towards the top of the individual Units corresponding to the facies change from channel to floodplain. On comparison with the texture it is observed that the silica variation positively correlates with the variation pattern of the sand fraction and is negatively correlated with silt and clay percentage (Fig 4.2). This would imply that the coarser fraction is enriched in quartz. As expected the downcore Al_2O_3 content exhibits antipathetic patterns with that of SiO_2 content and in top 2.7 m, i.e. in zone VIII reaches value as high as 25%. Al_2O_3 closely follows the depth wise variation trend of silt and clay. FeO, MgO, MnO_2, P_2O_5 and TiO_2 show positive correlation with Al_2O_3, silt and clay content and a negative correlation with SiO_2. Within this general trend MnO_2 exhibits exceptionally high concentration at various depths, 22.8 m in Unit II, 19.1m and 18.2 m in Unit III, 14.8 m in Unit IV , 10.7 m in Unit V, 6.6 m in Unit VII and 2.4 m in Unit VIII. The depth range where Mn show abnormal high concentration is observed to correspond with the top horizon of each facies assemblage cycle that has undergone variable degree of Pedogenessis and contain Fe and Mn concretionary nodules or the horizons having lateritic pebble. Most of these horizons are finely laminated and represent flood plain deposit or deposition under water in flood plain swamps or lakes under low energy which got later exposed and underwent different degree of pedogenesis. The pedogenic layers indicate period of non-deposition, whereas the presences of lateritic pebbles indicate increase input probably from the local sources that is the laterite capped Mio-Pliocene sandstone and mud stone exposed to the immediate west of the core location in the southern part of the delta. The Fe and Mn nodules are formed due to the precipitation from the solution.

Na_2O, K_2O and CaO show a weak but positive correlation with SiO_2 and sand %, and negative correlation with Al_2O_3 and silt % in lower part i.e. Unit I to VI, which corresponds to the Pleistocene deposits, whereas in upper part i.e. Unit VII and VIII they exhibit negative correlation with SiO_2 and sand and positive correlation with Al_2O_3 and silt (Fig 4.2). This may imply that in zone I to VI, i.e. 28 m to ~8 m depth, feldspar is dominantly held in sand fraction, whereas in zone VII and VIII it is predominantly in silt fraction or K and Na are held in clays in addition to feldspar.

The vertical down core distribution characteristics of trace elements are shown in (Fig 4.3) Ni, Cr and to some extent Y show depth wise trend parallel to the Al and opposite to Si. This indicates that these elements are held in the finer size fraction. Variation of Sr is seen to follow the trend of Ca, Na and K signifying feldspar to be the phase holding it. Ba shows some resemblance in depth wise variation with Al but with significant enrichment along some bands. It is worth noting here that the Ba enriched band coincides or preceeds bands exhibiting Mn enrichment.

Enrichment of Mn indicates deposition from solution. A sharp and sudden change in solubility of Mn takes place along the oxic-anoxic interface. Dissolved Mn^{2+} in favored in solution at low Eh values of anoxic waters (Force and Cannon, 1988). If anoxic water front happens to encounter and mix with the oxic water, dissolved Mn^{2+} precipitates immediately as MnOx. Hydrogenetic and diagenetic processes are known to result in Mn mobilization, precipitation and enrichment. The Organic matter buried with sediments is known to create the anoxic oxic boundary resulting in mobilization of Mn^{2+} in part it is decaying anaerobically. The mobilized Mn^{2+} whenon moving upward in pore water crosses the organic zone it meets the oxic water resulting in its precipitation. Thus often we see relation between the position of organic matter layer and the Mn concentration (Roy et al., 2010, Drittrich et al., 2009). When organic matter decays from top to bottom, the Mn precipitation zones also moves with it and thus the Mn enrichment zone associated with the last phase of organic matter decay is located at the bottom of organic zone. Ba gets enriched in organic matter and thus it acts as a proxy for organic matter after its decay. Its enrichment in any zone may thus indicate earlier presence of organic material. Thus the associated enrichment of Mn and Ba indicates formation by

above process. Thus in the present study also we can use bands with Mn and Ba enrichment showing above relation as proxy for paleosol development.

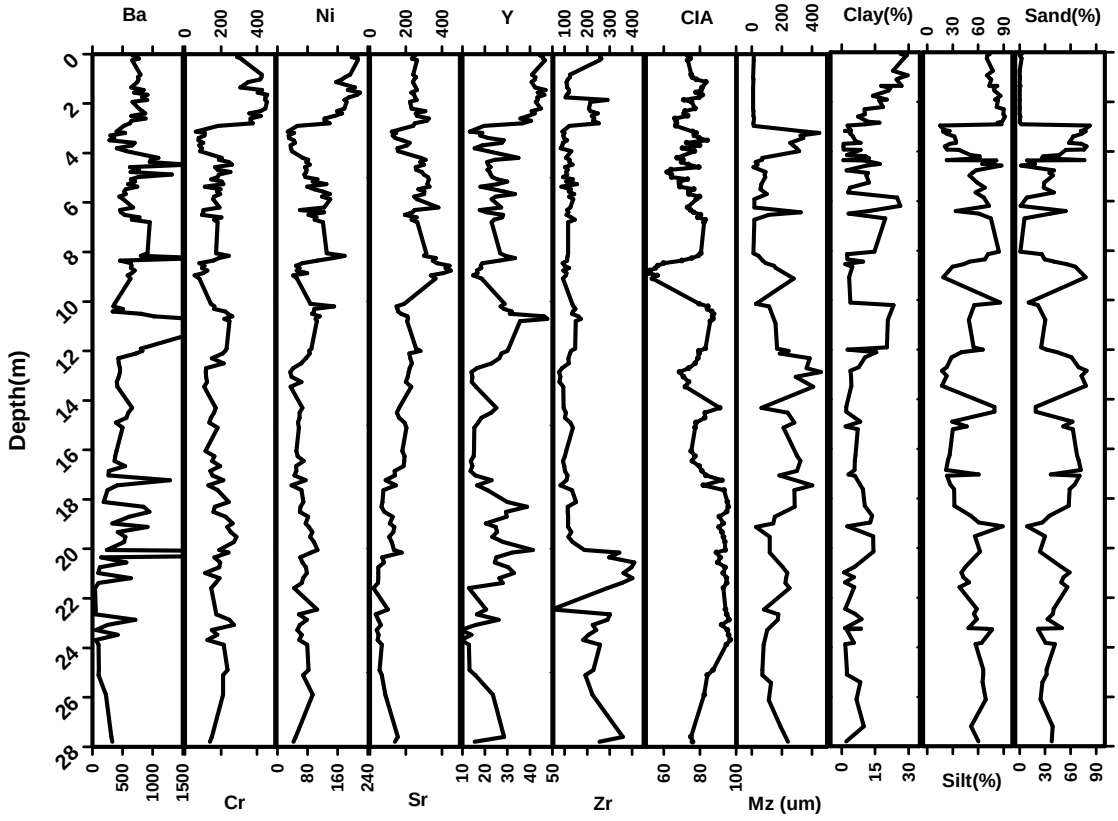

Figure 4.3: Depth wise variation in concentration of Trace elements (ppm) For comparison are plotted the Mean grain size (Mz) (μm), (%), Clay (%), Silt (%), Sand (%) along with value of CIA in core sediments from Uttrangudi borehole.

Another method by which Mn may get enriched is diagenetic, i.e. formed within the sediments by early diagenesis. In such case the bottom water and pore water in top thin layer of surface sediments remain oxic, whereas anoxic conditions prevail in the subsurface sediments. The anoxic pore water conditions in the subsurface sediments results in dissolution and mobilization of Mn which on moving upward encounters the oxic porewater near the surface sediments where Mn gets continuously precipitated and enriched. The second scenario fits better in case where Mn enrichment is not associated with Ba enrichment.

4.2.1.5 Interelemental relationship:

As expected SiO_2 in Uttrangudi core sediments exhibit strong negative correlation with almost all the major and trace elements (Ti, Fe, Mg, K, Na, P, Ni, Cr and Y) except Ca, Mn, Ba and Sr with which it exhibits lower degree of negative correlation (Table 4.3).The elements that have strong negative correlation with SiO_2 on the other hand exhibit strong positive correlation with Al_2O_3. The elements such as Ca, Mn, Ba and Sr which are having lower negative correlation with SiO_2 exhibit lower positive correlation with Al_2O_3. Thus SiO_2 and Al_2O_3 are found to control the first order variation in majority of elements. The lesser control of above on Mn and Ba is primarily because of the addition of these elements by secondary sources as discussed above. Good positive correlation among Ca, Na, K and Sr indicate their control by feldspar. Poor negative and positive correlation of Ca and Sr with SiO_2 and Al_2O_3 respectively may be due to weathering variability. The differential breakdown of calcic feldspar may lead to its presence both in coarser and finer fraction and also variable losses of Ca and Sr at different times. Good positive correlation of Al_2O_3 with K_2O and moderate correlation with Na_2O indicates that feldspar (sodic and pottasic) and muscovite are reduced in size and are dominantly fine grained. The strong correlation among Fe, Mg, Ti, Ni and Cr suggest that these elements are held in mafic minerals. Further their good correlation with Al_2O_3 and mud percentage indicates that they are held in finer fraction. Similarly good correlation of P_2O_5 and Y with Al_2O_3 and mud suggest their enrichment in finer fraction. SiO_2 exhibit positive correlation with sand and negative correlation with mud suggesting that the quartz is dominantly held in coarse fraction. Thus we observe that the mafic minerals and even feldspar are fine grained and the overall variation in chemistry is influenced by process of fluvial sorting except for elements such as Mn, Ba, Ca and Sr. The latter group of elements are influenced by secondary modifications.

Table 4.3. Correlation matrix for major and trace element concentration and CIA of sediments from Uttrangudi borehole.

	SiO_2	$Al2O_3$	TiO_2	Fe_2O_3	MgO	MnO	Ca*O	$Na*_2O$	K_2O	P_2O_5	CIA	Ba	Cr	Ni	Sr	Y	Clay(%)	Silt(%)	Sand(%)	Mud	Mean
SiO_2	1.00																				
$Al2O_3$	-0.98	1.00																			
TiO_2	-0.73	0.75	1.00																		
Fe_2O_3	-0.94	0.94	0.77	1.00																	
MgO	-0.92	0.88	0.66	0.83	1.00																
MnO	-0.43	0.43	0.52	0.48	0.41	1.00															
Ca*O	-0.44	0.32	0.05	0.16	0.47	0.00	1.00														
$Na*_2O$	-0.68	0.58	0.25	0.45	0.66	0.07	0.81	1.00													
K_2O	-0.81	0.73	0.43	0.63	0.80	0.24	0.72	0.83	1.00												
P_2O_5	-0.73	0.69	0.49	0.66	0.67	0.19	0.33	0.71	0.63	1.00											
CIA	0.25	-0.12	0.11	0.03	-0.34	0.12	-0.92	-0.77	-0.68	-0.27	1.00										
Ba	-0.26	0.25	0.32	0.23	0.28	0.36	0.14	0.14	0.18	0.09	-0.08	1.00									
Cr	-0.71	0.73	0.66	0.77	0.55	0.36	0.00	0.35	0.44	0.61	0.12	0.14	1.00								
Ni	-0.91	0.91	0.71	0.92	0.79	0.44	0.26	0.46	0.65	0.57	-0.06	0.19	0.72	1.00							
Sr	-0.37	0.29	0.10	0.17	0.48	0.07	0.72	0.55	0.59	0.22	-0.66	0.19	0.03	0.22	1.00						
Y	-0.77	0.78	0.72	0.79	0.63	0.61	0.15	0.36	0.50	0.51	0.03	0.30	0.64	0.81	0.17	1.00					
Clay(%)	-0.57	0.59	0.52	0.57	0.51	0.33	0.15	0.18	0.46	0.19	-0.02	0.24	0.35	0.63	0.20	0.51	1.00				
Silt(%)	-0.61	0.60	0.54	0.62	0.61	0.28	0.09	0.31	0.44	0.48	0.01	0.14	0.52	0.57	0.14	0.41	0.43	1.00			
Sand(%)	0.68	-0.68	-0.60	-0.69	-0.66	-0.33	-0.12	-0.31	-0.50	-0.46	0.00	-0.19	-0.54	-0.66	-0.17	-0.49	-0.65	-0.97	1.00		
Mud	-0.68	0.68	0.60	0.69	0.66	0.33	0.12	0.31	0.50	0.46	0.00	0.19	0.54	0.66	0.17	0.49	0.65	0.97	-1.00	1.00	
Mean	0.52	-0.49	-0.35	-0.47	-0.53	-0.18	-0.25	-0.41	-0.48	-0.40	0.16	-0.09	-0.35	-0.47	-0.23	-0.24	-0.42	-0.79	0.79	-0.79	1.00

4.2.2 Porayar Borehole:

Another core discussed in the present study has been taken from Porayar, located north of the axial part of the delta. The coring site is only 2 km inland from the present coastline along the Bay of Bengal. A 26.5 m deep core was recovered from the above location. The bottom ~7 m of the core is believed to be of Mio-Pliocene age over which the unconformably lie the 20 m section of sediments deposited mainly during the Holocene period (Fig 4.4 & Table 4.4). The unconformity suggests erosion of coastal part in this region up to ~20 m depth during the period of lower sea level. The bottom ~7 m is consolidated to semi consolidated sediments. The Holocene part of the section shows both marine and fluvial signature. For most of the part the Holocene section is characterized mainly by dark grey to black colored organic rich mud to fine sand sediments that contains microfossils, mainly foraminifera, along with some marine mega fossil shells except near the top where fossils are absent. The sand fraction contains grains mostly of size up to fine sand. The sand ranges between 0 and 80%, whereas silt ranges between 18% and 98 %. Clay in the overall section is less than 16%. The Holocene section of the sediments from this core is inferred to have been deposited in an estuarine/bay setting during the period of sea level rise after the last glacial maxima (LGM) (Singh et al., 2013).On the basis of texture and color the Porayar core has been divided into 6 units.

Unit I: The bottom ~7m (26.5 m to ~20 m) of the core identified as older sequence (Mio/Pliocene or Creataceous) is made up of compacted sand stone with fossil impression and pebble beds and is overlain by compacted clays. The bottom 26.5 m to 22.6 m of this unit constitutes reddish sandstone. The overlying mud stone is yellowish in color and highly compacted. The top of this marks an unconformity over which later deposition resumed only during the end of Pleistocene and continued through the Holocene.

Unit II: The bottom of this unit contains thin band of sand that rests unconformably over Mio/Pliocene or Creataceous sedimentary rocks. This is followed by 1.4 m (18.25 m to 19.65 m) thick well laminated brown to grey mud that contains predominantly silt and minor amount of clay and sand.

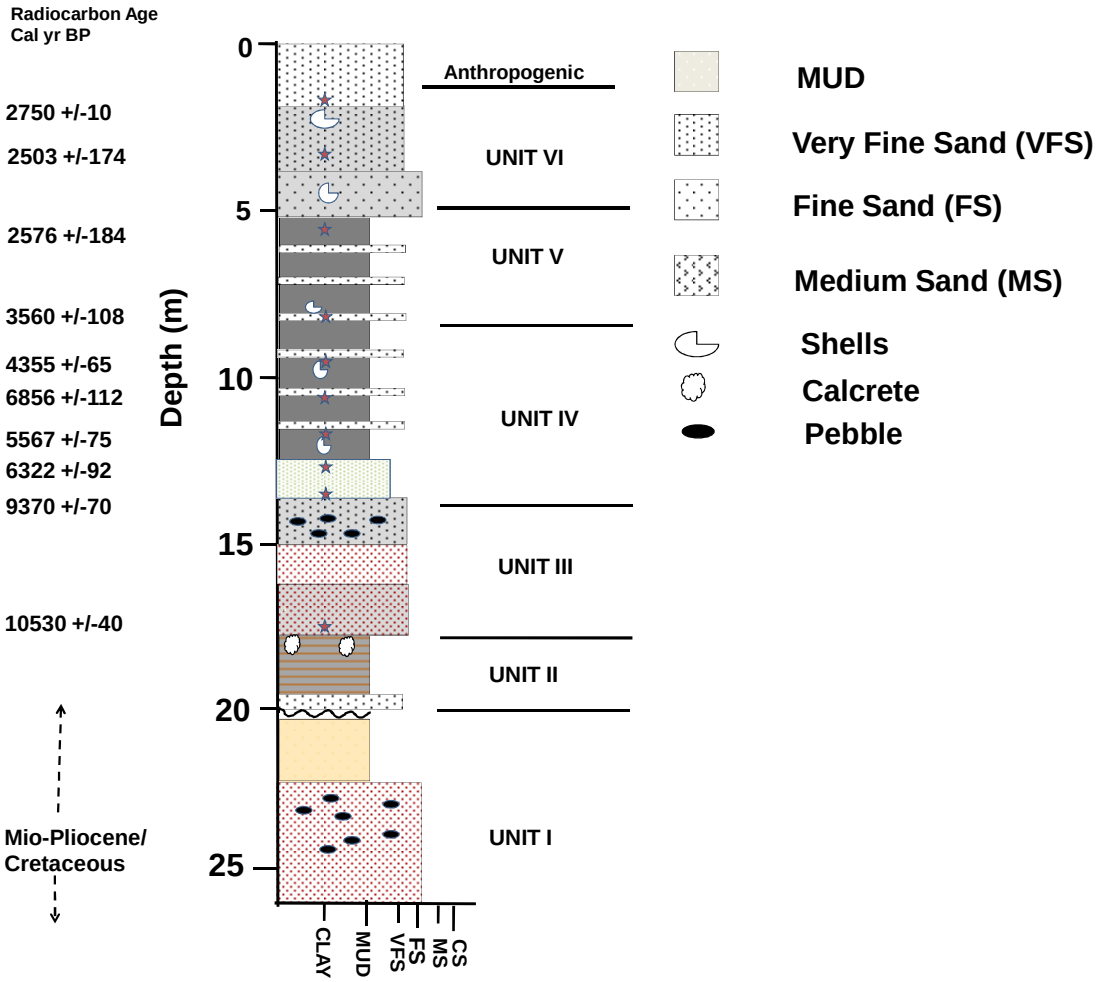

Figure 4.4 Bore hole lithology and stratigraphic position of radiocarbon dated level for Porayar (PR) core from central marginal part of delta plain

* Radicarbon dates after Srikanth (2012)

Unit III: The bottom 1.3m (16.95-18.25 m) of this unit is made up of grey to brownish colour mud to silty sand unit that contains dispersed calcrete nodules. The AMS radiocarbon date obtained at 17.6 m is 10, 530 yrs B.P. This is overlain by ~2 m thick band (16.95-15.0 m) of brown to dark grey silty sand unit. This unit is overlain by 1m thick unit (~15 m – 14 m) of greyish black pebbly and silty sandstone. The environment appears to be lagoonal or intertidal at the beginning of this unit that probably gradually got submerged and transformed towards estuarine.

Unit IV: Above the above unit i.e. from 14 m (~6000 calyr B.P.) up to ~8.0 m (3820 calyr B.P.) depth, the sediment show gradual increase of silt and clay percentage with corresponding decrease of sand percentage. This horizon contains intermittent thin layers of silty sand unit of 3 to 4 cm thickness. This Unit is dark greyish black in colour, rich in organics and exhibit presence of benthic microfossils of estuarine affinity. It indicates increase in water depth of the depositional environment probably because of sea level rise during this time Banerjee P.K., (2000). This may have led to better preservation of organics in bottom sediment due to anoxic conditions in deeper water.

Unit V: From 8m upward (from 3820 yr B.P.) upto ~ 5 m depth, the sediment starts showing coarsening upward sequence that may be as a result of shallowing of estuary due to gradual aggradation and progradation resulting into facies change. The sediments in this unit also are rich in organic material imparting it black/greyish black colour and also contains microfossils including benthic foraminifera.

Unit VI: This unit (5 m to 1.5 m) probably marks the last stages of estuary filling as indicated by sandy nature of the sediments that suggests increase in energy condition. The horizon above this is identified as dumped material and is not considered.

4.2.2.1 Porayar Major and Trace elements:

The Porayar core has been analyzed for chemical composition up to 24 m depth and the results for the major and trace elements are presented in (Table 4.5). SiO_2 concentration in Porayar sediments ranges from 56.2% to 80.31% with an average of 69.6%, except the top most sample which shows 90.13 %.

Table 4.5: Major (%) and trace (ppm) element concentrations along with CIA of Porayar borehole sediments from Cauvery delta.

Sample	Depth(cm)	SiO_2	Al_2O_3	TiO_2	Fe_2O_3	MgO	MnO	Ca*O	$Na*_2O$	K_2O	P_2O_5	Ba	Cr	Ni	Sr	Y	CIA
PR 153	153	90	6	0.2	1.1	0.5	0.01	1.0	0.8	0.7	0.08	217	34	26	128	4	59
PR 176	176	74	14	0.4	3.4	1.3	0.03	2.4	2.4	2.2	0.41	638	117	75	339	14	57
PR 199	199	73	14	0.5	3.9	1.4	0.03	2.3	2.4	2.3	0.32	614	131	77	329	14	57
PR 283	283	75	13	0.4	2.7	1.3	0.03	2.6	2.7	2.2	0.25	684	105	84	384	12	53
PR 306	306	72	14	0.5	3.5	1.6	0.03	2.7	2.8	2.2	0.35	648	119	80	376	14	54
PR 329	329	74	14	0.5	3.4	1.3	0.04	2.6	2.3	1.9	0.07	595	80	31	343	12	57
PR 403	403	74	15	0.2	1.8	0.9	0.03	3.0	2.9	2.1	0.33	702	56	20	405	7	54
PR 426	426	75	14	0.2	1.5	0.8	0.03	2.6	2.8	2.0	0.28	779	52	68	466	6	55
PR 449	449	73	14	0.5	2.7	1.4	0.05	3.3	2.8	1.9	0.19	737	112	72	465	13	52
PR 525	525	66	17	0.6	5.7	2.3	0.08	3.0	2.5	2.0	0.42	647	180	99	406	23	60
PR 548	548	61	20	0.8	7.4	2.9	0.09	2.8	2.4	2.3	0.33	566	231	120	351	25	63
PR 571	571	69	16	0.5	4.4	2.0	0.06	3.1	2.6	2.1	0.37	701	145	97	444	18	57
PR 645	645	67	17	0.6	5.4	2.3	0.08	3.0	2.4	2.1	0.55	648	174	98	412	20	60
PR 668	668	62	20	0.8	8.0	2.9	0.10	2.2	1.6	2.1	0.48	516	240	121	309	28	69
PR 691	691	65	19	0.6	5.9	2.3	0.08	2.6	2.2	2.1	0.43	592	203	118	375	22	64
PR 775	775	63	19	0.8	7.0	2.5	0.10	2.6	2.0	2.2	0.17	538	199	107	332	23	65
PR 803	803	56	23	1.0	11.1	3.4	0.15	1.3	1.1	2.5	0.17	350	301	140	197	36	77
PR 831	831	56	23	1.0	11.3	3.5	0.15	1.3	1.1	2.5	0.18	368	297	141	207	37	77
PR 842	842	65	19	0.8	8.8	2.7	0.12	1.1	1.0	1.9	0.10	340	327	123	196	31	76
PR 865	865	58	21	1.1	11.2	3.9	0.17	0.8	0.6	2.5	0.19	286	300	127	171	36	80
PR 898	898	62	19	0.9	7.3	2.8	0.10	2.6	2.0	2.6	0.13	520	206	111	351	26	64
PR 945	945	62	20	0.9	8.7	3.1	0.10	1.9	1.4	2.4	0.14	431	219	121	289	24	70
PR 973	973	67	17	0.9	6.6	2.4	0.07	2.0	1.8	2.3	0.09	516	204	104	328	23	66
PR 1001	1001	70	16	0.7	5.3	1.8	0.06	2.6	2.0	1.9	0.09	510	128	49	327	16	61
PR 1029	1029	80	11	0.5	2.9	1.3	0.06	1.8	1.3	1.0	0.13	562	98	67	329	12	63
PR 1057	1057	63	20	0.8	8.6	3.3	0.12	1.7	1.1	2.0	0.05	329	193	81	230	20	73
PR 1170	1170	72	15	0.6	5.2	1.9	0.05	1.7	1.3	2.0	0.09	492	147	82	297	15	66
PR 1198	1198	63	20	0.8	8.4	3.1	0.06	1.7	1.1	1.9	0.05	340	180	73	249	20	74
PR 1226	1226	76	14	0.6	4.3	1.7	0.04	1.7	1.2	1.0	0.10	504	138	81	306	14	69

Sample	Depth(cm)	SiO_2	Al_2O_3	TiO_2	Fe_2O_3	MgO	MnO	Ca*O	$Na*_2O$	K_2O	P_2O_5	Ba	Cr	Ni	Sr	Y	CIA
PR 1249	1249	66	18	0.8	7.4	2.8	0.07	1.9	1.1	1.8	0.05	374	158	60	276	17	71
PR 1279	1279	77	13	0.5	3.1	1.2	0.05	2.1	1.7	1.9	0.04	565	90	65	354	13	59
PR 1328	1328	74	15	0.6	3.7	0.9	0.03	2.5	2.4	1.6	0.04	591	93	28	342	12	59
PR 1351	1351	78	13	0.5	2.8	1.0	0.04	2.2	1.7	1.0	0.10	631	98	76	355	13	62
PR 1423	1423	72	15	0.7	3.9	1.3	0.04	3.1	2.3	1.6	0.03	658	144	52	426	19	57
PR 1453	1453	72	15	0.7	3.3	1.3	0.04	2.8	2.2	2.2	0.03	645	132	45	442	23	58
PR 1483	1483	73	14	0.6	3.8	1.3	0.04	3.1	2.4	1.6	0.04	693	135	56	479	23	56
PR 1573	1573	72	15	0.7	4.0	1.5	0.05	3.3	2.5	1.7	0.05	709	138	58	451	20	55
PR 1603	1603	71	16	0.7	4.2	1.5	0.05	3.3	2.5	1.7	0.07	631	121	114	412	24	57
PR 1643	1643	74	13	0.7	3.9	1.4	0.05	3.1	2.2	1.5	0.07	679	153	109	443	23	55
PR 1683	1683	74	13	0.7	3.7	1.4	0.05	3.3	2.4	1.6	0.04	653	129	45	415	19	53
PR 1718	1718	80	9	0.5	2.6	1.0	0.06	1.8	2.6	1.7	0.06	580	90	27	285	14	50
PR 1753	1753	72	11	0.5	3.8	1.6	0.07	8.6	1.2	1.4	0.06	462	101	48	291	16	67
PR 1785	1785	74	13	0.6	4.7	1.7	0.14	2.0	1.5	2.2	0.04	646	146	57	307	22	61
PR 1833	1833	62	20	0.9	8.8	3.0	0.06	1.0	1.0	2.3	0.14	408	279	108	211	26	77
PR 1863	1863	63	20	0.9	9.2	2.7	0.07	1.1	1.2	2.3	0.05	548	271	103	256	35	76
PR 1893	1893	64	20	0.8	8.0	2.5	0.10	1.0	1.4	2.3	0.09	393	230	92	239	25	75
PR 1923	1923	65	19	0.8	6.7	2.1	0.07	1.8	1.9	2.4	0.06	462	200	77	290	23	68
PR 1953	1953	69	17	0.7	4.5	1.5	0.06	2.2	2.4	2.4	0.05	549	208	54	354	16	62
PR 2170	2170	79	12	0.5	3.9	1.2	0.02	1.5	1.4	1.2	0.02	307	120	38	240	12	65
PR 2348	2348	70	14	0.7	5.1	1.7	0.04	3.8	2.5	1.7	0.04	473	191	70	329	21	58

The top ~ 4.5 meters show higher concentration of SiO_2 with an average of more than 75%. This is expected as the top portion of the core contains higher percentage of sand. The Al_2O_3 also shows variable range from 5.5% to 22.9 % with an average of 16.0 % in the sediments. The other major oxides like CaO* (CaO in silicate) ranges from 0.8% to 3.77% at an average of 2.26%; $FeO(_T)$ concentration ranges from 1.07% – 11.26 % at an average of 5.37 %; MgO ranges from 0.52% to 3.9 % at an average of 1.94 %; MnO ranges from 0.01 to 0.17 % at an average of 0.07%. P_2O_5 ranges from 0.02% to 0.55% with an average of 0.15%; TiO_2 ranges from 0.16% to 1.07% with an average 0.65%; K_2O ranges from 0.71% to 2.56% with an average of 1.94% and Na_2O ranges from 0.63%- 2.94 % with an average of 0.63 %.

Similarly among trace elements Ba ranges from 217 ppm to 779 ppm with an average 540 ppm, Cr ranges from 34 ppm to 327 ppm at an average of 163 ppm, Ni shows range of 20-141 ppm at an average of 79 ppm, Sr concentration ranges from 128 ppm to 479 ppm at an average of 331 ppm, Y ranges from 4 ppm to 37 ppm with an average of 20 ppm (Table 4.5)

4.2.1.2 Down core variation of chemistry in Porayar core:

The depth wise variation in chemistry is presented in (Fig 4.5) and divided into VI Units (I to VI from bottom to top). The depth wise concentration of silca show higher abundance in zones I, III and VI, whereas Al, Fe, Mg, Mn and Ti show lower abundances in these zones, although with variation within it. The opposite trend of these elements with respect to Silica is similar to the relation observed in Uttrangudi borehole sediments. It implies that the variation in their concentration is primarily due to the dilution effect of quartz. Further on comparison with texture, it is also observed to have exerted its control on the chemistry as also observed in sediments from Uttrangudi core. The zone having higher sand percentage and, lower silt and clay, show higher abundance of Si and lower abundance of above elements. On the contrary the zones having higher percentage of silt and clay, and lower sand percentage, show higher concentration of above elements (Al, Fe, Mg, Mn and Ti) except silica. The observed correlation of silica with sand percentage, and of Al, Fe, Mg, Mn and Ti with silt and clay would indicate that the sand

is having higher percentage of quartz, whereas the mafic minerals such as pyroxene and amphibole along with other clay minerals constitutes the finer fractions. Thus to the first approximation the major control over the concentration of Si, Al, Fe, Mg, Mn and Ti is probably due to variation in texture because of selective sorting of mafic minerals and quartz in finer and coarser size fractions respectively. Na_2O, CaO and to a great extent K_2O show behavior similar to SiO_2 suggesting that feldspar in Porayar sediments are also mostly hosted in sand i.e. they constitute the coarser fraction. This is similar to the relation observed in Pleistocene sediments from Uttrangudi core albeit with different concentration, and is unlike the Holocene sediments of Uttrangudi borehole where major feldspar population is observed to reside in fines and exhibit behavior similar to Al_2O_3. The similarity in variation pattern of Fe, Mg and Mn suggest that they are held in similar mafic minerals or different minerals having similar hydrodynamic behavior.

Among the trace elements the variation trend in Ni, Cr and Y correspond to the variation pattern of Al, Fe, Mg, Mn and Ti, indicating that these elements are held in mafic and clay minerals (Fig 4.6). Ba and Sr are observed to exhibit similar variation pattern and their similarity with the variation pattern of Na, Ca and K suggests that these elements are also held in feldspar.

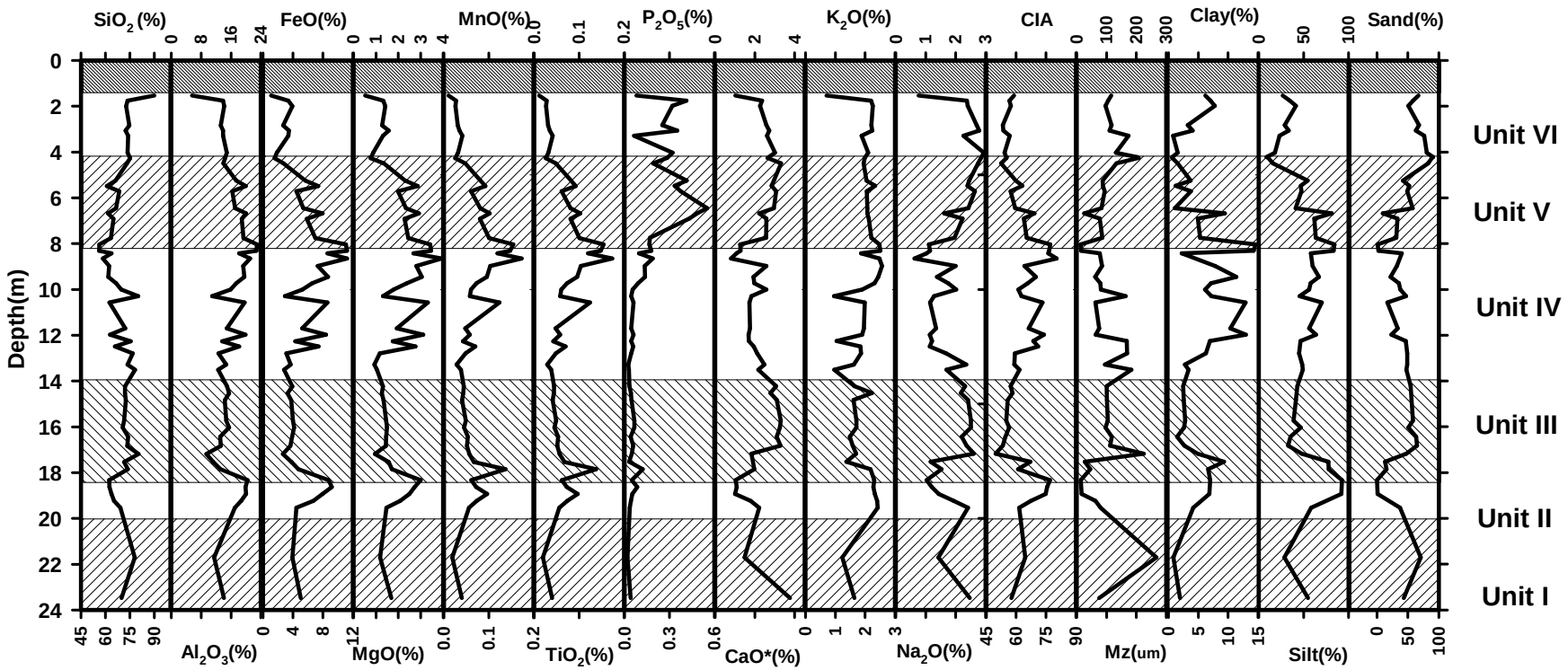

Figure 4.5: Depth wise variation in concentration of Major element oxide (%), Clay (%), Silt (%), Sand (%) and Mean grain size (Mz) in μm along with value of CIA in core sediments from Porayar borehole.

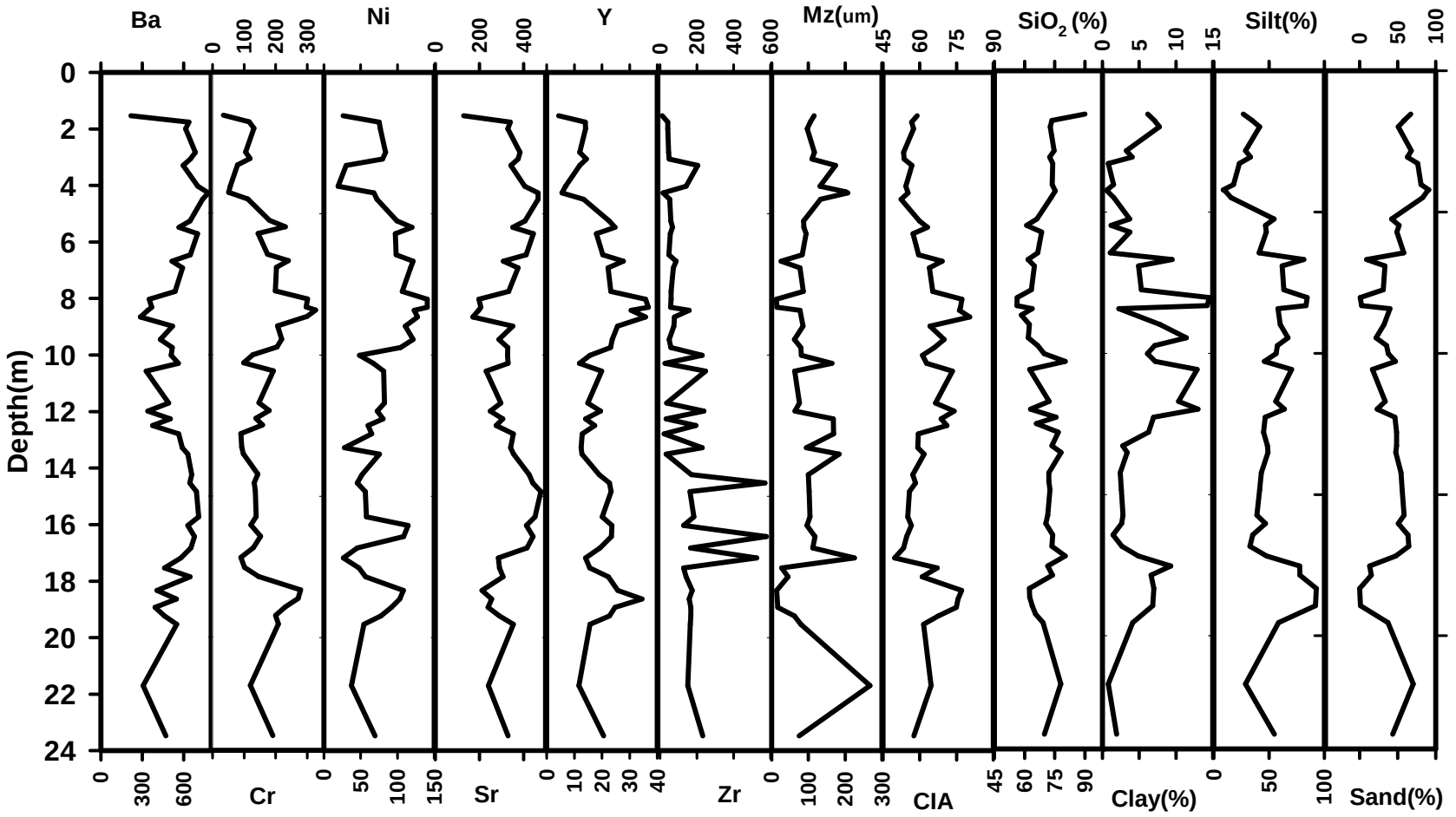

Figure 4.6: Depth wise variation in concentration of Trace element oxides (ppm), Mean grain size (Mz) (μm), CIA, SiO_2 (%), Clay (%), Silt (%) and Sand (%) in core sediments from Porayar location.

4.3 Discussion:

4.3.1 Geochemical Classification:

The chemical composition of sediment depend on the source rock composition, degree to which the clastic material has altered during the processes of weathering, the hydraulic differentiation during transportation and the environment in which it gets deposited (Bhatia, 1983; Taylor and McLennan., 1985; Wronkiewicz and Condie, 1987; Cullers et al., 1988; Nesbitt and Young, 1996; Tripathi and Rajamani, 1999, 2007; Singh and Rajamani, 2001a, b; Singh, 2009). With increase in maturity the sediments tend to increase in quartz at the expense of feldspar, mafic minerals and lithic fragments in the Riverbed sediments and at the same time the suspended load gets enriched in clay and more weatherable minerals, mostly the mafics. The above processes lead to increase of SiO_2 in River bed sediments at the expense of Na, K, Ca, Al, Fe, Mg, Mn and other trace elements. The opposite is true for suspended load and the floodplain deposits that result from their deposition. The above changes effects the ratios of some elements such as SiO_2/Al_2O_3, Na_2O/K_2O, Fe_2O_3/K_2O and Fe_2O_3/SiO_2 that are used as an indicator of sediment maturity (Pettijohn et al., 1972; Herron, 1988). The SiO_2/Al_2O_3 ratio reflects the abundance of quartz as well as clay and feldspar content (Potter, 1978). With increased maturity the SiO_2/Al_2O_3 ratios tend to increase, whereas Fe_2O_3/SiO_2 and Al_2O_3/SiO_2 ratios decrease. Most of the Uttrangudi borehole sediments plot in litharenite and subarkosic field of log Na_2O/K_2O vs. SiO_2/Al_2O_3 diagram of Pettijohn et al., (1972), except for few sediments from greater depth that plot in arkosic field (Fig 4.7a). The sediments from depth upto ~16m depth plot within a narrow range of log Na_2O/K_2O but exhibit higher range of SiO_2/Al_2O_3. This suggests that the variation in their spread is mostly controlled by variation in quartz and clay as a result of sorting. The sediments that are fine plot towards the lower SiO_2/Al_2O_3 value and the coarser ones have higher, whereas the unsorted sediments lie in-between. The sediments from greater depth plotting in the arkosic field have lost higher amount of Na i.e. undergone greater degree of plagioclase weathering. In comparison all the sediments from Porayar plot in the litharenite field and are poorly sorted (Fig 4.7b). The above observation suggests that the sediments are immature.

In log SiO_2/Al_2O_3 vs. logFe_2O_3/K_2O diagram of Heron (1988), the sediments from Uttrangudi borehole plot in the field of Fe-sandstone and Fe-shale, whereas the Porayar sediments plot below the Uttrangudi sediments in the field of wacke and shale(Fig 4.7c & d). The Uttrangudi sediments show higher variation in the FeO/K_2O ratios, with higher ratios in deeper sediments below 16 m depth. The higher FeO/K_2O ratios in deeper sediments from Uttrangudi borehole inspite of their higher silica percentage rule out the influence of sorting. The higher ratio is probably because the combined effect of Fe addition due to early diagenetic processes whereby Fe may have got added from the solution as indicated by higher mottling seen in sediments from this zone and higher degree of weathering exhibited by their lower Na and K concentrations.

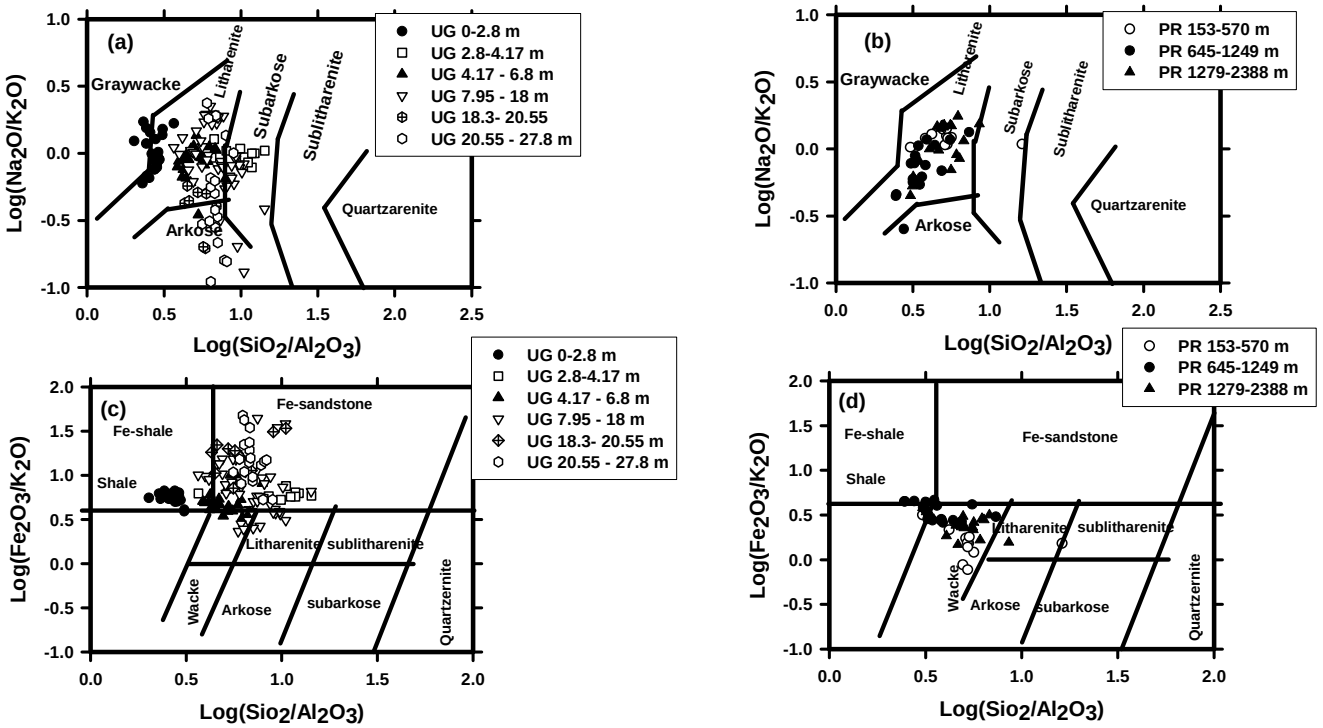

Figure 4.7: Plot of all the sediments in Log Na_2O/K_2O vs Log SiO_2/Al_2O_3 diagram for **(a)** Uttrangudi and **(b)** Porayar core sediments (after Pettijohn et al., 1972). Plot of all the sediments in Log FeO/K_2O vs. Log SiO_2/Al_2O_3 diagram for **(c)** Uttrangudi and **(d)** Porayar core sediments (Herron, 1988). Note that most of the samples from Uttrangudi core fall in litharenite and subarkosic field while the Porayar samples fall in litharenite field. In .Herron (1988) the Uttrangudi sediments fall in the field of Fe-sandstone, Fe-shale and greywacke area where as the Porayar sediments plot in the field of wacke suggesting towards diagenitic enrichment of Fe & greater loss of K in Uttrangudi sediments.

4.3.2 Spatial and temporal variation in weathering:

The sediments from both the bore holes have been grouped as silty and sandy based upon their mean size for comparison of their chemistry with the composition of upper continental crust (UCC) to understand the influence of weathering, sorting and diagenetic changes. On normalizing the average composition of major and trace elements in silty and sandy sediments with that of the UCC (Fig. 4.8), it is observed that the sandy sediments of Uttrangudi borehole show greater depletion of the mobile elements such as CaO, MgO, K_2O, Na_2O and Sr in comparison with the silty sediments, whereas SiO_2 exhibits enrichment. The depletion of these elements in both sandy and silty sediments indicates their loss due to weathering. The observed variation in depletion among silty and sandy sediments is inferred to be due to the greater dilution by silica in sand, and at the same time suggests higher concentration of feldspars in silt. Similar or higher concentration of Fe, Mn, Ti, Ba, Ni, Cr and Y in comparison with the UCC, both in case of sandy and silty sediments, although with different magnitude, suggest their addition or residual enrichment.

When we consider the average of Holocene sediments from Uttrangudi core we observe that it differs from above in respect to Mg, Ca, Na, K and Sr. The Holocene sediments show lower depletion of above set of mobile elements, whereas Mg shows an enrichment. If we consider the silty sediments of Holocene period separately, the above element show still lower depletion, indicating that unlike the Pleistocene sediments the feldspar in Holocene sediments of this core is preferentially enriched in silt fraction and is less weathered.

In Porayar borehole both sandy and silty sediments show depletion of Ca, Na and K in comparison to the UCC suggesting their loss due to weathering. Unlike the Pleistocene sediments of Uttrangudi borehole, the Porayar sediments exhibit higher concentration of Ca, Na and K in the sandy sediments suggesting higher percentage of feldspars constituting coarser fraction. Similar behavior of above elements is observed in the Holocene sediments of Uttrangudi borehole. Al and Ti in this core show enrichment in silty sediments and similar values in sandy sediments in comparison to UCC. Fe, Mg, Mn also show enrichment in silty sediments, whereas they are depleted in sandy

sediments compared to UCC. This suggests that the mafic minerals or their weathering product are preferentially concentrated in silt and clay fraction. Depleted values of Fe and Mn in Porayar sandy sediments contrast with that of the sandy sediments from Uttrangudi location where Fe was found to be almost similar to UCC and Mn to be enriched in the sandy sediments. We have in earlier section observed that Fe and Mn have got added by secondary diagenetic process in Uttrangudi sediments. Among the trace elements, Ni and Cr show enrichment both in silty and sandy sediments in Porayar core similar to that observed in Uttrangudi sediments. Ba and Sr exhibit behavior similar to Ca and Na suggesting their control by feldspars. Y shows concentration similar to UCC in silty sediments, whereas it is depleted in sandy sediments.

Overall we may be able to conclude that the Pleistocene sediments of Uttrangudi are different in their chemistry compared to the Holocene sediments of the same core and the Porayar core. The major difference is in terms of mobile elements. In contrast, the Holocene sediments of Uttrangudi and Porayar show somewhat similar character. Further reduced loss of mobile elements in Holocene sediments of both location compared to Pleistocene sediments suggest that the Holocene sediments are weathered to lesser degree.

To explore further into the difference and similarity in weathering of sedimets from the two locations and of different time period we have calculated a parameter known as chemical index of alteration (CIA) that is used to quantify the degree of weathering of soils and sediments (Nesbitt and Young 1982., 1984). CIA is defined as

$$CIA\ [= [Al_2O_3/(Al_2O_3+CaO^*+Na_2O+K_2O)]\times 100]$$

where the oxides are in molecular proportions, and CaO* is the amount of CaO incorporated in the silicate fraction of rocks. Unweathered igneous rocks have CIA values close to 50, and reflects cold or arid climate, whereas CIA range of ~65 to 80 indicate moderate degree of chemical weathering. Severely weathered sediments have CIA >80 (Fedo et al., 1996; Hofmann et al., 2003) and such severe weathering is related to a CO_2-rich atmosphere or an elevated surface temperature and a humid climate (Kasting, 1993; Knauth and Lowe, 2003, Nesbitt and Young, 1982).

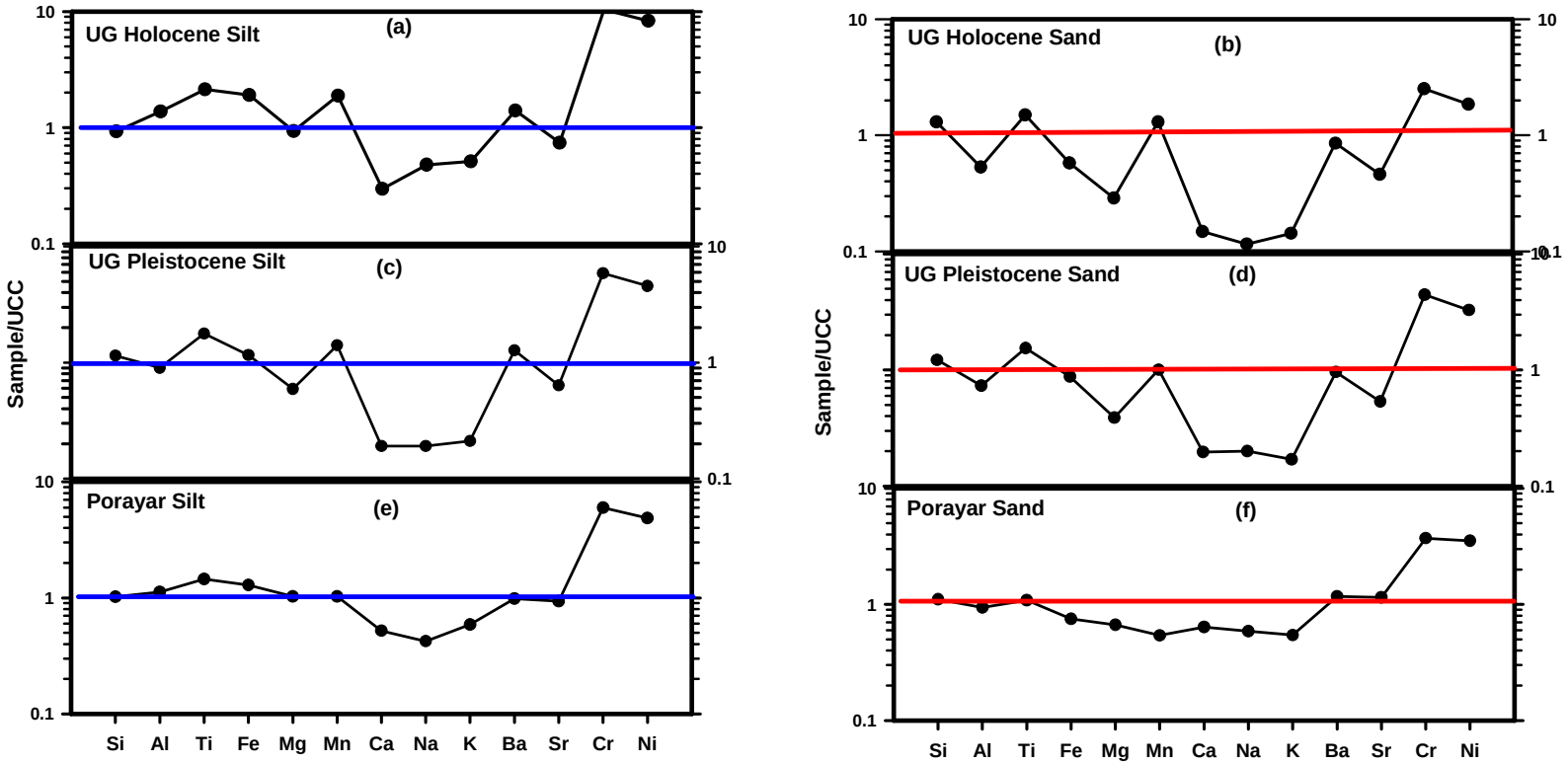

Figure 4.8: UCC normalized plot of silt and sand dominated sediments of Holocene and Pleistocene age from Uttrangudi (UG) and Porayar (PR) locations. Note the higher loss of mobile elements in all suites in comparison to the suites of sediments from Uttrangudi location in comparsion to the suites of Porayr location. **(a)** UG Holocene silt **(b)** UG Holocene sand **(c)** UG Pleistocene Silt **(d)** UG Pleistocene Sand (**e)** Porayar Silt and **(f)** Porayar sand.

In the studied cores the CIA values of Uttrangudi sediments exhibit a wide range from around 52 to 97. The range of CIA indicates that sediments have been derived from the source that has undergone moderate to strong degree of chemical weathering. The average CIA value of sediment between 27.8 m to 17.2 m is 91 (range 75 to 97), whereas between 17 m-10 m it reduces to 82 (range 69 to 91). On moving upward the average CIA value further reduces to 75 (range 62 to 84) with an exception for sediments between ~8.5 m to 9 m, which show much lower values with an average value of 56 (range 51to 60). The XRD results of sediments between 8.5m and 9m exhibit higher percentage of feldspar conent and are different from the overlying and underlying sediments. The sediments from this zone exhibit higher values of felsic component i.e. Si, Ca, Na and K and lower values of mafic components i.e. Fe, Mg, Mn, Ni and Cr. The reason for such short period change needs to be further explored. In general the CIA values show a gradual decrease from older sediments to younger (Fig 4.2). The sediments showing higher degree of weathering are of Pleistocene age, varying in age between ~3 to 1.93 lakh years B.P., whereas the Holocene sediments which represent top ~7 m show comparatively less weathering.

The CIA values of Porayar sediments which represent the Holocene period for most of its part ranges from 50 to 80 (Table 4.3). The range of CIA values indicates that sediments have been derived from the source that has undergone low to moderate weathering. The extreme weathering exhibited by the lower section of the Uttrangudi core is absent in Porayar core.

To explore the changes that have occurred with increasing degree of weathering we have plotted the sediments of Pleistocene and Holocene period from Uttrangudi borehole in the Al_2O_3- CaO* + Na_2O–K_2O (A-CN-K) triangular plot (Nesbitt and Young, 1984; Nesbitt et al., 1996) which gives the weathering trend. Similarly the Holocene sediments from Porayar borehole are also plotted in the same diagram. The A-CN-K diagram is the plot of molecular proportion of Al_2O_3, CaO*, Na_2O and K_2O. During weathering, alkali and alkaline earths are released into solution, whereas alumina is preferentially retained in the weathered residue. Ca and Na rich mineral phases (e.g., amphiboles and plagioclase) tend to degenerate earlier than K-rich phases (e.g.,

orthoclase and micas). Thus, progressive weathering of an igneous rock tends to drive the composition up and parallel to A-CN join to the right on this plot, so that more extremely weathered rocks will have more aluminous compositions plotting higher on the diagram. As weathering progresses and the residue begins to loose K, the composition of the residue starts moving parallel to the A-K join towards the A apex. Extreme weathering produces residuals completely depleted in alkali and alkaline earths that plot at A = 100 (Kaolinite and gibbsite clays, bauxite). The major oxide data for all the core sediments and for reference some rocks from source area have been plotted in Al_2O_3-CaO* Na_2O-K_2O (A-CN-K) compositional space (molecular proportions).Weathering trends for all sediments seem to be emanating from the same point on the feldspar join, which is considered to be indication of plagioclase and K- feldspar ratio in the source rock.

The plot of Pleistocene and Holocene sediments of Uttrangudi borehole exhibit trend parallel to the Al_2O_3 - CaO*+ Na_2O join (Fig 4.9a & b) in A-CN-K plot suggesting that the shift in the positions of plot is mainly because of mobilization of Ca and Na. In general the field of plot of Pleistocene sediments (with exception of sediments between ~8.5 m to 9 m) shows a greater shift away from feldspar tie line and closer to the 'A' end between CN range of 30-0. This would suggest greater loss of Ca and Na in them. In contrast to the Pleistocene sediments the field of plot of Holocene sediments lies relatively closer to the feldspar tie line and between 40-15 CN value. Similarly the Holocene sediments of Porayar core lie much closer to feldspar tie line similar to the Holocene sediments of the Uttrangudi borehole. Only difference between Holocene sediments of Uttrangudi and Porayar core is in behavior of K as indicated by the gradual shift of trend line towards higher proportion of K in Porayar core sediments as the points move towards the A end. This indicates increase in relative proportion of K with increase in weathering. This may suggest lesser mobilization of K in Porayar sediments in comparison to Uttrangudi sediments. Illite clay mineral is present throughout Porayar borehole which may have lead to greater retention of K and their enrichment.

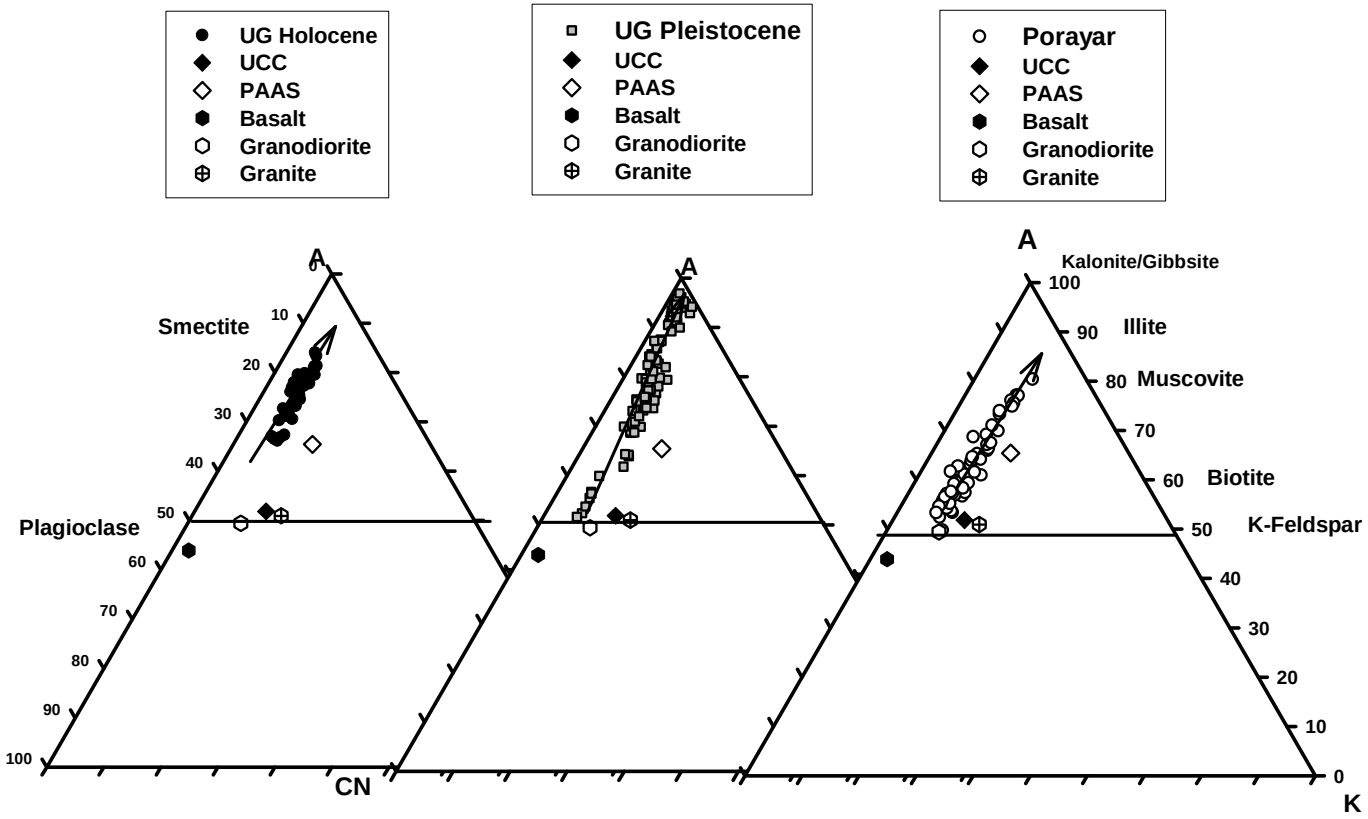

Figure 4.9: A-CN-K plots (Nesbit and Young, 1984) for (**a)** Holocene sediments and **(b)** Pleistocene sediment of Uttrangudi core site along with the plot for **(c)** Porayar sediments. Plotted for reference are the UCC, PASS, Granite, Granodiorite and Basalt. Note the increasing order of weathering from Porayar sediments to Holocene sediments from Utrrangudi to the Pleistocene sediments from Uttrangudi as indicated by increasing shift of plot towards the A apex.

The relatively lower weathering of Holocene sediments from both boreholes indicated by their overall closeness to the feldspar tie line in comparison to Pleistocene sediments leads to suggest as a first approximation that during the late Mid-Pleistocene period the climate was more wet and humid in comparison to Holocene.

To further understand the effect of sorting in addition to weathering the studied sediments are plotted in the A-CNK-FM diagram involving molecular proportion of Al_2O_3, CaO*, Na_2O, K_2O, FeO and MgO. This diagram help in understanding the weathering and sorting related changes involving Fe-Mg bearing minerals (Nesbitt and Young, 1984; 1089). In the A-CNK-FM diagram (Fig 4.10a-b) the sediments from the Uttarangudi borehole exhibit a trend moving away from the CNK end towards the A-FM join. The plot of samples trend away from CNK-FM line towards increasing "A" with a shift towards the A-FM line. The movement away from CNK & FM indicates mobilization of Ca, Na, K, Fe and Mg in all suites of Uttrangudi sediments and enrichment of Al in finer ones. This is also indicated in UCC normalized plot of silty and sandy sediments of Uttrangudi borehole where sandy sediments and silty sediments are seen to show larger difference in their Al content, whereas both sediments show depletion of Mg, Ca, Na and K . This suggests that the trend is as a result of weathering.

The plots of Porayar sediments show overall trend line parallel to the CNK-FM line with a shift towards the A-FM line suggesting negligible influence of Al.(Fig 4.10c). The variation in plots is mainly due to the change in the relative proportion of CNK and FM, whereas "Al" has remained same. This would suggest that the trend is mainly as a result of varying proportion of feldspar and mafic minerals. This is also observed in the UCC normalized plot of silty and sandy sediments from Porayar in which Al shows little variation, whereas both Fe and Mg show larger variation suggesting enrichment of mafic minerals in finer sediments. Also to be noted is higher concentration of feldspar in the coarser sediments of Porayar as indicated by its relatively higher value of Ca, Na and K. Thus mineral variation as a result of sorting has governed the trend line exhibited by Porayar sediments which is attributed to be process related, whereas in Uttrangudi sediments the trend is governed by weathering difference.

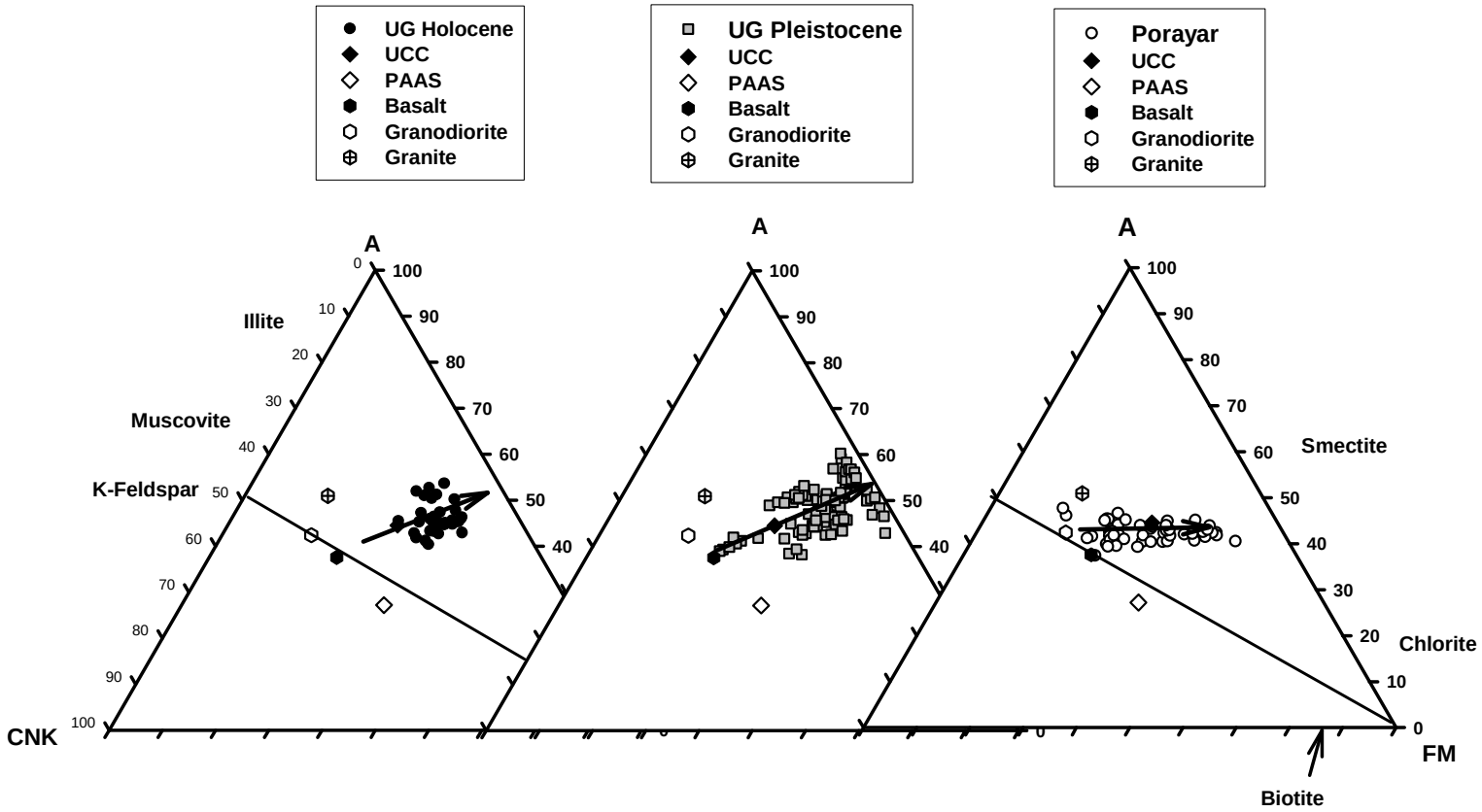

Figure 4.10: A-CNK-FM plots (Nesbit and Young, 1984) for **(a)** Holocene sediments of Uttrangudi **(b)** Pleistocene sediment of Uttrangudi core site and **(c)** Porayar core sediments showing weathering trends plotted along with UCC, PASS, Granite Granodiorite and Basalt. The trend of sediments in both Holocene and Pleistocene sediments from the Uttrangudi core suggest loss of CNK along with FM. The trend of plots in Porayar sediments suggests the effect of sorting.

4.3.3 Provenance:

The potential provenance for the Uttrangudi and Porayar sediments are the rocks of Archean age exposed in the catchment area of the Cauvery River. These include the two major terrains, (i) the northern greenstone granite terrain of Dharwar craton (DC) consisting of granite Gneisses and minor mafic supracrustal rocks and (ii) the Southern Granulite Terrain (SGT) composed of felsic to intermediate charnockites that are transected by several shear zones. The major shear zones comprise Moyar, Bhavani, Palghat, Cauvery and Attur shear zones. The charnockites in the SGT form high standing hills, whereas the gneisses in Dharwar craton and the shear zones form the low relief areas at different elevations.

The bulk composition of the sediments apart from the source also depends on the degree of weathering and later sorting during transportation. During the process of transport and deposition, differential enrichment and depletion of different elements takes place in finer and coarser sediments due to the resultant mineral sorting. Coarser sediments in general are enriched in silica and depleted in other elements particularly Al, Fe, Mg, Mn in comparison to the source due to concentration of mafic minerals in the finer size fraction constituting the finer sediments. As a result the plot among the ratios of above elements particularly the immobile elements and silica shows a wide linear array passing through the plot for the source. We in the present study as a first step have plotted the ratio of Al/Si vs Fe/Si of the sediments along with the probable source rocks from different part of the catchment region (Fig 4.11a). It is observed that the Holocene sediments from the Uttrangudi show a wider spread extending towards higher values of Fe/Si and Al/Si. This is expected as the part of the Uttrangudi Holocene sediments does not contain any sand as observed in the earlier section. On comparison of plots of Uttrangudi sediments in the above diagram with the plot of the probable source it is noted that the Gneisses from the Dharwar Craton do not fall within the linear array of Uttrangudi sediments and have lower Fe/Si ratios. This would suggest that they may not have acted as the source to the sediments. On the other hand the averages of Gneiss and charnockites from the transition zone between the DC and SGT, Enderbites from Nilgiri hills, Charnockite and migmatitic gneiss from northern Madurai Block (NMB) and

Cauvery Shear Zone from Madurai block domain (CSZ/MB) plot within or much closer to the trend line of the sediments in figure 4.11.

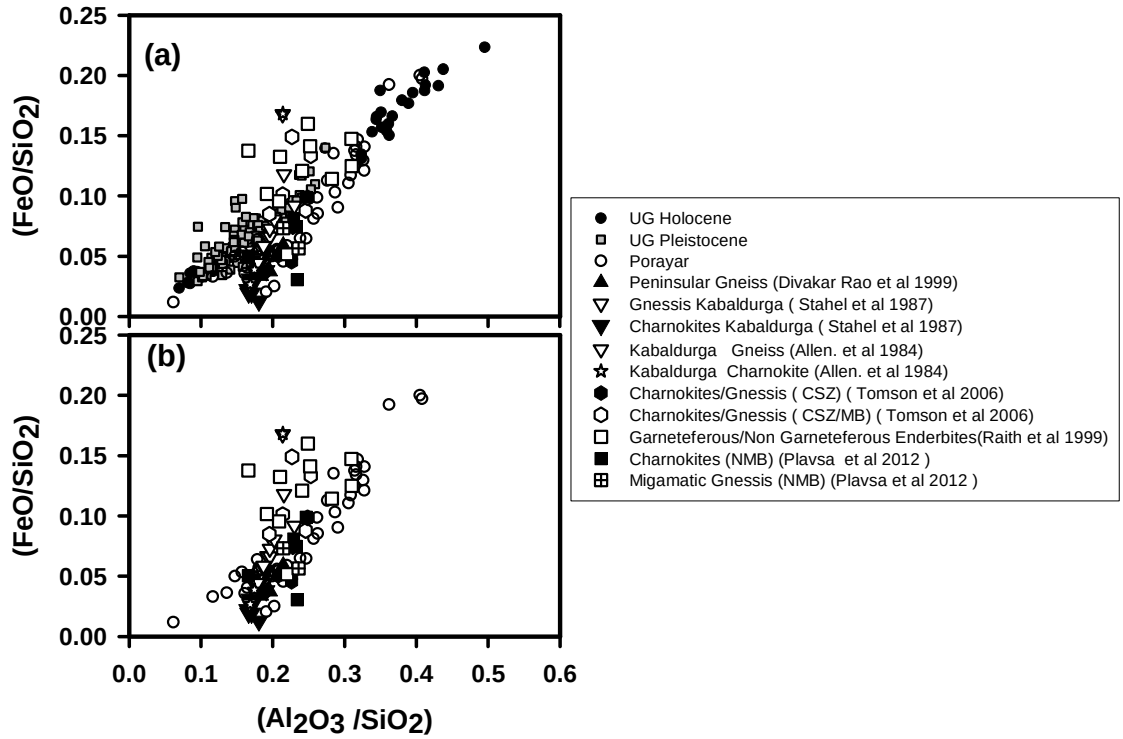

Figure 4.11 FeO/SiO_2 vs Al_2O_3/SiO_2 ratio diagram of the **(a)** Holocene and Pleistocene sediments from Uttrangudi core and **(b)** Porayar sediments along with various source rock compositions.

This as a first approximation would lead to conclude that various lithologies of the SGT acted as the dominant source for the Uttrangudi sediments, whereas the contribution from the gneisses of DC from upper catchment was negligible. In comparison to the Uttrangudi sediments the Porayar sediments show a narrower spread in Fe/Si vs Al/Si diagram (Fig 4.11b) suggesting lower degree of sorting and higher immaturity. Unlike the Uttrangudi sediments the trend line of the plots of Porayar sediments pass through the Gneisses of DC in addition to various lithologies from the SGT. This to first approximation would suggest that they have derived sediments from the mixed sources comprising DC and the SGT. One thing to note is that instead of following a linear trend expected due to the effect of sorting, the Porayar sediments take a curvilinear trend towards lower Fe/Si ratios. This may suggest that Fe has got mobilized to some extent in these sediments

which has led to pulling down of the trend line forcing it to pass through the plots of Gneisses from the DC. The loss of Fe can easily be explained as the sediments as inferred earlier have got deposited under water and contains substantial amount of carbon (Prayan, personal communication) which may have lead to anoxic condition facilitating Fe mobilization. Therefore the contribution of DC as inferred for Porayar sediments above may not be true.

Thus to better constrain the source we have further used the ratio plots among the immobile elements. Such plots lead to collapsing of the field of points within a narrow field as the ratios between the immobile elements generally do not get affected by the sorting if the elements used have similar mineralogical and size preferences (Frallick and Kronberg 1997; Singh, 2009). Among the several major elements Fe, Ti and Al are observed to have suffered least degree of mobilization, therefore we have plotted the sediments along with the probable source rocks in Fe/Ti vs Ti/Al diagram (Fig 4.12a).The plot of sediments in present study show clustering of data points of Pleistocene sediments from Uttrangudi and Holocene sediments from Porayar. Unlike the above two the Holocene sediments from Uttrangudi do not cluster together, but instead form a linear array displaying large variation. This would suggest that the Holocene sediments of the Uttrangudi have received input from differing sources at different times. On comparison with various lithologies we find that the Gneisses of DC separate out in this diagram and plot away from the sediments from Uttrangudi as well as Porayar sediments. The sediments from Porayar show an overlap with the field of plot of Charnockites and the Gneisses from the transition zone and charnockite from the Cauvery shear zone/Madurai block, Cauvery shear zone, Kodaikanal region and Non garnetiferous charnockite from Nilgiri hills (Fig 4.12b). This would suggest that the SGT rocks have acted as the major source for Porayar sediments. Unlike Porayar, the Pleistocene sediments from Uttrangudi do not show any overlap with the above mentioned catchment lithologies and plot towards lower Fe/Ti and higher Ti/Al end.

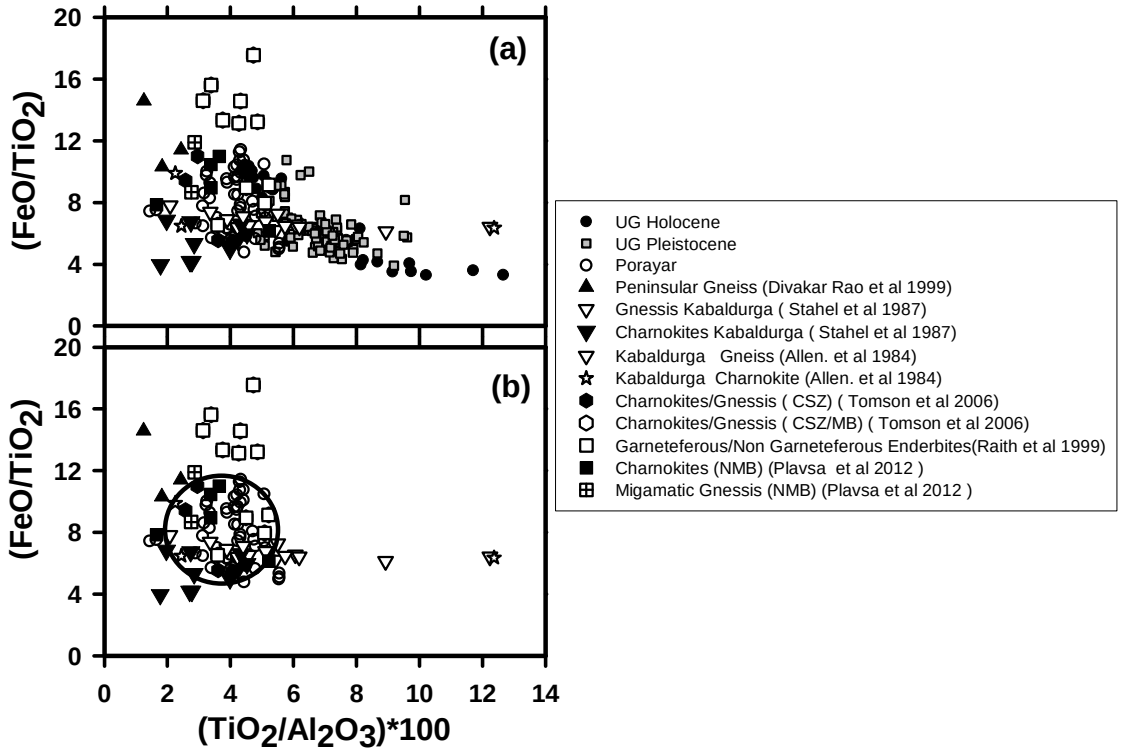

Figure 4.12: FeO/TiO_2 vs. TiO_2/Al_2O_3 ratio diagram comparing the **(a)** Uttrangudi Holocene and Pleistocene and **(b)** Porayar core sediments (encircled) with various source rocks.

It is interesting to find that these sediments show overlap with the plots of representative Tertiary rocks exposed west of Uttrangudi location (Fig 4.13). This would suggest that the source for Uttrangudi was local and it did not receive sediments from the upper catchment region during the Pleistocene. This appears to be true in light of the lower sea level during the time of deposition of these sediments which would have exposed the adjoining shelf region (Banerjee P.K., 2000). The maximum depth of sea towards the southern part of the delta separating it from Sri Lanka is 10 m). This implies that during the time of deposition of these sediments the sea may have retreated much away and India would have got connected by land with Srilanka due to the exposure of low gradient shelf. Similarly the sea had retreated on the eastern margin exposing the shelf in this region also. The resulting gradient towards the eastern margin was much greater and the sea was also nearer in comparison to the southern margin of the delta. This would have lead to the avulsion and migration of the distributary channels towards the middle and northern part of the delta abandoning the channels flowing south. Due to above

reason the supply of sediments from upper catchment to the Uttrangudi region would have got cut and it may have received sediments only from the erosion of the Tertiary rocks exposed towards the S/W of the delta. The Tertiary rocks in this part form the highlands and are highly dissected. Unlike the Pleistocene sediments the Holocene sediments of Uttrangudi shows wider spread and show overlap with Porayar sediments. This would suggest that Rivers in this region again became active during the Holocene and in addition to Tertiary rocks the region started receiving the sediments also from the upper catchment regions. This is indicated by the spread of the plots from Pleistocene sediments from Uttrangudi to the Holocene sediments from the Porayar.

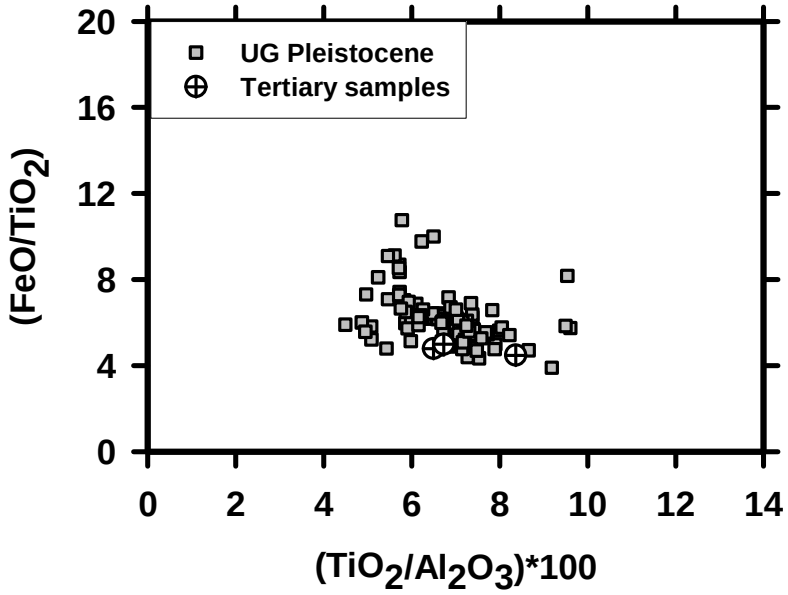

Figure 4.13: FeO/ TiO_2 vs. TiO_2 /Al_2O_3 ratio diagram comparing the Uttrangudi Pleistocene sediments with representative Tertiary sedimentary rocks exposed west of Uttrangudi location.

Thus from the above dicussion we may conclude that

(i) The first order control over the concentration of elements is due to variation in texture because of selective sorting of mafic minerals and quartz in finer and coarser size fractions respectively.

(ii) Higher CIA values, in conjunction with low absolute contents of Sr, Ca and Na in Pleistocene sediments, reflect an intensely weathered provenance and

indicate wetter climate during upper mid Pleistocene. The relatively lower CIA values with higher Sr, Ca and Na in Holocene sediments indicate relatively lower weathering and overall reduced rainfall during Holocene compared to Pleistocene period.

(iii) The bi-variant plot of the immobile major element ratios (Fe/Ti vs Ti*100/Al) suggest that the Porayar core sediments and the Holocene sediments from Uttrangudi core have been derived from the mix of various lithologies exposed in the Southern Granulite Terrain.

(iv) Unlike the Holocene sediments the Pleistocene sediments from Uttrangudi core appears to have been derived from recycling of Tertiary sedimentary rocks exposed towards the west of the core location.

Table 4.1: Textural data (clay, silt, and sand) in (%) of Uttarangudi coreSediments from Cauvery delta.

Sample Name	Depth	Mean	Clay(%)	Silt(%)	Sand(%)
UG 6	6	12.7	26.4	71.0	2.6
UG 8	8	7.8	26.7	73.3	0.0
UG 12	12	8.5	29.2	70.8	0.0
UG 25	25	11.9	27.8	69.9	2.3
UG 75	75	8.4	22.9	77.1	0.0
UG 83	83	74.0	2.1	50.8	47.1
UG 93	93	8.0	29.6	70.4	0.0
UG 103	103	9.4	26.2	73.2	0.6
UG 109	109	8.3	24.6	75.4	0.0
UG 113	113	95.0	3.1	60.5	36.5
UG 135	135	9.3	26.8	73.1	0.1
UG 136	136	8.8	17.6	82.4	0.0
UG 145	145	7.5	21.8	78.2	0.0
UG 161	161	7.7	21.0	79.0	0.0
UG 175	175	8.3	14.0	86.0	0.0
UG 191	191	9.0	20.3	79.7	0.0
UG 193	193	7.1	16.8	83.2	0.0
UG 227	227	8.5	18.6	81.5	0.0
UG 230	230	10.7	10.2	89.8	0.0
UG 232	232	50.0	2.2	65.6	32.2
UG 240	240	109.3	1.6	45.3	53.1
UG 252	250	9.7	10.3	89.7	0.0

Conti……

Sample Name	Depth	Mean	Clay(%)	Silt(%)	Sand(%)
UG 260	260	14.3	7.4	91.6	1.1
UG 280	280	11.6	11.7	88.2	0.1
UG 284	284	12.4	16.9	82.6	0.5
UG 290	290	12.5	10.7	87.2	2.0
UG 295	295	505.3	2.6	15.0	82.4
UG 313	313	356.5	4.1	20.2	75.7
UG 317	317	272.0	1.4	26.5	72.1
UG 319	319	450.0	4.1	18.5	77.4
UG 331	331	323.9	3.9	23.4	72.7
UG 339	339	341.8	5.1	31.9	63.0
UG 359	359	254.5	6.3	34.1	59.7
UG 365	365	242.0	8.4	33.7	57.8
UG 369	369	275.5	1.0	26.7	72.3
UG 380	380	297.6	0.8	20.6	78.6
UG 392	392	314.5	0.9	23.3	75.7
UG 394	394	252.3	8.5	37.2	54.4
UG 414	414	233.9	2.3	50.9	46.8
UG 417	417	69.9	10.7	61.7	27.6
UG 425	425	67.8	12.2	61.5	26.3
UG 435	435	284.0	0.8	23.0	76.2
UG 437	437	25.4	9.9	81.3	8.8
UG 449	449	39.2	15.4	68.4	16.2
UG 451	451	46.4	17.1	64.7	18.1

Sample Name	Depth	Mean	Clay(%)	Silt(%)	Sand(%)
UG 457	457	10.5	11.2	87.2	1.7
UG 477	477	91.5	2.3	57.3	40.5
UG 479	479	86.0	11.9	53.0	35.2
UG 495	495	88.9	11.1	49.7	39.2
UG 506	506	70.3	12.6	57.0	30.4
UG 516	516	69.1	12.7	57.7	29.7
UG 521	521	63.1	12.3	58.6	29.1
UG 526	526	77.6	12.3	54.0	33.7
UG 536	536	77.6	15.4	58.3	26.3
UG 546	546	26.4	18.1	69.2	12.7
UG 556	556	57.9	15.0	59.1	25.9
UG 566	566	100.5	2.9	56.8	40.3
UG 576	576	21.3	17.9	72.1	10.1
UG 581	581	18.1	24.9	66.6	8.5
UG 586	586	42.5	18.7	60.7	20.6
UG 620	620	44.8	16.6	62.2	21.2
UG 626	626	17.7	26.2	72.6	1.2
UG 630	630	97.4	11.9	47.1	41.0
UG 640	640	99.2	12.0	48.7	39.3
UG 641	641	325.8	12.3	33.6	54.2
UG 650	650	113.1	3.1	60.5	36.5
UG 660	660	58.8	16.5	59.7	23.8
UG 670	670	56.1	17.5	59.5	23.0
UG 676	676	18.1	19.5	74.7	5.8
UG 680	680	53.3	16.1	61.3	22.7
UG 805	805	41.1	13.0	69.7	17.3

Sample Name	Depth	Mean	Clay(%)	Silt(%)	Sand(%)
UG 811	811	11.2	14.7	84.3	1.0
UG 815	815	45.1	2.4	71.6	26.0
UG 825	825	63.0	12.5	61.5	26.1
UG 835	835	72.5	2.6	67.9	29.5
UG 836	836	93.2	9.7	49.9	40.3
UG 845	845	179.9	4.6	28.4	67.0
UG 855	855	195.5	3.4	23.0	73.6
UG 865	865	184.9	2.3	25.6	72.1
UG 866	866	160.4	4.8	29.8	65.5
UG 875	875	200.5	2.6	24.0	73.5
UG 885	885	189.0	1.3	24.0	74.7
UG 895	895	161.4	2.7	31.6	65.7
UG 901	901	279.1	3.4	19.0	77.6
UG 908	908	317.0	2.7	19.0	78.3
UG 1010	1010	28.0	3.9	85.6	10.5
UG 1020	1020	84.0	18.0	51.9	30.1
UG 1026	1026	114.7	23.2	55.3	21.5
UG 1030	1030	86.3	17.2	51.2	31.6
UG 1040	1040	651.7	6.1	17.0	76.9
UG 1050	1050	607.3	6.9	19.1	74.0
UG 1060	1060	820.6	6.5	17.5	76.0
UG 1070	1070	608.7	6.9	19.8	73.3
UG 1077	1077	157.1	20.7	48.9	30.4
UG 1190	1190	94.0	13.9	49.9	36.3
UG 1191	1191	168.2	20.3	54.5	25.2
UG 1200	1195	245.5	2.7	65.6	31.7

Sample Name	Depth	Mean	Clay(%)	Silt(%)	Sand(%)
UG 1216	1216	185.8	15.5	40.4	44.2
UG 1220	1220	454.8	5.8	22.9	71.3
UG 1230	1230	431.6	5.6	22.0	72.4
UG 1236	1236	384.9	10.5	28.6	60.9
UG 1250	1250	364.3	5.7	24.3	70.1
UG 1266	1266	364.8	7.7	23.0	69.3
UG 1270	1270	751.8	1.3	6.1	92.6
UG 1281	1281	459.5	3.9	17.3	78.9
UG 1285	1285	480.5	3.5	18.0	78.4
UG 1305	1305	502.4	4.7	17.2	78.1
UG 1311	1311	292.2	4.3	22.9	72.8
UG 1325	1325	388.2	5.1	26.0	68.9
UG 1345	1345	411.6	5.3	26.5	68.2
UG 1346	1346	409.1	4.3	17.6	78.2
UG 1430	1430	63.0	2.1	78.9	19.0
UG 1440	1440	188.8	0.0	12.1	87.9
UG 1450	1450	334.7	8.2	33.8	58.1
UG 1456	1456	239.0	2.1	78.9	19.0
UG 1486	1486	284.0	8.3	29.3	62.3
UG 1490	1490	335.6	6.1	31.7	62.3
UG 1500	1500	88.9	12.6	51.1	36.4
UG 1510	1510	210.7	1.8	46.8	51.4
UG 1520	1520	84.1	5.0	49.2	45.8
UG 1521	1521	285.0	7.2	30.1	62.7
UG 1621	1621	301.5	6.3	26.3	67.5
UG 1645	1645	590.9	1.5	8.6	89.9

Sample Name	Depth	Mean	Clay(%)	Silt(%)	Sand(%)
UG 1651	1651	322.9	5.9	24.6	69.5
UG 1665	1665	952.0	3.0	16.2	80.7
UG 1681	1681	300.1	5.7	22.2	72.0
UG 1685	1685	498.1	2.9	15.1	82.0
UG 1703	1703	183.5	3.1	60.5	36.5
UG 1709	1709	315.8	6.0	23.5	70.5
UG 1739	1739	401.6	8.2	27.0	64.8
UG 1743	1743	490.6	3.2	16.5	80.3
UG 1764	1764	282.9	9.6	31.5	58.9
UG 1826	1826	284.2	10.4	31.8	57.8
UG 1830	1830	600.4	2.9	13.3	83.8
UG 1845	1845	446.7	4.4	18.9	76.7
UG 1870	1870	337.2	5.3	27.9	66.8
UG 1886	1886	152.9	13.7	51.1	35.2
UG 1890	1890	80.6	10.3	56.2	33.5
UG 1902	1902	141.4	12.8	60.5	26.7
UG 1903	1903	95.4	10.0	50.8	39.2
UG 1912	1912	28.5	2.5	88.8	8.7
UG 1948	1948	117.9	14.2	56.1	29.7
UG 1953	1953	133.2	8.9	39.8	51.3
UG 1972	1972	113.5	10.4	44.1	45.5
UG 2005	2005	331.8	6.6	25.7	67.7
UG 2013	2013	119.2	14.2	62.1	23.7
UG 2076	2076	205.9	5.9	45.3	48.8
UG 2098	2098	235.7	1.1	40.2	58.7
UG 2098	2098	653.5	2.0	9.8	88.2

Sample Name	Depth	Mean	Clay(%)	Silt(%)	Sand(%)
UG 2118	2118	323.4	5.6	21.2	73.2
UG 2124	2124	228.2	5.6	42.7	51.7
UG 2138	2138	224.0	1.6	49.5	49.0
UG 2154	2154	251.6	5.7	38.0	56.3
UG 2158	2158	383.9	5.1	19.6	75.3
UG 2245	2245	21.2	19.3	70.9	9.8
UG 2256	2256	175.9	5.9	54.9	39.1
UG 2275	2275	891.1	1.4	7.1	91.5
UG 2287	2287	1000.6	1.3	6.9	91.8
UG 2291	2291	172.8	8.9	58.2	32.9
UG 2307	2307	74.3	6.5	66.5	27.1
UG 2323	2323	46.0	1.5	48.7	49.8
UG 2326	2326	101.9	8.6	69.4	22.0
UG 2328	2328	10.0	8.8	91.2	0.0
UG 2368	2368	123.7	0.7	11.7	87.6
UG 2382	2382	136.7	5.5	64.0	30.5
UG 2388	2388	58.9	2.0	77.2	20.9
UG 2490	2490	70.0	2.3	65.8	31.9
UG 2495	2495	11.4	5.3	94.7	0.0
UG 2515	2515	70.0	2.3	65.8	31.9
UG 2541	2541	127.8	8.4	64.9	26.7
UG 2595	2595	54.9	5.3	74.5	20.2
UG 2611	2611	112.8	6.6	68.9	24.5
UG 2719	2719	191.7	9.9	51.4	38.7
UG 2760	2760	424.6	1.2	41.7	57.1
UG 2771	2771	240.4	2.0	60.3	37.7

Sample Name	Depth	Mean	Clay(%)	Silt(%)	Sand(%)
UG 2780	2780	719.7	0.6	25.5	73.9
UG 2821	2821	158.7	6.0	60.6	33.4
UG 2856	2856	151.5	6.1	59.0	35.0
UG 2926	2926	187.7	4.0	54.5	41.6
UG 2975	2975	73.5	4.9	68.2	26.8
UG 3007	3007	195.2	2.0	55.5	42.5
UG 3169	3169	226.2	3.1	47.2	49.7
UG 3191	3191	73.4	5.6	57.2	37.1

Table 4.4: Textural data (clay, silt, and sand) in (%) of Porayar core sediments from Cauvery delta.

Sample name	Depth	Mean	Clay (%)	Silt (%)	Sand (%)
PR 150-153	153	115.9	6.2	26.6	67.2
PR 173-176	176	105.6	7.1	34.6	58.3
PR 196-199	199	96.9	7.7	41.4	50.8
PR 280-283	283	116.8	3.3	28.8	68.0
PR 303-306	306	110.0	4.0	33.2	62.8
PR 329-331	331	174.0	0.8	23.0	76.2
PR 400-403	403	131.7	1.5	17.8	80.7
PR 420-422	422	201.4	0.6	8.5	90.9
PR 420-426	426	207.0	0.7	10.3	89.0
PR 446-449	449	133.3	1.5	15.6	82.9
PR 522-525	525	87.1	3.7	54.5	41.8
PR 545-548	548	88.0	1.2	46.8	52.0
PR 568-571	571	93.7	3.8	47.4	48.8
PR 645-647	647	83.1	1.1	41.1	57.9
PR 665-668	668	25.6	9.5	81.4	9.2
PR 688-691	691	76.9	4.9	61.8	33.3
PR 772-775	775	86.2	5.3	63.4	31.3
PR 800-803	801	13.0	14.5	84.5	1.0
PR 828-831	831	14.6	14.2	83.3	2.4
PR 840-842	842	77.7	2.2	58.0	39.8
PR 895-898	898	85.3	7.8	60.0	32.2
PR 942-945	945	62.1	11.4	67.0	21.6
PR 970-973	973	79.4	7.1	57.5	35.3
PR 998-1001	1001	80.9	6.1	56.2	37.7

Sample name	Depth	Mean	Clay (%)	Silt (%)	Sand (%)
PR 1026-1029	1029	163.9	7.2	45.6	47.2
PR 1054-1057	1057	62.9	12.9	70.2	16.9
PR 1167-1170	1170	75.6	10.4	56.1	33.5
PR 1195-1198	1198	63.6	13.0	63.9	23.1
PR 1223-1226	1226	168.1	7.0	46.5	46.5
PR 1276-1279	1279	168.8	6.3	44.9	48.8
PR 1325-1328	1328	94.5	2.8	48.5	48.7
PR 1348-1351	1351	183.6	3.4	49.1	47.5
PR 1420-1423	1423	100.1	2.4	43.1	54.5
PR 1480-1483	1483	101.9	2.6	41.4	56.0
PR 1570-1573	1573	104.2	2.8	38.8	58.4
PR 1600-1603	1603	96.2	2.6	46.6	50.8
PR 1641-1643	1643	118.0	1.5	35.2	63.4
PR 1680-1683	1683	112.3	2.7	32.6	64.7
PR 1715-1718	1718	225.1	4.9	47.8	47.3
PR 1750-1753	1753	27.5	9.3	77.6	13.1
PR 1780-1785	1785	45.2	6.6	77.8	15.5
PR 1830-1833	1833	13.7	7.0	92.9	0.1
PR 1890-1893	1893	16.7	6.9	92.1	1.0
PR 1920-1923	1923	62.4	5.8	74.4	19.8
PR 1950-1953	1953	79.9	4.1	58.5	37.4
PR 2170-2173	2173	267.3	0.8	28.6	70.7
PR 2345-2348	2348	75.0	1.9	54.8	43.3

Chapter 5

Rare Earth Element, Rb-Sr and Sm-Nd isotope studies on the Core sediments from the Cauvery delta.

5.1. Introduction

It is now a well-established fact that the chemical and mineralogical compositions of clastic sedimentary rocks is the manifestation of composite interaction of various variables including source rock composition, weathering, erosion, transportation and sedimentation processes such as mechanical sorting, decomposition and diagenesis (McLennan et al., 1993). In-spite of the above intermediate processes operating between the times the soil is eroded from the source region and sediments are deposited in different basins, the sediments are believed to preserve the chemical signature of their provenance. Among the various chemical parameters, the immobile elements including the rare earth elements (REE's), are thought to be carried as such without any losses (Taylor and McLennan, 1985). The REEs are comparatively insoluble and present in very low concentrations in sea and river water. Therefore, the provenance of sediments is considered to be the most important factor contributing to the REE content of clastic sediments (Fleet., 1984; McLennan, 1989). The REE's because of their similar behavior are expected to retain their pattern and the ratios among them that are similar to their source (Fralick and Kronberg, 1997). In view of above the REE's have also been widely used to understand the evolution of continental crust (Taylor and McLennan, 1985, 1995; McLennan and Taylor, 1991; Condie., 1993; Lahtinen, 2000) particularly the Precambrian crust, where either the source rock has been subjected to erosion or exhumed by subduction processes (Feng and Kerrich., 1990; Hofmann., 2005; Hofmann et al., 2003; Holland., 1984; Johnson., 1993).

In addition to above Sm–Nd analyses of fine-grained clastic sediments is also a powerful geochemical tool to elucidate their provenance. Being relatively immobile REEs and having no further parent-daughter fractionation occurring after mantle-crust differentiation (O'Nions et al., 1983; Chaudhuri and Clauer, 1992), they are believed to be transported together without significant fractionation during sedimentary processes (McCulloch and Wasserburg., 1978). As such they can retain isotope ratios that reflect those of the source area (Nelson and DePaolo., 1988), which when coupled with other trace element data can provide significant information on sediment provenance. The advantage of Sr and Nd isotopes is that they act as fingerprints for source regions and

transport pathways of detrital sediments (Innocent et al., 2000; Rutberg et al., 2005). Isotopic ratios of Sr and Nd vary according to the age and geological history of crustal rocks. This results in an inverse relationship between $^{87}Sr/^{86}Sr$ and εNd_0 (Goldstein and Jacobsen., 1987). Sediments of rivers draining older crust have more radiogenic Sr and non-radiogenic Nd than rivers draining the younger crust. Depleted mantle Nd model ages (T_{DM}) add a temporal dimension to the provenance study of sediments by providing extraction ages of the sediment sources from the depleted mantle.

This chapter presents results on Rare earth elements (REE's), Sr and Nd isotopic compositions of sediments from the two core i.e. from Uttrangudi and Porayar sites taken from the Cauvery Delta. These results are interpreted to derive information on the provenance of sediments of the Cauvery delta. The rock types in the catchment region of River Cauvery includes predominantly granitic gneisses along with supracrustal rocks of Dharwar craton that are characterized by high $^{87}Sr/^{86}Sr$ ratio and lower εNd in the upper part in the northern part, whereas in the southern and eastern part of the catchment granulite grade charnockite forming the highlands and migmatitic gneisses forming the shear zones have less radiogenic $^{87}Sr/^{86}Sr$ and higher εNd_o values. In addition we have also carried Sr isotopic analysis on several secondary phases associated with the sediments and attempted to infer the temporal and spatial variation in the ground water composition.

5.2 Results

5.2.1 REE Characteristics:

REE analysis was carried out on limited number of samples selected on the basis of changes observed in texture and chemistry of the sediments as discussed in Chapter 4. The results of the REE for sediments from Uttrangudi and Porayar core are given in (Table 5.1 and Table 5.2) respectively. The number associated with the sample denotes the depth in cm. The total REE (∑REE) concentration of sediments from Uttrangudi core ranges from 52 to 246 ppm with an average value of 157 ppm. The average ∑REE concentration of sediments from Porayar site is 136 ppm, ranging from 46 to 215 ppm, except one sample at 8.3 m having value of 270 ppm. The variation and concentration of

REE is higher in the Uttrangudi sediments. As expected, the concentration of the most individual REEs shows good correlation with each other and with ∑REE, with correlation coefficient (r) ranging between 0.81 and 0.99 in Uttrangudi sediments and between 0.93 and 1.0 in Porayar sediments. The range of $(Ce/Yb)_N$, $(Ce/Sm)_N$ and $(Gd/Yb)_N$ ratios of Uttarangudi sediments are 7.4 to 10.9 except for three samples at 22.45 m, 23.28 and 23.88 that have values of 3.5, and 3.7 (avg. 8.2); 2.3 to 4.0 (avg. 3.1) and 1.5 to 2.7 (avg. 1.7) except for lower value of 1 for sample at 22.45, 23.28 and 23.88 m depth. respectively, whereas for Porayar sediments their ranges are 5.3 to 8.3 (avg. 7.1), 2.2 to 3.3 (avg. 2.7) and 1.4 to 2.1(avg. 1.7) respectively (Table 5.2). The Uttrangudi sediments exhibit slight to negligible negative Eu anomaly ranging between 0.79 and 0.97, whereas Porayar sediments exhibit negative to slightly positive Eu anomalies ranging between 0.7 and 1.2, except one sample which shows value of 1.6. The chondrite normalized REE plots for sediments indicate fractionated pattern (Fig 5.1a and 5.1b).

Rb-Sr and Sm-Nd isotope systematics:

Rb is an alkali metal with an ionic radius (1.48 A°) similar to that of Potassium (1.33 A°) and can substitute the later in K-bearing minerals such as Biotite, Muscovite, feldspar and clay minerals and evaporite minerals. Rb has two naturally occurring isotopes $^{85}_{37}Rb$ and $^{87}_{37}Rb$. Rb is radioactive and decays to stable ^{87}Sr by emission of negative beta particle (negatron) which can be expressed in the form of following equation:

$$^{87}_{37}Rb \rightarrow {}^{87}_{38}Sr + \beta^- + \ddot{\nu} + Q \qquad \longrightarrow \qquad (5.1)$$

Where β^- is the beta particle (negatron), $\boldsymbol{\nu}$ is an antineutrino and Q is the decay energy 0.275 MeV/atom.

The growth of radiogenic ^{87} Sr can be expressed relative to a stable non radiogenic isotope^{86}Sr as :

$$^{87}_{86}\mathrm{Sr} = \left(\frac{^{87}\mathrm{Sr}}{^{86}\mathrm{Sr}}\right)_i + \frac{^{87}\mathrm{Rb}}{^{86}\mathrm{Sr}}\left(e^{\lambda t} - 1\right) \qquad \longrightarrow \qquad (5.2)$$

where, i represents the initial isotopic composition of Sr and $\boldsymbol{\lambda}$ is the decay constant which is equal to 1.42 X $10^{-11}y^{-1}$ (Steiger and Jager 1977).

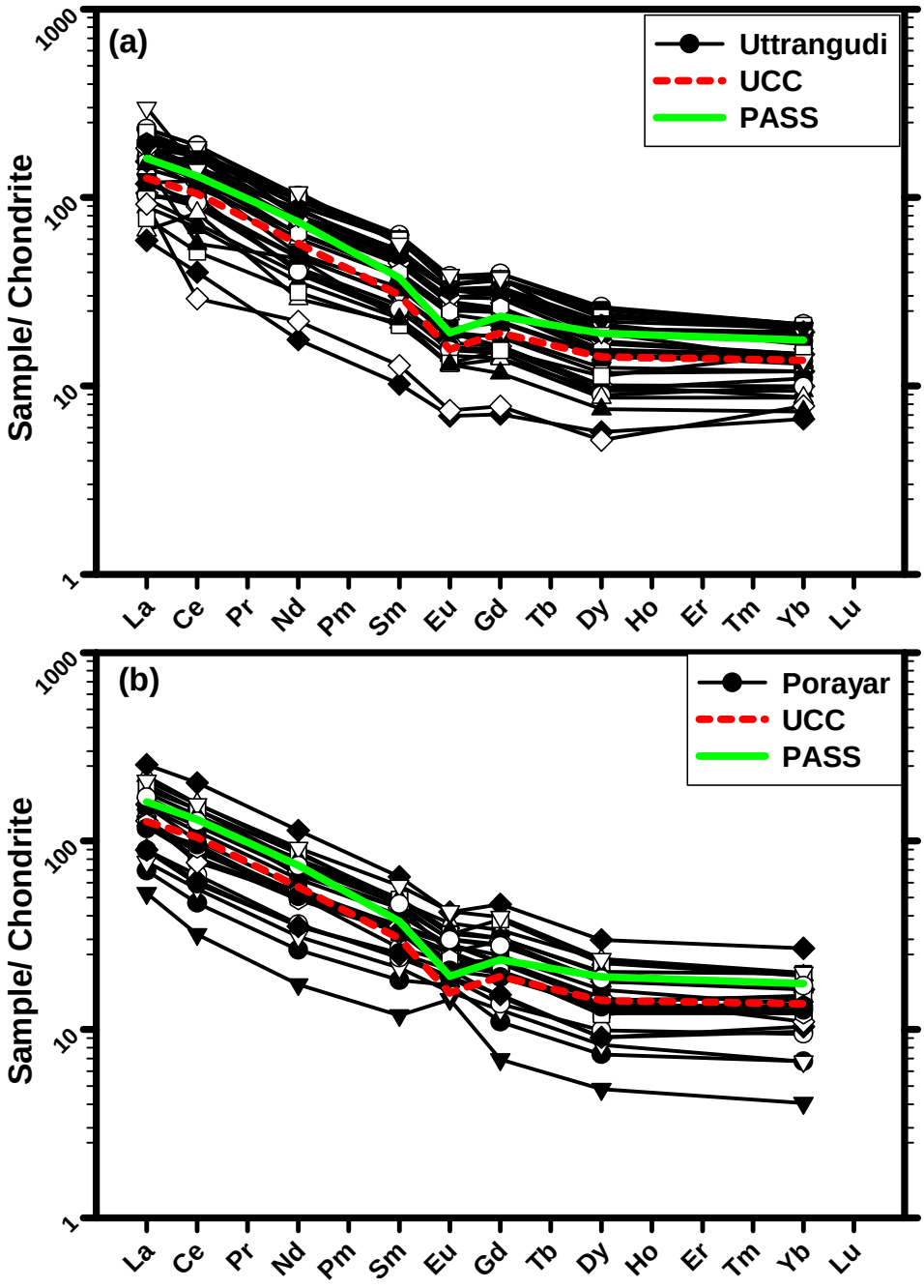

Figure 5.1: Chondrite normalized REE plots of sediments from **(a)** Uttrangudi (UG) and **(b)** Porayar (PR) cores, Also plotted for comparison are chondrite normalized REE plots of UCC and PAAS.

Table 5.1. Rare earth element (REE) abundances along with Th, Rb (ppm) and chondrite normalized ratios in selected samples from Uttrangudi borehole.

Sample	Depth(cm)	La	Ce	Nd	Sm	Eu	Gd	Dy	Yb	Lu	ΣREE	Sc	Co	Th	Rb	$(La/Yb)_N$	$(Ce/Yb)_N$	$(Eu^*)_N$	$(La/Sm)_N$	$(GD/Yb)_N$	$(Ce/Sm)_N$
UG 83	83	55	116	45	9.3	2.1	7.8	6.3	3.4	0.5	245	19.8	34.8	18.9	69.6	10.9	8.9	0.7	3.7	1.8	3.0
UG 113	113	55	115	47	9.4	2.2	7.9	6.5	3.4	0.5	247	21.3	34.6	20.2	82.8	10.9	8.9	0.8	3.7	1.9	3.0
UG 185	185	51	104	44	8.8	1.9	7.3	5.9	3.2	0.5	227	15.7	29.4	14.3	80.8	10.6	8.4	0.7	3.6	1.8	2.9
UG 220	220	48	103	41	8.8	1.9	7.2	6.0	3.2	0.5	220	39.3	74.4	16.5	195.9	10.3	8.6	0.7	3.4	1.8	2.8
UG 240	240	46	102	41	8.9	2.0	7.3	6.2	3.3	0.5	218	34.1	79.3	14.7	176.7	9.5	8.1	0.7	3.2	1.8	2.8
UG 260	260	52	106	46	8.8	2.1	7.4	5.7	3.4	0.6	233	27.6	57.1	14.1	147.0	10.6	8.3	0.8	3.7	1.8	2.9
UG 280	280	28	58	22	4.4	1.1	3.6	2.9	1.9	0.2	122	17.5	30.2	11.7	96.0	9.9	7.9	0.8	3.9	1.5	3.1
UG 313	313	25	55	19	4.0	1.0	3.2	2.5	1.6	0.4	112	9.3	46.4	8.0	40.3	10.6	9.0	0.8	3.9	1.6	3.3
UG 380	380	21	42	16	3.4	0.8	2.8	2.3	1.5	0.2	91	12.8	35.0	9.9	59.4	9.5	7.4	0.8	3.9	1.5	3.0
UG 392	392	29	55	22	4.5	1.0	3.7	3.1	1.9	0.3	120	10.0	33.5	10.6	55.9	10.4	7.5	0.8	4.1	1.6	2.9
UG 419	419	45	77	36	7.0	1.8	6.6	5.2	2.7	0.4	181	15.7	41.7	13.3	93.9	11.5	7.6	0.8	4.0	2.0	2.6
UG 427	427	35	83	29	5.9	1.4	4.9	3.7	2.3	0.3	165	21.0	38.2	14.3	109.7	10.2	9.4	0.8	3.7	1.7	3.4
UG 457	457	39	90	32	6.5	1.5	4.9	3.9	2.2	0.4	181	19.4	47.0	13.7	114.0	12.1	10.9	0.8	3.7	1.8	3.3
UG 477	477	45	89	39	7.7	1.8	6.2	4.8	2.8	0.6	197	21.4	33.7	12.5	97.4	11.0	8.5	0.8	3.6	1.8	2.8
UG 526	526	40	86	33	6.7	1.6	5.1	4.1	2.4	0.5	179	21.5	41.7	14.0	114.4	11.4	9.5	0.8	3.7	1.7	3.1
UG 546	546	34	73	28	5.6	1.4	4.4	3.6	2.1	0.3	152	23.2	37.6	12.9	133.8	10.7	9.0	0.8	3.7	1.7	3.1
UG 566	566	42	90	34	7.4	1.8	6.2	5.0	2.8	0.6	189	22.5	39.7	12.4	128.5	10.0	8.3	0.8	3.5	1.8	2.9
UG 650	650	38	69	30	5.9	1.4	5.0	3.6	2.1	0.4	155	16.9	33.8	10.6	73.5	12.2	8.6	0.8	4.0	1.9	2.8
UG 815	815	37	100	32	6.9	1.7	6.2	4.9	3.1	0.6	192	26.6	66.9	14.2	88.1	8.0	8.5	0.8	3.3	1.6	3.5
UG 825	825	43	72	35	6.6	1.7	5.8	4.3	2.4	0.4	171	21.7	37.7	12.2	75.7	12.4	8.0	0.8	4.1	2.0	2.6
UG 855	855	23	44	18	3.6	1.1	3.2	2.5	1.4	0.2	98	10.9	25.1	5.6	52.3	11.3	8.3	1.0	4.1	1.9	3.0
UG 1010	1010	45	113	37	7.6	1.8	6.4	5.0	3.0	0.6	219	17.6	40.5	12.4	54.3	10.2	9.9	0.8	3.7	1.7	3.6
UG1200	1200	46	82	40	7.2	1.8	6.0	4.5	2.8	0.5	191	19.0	32.6	11.6	59.7	11.3	7.7	0.8	4.0	1.8	2.7
UG 1430	1430	37	77	29	5.9	1.4	5.2	3.8	2.4	0.5	162	15.0	40.8	10.1	43.2	10.6	8.6	0.8	3.9	1.8	3.2
UG 1510	1510	24	62	18	3.7	0.9	3.1	2.4	1.8	0.4	116	11.9	25.2	10.1	50.5	9.2	9.2	0.8	4.1	1.4	4.0
UG 1703	1703	24	57	18	3.8	0.9	3.0	2.2	1.6	0.4	112	12.5	23.0	9.3	38.4	10.4	9.5	0.8	4.0	1.5	3.7
UG1912	1912	44	101	36	7.8	1.8	6.6	5.4	3.3	0.7	207	17.2	42.8	10.3	38.7	9.1	8.1	0.8	3.5	1.6	3.1
UG 2098	2098	16	51	13	3.2	0.7	2.8	2.1	1.4	0.3	90	14.5	33.0	10.1	26.1	7.7	9.6	0.7	3.1	1.6	3.8
UG 2138	2138	28	75	23	4.9	1.1	4.3	3.5	2.2	0.4	143	n.d	n.d	n.d	n.d	8.8	9.0	0.7	3.6	1.6	3.7
UG 2245	2245	18	32	14	3.1	0.7	3.1	2.8	2.4	0.6	77	n.d	n.d	n.d	n.d	5.2	3.5	0.7	3.7	1.0	2.5
UG 2328	2328	14	25	8	1.5	0.4	1.4	1.4	1.1	0.2	53	14.4	15.0	9.9	24.9	8.9	6.0	0.8	5.8	1.1	3.9
UG 2388	2388	22	18	10	1.9	0.4	1.6	1.3	1.3	0.3	56	20.8	24.1	13.1	41.5	7.9	3.7	0.7	4.8	1.0	2.3
UG 2490	2490	36	35	22	3.3	0.7	2.3	1.8	1.2	0.2	102	15.3	21.6	8.5	28.8	20.6	7.8	0.8	6.7	1.6	2.5
UG 2760	2760	71	86	49	8.4	2.2	7.4	4.7	2.2	0.4	231	n.d	n.d	n.d	n.d	21.8	10.2	0.8	5.3	2.7	2.5

Table 5.2. Rare earth element (REE) abundances along with Th, Rb (ppm) and chondrite normalized ratios in selected samples from Porayar borehole.

Sample	Depth(cm)	La	Ce	Nd	Sm	Eu	Gd	Dy	Yb	Lu	ΣREE	Sc	Co	Th	Rb	$(La/Yb)_N$	$(Ce/Yb)_N$	$(Eu^*)_N$	$(La/Sm)_N$	$(GD/Yb)_N$	$(Ce/Sm)_N$
PR 283	283	16.5	28.7	12.1	2.7	1.0	2.2	1.8	1.1	0.2	66.2	8.0	14.3	4.0	77.8	10.3	6.9	1.2	3.8	1.6	2.6
PR 329	329	31.3	47.4	23.4	4.0	1.3	4.0	3.3	2.1	1.0	117.7	12.0	20.4	6.1	88.5	10.0	5.8	1.0	4.9	1.5	2.9
PR 426	426	12.5	19.6	7.9	1.8	0.8	1.4	1.2	0.7	0.1	46.0	4.5	7.3	1.7	70.7	13.0	7.9	1.6	4.5	1.7	2.7
PR 548	548	52.3	96.5	40.1	7.0	2.1	6.7	5.8	3.1	0.4	214.0	13.8	24.4	6.5	104.5	11.4	8.1	0.9	4.6	1.7	3.3
PR 645	645	44.4	90.4	35.4	7.1	1.8	6.0	5.0	3.2	0.5	193.8	12.6	24.4	5.2	95.9	9.5	7.5	0.8	3.9	1.5	3.1
PR 775	775	47.2	89.6	39.2	7.2	1.8	7.6	5.5	3.1	0.6	201.9	17.1	26.6	8.7	135.4	10.3	7.6	0.7	4.1	2.0	3.0
PR 831	831	60.2	124.6	51.9	9.6	2.4	9.2	7.3	4.3	0.7	270.2	27.4	44.0	12.5	202.7	9.4	7.5	0.8	3.9	1.7	3.1
PR 842	842	37.1	73.8	31.4	6.5	1.4	5.9	4.4	2.6	0.4	163.7	19.8	34.1	8.9	135.0	9.6	7.4	0.7	3.6	1.8	2.7
PR 945	945	42.6	83.6	36.6	7.3	1.9	6.1	4.9	2.7	0.6	186.2	21.6	35.7	9.8	157.2	10.8	8.2	0.9	3.6	1.8	2.8
PR 1029	1029	18.3	34.1	14.2	3.1	0.9	2.5	2.0	1.1	0.2	76.5	9.5	16.7	5.6	78.6	11.4	8.2	1.0	3.6	1.9	2.6
PR 1170	1170	28.3	55.4	22.8	5.0	1.4	4.0	3.0	2.0	0.5	122.3	13.9	22.4	7.1	107.6	9.8	7.4	1.0	3.6	1.7	2.7
PR 1226	1226	28.2	50.1	22.2	4.9	1.4	4.0	3.1	2.2	0.5	116.6	n.d	n.d	n.d	n.d	8.9	6.1	1.0	3.6	1.5	2.5
PR 1279	1279	21.0	36.2	16.2	3.8	1.2	3.0	2.2	1.6	0.4	85.5	8.9	15.5	5.6	77.2	9.1	6.1	1.1	3.5	1.5	2.3
PR 1351	1351	21.2	40.4	16.5	3.5	1.1	2.7	2.4	1.5	0.3	89.7	10.5	17.3	4.8	70.9	9.5	7.0	1.0	3.7	1.4	2.7
PR 1453	1453	30.0	49.6	23.7	5.1	1.6	4.5	3.4	2.4	0.5	120.8	11.9	23.3	6.0	64.9	8.4	5.3	1.0	3.7	1.5	2.4
PR 1483	1483	30.4	53.8	23.7	5.3	1.6	4.5	3.5	2.4	0.6	125.9	n.d	n.d	n.d	n.d	8.6	5.9	1.0	3.6	1.5	2.4
PR 1573	1573	28.8	54.1	24.2	4.9	1.2	3.9	3.1	2.0	0.4	122.7	n.d	n.d	n.d	n.d	9.9	7.2	0.9	3.7	1.6	2.7
PR 1643	1643	36.3	61.4	25.8	5.0	1.5	4.1	3.0	2.3	0.2	139.5	12.5	16.8	6.6	68.5	10.5	6.9	1.0	4.6	1.4	3.0
PR 1718	1718	21.2	37.7	16.1	3.7	1.1	3.0	2.2	1.7	0.4	87.1	12.5	15.6	7.2	47.5	8.7	6.0	1.0	3.6	1.5	2.5
PR 1785	1785	30.3	47.0	25.2	5.2	1.3	4.6	3.6	1.8	0.3	119.3	n.d	n.d	n.d	n.d	11.6	7.0	0.8	3.6	2.1	2.2
PR 1833	1833	37.0	83.9	30.2	6.5	1.7	5.6	4.4	2.8	0.6	172.7	13.9	29.3	6.8	85.0	9.0	7.9	0.9	3.6	1.6	3.1
PR 1863	1863	49.4	95.8	41.9	8.6	2.4	7.9	5.8	3.2	0.6	215.5	24.3	36.1	8.9	136.4	10.4	7.8	0.9	3.6	2.0	2.7
PR 1923	1923	35.9	68.8	28.7	6.0	1.6	4.9	4.0	2.2	0.4	152.4	19.3	32.1	7.6	122.8	11.3	8.3	0.9	3.8	1.8	2.8
PR 1953	1953	29.3	56.2	24.2	4.8	1.3	4.1	3.3	1.9	0.4	125.4	14.6	23.3	7.0	90.9	10.3	7.6	0.9	3.8	1.7	2.8
PR 2170	2170	27.6	58.5	23.2	4.8	1.2	3.8	3.2	2.0	0.3	124.6	12.6	14.7	4.8	65.2	9.2	7.5	0.8	3.6	1.5	2.9
PR 2348	2348	40.4	77.6	33.8	6.8	1.7	5.5	4.5	2.7	0.5	173.6	13.3	24.8	7.3	77.7	10.0	7.4	0.8	3.7	1.6	2.7

The common primary minerals like biotite, K feldspar and muscovite have relatively higher Rb/Sr ratios, while plagioclase, apatite, pyroxene and amphiboles have relatively lower Rb/Sr ratios.

The Sm and Nd are rare earth elements that are found in majority of minerals in silicates. One of the radioactive isotopes of Sm, ^{147}Sm, decays by alpha emission to stable ^{143}Nd. Sm and Nd are considered less mobile in various geochemical environments than Rb and Sr and hence the Sm-Nd isotopic system is considered more robust in sediments. The decay of ^{147}Sm to ^{143}Nd can be expressed in the form of an equation as follows:

$$^{147}_{62}\text{Sm} \rightarrow {}^{143}_{60}\text{Nd} + \alpha + Q \qquad \longrightarrow \qquad (5.3)$$

Where, α is the alpha particle and Q = 4.32 MeV/atom. Radiogenic growth of ^{143}Nd in rocks can be expressed relative to the stable non-radiogenic isotope ^{144}Nd as:

$$\frac{^{143}Nd}{^{144}Nd} = \left(\frac{^{143}Nd}{^{144}Nd}\right)_i + \frac{^{147}Sm}{^{144}Nd}\left(e^{\lambda t} - 1\right) \qquad \longrightarrow \qquad (5.4)$$

where, i represents the initial isotopic composition of Nd and $\boldsymbol{\lambda}$ is the decay constant of ^{147} Sm which is equal to 6.54 X $10^{-12}y^{-1}$ (Lugmair and Marti, 1978).

Sm/Nd ratios are comparatively higher for the common rock forming minerals like garnet, clinopyroxene and hornblend whereas olivine plagioclase and K-feldspar have lower Sm/Nd ratios than chondrite. DePaolo and Wasserburg (1976) observed that the initial ^{143}Nd/^{144}Nd. ratios of the Archean terrestrial rocks were consistent with the evolution line of the Chondritic Uniform Reservoir (CHUR) in a plot of age vs initial ^{143}Nd/^{144}Nd. Sm and Nd have very similar geochemical properties and undergo only slight relative fractionation during crystal-liquid processes. Also the decay constant for decay of ^{147}Sm to ^{143}Nd is very small. DePaolo and Wasserburg (1976) therefore developed a notation where by initial ^{143}Nd/^{144}Nd ratio could be represented in parts per 10^{4} deviations from the CHUR evolution line, termed epsilon units (εNd) which can be expressed as:

$$\varepsilon_{Nd}^{0} = \left[\frac{\left(\frac{^{143}Nd}{^{144}Nd}\right)_s}{\left(\frac{^{143}Nd}{^{144}Nd}\right)^{0}_{CHUR}} - 1\right] \times 10^4 \longrightarrow \quad (5.5)$$

Where $(^{143}Nd / ^{144}Nd)_s$ is the ratio measured in the sample today and $(^{143}Nd / ^{144}Nd)^0_{CHUR}$ is the present day $^{143}Nd/^{144}Nd$ in the CHUR (Chondritic Uniform Reservoir), which represents a bulk earth Nd isotopic composition whose value for the present day is given as 0.512638 (Hamilton *et al* 1983).

A 'model age' can be calculated from the $^{143}Nd/^{144}Nd$ and $^{147}Sm/^{144}Nd$ ratios of crustal rocks which reflect the time elapsed since the precursor first separated from the mantel. Faure (1986), McCulloch and Wasserburg (1978) indicated that since the Sm/Nd ratios of the sediments are not appreciably altered during weathering, transport, deposition and diagenesis, the Sm/Nd model dates calculated relative to CHUR or Depleted Mantle reflects the ages of the rocks from which they were derived and may be helpful in identifying their sources. As T_{DM} model ages, are considered as a more accurate indication of 'crustal formation age' than T_{CHUR} ages, the T_{DM} ages are widely used in provenance studies. It can be calculated as follows using present day depleted mantel values of $^{147}Sm/^{144}Nd = 0.2137$, $^{143}Nd/^{144}Nd = 0.51315$ (White., 2007) and decay constant of 6.54 X 10^{-12} y-1.

$$T_{DM} = \frac{1}{\lambda}\, 1n\left[1 + \frac{\left(\frac{^{143}Nd}{^{144}Nd}\right)_{sample} - \left(\frac{^{143}Nd}{^{144}Nd}\right)_{DM}}{\left(\frac{^{147}Sm}{^{144}Nd}\right)_{sample} - \left(\frac{^{147}Sm}{^{144}Nd}\right)_{DM}}\right] \longrightarrow \quad (5.7)$$

The deviations of the present ratio of Sm-Nd in samples from the bulk earth values is expressed in parameter f defined as:

$$f_{Sm/Nd} = \left[\left(\frac{\left(\frac{^{147}Sm}{^{144}Nd}\right)_s}{\left(\frac{^{147}Sm}{^{144}Nd}\right)_{CHUR}}\right) - 1\right] \longrightarrow \quad (5.8)$$

Where $\left(\frac{^{147}Sm}{^{144}Nd}\right)_s$ is the ratio in the sample and $\left(\frac{^{147}Sm}{^{144}Nd}\right)_{CHUR}$ is the ratio in the CHUR (Chondritic Uniform Reservoir). $\left(\frac{^{147}Sm}{^{144}Nd}\right)_{CHUR} = 0.1967$ (Hamilton et al., 1983). Positive values ($f_{Sm/Nd}>0$) indicate higher Sm/Nd ratios than the CHUR.

In the present study the sediments were subjected to 7 step sequential extraction procedure of Leleyter and Probst, (1999). The Sr isotopic measurements were carried out on four leachate fractions (Exchangeable, Carbonate, Fe-Mn and organic phases) and the residual silicate phase. Nd isotopic measurement was carried out only in the residual silicate phase. The detail of extraction process is given in chapter 3.

5.2.2 Sr and Nd isotopic compositions in residual:

The Sr and Nd concentrations in the residual phase of sediments from Uttrangudi core range are presented in (Table 5.3). The $^{87}Sr/^{86}Sr$ values lies between 0.71268 and 0.71901 and $^{143}Nd/^{144}Nd$ ranges between 0.510909 and 0.511316. The measured εNd_0 values vary from -25.78 to -33.72 with Nd model ages varying from 2.15 to 3.16 Ga**.** Sr and Nd isotopic composition of residual silicate phase of sediments from Porayar core are presented in (Table 5.4). The measured εNd_o and $^{87}Sr/^{86}Sr$ values range between -24.14 to - 33.74 and 0.712009 to 0.721514 respectively and $^{143}Nd/^{144}Nd$ ranges between 0.510908 and 0.5114.

5 .2.3 $^{87}Sr/^{86}Sr$ in leachate fraction:

The $^{87}Sr/^{86}Sr$ for four leachates of sediments from Uttrangudi core (i) exchangeable phase (Exch) (ii) carbonate phase (Carb), (iii) Fe-Mn phase and (iv) Organic phase (ORG) range between 0.71137 to 0.71348, 0.71428 to 0.71428, 0.71143 to 0.71497 and 0.71128 to 0.71544 respectively (Table 5.5).

Similarly the $^{87}Sr/^{86}Sr$ ratio measured in carbonate, Fe-Mn and organic phases in sediments from Porayar core ranges between 0.708181 to 0.714737, 0.709610 to 0.714816 and 0.709002 to 0.711886 respectively (Table 5.6).

Table 5.3: Rb-Sr and Sm-Nd isotope data for residual silcate fraction of sediments Uttrangudi borehole. An uncertainty of 0.6 % (1σ) was assigned for the calculations of $^{87}Rb/^{86}Sr$ and $1/^{86}$ Sr ratios. An uncertainty of 0.5% (1σ) was assigned for the calculation of $^{147}Sm/^{144}Nd$. Uncertainties for $^{87}Sr/^{86}Sr$ and $^{143}Nd/^{144}Nd$ are expressed as Standard Error (SE).

Sample	Depth(m)	87Rb/86Sr	$^{87}Sr/^{86}Sr$	± SE	Rb	Sr	$^{147}Sm/^{144}Nd$	$^{143}Nd/^{144}Nd$	± SE	Sm(conc)	Nd(conc)	eNd_o	fSm/Nd	TDM
UG 83	83	1.0553	0.715734	± 3	2.6	159.8	0.0903	0.511210	± 1.4	2.56	15.0	-27.9	-0.54	2.4
UG 185	185	1.3575	0.717570	± 4.2	3.0	165.5	0.0872	0.511275	± 1.3	3.05	18.5	-26.6	-0.56	2.2
UG 226	226	n.d	0.719012	± 4.2	n.d	n.d	0.6983	0.511249	± 7.7	n.d	n.d	-27.1	n.d	n.d
UG 240	240	1.4500	0.717818	± 4.5	3.3	151.6	0.0919	0.511268	± 1.4	3.30	19.0	-26.7	-0.53	2.3
UG 380	380	0.8363	0.712958	± 3	1.2	117.6	0.0880	0.511083	±1.5	1.21	7.3	-30.3	-0.55	2.5
UG 457	457	0.5269	0.714052	± 5	5.0	467.8	0.0857	0.511211	± 2.0	5.05	31.2	-27.8	-0.56	2.3
UG 546	546	n.d	0.714746	± 3.3	2.1	n.d	n.d	0.511316	± 5.5	2.13	n.d	-25.8	n.d	n.d
UG 650	650	1.9834	0.712891	± 3	0.9	106.4	0.0772	0.511179	± 3.0	0.85	5.8	-28.5	-0.61	2.2
UG 815	815	0.3974	0.712996	± 3	3.6	186.8	0.1023	0.511222	± 2	3.58	18.5	-27.6	-0.48	2.6
UG 1010	1010	0.9125	0.712685	± 4	1.8	129.6	0.0872	0.511228	± 2	1.77	10.8	-27.5	-0.56	2.3
UG1200	1200	0.1957	0.713042	± 7.2	0.7	150.9	0.0903	0.511152	± 2.7	0.67	3.9	-29.0	-0.54	2.5
UG 1430	1430	3.2893	0.714151	± 3	0.5	4.8	0.0793	0.511140	± 1.8	0.46	3.0	-29.2	-0.60	2.3
UG 1510	1510	21.1053	0.715334	± 1.7	0.4	8.0	0.0691	0.510909	± 4.3	0.36	2.7	-33.7	-0.65	2.4
UG 1703	1703	0.8963	0.713782	± 6.3	0.3	97.8	0.0694	0.510911	± 9	0.29	2.2	-33.7	-0.65	2.4
UG1912	1912	1.2920	0.713781	± 2.4	0.4	80.5	0.0793	0.511034	± 2.7	0.38	2.6	-31.3	-0.60	2.4
UG 2098	2098	6.0289	0.713871	± 1.5	0.2	12.6	0.1234	0.511263	± 5.0	0.23	1.0	-26.8	-0.37	3.2
UG 2245	2245	6.7754	0.715297	± 7.3	0.4	7.1	0.0961	0.51122	± 3.5	0.41	2.2	-27.7	-0.51	2.5
UG 2388	2388	0.5843	0.716031	± 5.3	0.1	12.9	0.0844	0.511313	± 7.7	0.14	0.9	-25.8	-0.57	2.2

Table 5.4: Rb-Sr and Sm-Nd isotope data for residual silcate fraction of sediment samples from Porayar borehole. An uncertainty of 0.6 % (1σ) was assigned for the calculations of $^{87}Rb/^{86}Sr$ and $1/^{86}$ Sr ratios. An uncertainty of 0.5% (1σ) was assigned for the calculation of $^{147}Sm/^{144}Nd$. Uncertainties for $^{87}Sr/^{86}Sr$ and $^{143}Nd/^{144}Nd$ are expressed as Standard Error (SE).

Sample Name	Depth(cm)	87Rb/86Sr	$^{87}Sr/^{86}Sr$	± SE	Rb	Sr	$^{147}Sm/^{144}Nd$	$^{143}Nd/^{144}Nd$	± SE	Sm(conc)	Nd(conc)	eNd_o	fSm/Nd	TDM
PR 280	280	0.2350942	0.712903	± 5.3	16.0	196.54		0.511103	± 4.8	1.09	2.91	-29.94	n.d	n.d
PR 426	426	0.2208421	0.7134009	± 1.2	38.3	502.65	0.10	0.5114	± 4	1.57	8.69	-24.15	-0.5138125	2.25
PR 647	647	0.4170895	0.713496	± 5.4	59.3	411.78	0.09	0.511012	± 5	3.08	17.59	-31.72	-0.5291647	2.68
PR 842	842	1.6031682	0.718192	± 5.2	7.8	14.04	0.09	0.511287	± 4.2	n.d	1.11	-26.35	-0.5315983	2.33
PR 1029	1029	0.2961683	0.713493	± 6.3	34.8	339.86	S.D	0.510908	± 4.2	0.19	16.85	-33.75	n.d	n.d
PR 1351	1351	0.4106242	0.712976	± 5.4	0.6	3.91	0.10	0.511105	± 8.3	0.02	0.10	-29.90	-0.5059223	2.66
PR 1573	1573	0.2762633	0.713298	± 5.4	3.8	39.62	0.09	0.510981	± 4.1	0.09	0.56	-32.32	-0.5494451	2.63
PR 1785	1785	0.6498292	0.721513	± 4.6	4.6	20.37	0.09	0.511176	± 3.6	0.14	0.82	-28.52	-0.5349244	2.45
PR 1923	1923	0.6826609	0.713347	± 4.1	54.9	232.66	0.09	0.511187	± 2.1	2.22	13.11	-28.30	-0.5445784	2.40
PR 1953	1953	0.3531921	0.712311	± 4.1	44.1	361.23	0.09	0.511086	± 2.5	2.16	12.91	-30.27	-0.5505164	2.50
PR 2173	2173	0.4178332	0.712546	± 3.3	49.0	339.33	0.09	0.511026	± 2.3	3.04	18.33	-31.45	-0.5538969	2.56
PR 2348	2348	0.2899472	0.7120089	± 6.6	44.0	439.64	0.09	0.510956	± 1.3	3.65	22.08	-32.81	-0.5547982	2.64

Table 5.5: $^{87}Sr/^{86}Sr$ ratios with errors (2σ) determined on Exchangeable (Exch), Carbonate (CARB), Fe-Mn phase (Fe-Mn) and Organic (ORG) leachates of sediments from Uttrangudi borehole from Cauvery delta. . Uncertainties for $^{87}Sr/^{86}Sr$ is expressed as Standard Error (SE).

Sample Name	Depth(cm)	Exch	± SE	CARB	± SE	Fe-Mn	± SE	ORG	± SE
UG 83	83	0.713481	±2	0.71318	± 3.3	0.713698	± 10	0.715012	± 12
UG 185	185	0.71268	± 20	0.712613	± 11	0.712833	± 2.5	0.713401	± 9.2
UG 226	226	0.712657	± 4	0.713816	± 5.7	0.714025	± 7	0.714872	± 5
UG 240	240	0.712481	± 11	0.71257	± 5	0.712439	± 5.3	0.712576	± 7.5
UG 380	380	0.712361	± 18	0.71428	± 5	0.714971	± 5	0.715251	± 2
UG 457	457	0.711867	± 11	0.711868	± 7	0.711984	± 3	0.713651	± 1.6
UG 546	546	0.711933	± 3.5	0.714179	± 5.3	0.712905	± 4.7	0.715437	± 4.5
UG 650	650	0.711661	± 10	n.d		0.711849	± 3	0.712231	± 2.7
UG 815	815	0.711576	± 6	0.711548	± 3	0.711715	± 3	0.712291	± 2.3
UG 1010	1010	0.711379	± 9	0.711458	± 14	0.711534	± 6.1	0.711281	± 1.3
UG1200	1200	0.711431	± 2.4	0.71137	± 8	0.71197	± 1.2	0.711504	± 8
UG 1430	1430	0.711431	± 1.4	n.d		0.711927	± 4.4	0.712221	± 3
UG 1510	1510	0.711841	± 7	n.d		0.711782	± 6	0.711333	± 6
UG 1703	1703	0.711643	± 7.2	n.d		0.712148	± 7.4	0.712531	± 8
UG1912	1912	0.711433	± 7	n.d		0.711433	± 4.6	0.712318	± 7
UG 2098	2098	0.711454	± 8.4	0.71145	± 4.1	0.711568	± 7	0.712111	± 3
UG 2245	2245	0.711531	± 1.4	0.711958	± 9.2	0.71153	± 7.2	0.711875	± 8
UG 2388	2388	0.711701	± 6	0.711511	± 2	0.711444	± 9	0.712721	± 2.4

Table 5.6: $^{87}Sr/^{86}Sr$ ratios with errors (2σ) determined on Exchangeable (Exch), Carbonate (CARB), Fe-Mn phase (Fe-Mn) and Organic (ORG) leachates of sediments from Porayar borehole from Cauvery delta. Uncertainties for $^{87}Sr/^{86}Sr$ is expressed as Standard Error (SE).

Sample Name	Depth	CARB	± SE	Fe-Mn	± SE	ORG	± SE
PR 280	280	0.714736	± 4	0.714629	± 4	0.711665	± 3.4
PR 426	426	0.70993	± 6.2	0.7138	± 1.1	0.710718	± 4
PR 647	647	0.709934	± 7.4	0.714815	± 4.1	0.709841	± 7.6
PR 842	842	0.710263	± 7.7	0.712431	± 3.7	0.710598	± 4
PR 1029	1029	0.710731	± 5.2	0.712356	± 4.6	0.710028	± 4
PR 1351	1351	0.710193	± 4.7	0.710636	± 3.8	0.711714	± 5.7
PR 1573	1573	0.709615	± 1.2	0.712464	± 5.2	0.710652	± 5.3
PR 1785	1785	0.709591	± 1.1	0.70961	± 5.3	0.710151	± 7
PR 1923	1923	0.710661	± 2.9	n.d		0.710676	± 4.8
PR 1953	1953	0.710061	± 5.8	0.710669	± 8.4	0.71072	± 7.3
PR 2173	2173	0.710801	± 2.4	0.711999	± 6.6	0.711885	± 4.6
PR 2348	2348	0.708181	± 5.9	0.710136	± 8.7	0.709002	± 4.5

5.3 Discussion

Chemical composition of the clastic sediments is the net result of a number of geological factors. This may include other than source rocks, the intensity of their chemical weathering, rate of sediment supply, sorting and post depositional changes(Campos Alvarez and Roser 2007; Bhatia, 1983;Condie et al., 1995; Cullers, 1987, 1994, 2000; Huntsman-Mapila et al., 2009; McLennan et al., 1990, 1993). Each of these factors must be evaluated before drawing conclusions on the nature of source rocks and tectonics of the region. In the following discussion we have first considered the compositional features of sediments that may result from chemical weathering and fluvial process of sorting. Then we have tried to determine the provenance and evaluate the influence of climate and relief in the area on the varying sediment input of the sediment from different parts of the catchment region.

5.3.1 Textural and mineralogical control on REE :

The depth wise plot of individual REE and ∑REE along with the texture for both Uttrangudi and Porayar sediments are shown in figures 5.2 and 5.3. All the REE's are observed to show good positive correlation among them and with silt (%) and negative correlation with sand (%). It is observed that the finer sediments are having higher concentration of REE. The good positive correlation of various REE's with silt and clay and their negative correlation with sand percentage would suggest that in the studied sediments majority of the REE holding mineral phases are concentrated in the silt fraction and REE's are also held in clays. Thus to the first approximation the first order variation in concentration of REE in the studied sediments is because of the varying percentage of sand which in present case acts as a diluting agent for REE.

On comparison of REE's from both the cores with other compositional variables of the sediments, it is observed that sediments from both the cores show some similarities and differences. The REE's in Uttrangudi sediments show good postive correlation with Th and Y; moderate positive correlation with Al, Fe, Mg, Mn, Ni, Cr, Sc, Co, and poor correlation with Ti (Table 5.7). In contrast the REE's in Porayar sediments show strong positive correlation with Al, Fe, Mg, Ti, Th, Y, Ni, Cr, Sc and Co and moderate correlation with Mn (Table 5.8). Good to moderate correlation with Al, Fe, Mg, Ni, Cr, Sc and Co in both the cores suggest, to some extent, the control of mafic minerals and clay. Strong correlation of REE's with Ti, Th and Y in Porayar sediments may suggest control of Allanite, Titanite, Monazite and zircon. In contrast poor correlation of REE's with Ti and their good correlation with Th and Y in Uttrangudi sediments suggest control of monazite and zircon.

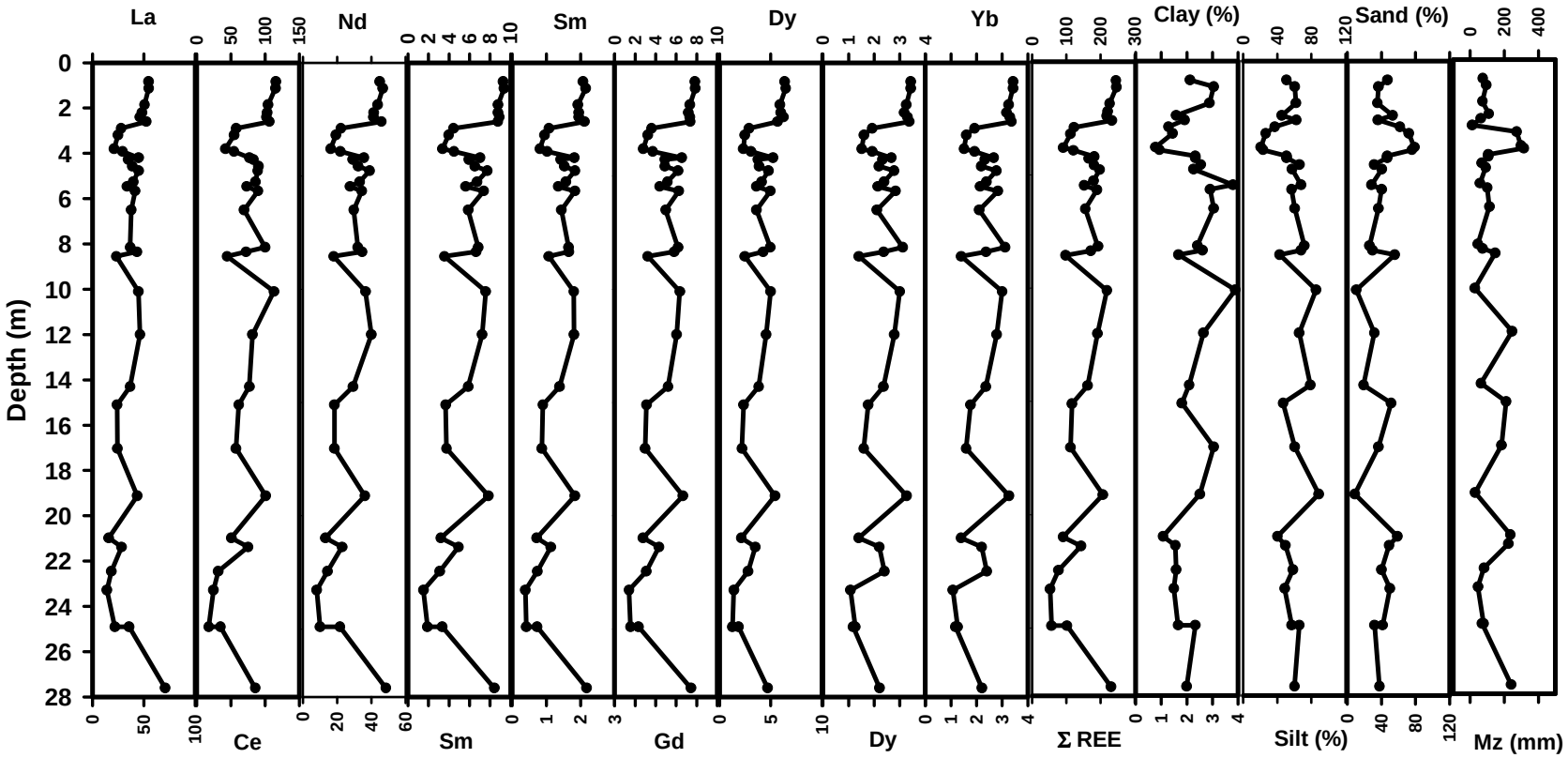

Fig 5.2: The depth wise plot of individual REE's and Total REE (∑ REE) along with the texture for Uttrangudi core. All the REE's are observed to show good positive correlation among them and with Silt (%). It is also observed that the finer sediments are having higher concentration of REE.

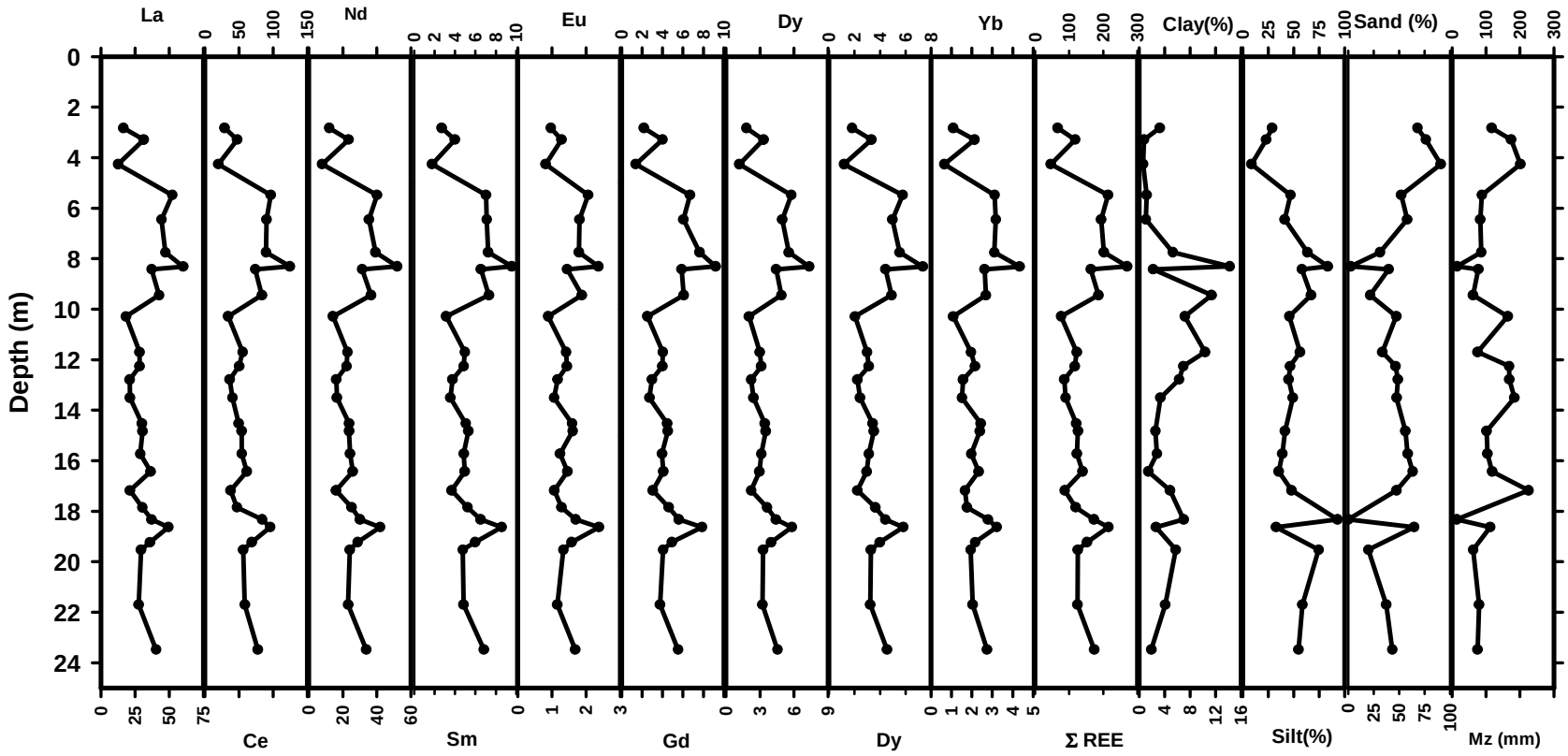

Fig 5.3: The depth wise plot of individual REE and Total REE (∑ REE) along with the texture in sediments from Porayar borehole. All the REE's are observed to show good positive correlation among them and with Silt (%).

Table 5.7: Correlation matrix for major and trace element concentration and ∑REE of samples from Uttrangudi borehole.

	SiO_2	$Al2O_3$	TiO_2	Fe_2O_3	MgO	MnO	Ca*O	$Na*_2O$	K_2O	P_2O_5	*Ba*	*Sr*	*Cr*	*Ni*	*Sc*	*Co*	*Th*	*U*	*Y*	*Rb*	*La*	*Ce*	*Nd*	*Sm*	*Eu*	*Gd*	*Dy*	*Yb*	*Lu*	*∑REE*
SiO_2	1.00																													
$Al2O_3$	-0.98	1.00																												
TiO_2	-0.73	0.68	1.00																											
Fe_2O_3	-0.97	0.97	0.76	1.00																										
MgO	-0.93	0.88	0.63	0.88	1.00																									
MnO	-0.58	0.54	0.48	0.56	0.59	1.00																								
Ca*O	-0.53	0.39	0.37	0.39	0.62	0.38	1.00																							
$Na*_2O$	-0.82	0.73	0.56	0.70	0.78	0.44	0.77	1.00																						
K_2O	-0.86	0.78	0.62	0.75	0.84	0.50	0.71	0.88	1.00																					
P_2O_5	-0.80	0.76	0.70	0.78	0.67	0.36	0.38	0.80	0.72	1.00																				
Ba	-0.59	0.52	0.44	0.50	0.66	0.78	0.61	0.61	0.69	0.35	1.00																			
Sr	-0.56	0.45	0.31	0.43	0.68	0.46	0.90	0.67	0.71	0.29	0.71	1.00																		
Cr	-0.85	0.88	0.57	0.84	0.72	0.47	0.25	0.67	0.69	0.67	0.50	0.27	1.00																	
Ni	-0.85	0.87	0.52	0.88	0.76	0.51	0.27	0.54	0.62	0.56	0.44	0.36	0.83	1.00																
Sc	-0.75	0.75	0.44	0.76	0.79	0.45	0.26	0.50	0.61	0.59	0.38	0.34	0.66	0.72	1.00															
Co	-0.52	0.50	0.25	0.52	0.59	0.63	0.24	0.40	0.46	0.40	0.54	0.29	0.41	0.50	0.77	1.00														
Th	-0.75	0.77	0.61	0.77	0.70	0.41	0.17	0.39	0.64	0.47	0.47	0.26	0.74	0.76	0.65	0.42	1.00													
U	-0.71	0.69	0.42	0.73	0.77	0.46	0.35	0.40	0.65	0.42	0.46	0.47	0.54	0.79	0.73	0.55	0.76	1.00												
Y	-0.76	0.76	0.50	0.76	0.65	0.56	0.28	0.57	0.67	0.57	0.60	0.39	0.72	0.79	0.62	0.56	0.72	0.71	1.00											
Rb	-0.73	0.67	0.45	0.66	0.81	0.48	0.52	0.66	0.82	0.64	0.54	0.55	0.53	0.54	0.84	0.74	0.57	0.73	0.58	1.00										
La	-0.55	0.53	0.32	0.54	0.57	0.45	0.36	0.47	0.50	0.24	0.57	0.42	0.58	0.51	0.56	0.46	0.71	0.63	0.64	0.53	1.00									
Ce	-0.65	0.63	0.43	0.63	0.63	0.68	0.38	0.49	0.61	0.33	0.70	0.49	0.62	0.65	0.55	0.59	0.71	0.66	0.79	0.56	0.81	1.00								
Nd	-0.65	0.62	0.41	0.62	0.65	0.57	0.43	0.56	0.62	0.33	0.68	0.52	0.65	0.60	0.59	0.52	0.71	0.66	0.76	0.59	0.97	0.91	1.00							
Sm	-0.69	0.66	0.44	0.67	0.68	0.66	0.43	0.57	0.65	0.38	0.72	0.52	0.68	0.67	0.62	0.59	0.73	0.70	0.82	0.62	0.92	0.95	0.98	1.00						
Eu	-0.64	0.59	0.39	0.61	0.65	0.63	0.48	0.55	0.63	0.32	0.73	0.58	0.59	0.60	0.58	0.56	0.68	0.69	0.77	0.61	0.93	0.93	0.98	0.99	1.00					
Gd	-0.66	0.63	0.42	0.65	0.65	0.64	0.41	0.55	0.62	0.37	0.72	0.52	0.65	0.66	0.59	0.58	0.71	0.69	0.83	0.57	0.91	0.94	0.97	0.99	0.99	1.00				
Dy	-0.72	0.70	0.48	0.71	0.68	0.70	0.40	0.57	0.66	0.43	0.74	0.50	0.72	0.73	0.61	0.59	0.74	0.70	0.87	0.59	0.85	0.94	0.94	0.98	0.96	0.98	1.00			
Yb	-0.69	0.68	0.51	0.70	0.64	0.70	0.32	0.52	0.61	0.44	0.70	0.46	0.72	0.75	0.60	0.55	0.72	0.66	0.83	0.52	0.75	0.91	0.86	0.92	0.89	0.93	0.96	1.00		
Lu	-0.31	0.32	0.17	0.35	0.26	0.49	0.02	0.15	0.22	0.12	0.39	0.20	0.44	0.54	0.38	0.35	0.34	0.38	0.51	0.17	0.46	0.65	0.56	0.62	0.60	0.64	0.65	0.78	1.00	
∑REE	-0.65	0.63	0.42	0.64	0.65	0.63	0.41	0.53	0.61	0.33	0.70	0.50	0.65	0.64	0.58	0.57	0.73	0.68	0.78	0.58	0.93	0.97	0.98	0.99	0.98	0.98	0.96	0.90	0.62	1.00

Table 5.8: Correlation matrix for major and trace element concentration and ∑REE of samples from Porayar borehole.

	SiO_2	$Al2O_3$	TiO_2	Fe_2O_3	MgO	MnO	Ca*O	$Na*_2O$	K_2O	P_2O_5	Mz	Ba	Sr	Cr	Ni	Sc	Co	Th	Y	Rb	La	Ce	Nd	Sm	Eu	Gd	Dy	Yb	Lu	∑REE
SiO_2	1.00																													
$Al2O_3$	-0.98	1.00																												
TiO_2	-0.77	0.73	1.00																											
Fe_2O_3	-0.92	0.89	0.84	1.00																										
MgO	-0.93	0.89	0.79	0.97	1.00																									
MnO	-0.66	0.61	0.62	0.73	0.74	1.00																								
Ca*O	0.20	-0.27	-0.26	-0.49	-0.40	-0.34	1.00																							
$Na*_2O$	0.26	-0.31	-0.47	-0.57	-0.52	-0.41	0.81	1.00																						
K_2O	-0.74	0.73	0.41	0.56	0.57	0.50	-0.10	0.08	1.00																					
P_2O_5	-0.31	0.30	-0.20	0.12	0.29	0.18	0.19	0.27	0.24	1.00																				
Mz	0.80	-0.76	-0.69	-0.74	-0.76	-0.65	0.04	0.23	-0.67	-0.15	1.00																			
Ba	0.33	-0.32	-0.45	-0.58	-0.50	-0.25	0.61	0.64	-0.05	0.21	0.12	1.00																		
Sr	0.31	-0.29	-0.38	-0.60	-0.52	-0.40	0.80	0.71	-0.11	0.19	0.14	0.88	1.00																	
Cr	-0.89	0.87	0.85	0.95	0.91	0.69	-0.43	-0.50	0.55	0.09	-0.79	-0.52	-0.53	1.00																
Ni	-0.80	0.79	0.58	0.80	0.86	0.63	-0.28	-0.44	0.40	0.43	-0.67	-0.29	-0.30	0.76	1.00															
Sc	-0.82	0.81	0.87	0.95	0.87	0.71	-0.55	-0.61	0.49	-0.14	-0.69	-0.55	-0.64	0.89	0.66	1.00														
Co	-0.83	0.81	0.83	0.93	0.88	0.82	-0.50	-0.58	0.58	-0.06	-0.79	-0.49	-0.61	0.88	0.64	0.95	1.00													
Th	-0.76	0.72	0.90	0.89	0.83	0.75	-0.40	-0.59	0.43	-0.22	-0.73	-0.51	-0.56	0.84	0.66	0.93	0.90	1.00												
Y	-0.84	0.79	0.88	0.88	0.83	0.74	-0.27	-0.41	0.53	0.00	-0.80	-0.29	-0.33	0.88	0.69	0.89	0.89	0.87	1.00											
Rb	-0.84	0.85	0.66	0.91	0.89	0.75	-0.57	-0.55	0.58	0.12	-0.64	-0.51	-0.63	0.79	0.74	0.88	0.88	0.83	0.73	1.00										
La	-0.88	0.81	0.83	0.86	0.87	0.66	-0.10	-0.30	0.51	0.23	-0.67	-0.37	-0.32	0.81	0.71	0.81	0.79	0.79	0.86	0.72	1.00									
Ce	-0.90	0.84	0.83	0.91	0.91	0.64	-0.20	-0.37	0.49	0.26	-0.67	-0.47	-0.41	0.86	0.75	0.83	0.80	0.79	0.85	0.76	0.98	1.00								
Nd	-0.88	0.82	0.85	0.89	0.89	0.69	-0.16	-0.36	0.51	0.18	-0.69	-0.43	-0.38	0.84	0.70	0.86	0.84	0.84	0.88	0.77	0.99	0.98	1.00							
Sm	-0.87	0.81	0.87	0.91	0.89	0.67	-0.22	-0.42	0.49	0.13	-0.72	-0.46	-0.41	0.86	0.69	0.88	0.87	0.84	0.91	0.77	0.96	0.97	0.98	1.00						
Eu	-0.87	0.82	0.81	0.85	0.84	0.56	-0.14	-0.31	0.54	0.17	-0.71	-0.30	-0.26	0.79	0.68	0.82	0.80	0.76	0.88	0.72	0.95	0.93	0.95	0.95	1.00					
Gd	-0.88	0.83	0.84	0.90	0.89	0.71	-0.22	-0.39	0.53	0.16	-0.70	-0.41	-0.40	0.85	0.70	0.87	0.86	0.84	0.90	0.80	0.97	0.97	0.99	0.98	0.95	1.00				
Dy	-0.89	0.84	0.82	0.90	0.90	0.70	-0.20	-0.37	0.53	0.21	-0.69	-0.43	-0.40	0.84	0.70	0.85	0.85	0.81	0.87	0.79	0.98	0.98	0.99	0.98	0.95	0.99	1.00			
Yb	-0.83	0.77	0.83	0.84	0.83	0.60	-0.13	-0.33	0.44	0.18	-0.63	-0.41	-0.33	0.79	0.65	0.80	0.78	0.79	0.86	0.70	0.96	0.96	0.96	0.96	0.94	0.96	0.96	1.00		
Lu	-0.48	0.46	0.53	0.49	0.48	0.26	-0.13	-0.23	0.33	-0.06	-0.29	-0.27	-0.25	0.37	0.15	0.53	0.54	0.53	0.45	0.51	0.58	0.53	0.58	0.56	0.60	0.61	0.60	0.65	1.00	
∑REE	-0.89	0.83	0.84	0.90	0.90	0.66	-0.17	-0.35	0.51	0.23	-0.68	-0.44	-0.38	0.85	0.73	0.84	0.82	0.81	0.87	0.76	0.99	1.00	1.00	0.98	0.95	0.98	0.99	0.97	0.57	1.00

Among the various LREE enriched mineral phases, addition of Monazite would lead to increase in total REE, LREE and $(La/Yb)_N$ ratios. In addition it would also lead to increase in $(Gd/Yb)_N$ ratios of the sediments. The REE in Uttrangudi sediments are observed to follow the above relation (Fig 5.4 a, b, d). The positive correlation among Gd_N and $(Gd/Yb)_N$ and$(La/Yb)_N$ and $(Gd/Yb)_N$ (Fig 5.4 e) also corroborates the control of monazite over the REE concentration in Uttrangudi sediments. Similar relations are observed for the Porayar sediments (Fig 5.5 a - i). Good positive correlation of Th with ∑ REE further supports control of monazite on REE in the studied sediments.

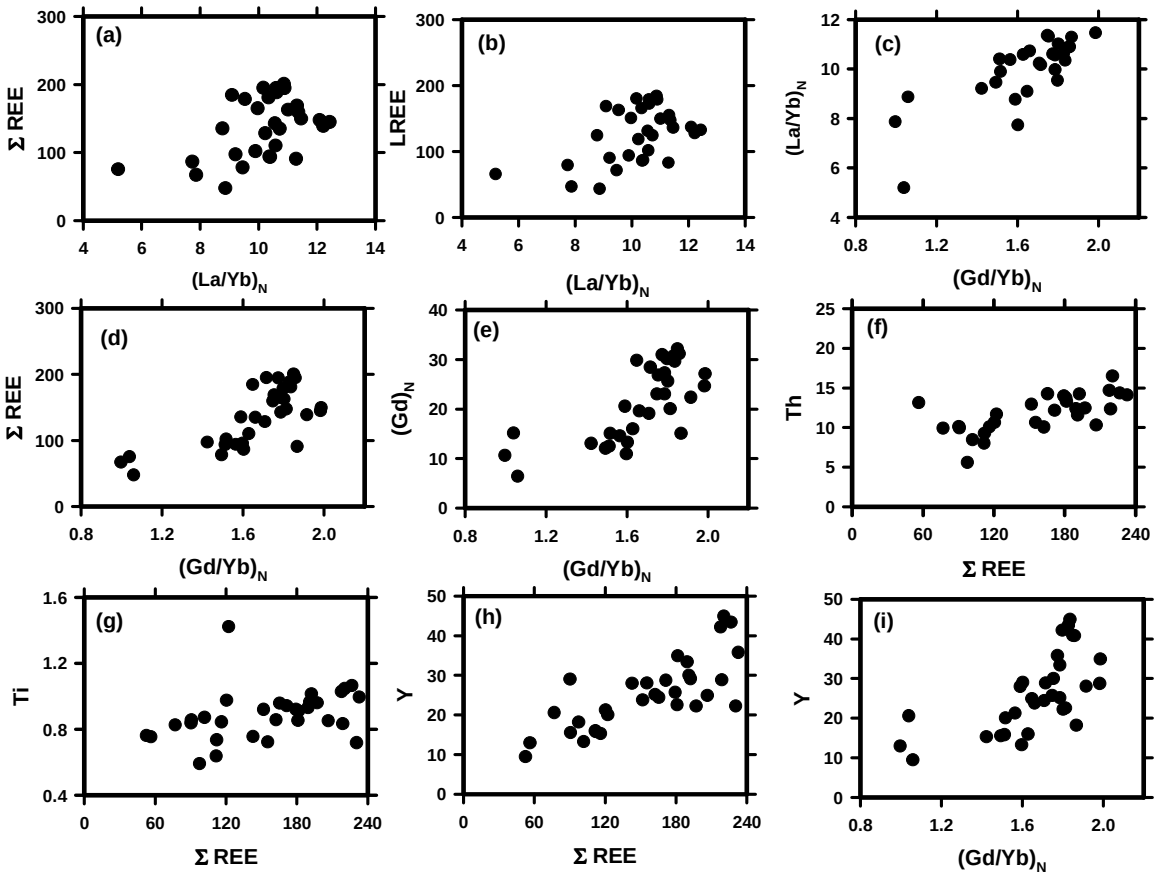

Figure 5.4: The bivariant plot of Ti, Th and Y with total REE, LREE and chondrite normalisedratios. The above correlations indicate control of Monazite, Allanite and titanite on the REE distribution in sediments from Uttrangudi as discussed in text.

.

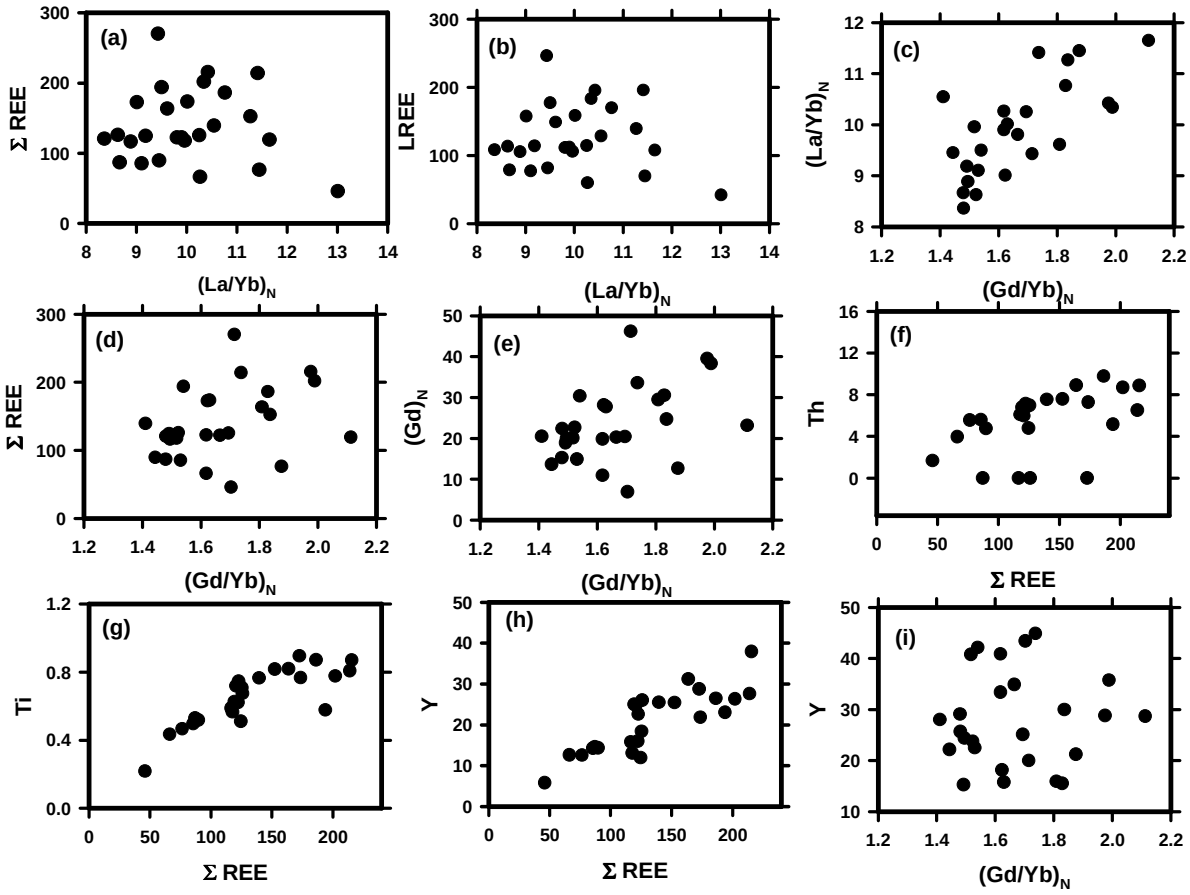

Figure 5.5: The bivariant plot of Ti, Th and Y with total REE, LREE and chondrite normalisedratios. The above correlations indicate control of Monazite, Allanite and titanite on the REE distribution in sediments from Porayar borehole sediments as discussed in text.

Ti and Y other than Th also show good positive correlation with ΣREE (Fig 5.4 g & h and Fig 5.5 g & h).This would suggest that other LREE enriched mineral phases particularly titanite and allanite have also contributed to the REE concentrations in the sediments. Strong positive correlation of Y with $(Gd/Yb)_N$ ratio, (Fig 5.4 i and Fig 5.5 i) would indicate the major contribution of Y from LREE bearing phase such as allanite. Since in case of HREE bearing minerals particularly zircon, the Yb concentration is expected to be higher, which may lower $(Gd/Yb)_N$ ratio. This should in turn result in development of negative correlation of $(Gd/Yb)_N$ with $(La/Yb)_{N..}$ Hence Y is also major element present in zircon, it should also show negative correlation of $(Gd/Yb)_N$ if it is

primarily contributed by zircon which is not the case in studied sediments. (Fig 5.4 c & i and Fig 5.5 c & i)

Thus as a first approximation we may conclude that the LREE enriched heavy mineral phases along with the mafic minerals have largely controlled the REE concentration and pattern in the sediments from both the studied locations.

5.3.2. Eu anomaly:

Eu systematic has been widely used to discriminate between Archean and Post-Archean sediments as it is believed to be inherited from the sediment sources (McLennan et al., 1980, 1993; Taylor and McLennan, 1985). Small Eu anomalies are usually attributed to be input of basic detritus, whereas large anomalies are related to felsic source (Taylor and McLennan., 1985; Cullers et al., 1987; Hassan et al., 1999; Cullers, 2000). According to McLennan et al. (1993) Archean sediments tend to have Eu anomalies higher than 0.85 and higher $(Gd/Yb)_N$ even more than 2.0. In contrast the sediments derived from the post Archean rocks tend to have Eu anomalies values lower than 0.85 and lower $(Gd/Yb)_N$. In the present study the sediments from both Uttrangudi and Porayar sites are plotted in the Eu/Eu* versus $(Gd/Yb)_N$ diagram (Fig.5.6 a and b). Sediments from both the locations show higher Eu/Eu* values of more than 0.72 and up to ~1.6. The Eu/Eu* value of Uttrangudi sediments ranges between 0.73 and 0.84 except one sample, which shows higher value of 0.96. The range of Eu/Eu* values in Porayar sediments is between 0.7 and 1.2, except one sample which shows value of 1.6. In general it is observed that Eu/Eu* values are higher in Porayar samples in comparison to Uttrangudi sediments. The $(Gd/Yb)_N$ shows similar range between 1.4 and 2 in sediments from both the locations except three samples from Uttrangudi location that show much lower value of around 1.0. It should be noted that in Eu/Eu* vs. $(Gd/Yb)_N$ diagram all samples plot above the field of UCC and PAAS. This is expected as the catchment of the Cauvery River dominantly comprises of Archean lithologies. It is noted that although the Uttrangudi and Porayar sediments show an overlap in the above diagram they differ primarily in their Eu/Eu* values.

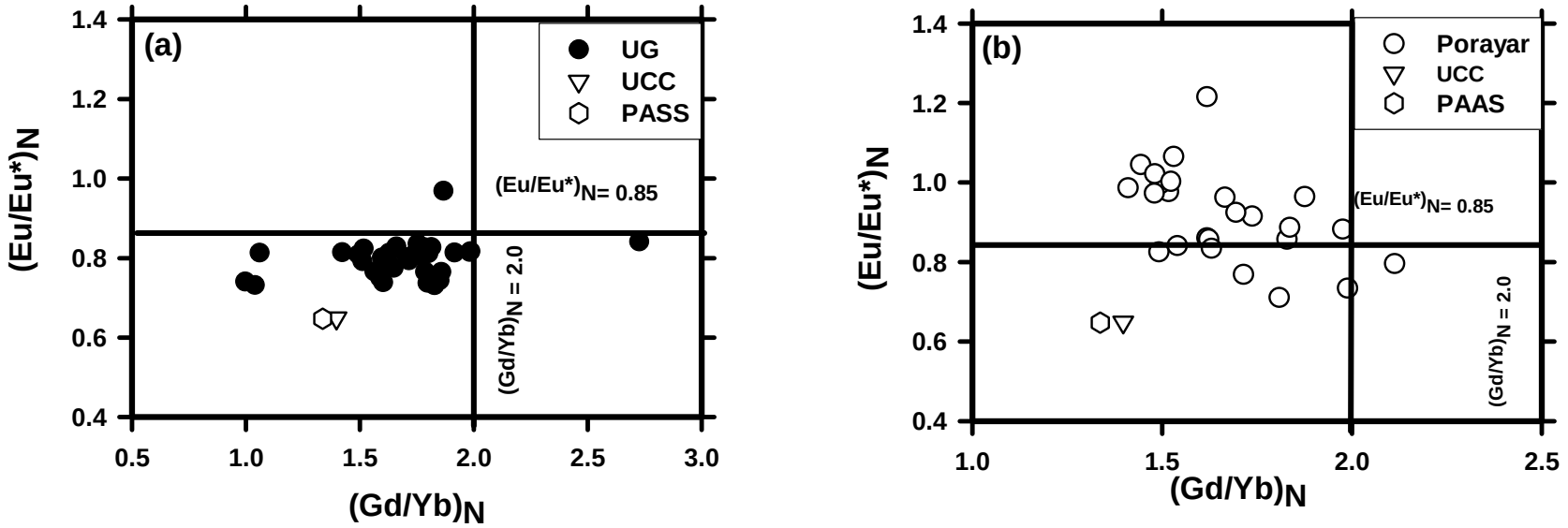

Figure 5.6: In the above plot sediments from both Uttrangudi and Porayar sites are plotted in the Eu/Eu* versus $(Gd/Yb)_N$ diagram (Fig.5.9a and b). Sediments from both the locations show higher Eu/Eu* values of more than 0.72 up to ~1.6. The Eu/Eu* value of Uttrangudi sediments ranges between 0.73 and 0.84 except one sample, which shows higher value of 0.96. The range of Eu/Eu* values in Porayar sediments is between 0.7 and1.2, except one sample which shows value of 1.6. It should be noted that all samples plot above the field of UCC and PAAS. This is expected as the catchment of the Cauvery River dominantly comprises of Archean lithologies. It is noted that although the Uttrangudi and Porayar sediments show an overlap in the above diagram they differ primarily in their Eu/Eu* values.

Further to evaluate the effect of weathering on Eu we have plotted the depth wise variation in Eu/Eu* values of sediments along with their CIA (Chemical Index of Alteration) from both the locations (5.7 a and 5.7 b). It is observed that in both the cores Eu/Eu* values show a significant anti correlation with the CIA values, particularly in Uttrangudi sediments. This would suggest that the Eu in sediments have been modified to different extent by the process of weathering effecting its loss and lowering of Eu/Eu* values. Eu is known to be mobile in Eu^{2+} state, whereas it remains immobile in Eu^{3+} state. Thus during weathering, Eu can get mobilized by chemical breakdown of feldspar only if the local environment has been reducing. But it is known that even if mobilized during weathering of rocks the REE get redistributed within the soil profile (Nesbit.,1979; 1989). Further on erosion the re-mixing of soil results in values similar to rock (Cullers et al. 1987). Other possibility is that Eu got mobilized from sediments after their deposition. This would imply post depositional weathering of feldspar under subsurface reducing conditions, where Eu^{3+} after their release got reduced to Eu^{2+}, and was carried away by ground water in dissolved state.

Further we have tried to evaluate the control of heavy mineral on Eu/Eu* value. In the present study as discussed earlier the trace elements Th, Y and Ti are found to be associated with the REE bearing heavy minerals such as monazite, allanite and titanite. For this we have plotted the depth wise variation trend of Th, Y and Ti with that of the Eu/Eu* (Fig 5.8 & 5.9). It is observed that like CIA, the above set of trace elements also exhibit negative co-relation with Eu/Eu* values. This would mean that enrichment of heavy minerals has resulted in relatively higher increase in LREE and HREE in comparison to Eu that is dominantly held in feldspars, which has resulted in decrease in value of Eu/Eu*.

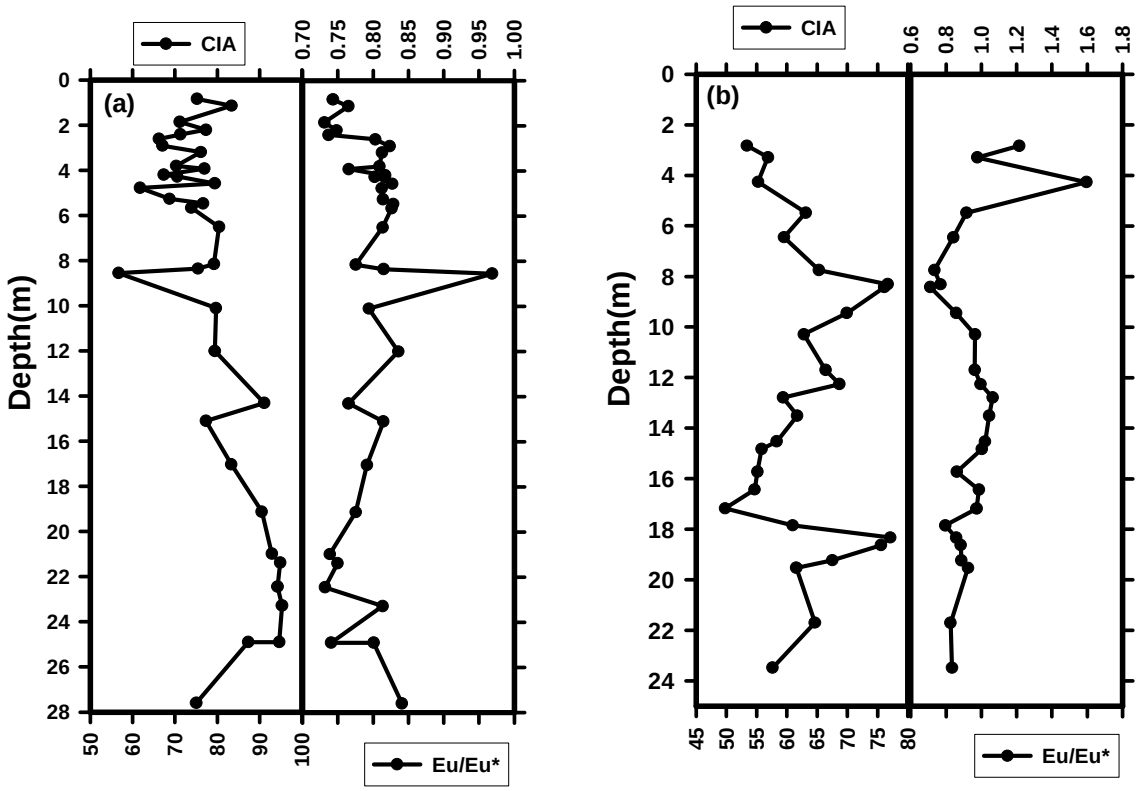

Figure 5.7 : The depth wise variation in Eu/Eu* values of **(a)** Uttrangudi and **(b)** Porayar sediments along with their CIA (Chemical Index of Weathering) from both the locations. Significant anti correlation Eu/Eu* with the CIA values, particularly in **(a)** suggest that the Eu in sediments have been modified by the process of weathering effecting its loss and lowering of Eu/Eu* values.

Thus we observe that Eu anomaly of sediments in the present study has been modified both by the variation in heavy mineral concentration and the weathering variability. The overall lower value of Eu/Eu* in Uttrangudi sediments in comparison to Porayar sediments, may thus be due higher degree of weathering exhibited by Uttrangudi sediments. This may partly be because of post depositional changes, as the Uttrangudi sediments are older (upper mid Pleistocene) for most of the part. Thus in absence of these changes we would expect the sediments to plot above their present position in Eu/Eu* vs $(Gd/Yb)_N$ diagram.

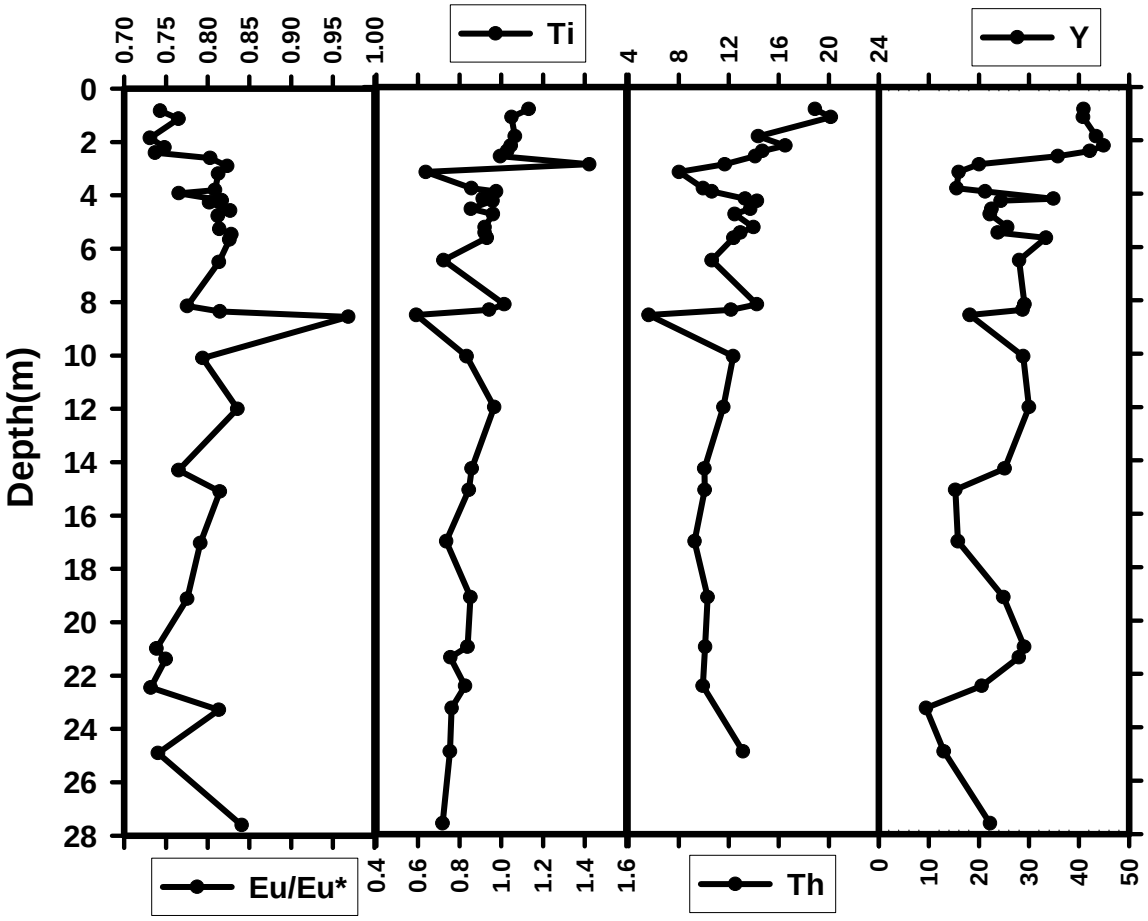

Figure 5.8: The depth wise variation trend of Th, Y and Ti with that of the Eu/Eu* for Uttrangudi sediments. The negative co-relation of these elements with Eu/Eu* values mean that enrichment of heavy minerals such as titanite, allanite and monazite has resulted in relatively higher increase in LREE and HREE in comparison to Eu leading in decrease of Eu/Eu*.

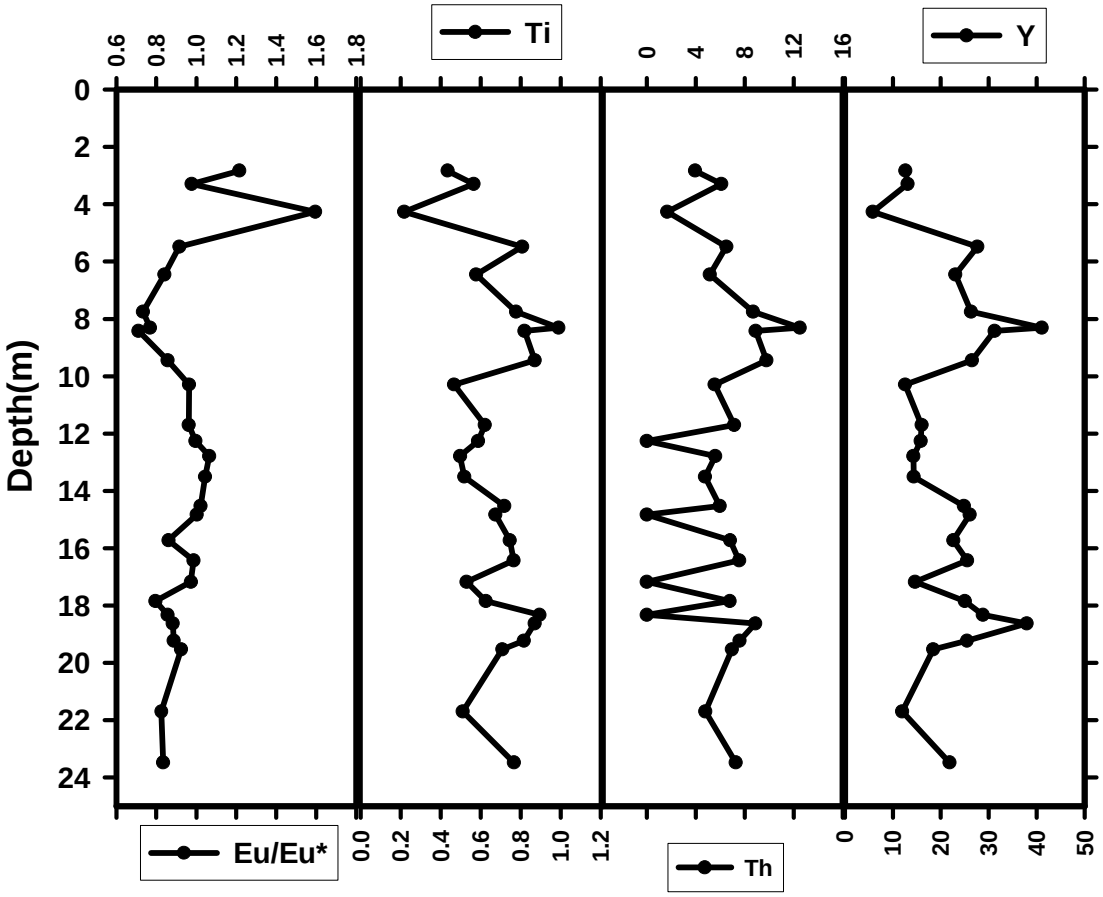

Figure 5.9: The depth wise variation trend of Th, Y and Ti with that of the Eu/Eu* for Porayar sediments.

5.3.3 Provenance:

The Cauvery River traverses from west to east through major lithologies that include Gneisses, Charnokites and Migmatatic Gneisses. Gneisses from Dharwar Craton (DC) popularly known as peninsular gneisses form the uppermost part of the catchment region on the Mysore plateau. Migmatitic Gneiss are predominantly found along the major shear zones in Moyar, Bhavni, Palghat and Cauvery Shear zones and Madurai block (MD). Charnockites form the major rock type in the Southern Granulite Terrain along with the above mentioned migmatitic gneiss. The gneisses form the high and low elevation region but with flatter topography and lower relief, whereas the Charnokites from Southern Granulite Terrain (SGT) form the uplands with higher relief in parts of BR

Hills and Nilgiri Hills towards its north and the Kodikanal and Palani hills of MB block towards its south. Among the major tributaries of Cauvery River, the *Hemavat R.*, drains through the northern upper reaches of the Cauvery catchment towards the western part of Western Ghats. The *Moyar R.* a major tributary of Cauvery originates from northern part of the Nilgiri hills and drains the valley between the northern slopes of the Nilgiri and the southern slopes of the BR Hills. *Bhavani R.* is another tributary that flows along south of the Nilgiri Hills. About 12 major rivulets join *Bhavani. R* draining the southern Nilgiri slopes. Further another major tributary of Cauvery that includes the *Amravati R.* drains Charnokitic rocks of Palani hills and Kodaikanal hills of Madurai block and joins the Cauvery at Karur. The main track of the Cauvery River follows the major shear zones. Here we have tried to evaluate the source for the sediments by comparing the REE and Sr, Nd isotopic compositions of sediments with that of UCC and various lithologies exposed in the catchment region.

5.3.4 Comparison with UCC:

In the UCC normalized REE pattern of Uttrangudi and Porayar core sediments are shown in (Fig 5.10 a and e). The sediments from both the cores show almost flat UCC normalized LREE and HREE pattern and slight enrichment of MREE including Eu. This implies that the sediments have been derived from less differentiated source in comparison to the UCC. On looking into details it observed that the Uttrangudi sediments show variation in terms of Ce. It can be distinguished into two groups, one without Ce anomaly and the other exhibiting slight positive Ce anomaly. The development of positive Ce anomaly may be related to post depositional weathering. Marsh (1991) in his study has suggested that preferential leaching of REE other than Ce in a weathering profile could result in development of positive Ce anomaly. Similar observation has been made by Tripathi and Rajamani (2007). The relation of Eu and CIA as discussed earlier (Fig 5.7a and 5.7b.) also indicates that the sediments have undergone some post depositional weathering. The sediments from both the cores also show positive Eu anomaly, which is probably related to the source, as the rocks exposed in the catchment area are of deep crustal origin primarily of Archean age. The difference in degree of Eu anomaly between Porayar and Uttrangudi sediments in UCC normalized plot is basically due to difference in their weathering intensities as discussed in the preceding section.

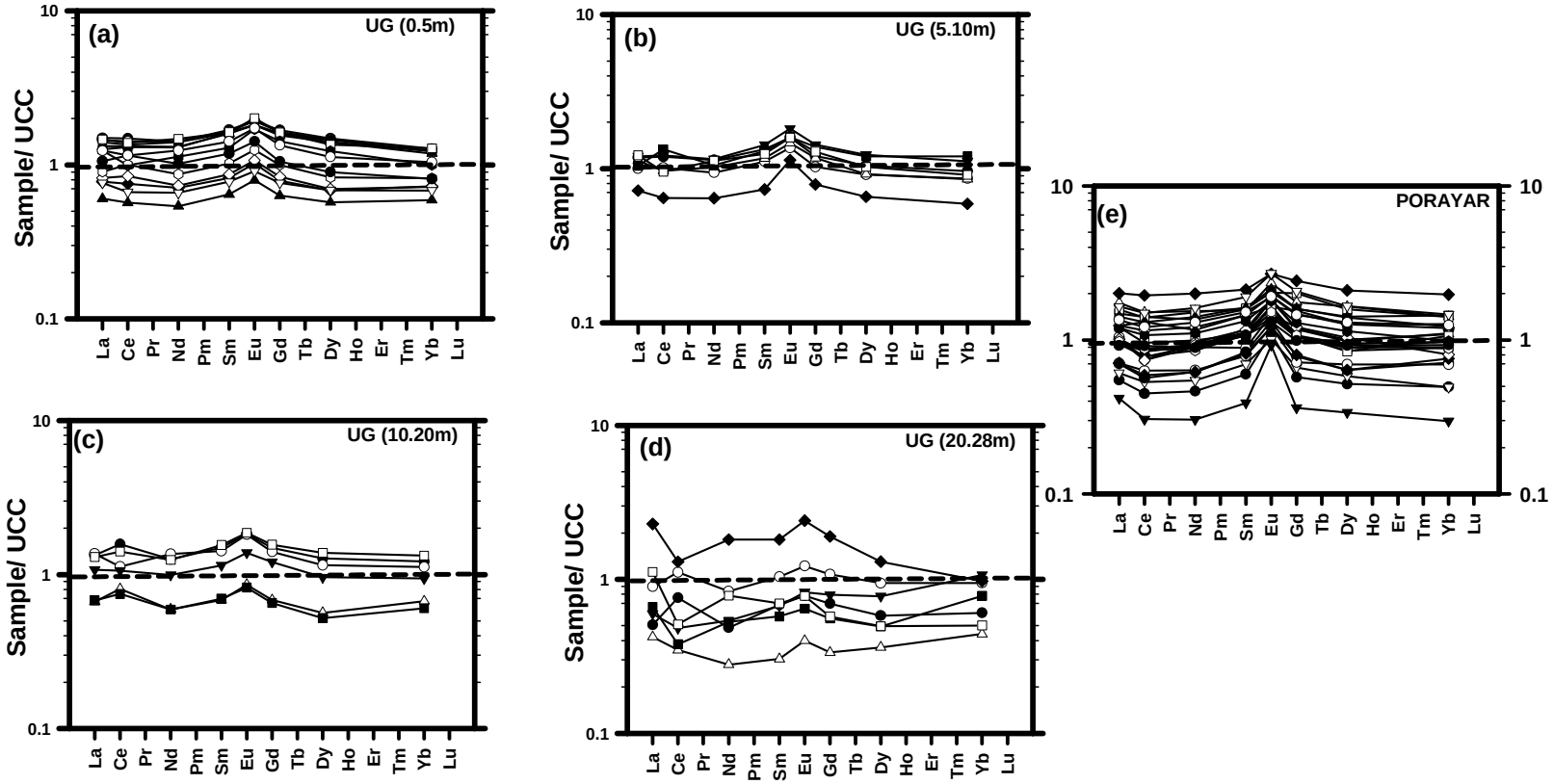

Figure 5.10: The above plot shows UCC normalized REE pattern of Uttrangudi **(a to d)** from different depths and **(e)** Porayar core sediments. The sediments from both the cores show almost flat UCC normalized LREE and HREE pattern and slight enrichment of MREE including Eu. This implies that the sediments have been derived from less differentiated source in comparison to the UCC.

Thus we may conclude that the variation, particularly in Eu and Ce between the two cores is due to post depositional changes. Uttrangudi may have suffered more alteration in comparison to the Porayar sediments because of their older age and slower rate of deposition. Other than the top ~7 m rest of the sediments in Uttrangudi are of upper mid Pleistocene, whereas almost the entire sediments in Porayar core are of Holocene age.

5.3.5 Comparison with the source rocks:

The REE's are considered to be to be immobile and hence preserve the signature of source rocks (Taylor and McLennan, 1985). The chondrite normalized REE patterns are less fractionated for mafic rocks, whereas it is more fractionated in felsic rocks. The chondrite normalized plots of REE in sediments from both the core are almost parallel to each other and exhibit similarly fractionated patterns (Fig 5.1a and 5.1b) with the $(Ce/Yb)_N$ ratio of ~8.2 although with large variations in their abundance. The similar patterns for individual samples may imply either uniform source rocks and/or efficient mixing of source lithologies during sedimentary transport and deposition (McLennan.,1989). The more fractionated nature of LREE and flatter HREE along with slight negative to positive Eu anomaly, suggests that the sediments have been derived from a rock of intermediate composition.

To further constrain the source we have plotted chondrite normalized value of studied sediments from both the cores with that of various rock types from different areas of catchment as described above. (Fig 5.11 a to f) & Fig 5.12 (a to f). These include (1) Gneisses from Mysore plateau (Upper catchment) (Bhaskar Rao et. al., 1991, Divakar Rao., et al 1999) (2) enderbites from the Nilgiri Hills (Raith et al., 1999) (3) Charnockites and Gnessis of BR Hills and Transation zone (Stahle et al 1987, Allen., et al 1984) (4) Charnokites and Migamatic gnessis from shear zones and Kodaikanal Hills (Catlos et al., 2011, Plavsa et al., 2012)

The gneissic rocks from Dharwar Craton forming the major rock type exposed in the upper catchment region show two type of chondrite normalized REE pattern. One group exhibit lower fractionation of REE with $(Ce/Yb)_N$ values ~7 (Bhaskar Rao et. al., 1991), whereas the other group shows higher fractionation with $(Ce/Yb)_N$ ~10 (Divakar

Rao., et al 1999), with both groups exhibiting consistently higher negative Eu anomalies. On comparison of REE plot of studied sediments with the above rock types we observe that there are some noticeable differences. The more fractionated gneissic rock show LREE fractionation similar to the sediments, whereas their HREE are more fractionated (Fig 5.11 a). The other group of gneiss show less fractionation of both LREE and HREE in comparison to the sediments. Apart from this both gneisses are having consistently higher negative Eu anomaly. This suggests that the Gneisses from the Dharwar Craton may not have acted as the source for the sediments. The River from this part enters into the SGT through the transition zone.

The transition zone litholgies comprise of grey gneiss, mafic gneiss and charnockites (Stahle et al., 1987). The gneisses from this region when compared to the studied sediments are distinctly different in having large negative Eu anomalies. In addition the gneisses from this region are much more enriched in HREE and thus less fractionated. The charnockites are much more depleted in HREE in comparison to gneisses and have negligible Eu anomaly. The HREE fractionation and concentration of the charnockites is very similar to the studied sediments although their LREE exhibit higher concentrations and fractionation. Among the above two the rock types, REE concentration and pattern of charnockite are closer to that of the sediments but with overall higher fractionation.

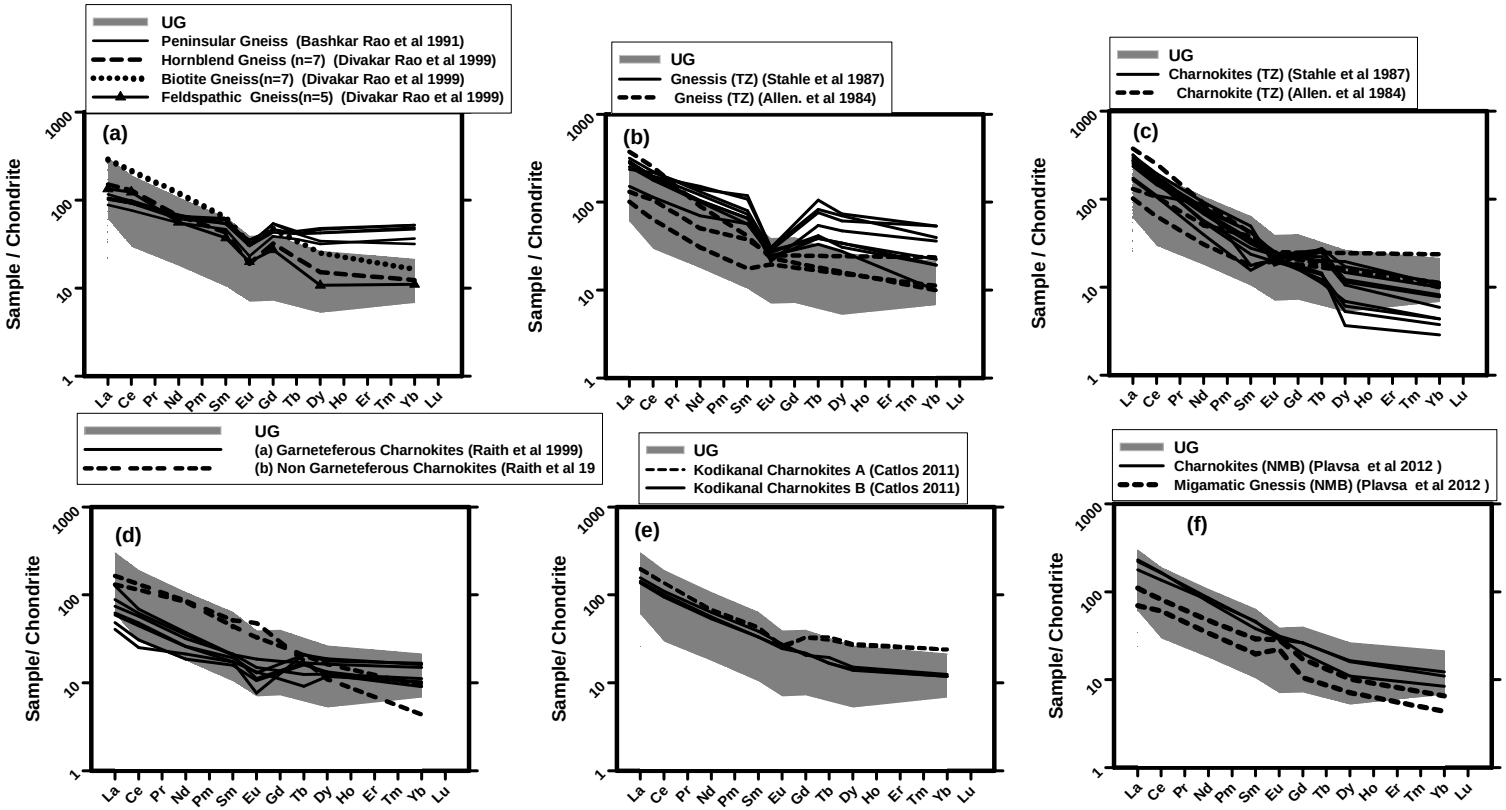

Figure 5.11: The chondrite normalized value of studied sediments from Uttrangudi core (shaded area) with that of various rock types from different areas of catchment. These include (a) Gneisses from Mysore plateau (Upper catchment) (Bhaskar Rao., et al 1991 and Divakar Rao.,et al 1999) (b & c) Gneisses and Charnockites of Transition zone (TZ) (Stahle et al 1987, Allen., et al 1984) (d) enderbites from the Nilgiri Hills (Raith et al., 1999) (e-f) Charnokites and Migmatitic gnessis from Kodaikanal Hills and Northern Madurai Block (NMB) (Tomson et al, 2006, Catlos et al. 2011, Plavsa et al., 2012) .

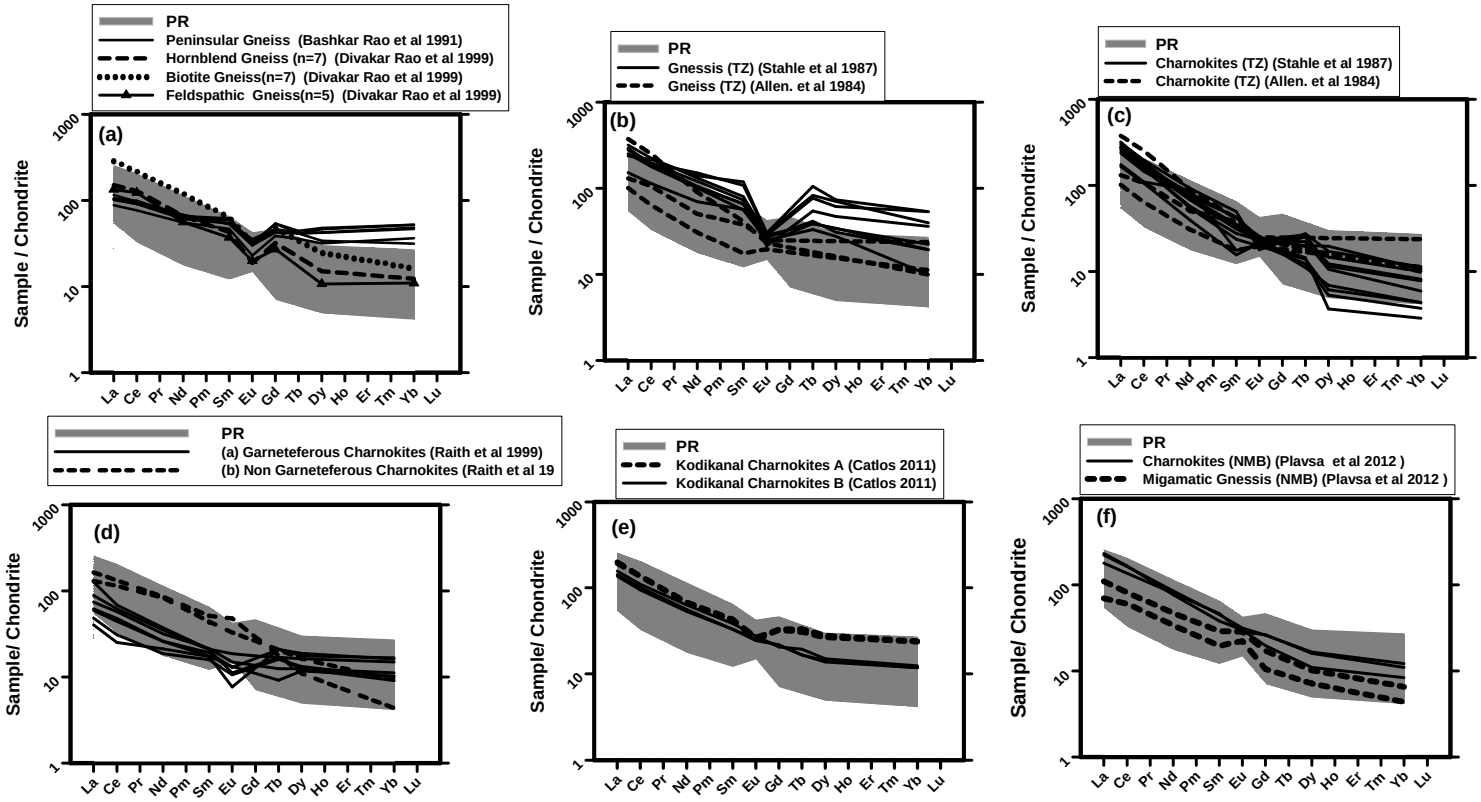

Figure 5.12: The chondrite normalized value of studied sediments from Porayar core (shaded area) with that of various rock types from different areas of catchment. These include (a) Gnessis Mysore plateau (Upper catchment) (Bhaskar Rao., et al 1991 and Divakar Rao.,et al 1999) (b & c) Gnessis and Charnockites of Transition zone (TZ) (Stahle et al 1987, Allen., et al 1984) (d) enderbites from the Nilgiri Hills (Raith et al., 1999) (e-f) Charnokites and Migmatitic gnessis from Kodaikanal Hills and Northern Madurai Block (NMB) (Tomson et al, 2006, Catlos et al. 2011,Plavsa et al., 2012).

The Cauvery River takes a bend and after Hogenekal and starts flowing in southerly direction and enters into plains after Mettur. In this part of its tract it is joined in west by Bhavani River, a major tributary formed by confluence of Moyar and Bhavani River flowing north and south of the Nilgiri hills. The Nilgiri hill in the southern granulite terrain comprises of intermediate charnockites that are of garnetiferous and non garnetiferous nature. It also consists of some pyroxenite bands. The garnetiferous charnockite is depleted in LREE and exhibit HREE enrichment and has negligible negative Eu anomaly. The overall resultant chondrite normalized REE pattern is less fractionated with (Ce/Yb) values of ~ 5. Compared to the sediments from both the cores; the garnetiferous charnockites is depleted in LREE, whereas the HREE exhibit similar abundance and similar or less fractionation. The non garnetioferous charnockites on the other hand show a complementary pattern. It is LREE enriched, which is similar to the sediments, but the HREE in these rocks show higher fractionation in comparison to the sediments. Thus individually the REE patterns of both the charnockites, except their Eu anomaly do not match that of the sediments. At the same time their mix in almost equal proportion may results in REE pattern and abundance similar to the sediments, including the Eu anomaly.

Further moving south, the River after Erode, takes an easterly turn and continues flowing east along the Cauvery Shear Zone (CSZ) until it drains into the Bay of Bengal. The southern part of the SGT grouped as the Southern Granulite Block (SGB) lies to the south of Cauvery River in this part. The SGB includes Northern Madurai Block (NMB) made of massif charnockites in Palani and Kodaikanal hill areas. The other dominant lithologies of this region are migmatitic gneiss and migmatised charnockite along the shear zones. In its middle, east flowing track, the main River is joined from south by another major tributary, the Amravati River. This tributary originates in the Palani and Kodaikanal hills and flows over the shear zone of Madurai Block domain before joining mainstream Cauvery River. On comparing the chondrite normalized REE plot of various above stated lithologies with the sediments it is observed that the charnockites from Kodaikanal and Palani hill region shows the closest resemblance with the sediments in terms of their REE abundance. The chondrite normalized REE plot of charnockites from

this region show fractionation and Eu anomaly similar to the studied sediments (Fig 5.11 e & 5.12 e). Similarly we observe the chondrite normalized REE pattern and Eu anomaly of the migmatitic gneiss from this region to resemble the studied sediments from both the cores (Fig 5.11 f & 5.12 f).

In the lower reaches the Cauvery delta is bordered towards south west by Tertiary rocks of Mio-Pliocene age. It is interesting to note that the chondrite normalized REE pattern of selected samples analysed from this Tertiary exposure, located towards the south west part of the delta, exhibit abundance, fractionation and Eu anomaly similar to the studied sediments (Fig 5.13). Their resemblance with the sediments from Uttrangudi location is more prominent. Similar resemblance with the Uttrangudi sediments was also observed in terms of major element chemistry as discussed in chapter 4.

Thus from our REE results we infer that the source to the sediments have been Charnokitic rocks from high standing hills of Nilgiri and Biligirirangan hills forming part of the Northern Block of the SGT charnokite and migmatitic gnessis from the Southern Block of SGT. In addition to above the migmatitic gneiss and charnockite from the NMB has also acted as the source. There is also probability of a local source in form of Tertiary rocks for the Uttrangudi sediments.

To further constrain the source the Sr and Nd isotopic composition of the sediments has been compared with that of all the probable source rocks. Before we do the above comparison we have analysed the temporal variation of these compositions in the studied core and tried to evaluate the reason for such variations.

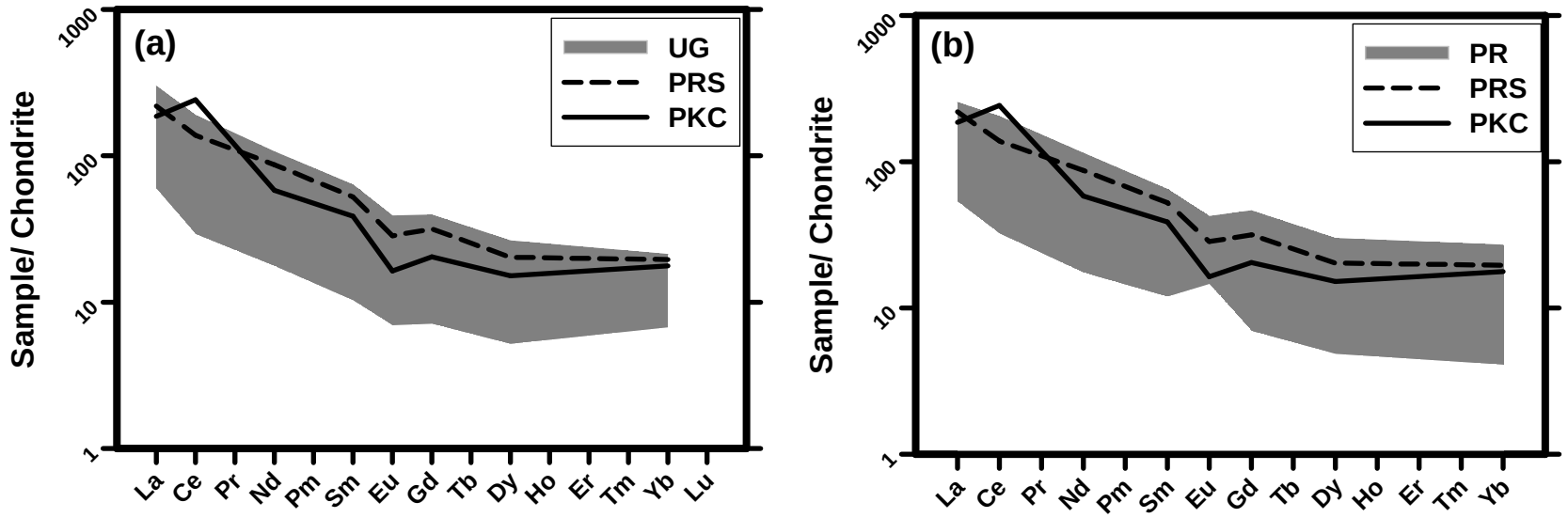

Figure 5.13: The chondrite normalized value of studied sediments from **(a)** Uttrangudi core (shaded area) and **(b)** Porayar core (shaded area) with plots of representative samples from the bordering SW margin of Cauvery Delta Territary rocks from Cauvery basin. PRS (Lateritic cover) & PKC (Mudstone).

5.3.6 Temporal variation in Sr and Nd isotope:

Sr-Nd isotopic compositions of sediments are considered to be reflect their continental source provided they are not affected by weathering and sorting i.e. grain size. The advantage of Sr and Nd isotopes is that they act as fingerprints for source regions and transport pathways of detrital sediments (Innocent et al., 2000; Rutberg et al., 2005). Isotopic ratios of Sr and Nd vary according to the age and geological history of crustal rocks, which results in an inverse relationship between $^{87}Sr/^{86}Sr$ and εNd_0 (Goldstein and Jacobsen., 1987). Sediments of rivers draining older crust have more radiogenic Sr and non-radiogenic Nd than rivers draining the younger crust. Out of the above two, Sm-Nd is considered more robust as their geochemical behaviors are very similar and thus are more difficult to fractionate (Goldstein et al., 1984; Revel et al., 1996), whereas on the other hand Sr isotope is known to get modified by weathering. Strontium being mobile during chemical weathering is easily removed from the source region (Palmer and Edmond., 1992, Blum and Erel, 1997, 2003,) and is more readily released into solution compared to Rb, which gets held up in clays. Thus the fine grained weathered sediments tend to exhibit increase in Sr isotope ratios. Thus the variations in the $^{87}Sr/^{86}Sr$ ratio of sediments is a powerful tool to identify changes in the continental hydrology and chemical weathering regimes (Gosz et al., 1983, Capo et al., 1998, Innocent et al., 2000, Blum and Erel, 2003; Kessarkar et al., 2003, Kuhlmann et al., 2004, Jung et al., 2004; Weldeab et al., 2002) and may prove to be less useful in provenance studies particularly where the sediments have been derived from highly weathered source. On the contrary, Nd isotopes are believed not to alter and therefore not fractionated during near surface processes, such as chemical weathering (Clift et al., 2002, Clift and Blusztajin., 2005. Hence, the isotopic composition of Nd has been established to be a reliable indicator of the provenance to the sediments (Blum and Erel, 2003; Fagel et al., 2002; Goldstein and O'Nions, 1981).Thus ruling out the effect of secondary processes becomes essential in case of Sr isotope before they are used for provenance determination along with Nd isotope.

In the present study the depth wise variation in Sr isotope ratios and εNd_0 values in the residual silicate phase of sediments are plotted in figure 5.14 and 5.15. Other

parameters plotted in the figure are Rb, Sr, CIA, Si, HREE, LREE, TREE, Sm, Nd and silt. In the Uttrangudi core below 12 m depth, Sr is observed to show anti correlation with the CIA, whereas Rb does not show any relation (Fig 5.14). $^{87}Sr/^{86}Sr$ ratio in this part is seen to exhibit an overall enrichment trend with increase in CIA, i.e. weathering, although the relation is not linear. Silica does not show much variation in this part of the core. Thus it appears that below 12 m depth the $^{87}Sr/^{86}Sr$ ratio has been modified, to small extent by the increase in weathering intensity leading to its corresponding enrichment. Above this the $^{87}Sr/^{86}Sr$ ratio in the core is observed to follow the trend exhibited by Rb and Sr, and weathering in this part is relatively less. The concentrations of Rb and Sr in this part show no relation to weathering intensity i.e. the CIA. Thus it appears that $^{87}Sr/^{86}Sr$ ratios of the sediments below 12 m has been modified, although to lesser degree, by weathering, whereas in upper part of the core lying above 12 m depth, the variation in $^{87}Sr/^{86}Sr$ ratios appears to follow the variation in source.

In case of Porayar core the variation in the $^{87}Sr/^{86}Sr$ ratios of sediments below 18m depth do not appear to be related to weathering (Fig 5.15). Above 18m depth upto top, we observe the variation in Rb concentration is positively related to weathering intensity and its enrichment and depletion follows the increase and decrease in weathering intensity i.e. the CIA. Sr is observed to show negative relation with weathering intensity. It is known as stated above that weathering leads to mobilization and loss of Sr and at the same time Rb is enriched. Thus the variation trend of these elements in the Porayar core in section above 18 m depth are inferred to be weathering controlled (Fig 5.15). Enrichment of Rb and loss of Sr should result in increase of $^{87}Sr/^{86}Sr$ ratio and vice-versa. The variation in the value of $^{87}Sr/^{86}Sr$ follows the trend as is theoretically predicted. Thus we may infer that the $^{87}Sr/^{86}Sr$ ratios of sediments in Porayar core are modified by weathering above 18 m depth.

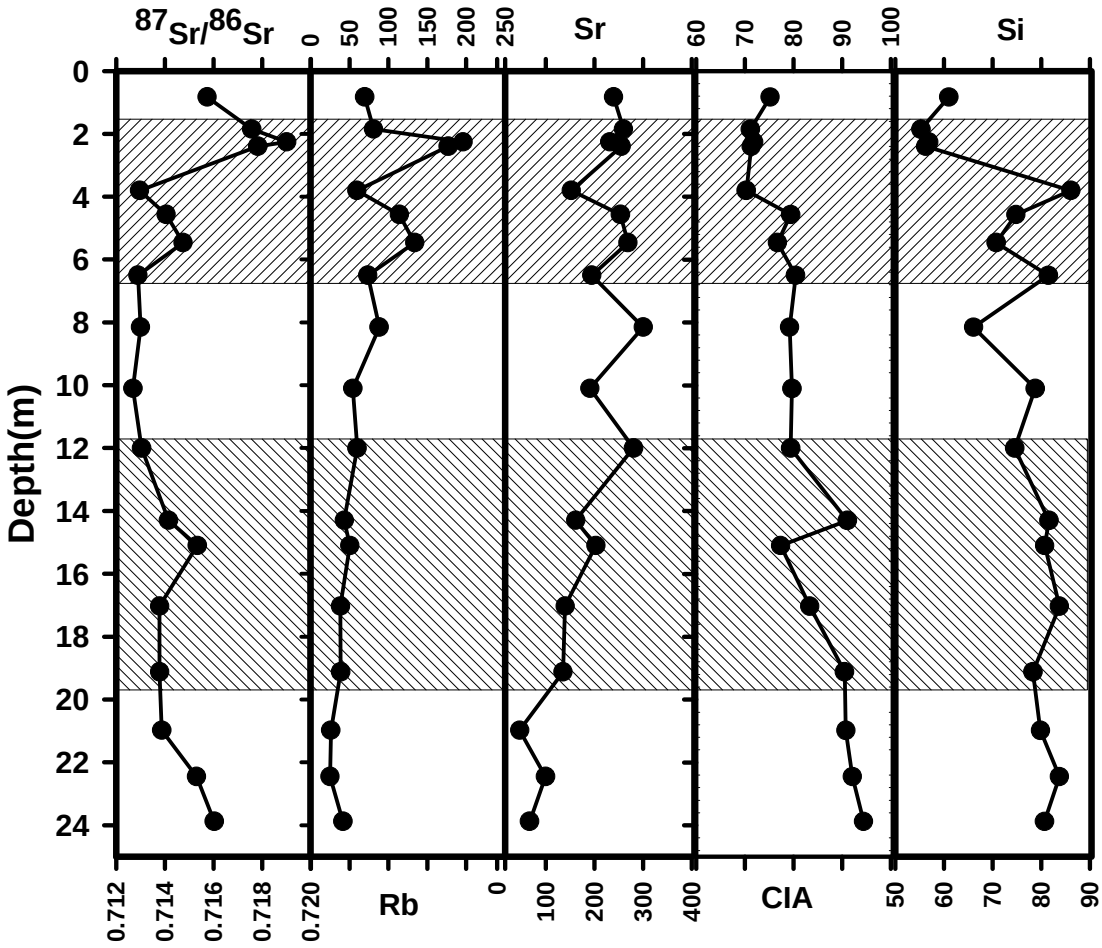

Figure 5.14: The depth wise variation in Sr isotope ratios in silicate fraction of sediments from Uttrangudi core are plotted in figure. Other parameters plotted in the figure are Rb, Sr, CIA and Si, In the core below 12 m depth, Sr is observed to show anti correlation with the CIA, whereas Rb do not show any relation. $^{87}Sr/^{86}Sr$ ratio in this part is seen to exhibit an overall enrichment trend with increase in CIA i.e. weathering.

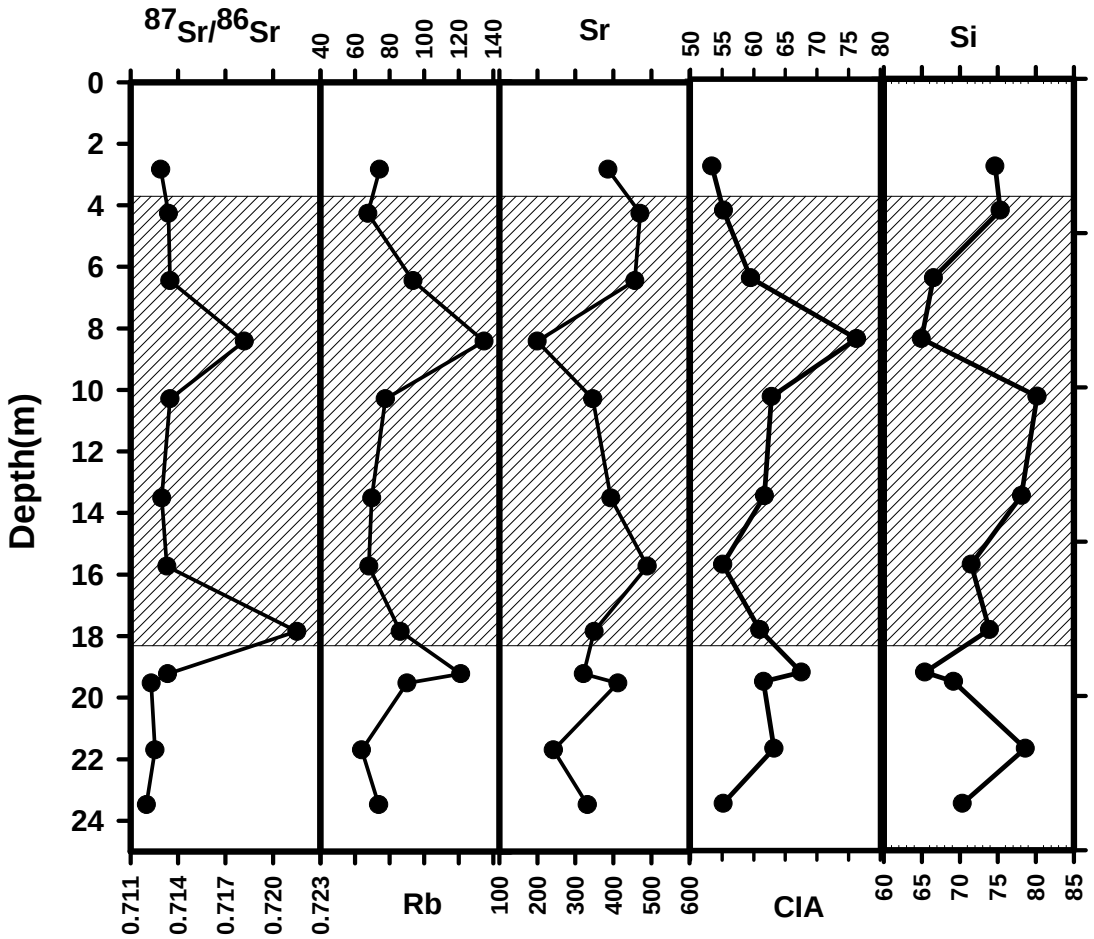

Figure 5.15: The depth wise variation in Sr isotope ratios of Porayar core. It should be noted that the variation in the $^{87}Sr/^{86}Sr$ ratios of sediments below 18m depth do not appear to be related to weathering. Above 18 m depth upto top, we observe the variation in Rb concentration is positively related to weathering intensity and its enrichment and depletion follows the increase and decrease in weathering intensity i.e. the CIA. Sr is observed to show negative relation with weathering intensity.

In contrast the εNd_0 appears unaffected by weathering. At first glance it appears to be controlled by grain size particularly the silt percentage. It is noted that in Uttrangudi sediments the variation in εNd_0 values follow the variation trend of silt percentage except for bottom three samples (Fig. 5.16). On closer examination it is observed that the silt percentage and εNd_0 do not show a linear relation although excursions in percentage silt corresponds to the excursions observed in εNd_0 values. This would suggest that observed grain size control is apparent and the observed correspondence in variations may be

coincident with the variation in source resulting in group shift of all the parameters at different depth. But one can still not rule out the role of grain size within different sectors illustrated with different shades. Similar variation of εNd_0 with percentage silt is observed in Porayar core sediments between 6 m and 22 m (Fig. 5.17). It should be also noted that variation trends in εNd_0 and percentage silt is also observed to positively correlate with the variation trends in HREE, LREE, ΣREE, Sm and Nd, although it is more prominent in Uttrangudi sediments. This would lead to infer that the variation in εNd_0 values in the studied core is ultimately due to the variation in proportion of different REE holding mineral phases that may be differently distributed in silt and sand. Thus the variation in silt and corresponding variation in sand may lead to variation in proportion of various REE holding minerals in the sediments that may have been derived from multiple sources, and thus having different εNd_0 values.

Therefore, based on the above observations, we may infer that the $^{87}Sr/^{86}Sr$ ratio in the studied sediments in some part have been slightly effected by weathering, and the not so prominent overall co-variation exhibited between silt and εNd_0 suggests that the little co-variation observed in small sectors may be apparent and due to variation in source for silt and sand.

Thus in the present study we have used εNd_0 along with Sr isotope compositions of sediments (keeping in mind that their Sr isotopic ratios may represent higher values in parts correlated to weathering) as the tracer of their source. The sediments have been compared with the major source rocks that comprise of Gnessises from the GGG Terrain of DC and of SGT. Late Archean to Proterozoic granulite facies rocks. The depth wise plot of the isotopic data show temporal variations in both Uttrangudi and Porayar cores (Fig 5.18). The Uttrangudi core represents sediments ranging in age from Upper mid Pleistocene to Holocene, whereas the Porayar core represents late upper Pleistocene to Holocene sediments. The εNd_0 and Sr isotope in Uttrangudi and Porayar sediments show large range indicating temporal variation of their source. In case of the Uttrangudi site the εNd_0 and Sr isotope values of the sediments ranges from -26 to -36 and 0.712 to 0.720 respectively. On comparison with source we find that the ranges of above isotopic values are much deviated from the isotopic composition of the predominant lithologies of ~3.0-

3.6 G.a Granite-Gneiss-Greenstone (GGG) terrain of the DC exposed in the upper part of the catchment region particularly in their Sr isotope. In the gnessis of DC the range of εNd_0 (-33 to - 40) and Sr ($^{87}Sr/^{86}Sr$ = 0.74 to 0.8) similar dissimilarity is exhibited by Porayar sediments with their εNd_0 and Sr isotope values ranging from -24 to -34 and 0.712 to 0.722 respectively. Thus it seems the above range of values in sediments fall within the values for different lithologies, forming part of the high grade Southern granulite terrain (SGT) that are exposed in the middle and southern part of the catchment region. Thus as a first approximation we may conclude that the sediments of the Cauvery delta region have been predominantly derived from the SGT and the contribution from the older rocks of DC is very minimal.

Therefore in the following section we have tried find to explore further the variation in input to the sediments from different parts within the Southern Granulite Terrain (SGT).The Precambrian Southern Granulite Terrain (SGT) of South India forming part of the Cauvery catchment is a mosaic of high grade granulite massifs separated by several shear zones. The SGT can broadly be distinguished into late Archaean granulite domain also known as the Northern granulite domain (NGD) and Proterozoic granulite terrains based on the age of regional granulite facies metamorphism at ~ 2.5 Ga and ca. 0.5 Ga. respectively. The two terrains are separated by crustal-scale Palghat-Cauvery shear zone (PCSZ). The 2.5 Granulite terrain north of PCSZ is distinguished into Nilgiri (NHG) and Biligirirangan (BRG) granulite terrain, whereas the 0.5 Ga terrain south of shear zone is the Madurai Block. The Nilgiri granulite terrain which forms the highland is predominantly made up of garnetiferous enderbites and subordinate mafic granulites. The protolith age of this terrain ranges between 2.9 and 2.6 Ga. The $^{87}Sr/^{86}Sr$ and εNd_0 value of this terrain ranges from 0.703887 to 0.731059 and -33 to -20 respectively (Raith et al 1999; Bhaskar Rao et al., 2003). The Biligirirangan granulites exhibit protolith ages between 3.5 and 3.0 Ga. and their $^{87}Sr/^{86}Sr$ and εNd_0 values ranges between 0.70756 to 0.71492 and -36 to - 46 (Bhaskar Rao.,et al., 2003). Both this terrain has been affected by widespread regional metamorphism around 2.5 Ga. The Cauvery shear zone (CSZ) located towards south of NGD and north of PCSZ comprise of charnockite gneiss associated with supracrustal rocks and migmatite gneisses.

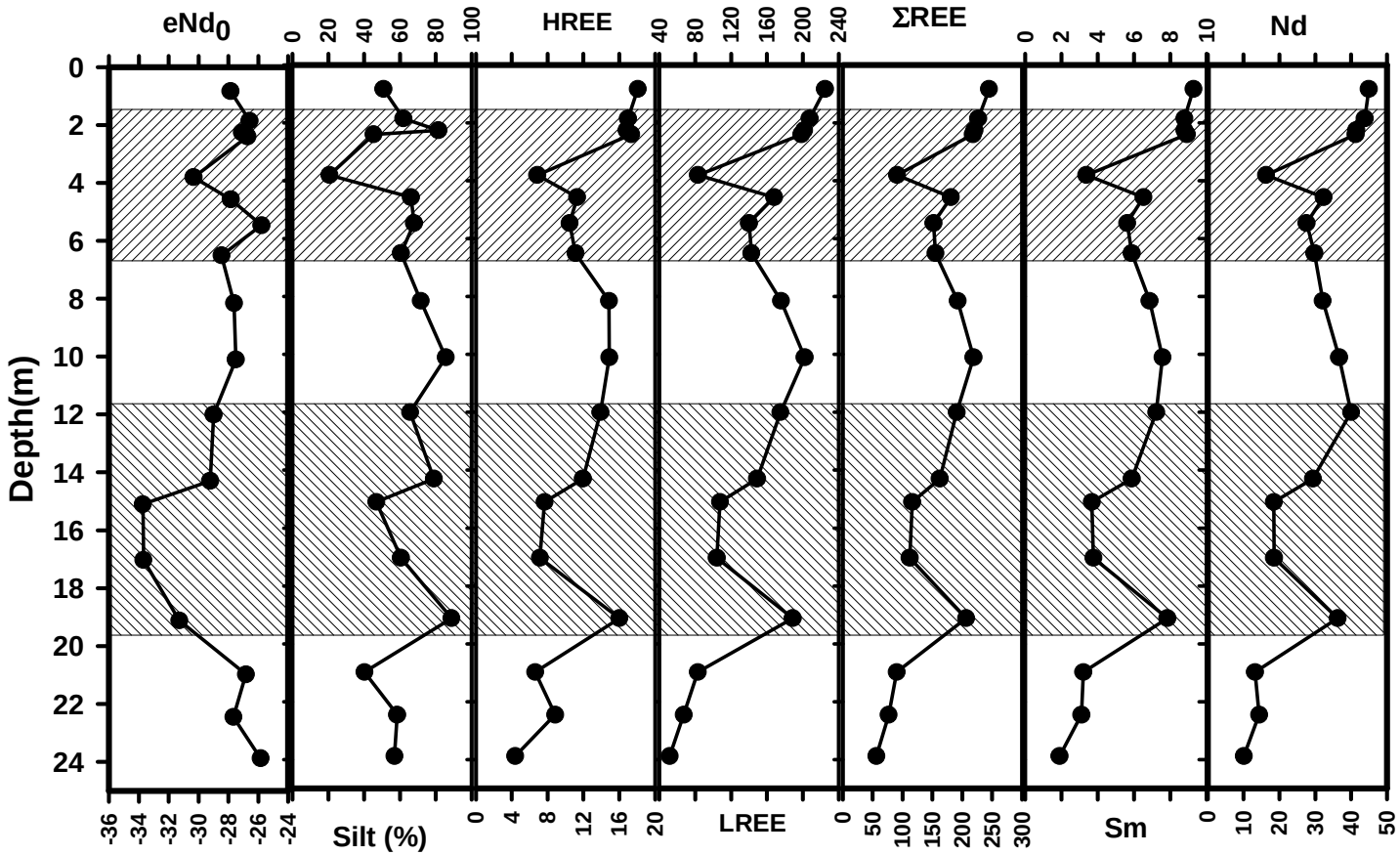

Figure 5.16: The depth wise variation in εNd_0 values for Uttrangudi is plotted in figure. Other parameters plotted in the figure are HREE, LREE, TREE, Sm, Nd and silt (%).

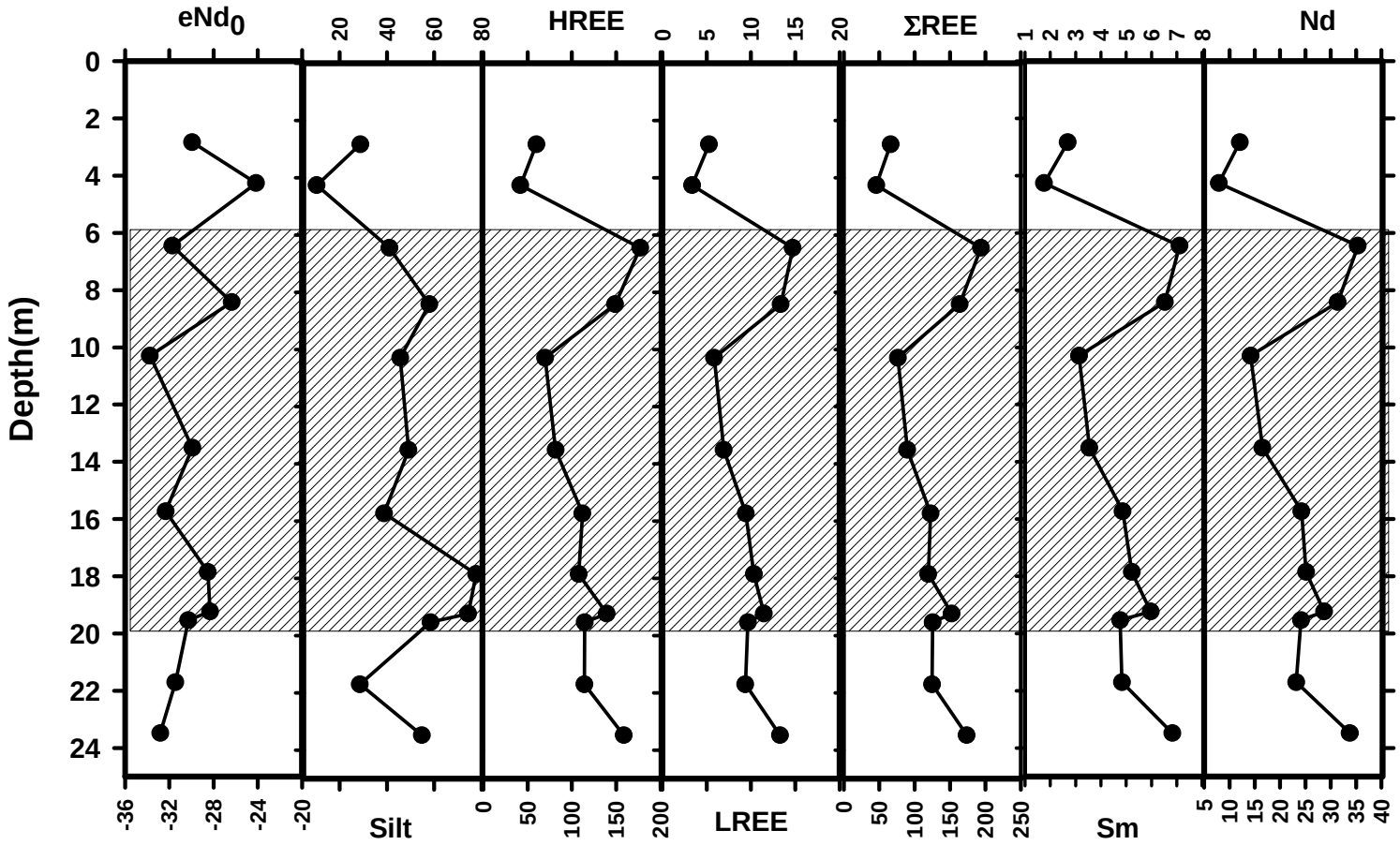

Figure 5.17: The depth wise variation in εNd_0 values in silicate phase of Porayar core sediments. Other parameters plotted in the figure are HREE, LREE, TREE, Sm, Nd and silt (%).

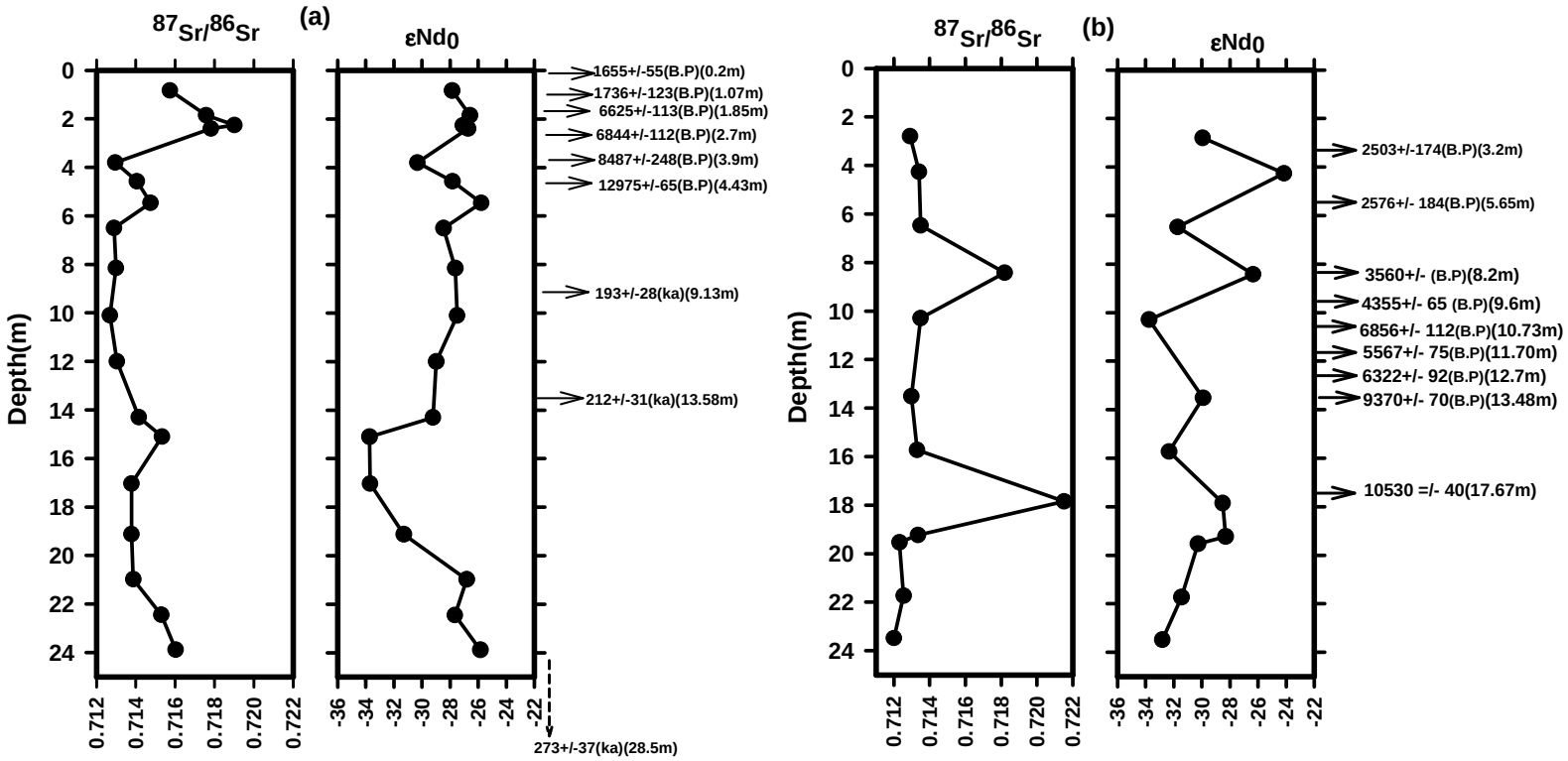

Figure 5.18: **(a)** Variation in Sr and Nd isotope of composition of the sediments with depth. Comparison of trends of εNd_o and $^{87}Sr/^{86}Sr$ ratios in the detrital phase of the Uttrangudi borehole sediments shows five excursions. **(b)** Variation in Sr and Nd isotope of composition of the sediments with depth. Comparison of trends of εNd_o and $^{87}Sr/^{86}Sr$ ratios in the detrital phase of the Porayar borehole sediments shows four excursions.

*Radiocarbon dates (B.P) Srikanth., 2012 and OSL dates (ka) Alappat et al 2010.

The granulites and high grade paragneisses are retrogressed to amphibolites facies leading to formation of mylonitic hornblende biotite gneiss. The CSZ exhibit protolith ages of 2.9 to 2.3 Ga. The shear zones have been reworked by later Pan-African deformations. The $^{87}Sr/^{86}Sr$ and εNd_0value of this terrain ranges from 0.70366 to 0.7546 and -38 to -44 respectively (Bhaskar Rao., 2003; Tomson et al., 2006). The PCSZ and the CSZ-MB (between PCSZ and MB) also yield protoloith and deformation ages similar to CSZ and the $^{87}Sr/^{86}Sr$ and εNd_0value of this terrain ranges from 0.71046 to 0.73157 and -18 to -32 respectively (Bhaskar Rao., 2003). The rocks of CSZ-MB comprise dominantly of charnockite gneiss and amphibolites grade quartzofeldspathic migmatite gneiss along with intrusive granite gneiss and granite. The Madurai block south of the PCSZ is composed of granulite grade charnockite gneiss along the northern slopes of Kodaikanal-Palani hills. In the eastern and south eastern margins the charnockite and migmatite gneiss are in contact with meta-sedimentary associations (Toshiaki and Santosh., 2003). The rocks in this terrain yield model Sm-Nd age of 2.1 to 3.0 Ga and younger ages of ~500 Ma corresponding to the later Pan-African granulite grade metamorphism in this terrain (Harris et al., 1994, Brandon and Meen., 1995). The $^{87}Sr/^{86}Sr$ and εNd_0 value of this terrain ranges from 0.70953 to 0.74326 and -32 to -24 (Bhaskar Rao et al., 2003) respectively. Thus we see that in general the εNd_0 values of NGB, particularly of BR hills is distinctly more negative in comparison to the values obtained for Nilgiri hills, shear zones and the Madurai block. The $^{87}Sr/^{86}Sr$ values for Nilgiri hill and Biligirirangan hills are lower and show an increase on moving south in the shear zones and the Madurai block. Thus to assess the erosion distribution of sediments from the granulite terrain we can form three end members (i) (BRG- BR hills granulites/Gnessis and CSZ north of PCSZ (BRG-CSZ) (ii) (NHG - Nilgiri hills charnokites and Moyar shear zone (MSZ) (NGH/MSZ) and (iii) CSZ/MB CSZ south of PCSZ and charnokites/Gnessis of Northern Madurai block (KDH, NMB, MB). BRG end member is distinctly different but NRG shows overlap in their $^{87}Sr/^{86}Sr$ values with BRG and of εNd_0 values with SZ/MB end member. The SZ/MB group is distinct from the BRG and NHG group only in their $^{87}Sr/^{86}Sr$ values.

The Cauvery delta receives sediments as discussed in earlier section by tributaries and main channel draining the above three end member lithologies. The main channel and tributaries mainly Chittar and Palar drain and erode the BRG, whereas the Rivers Bhavani and Moyar bring sediments eroded from the NHG. The major tributary Amravati drains through the northern part of the MB and southern part of CSZ in addition to the main channel flowing through the PCSZ. The major factor which may bring in the variation in erosion distribution in this region is the rainfall and the relief. As discussed earlier the Sr and Nd concentrations and their isotopic compositions are within the range of above three end member groups forming part of the Southern granulite terrain and falls outside the range of compositions of rocks from Dharwar Craton. Therefore we have attempted to interpret the variation in the $^{87}Sr/^{86}Sr$ and εNd_0 in the Uttrangudi and Porayar core sediments in terms of variation in mixing proportion of BRG, NH and CSZ/MB (Fig.5.19 and 5.20). The $^{87}Sr/^{86}Sr$ and εNd_0 of the sediments from Uttrangudi shows five major excursions at depths ~22, ~16, ~5.8, ~4 and ~2 m. The positive excursion in both εNd_0 and $^{87}Sr/^{86}Sr$ observed at ~22, ~5.8 and ~2 m indicate increased input from the SZ/MB as the rock types from this terrain is characterised by having both high $^{87}Sr/^{86}Sr$ ratio and εNd_0. The prominent excursion at ~16 m depth particularly towards lower εNd_0 indicate towards definite increase in input from the BRG as this terrain is having distinctly lower εNd_0 values. One may argue for the lowering of εNd_0 values due to input from the DC. But we rule out sourcing of sediments from the DC as they have distinctly higher values of $^{87}Sr/^{86}Sr$ (0.74 - 0.8) which is not reflected in the $^{87}Sr/^{86}Sr$ values of sediments at this depth, although they show a slight positive peak. As discussed in earlier section the slight positive excursion in $^{87}Sr/^{86}Sr$ at depth may be related to weathering related enrichment as the sediments at this depth are highly weathered Other negative excursion in $^{87}Sr/^{86}Sr$ and εNd_0 observed at ~4 m depth may also be due to increased input from BRG. The sediment between 6 to 14 m depth show anti relation between Sr and Nd as indicated by increase in εNd_0 value with the concomitant decrease in the $^{87}Sr/^{86}Sr$ values. This relation between $^{87}Sr/^{86}Sr$ and εNd_0 is observed in the rocks from NHG region suggesting them to have dominantly sourced the

sediments for this part. Thus we observe a temporal variation in the dominance of sediment supply from different regions of the granulite terrain.

The Uttrangudi sediments as stated vary in their age from Upper mid Pleistocene to Holocene. Only the top 7 m of the core is of Holocene age and the sediment at ~9 m depth has been dated ~193 ka. It is observed that the frequency of fluctuation in source of sediments at Uttrangudi site increased during the Holocene period. The sediments from Porayar location show uniform $^{87}Sr/^{86}Sr$ values of ~ 0.713 except for two excursions observed at ~18 m ($^{87}Sr/^{86}Sr$ = 0.72) and 8.3 m ($^{87}Sr/^{86}Sr$=718) depths. In contrast εNd_0 values show larger variations of upto -10 in their εNd_0 values with a range of -34 to -24. The excursions towards higher εNd_0 observed at 19.23, 17.85, 13.5, 8.42 and 4.26 m depth would suggest increase in input from the SZ/MB domain, whereas excursions at 23.48, 21.73, 15.73, 10.29 and 6.47 m depths suggests increase in input from BRG and NHG terrain. Thus we see that the sediments from Porayar core, which represents for most part the Holocene show frequent changes in the source domain as observed in case of the Holocene sediments from Uttrangudi core.

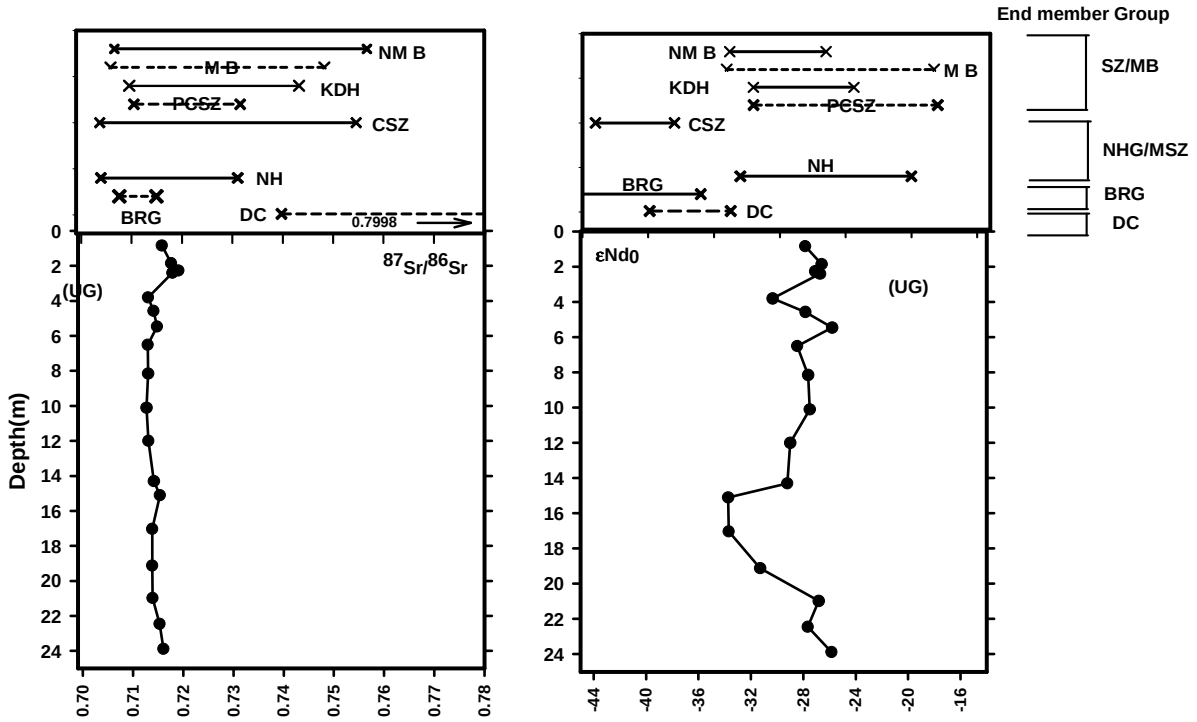

Figure 5.19: The depth wise variation of Sr isotope and εNd_0 values of Uttrangudi core along with the range of values for different lithologies in the source region shown in box above. The major lithologies include from bottom to top, **DC**-Gnessis Dharwar Craton (DC) (Bhaskar Rao., et al 1991 & Meisner., et al 2002); **BRG** Charnockites and Gnessis of BR Hills (Bhaskar Rao., et al 2003), **NHG/MSZ** enderbites from the Nilgiri Hills (Raith et al., 1999, Bhaskar Rao., et al 2003) /(Hbl Bi Gnessis Moyar Shear zone (MSZ) (Meisner., et al 2002) **SZ/MB** Charnokite gnessis(CSZ) (Bhaskar Rao., et al 2003),(Charnokites Palghat Cauvery Shear Zone (PCSZ) (Bhaskar Rao., et al 2003, Choudhary., et al, 2011), Charnokites and Migmatitic gnessis from Kodaikanal Hills (Bhaskar Rao., et al 2003), Madurai Block (MB) (Tomson et al., 2012) and Northern Madurai Block (NMB) (Plavsa et al., 2012).

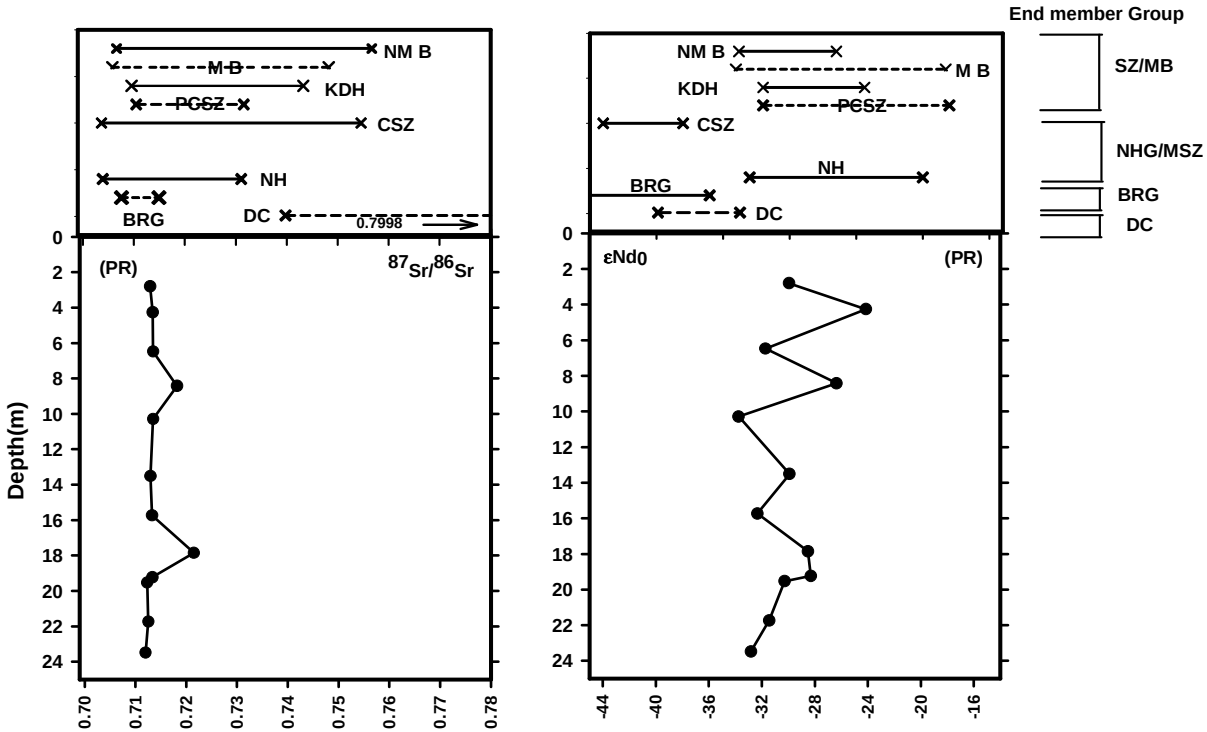

Figure 5.20: The depth wise variation of Sr isotope and εNd_0 values of Porayar core along with the range of values for different lithologies in the source region shown in box above. The major lithologies include from bottom to top, **DC**-Gnessis Dharwar Craton (DC) (Bhaskar Rao., et al 1991 & Meisner., et al 2002); **BRG** Charnockites and Gnessis of BR Hills (Bhaskar Rao., et al 2003), **NHG/MSZ** enderbites from the Nilgiri Hills (Raith et al., 1999, Bhaskar Rao., et al 2003) /(Hbl Bi Gnessis Moyar Shear zone (MSZ) (Meisner., et al 2002) **SZ/MB** Charnokite gnessis(CSZ) (Bhaskar Rao., et al 2003),(Charnokites Palghat Cauvery Shear Zone (PCSZ) (Bhaskar Rao., et al 2003, Choudhary., et al, 2011), Charnokites and Migmatitic gnessis from Kodaikanal Hills (Bhaskar Rao., et al 2003), Madurai Block (MB) (Tomson et al., 2012) and Northern Madurai Block (NMB) (Plavsa et al., 2012).

5.3.7 Isotope Mixing

The two component mixing component for Sr and Nd was derived by (Faure 1977). In the case of Sr having different concentration and isotope ratio the $^{87}Sr/^{86}Sr$ ratio of a mixture is

$$\left(\frac{87_{Sr}}{86_{Sr}}\right)_M = \left(\frac{87_{Sr}}{86_{Sr}}\right)_A f_A \left(\frac{Sr_A}{Sr_M}\right) + \left(\frac{87_{Sr}}{86_{Sr}}\right)_B \times (1 - f_A) \left(\frac{Sr_B}{Sr_M}\right) \longrightarrow \quad (5.9)$$

The equation contains two kind of weighting factors f_A and $1\text{-}f_A$ expressing the abundances of components A and B, whereas Sr_A/Sr_M and Sr_B/Sr_M are the fractions of Sr in the mixture contributed by components A and B, respectively.

The mixing hyperbola based on equation 5.1 was also used for Nd. The equations for Nd are

$$Nd_M = Nd_A f_A + Nd_B(1 - f_A) \longrightarrow \quad (5.10)$$

$$\left(\frac{143_{Nd}}{144_{Nd}}\right)_M = \left(\frac{143_{Nd}}{144_{Nd}}\right)_A f_A \left(\frac{Nd_A}{Nd_M}\right) + \left(\frac{143_{Nd}}{144_{Nd}}\right)_B \times (1 - f_A) \left(\frac{Nd_B}{Nd_M}\right) \longrightarrow \quad (5.11)$$

The isotope ratios of Sr and Nd are effective combination because the geochemical properties of the Rb-Sr system differ markedly from those of the Sm-Nd system .The Sr-Nd isotopic mixing hyperbola was used for components A, B and C which represent three source members.

On a Sr-Nd mixing diagram (Fig 5.21) we interpret the mixtures of the investigated sediments between three possible end members. The three end members as stated earlier include BRG - Charnokitic rocks from BRG hills and CSZ and other end member NHG include enderbites from Nilgiri high land massif and Moyar Shear zone (MSZ) and third end member CSZ/MB include Charnokitic rocks from CSZ/MB block and Kodaikanal region. The BRG and NHG end members are observed to have contributed 70% to 90% whereas the CSZ/MB domin is observed to vary between 10 to

30%. In four samples the CSZ/MB is observed to have higher contribution ranging between 45 to 50 %

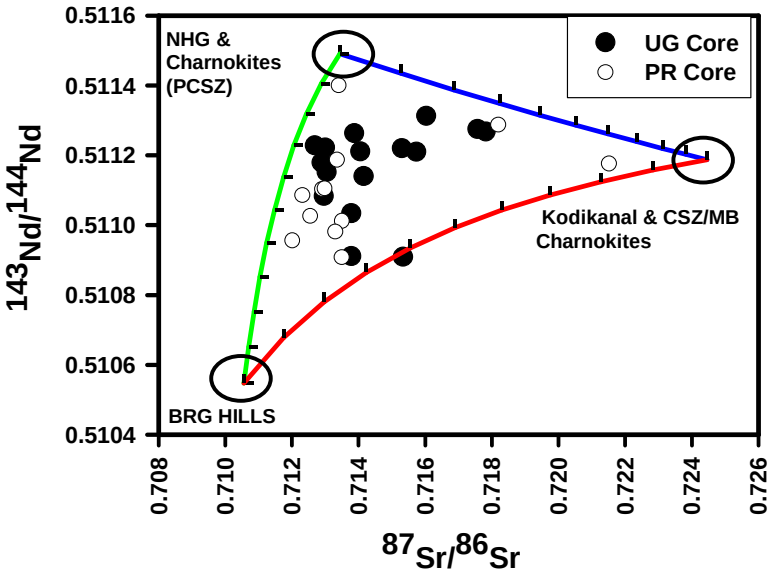

Figure 5. 21: Sr-Nd mixing diagram of the investigated sediments falling between three possible end members. The three end members are Charnokitic rocks from BRG hills, Enderbites from Nilgiri high land massif and Shear zone (PCSZ) and third end member Charnokitic rocks from CSZ/MB block and Kodaikanal region. The data for mixing diagram has been taken from (Raith et al., 1999, Bhaskar Rao., et al 2003, Choudhary., et al, 2011).

From the above discussion we may conclude that the sediment contribution during the Pleistocene period as observed in Uttrangudi core was dominantly from the BRG and NHG domains. The contribution from SZ/MB domain is observed to have mainly increased towards the late Pleistocene and continued through the Holocene. In contrast we observe that the contribution from DC has remained minimal for the entire period. Observations made on the basis of REE composition of these sediments also indicate predominant contribution from SGT and minimal input from the DC. The major factors which control the erosion of sediments are rainfall and relief. In the studied area we find that the entire catchment region of the Cauvery River lies in the rain shadow zone of south west monsoon that is blocked by the barrier formed by the Western Ghats located towards the west. The major contribution of rainfall in this region is from the NE monsoon. If we look into the rainfall distribution pattern (Fig 5.22) we observe that the

maximum rainfall is received in the Nilgiri hills and the Palani Hills of Madurai block. The annual rainfall in the Shear zone region, BR hills and the Upper catchment region is similar, but we observe that in BR hills and the shear zone region the maximum rainfall occurs over a shorter duration, whereas in Mysore Plateau region the rainfall is spread over longer period. Higher rainfall over shorter period leads to more surface run off leading to greater erosion in contrast to similar or lower rainfall, which is distributed over a longer period. In such case the surface runoff is reduced. In addition to this, the relief may have also led to variable erosion distribution. The upper catchment region comprising of DC has lower relief and form a large plateau with gently undulating topography (Fig 5.23). In contrast the SGT is the region of high relief particularly in the chrnockitic region. The charnockites in SGT form highland massifs with high relief that may facilitate erosion. Thus higher rainfall spread over shorter time period along with higher relief in the SGT, together, may have resulted in higher erosion of the SGT rock in comparison to the DC where rainfall is comparatively less and is spread over longer period along with the gentle topography of the region. The temporal variation in input from different parts of the granulite terrain may be due to the local variations in rainfall at different times as is common in monsoonal rain fed areas.

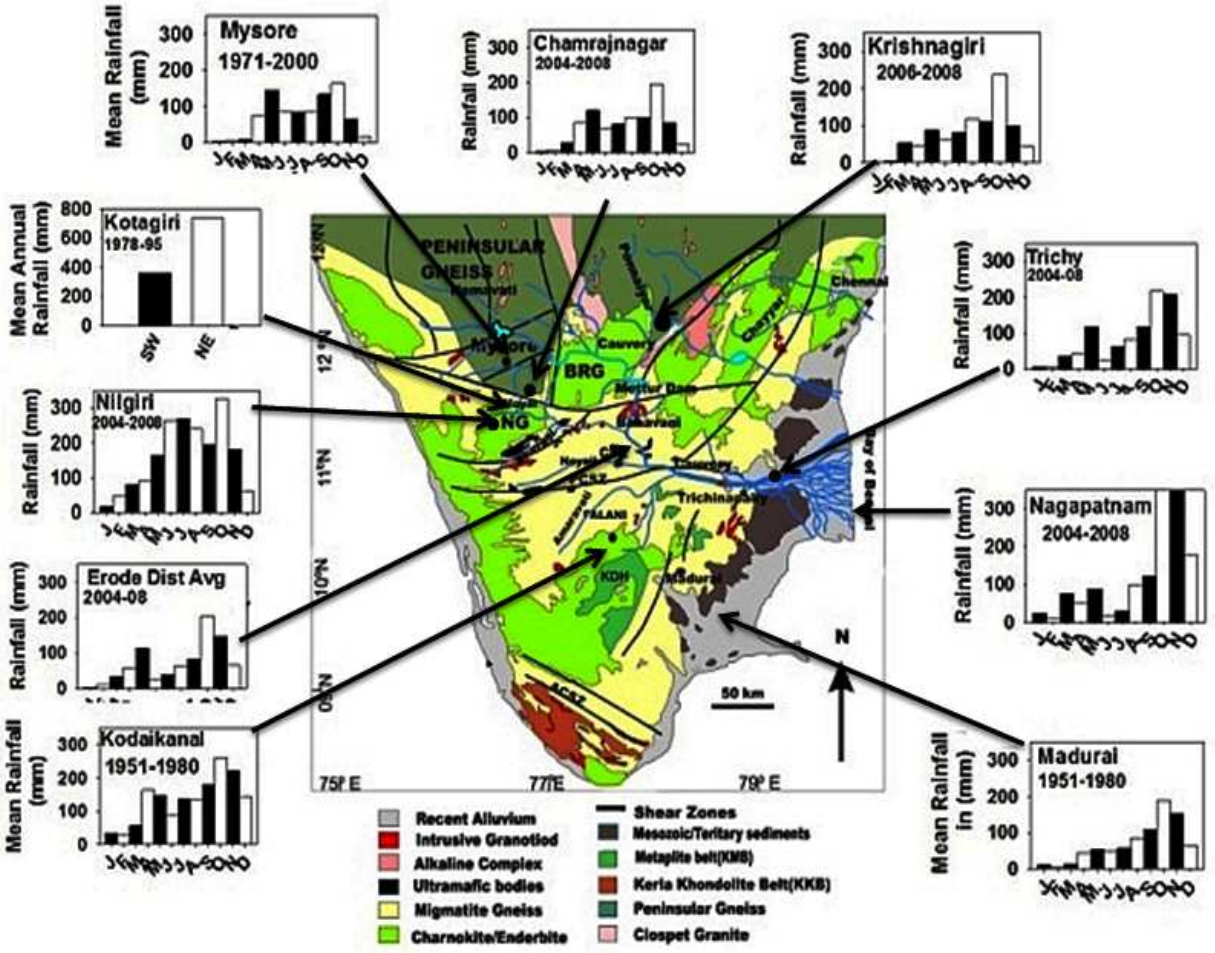

Figure 5.22: Rainfall distribution pattern in the study region [Data from Indian Meteorological Division (IMD)].

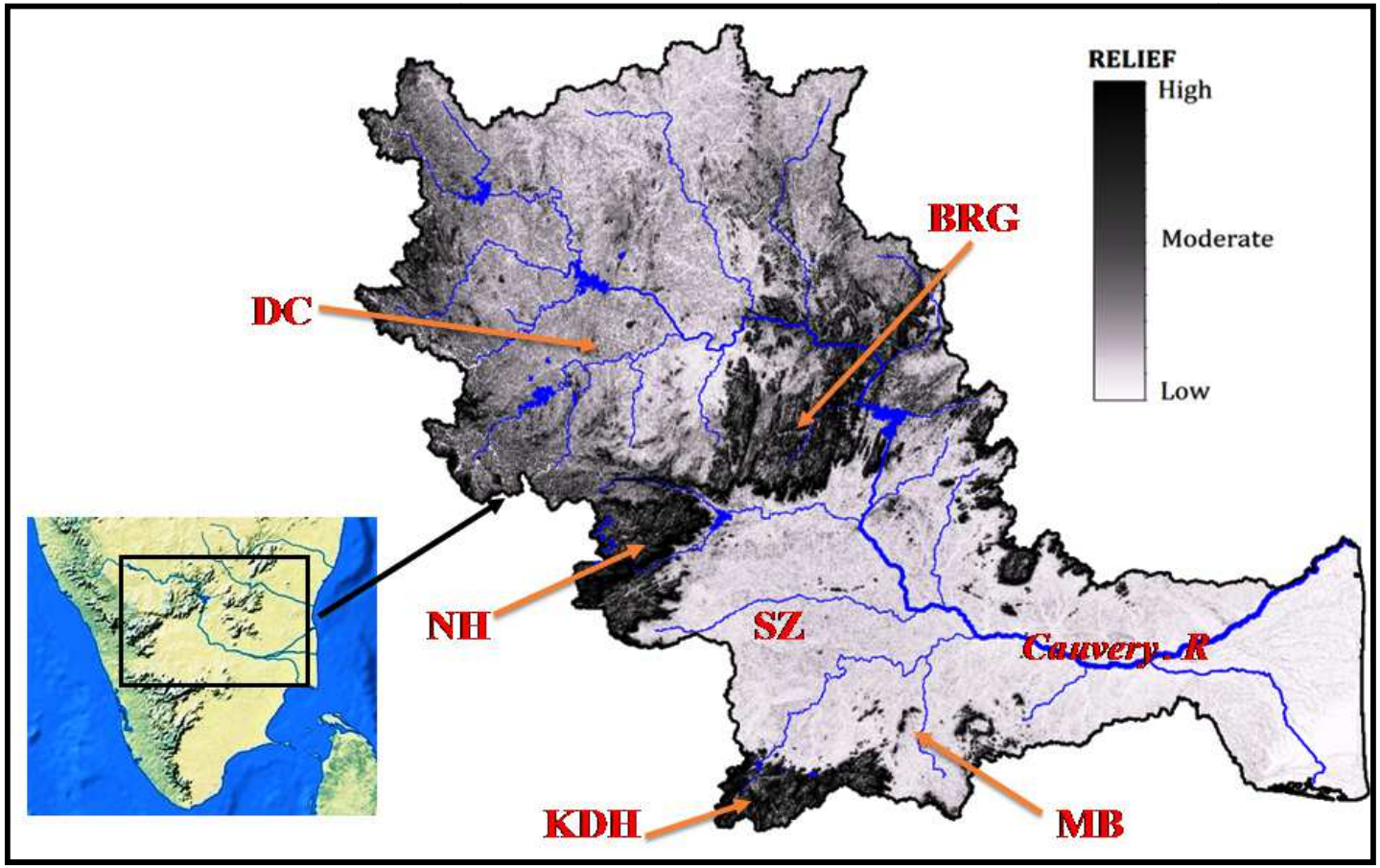

Figure 5.23: Shaded relief image of Cauvery basin southern India showing the different showing the distribution of major charnockite massifs. The different crustal blocks shown are Dharwar Craton (DC), Nilgiri Hills (NH), Biligirirangan Hills (BRG), Shear Zone (SZ), Kodaikanal Hills (KDH) & Madurai Block (MB).

5.3.8 $^{87}Sr/^{86}Sr$ in leachate fraction: *implication to temporal and spatial varation in groundwater chemistry.*

Sr is easily leached from mineral and is present in the dissolved state in the aquatic system including the pore waters. The Sr isotopes do not get further fractionated in the water by any chemical or biological process. The $^{87}Sr/^{86}Sr$ ratios in water may change only as a result of mixing of two different water masses. Sr from water is taken into many secondary solid phases hat precipitate out of the solution or that are in equilibrium with the water. Thus the $^{87}Sr/^{86}Sr$ isotopic of several secondary phases acts as the proxy for the ratios of water from which they have precipitated or equilibrated (Casanova and Négrel, 1995; Négrel et al.,1997; Holmden et al., 1997; Vonhof et al., 1998;Casanova et al., 1999).Sr is chemically and isotopically uniform in ocean water due to it longer residence time (2-5 Ma) that exceeds the mixing time of ocean water (~10^3 yr). The Sr isotopic composition found in streams and groundwater has been found variable depending upon the chemical weathering of different types of bed rocks (Faure et al, 1963). Thus Sr isotopic concentration has been found useful as a natural tracer to study the streams that drain through different kind of rock types and to recognize the subsurface movement and chemical evolution of groundwater (Eastin and Faure 1970; Stueber et al 1975; Fisher and Stuber 1976; Franklyn et al 1991; Aramstrong et al, 1998). We have performed sequential extraction to investigate the Sr isotopic composition of different secondary phase to evaluate the changes in the pore water chemistry at various times and its relation with the silicate phase of sediments and also with the continental and sea water. The results of $^{87}Sr/^{86}Sr$ analyses done in four leachates fractions on selected samples of Uttrangudi core and three leachates from Porayar core are given in (Table 5.5 and 5.6). The leachate fractions analysed are (i) exchangeable phase (Exch) (ii) carbonate phase (Carb) (iii) Fe-Mn phase and (iv) Organic phase (ORG). The $^{87}Sr/^{86}Sr$ ratios in different leachate fractions and the residual silicate phase are plotted in (Fig 5.24 & 5.25) along with Rb concentration of bulk sediment. For reference, line indicating $^{87}Sr/^{86}Sr$) value of sea water and present day Cauvery River water in delta region are also plotted. In Uttrangudi core we observe that the $^{87}Sr/^{86}Sr$ isotopic ratio values of the leachate fractions do not show much variation from bottom 24 m upto ~ 6 m depth and their values are also similar. The $^{87}Sr/^{86}Sr$ value of the residual phase also

exhibit gradual decrease from bottom up to 6 m depth without any major excursion except one noted at 15.1m. Similarly Rb also shows a gradual increase within a narrow range for this depth without any excursion. The $^{87}Sr/^{86}Sr$ ratios of exchangeable, carbonate, Fe-Mn and organic phases of the sediments within this depth exhibit similar trend falling between seawater and river water values i.e. 0.7091 and 0.71429 respectively. This would suggest that the Sr isotope signature of leachate fractions in this part has been determined by the mixing of river and saline water. Above 6 m depth that constitutes Holocene sediments we observe increase in $^{87}Sr/^{86}Sr$ values of leachate fractions with four positive and three negative excursions.

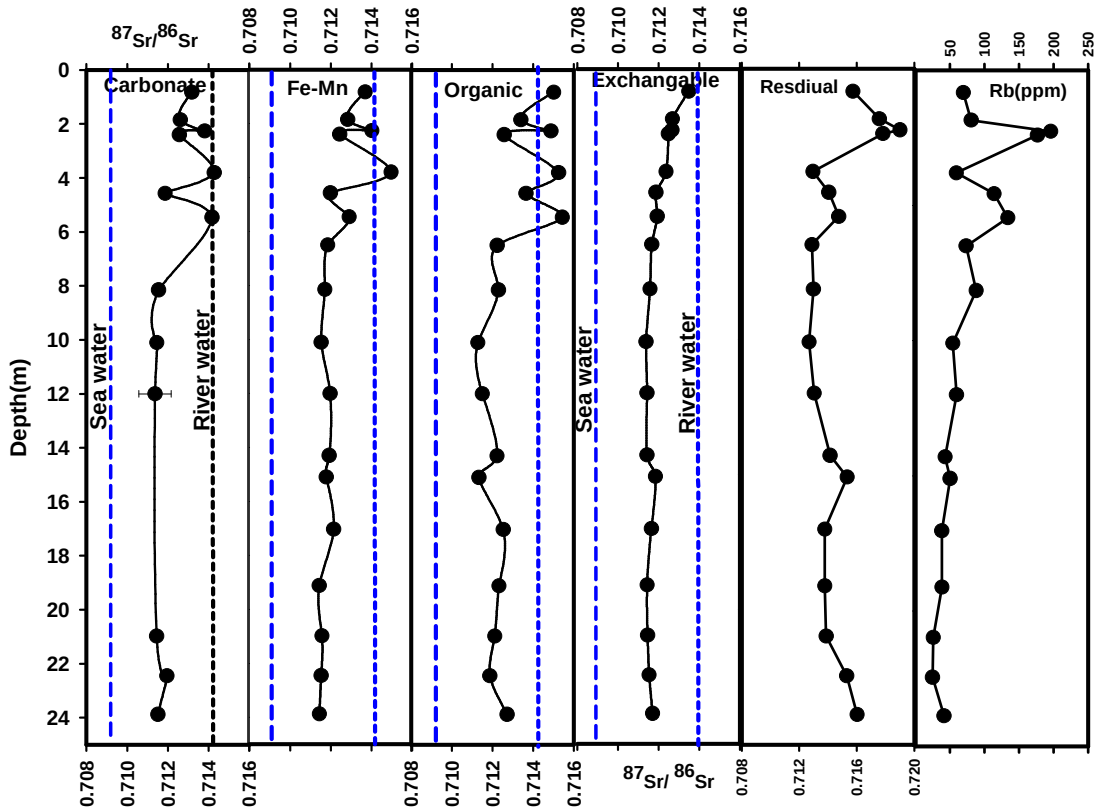

Fig-5.24: The $^{87}Sr/^{86}Sr$ ratios of exchangeable, carbonate, Fe-Mn and organic phases of the Uttrangudi core sediments exhibit similar trends falling between seawater and river water values (Pattanaik et al., 2006).. For comparsion are plotted $^{87}Sr/^{86}Sr$ ratios of residual silicate phase and Rb concentration (in ppm).

The $^{87}Sr/^{86}Sr$ values in this part are also seen to skew towards and center around the river water composition. Two major positive excursions coincide with the similar excursions of $^{87}Sr/^{86}Sr$ in residual silicate phase and the Rb in the bulk sediment. This would lead to infer that in this part there was diagenetic addition of Sr to the pore water by breakdown of minerals in the sediments, which are more radiogenic and further the influence of saline water had also reduced or ceased. It is also to be noted that the Sr isotopic values of leachate at 3.8 m depths exceeds the value in residual silicate phase. None the less the values of $^{87}Sr/^{86}Sr$ ratio in residual silicate phase in sediments underlying and overlying this part are higher than the leachate fraction at this depth. This would suggest addition of Sr into water at 3.8m depth from underlying and overlying sediments, which may have got diagenetically altered and released high radiogenic $^{87}Sr/^{86}Sr$ into the pore water. High radiogenic $^{87}Sr/^{86}Sr$ in sediments above 6 m depth indicates change in the source.

Similarly the $^{87}Sr/^{86}Sr$ ratios were measured in carbonate, Fe-Mn and organic phases in sediments from Porayar core and are plotted in Fig 5.25. The sediments in Porayar core for most of its part have been deposited in an estuarine environment and are Holocene in age except below ~20 m depth. The sediments below 20 m depth are older sediments of Tertiary or Cretaceous period. The sediments between 15.5 m and 20 m depth are fluvial in origin and are oxidized to different extent. The estuarine environment is interpreted to have established from ~15.5 m upwards as indicated by presence of foraminifera. The lower value of $^{87}Sr/^{86}Sr$ in carbonate, more closer to sea water values, indicate dominant control of saline water. The organic has relatively higher, although fluctuating value compared to carbonate phase upto 12 m depth from bottom. This would indicate that the organic added from the continental environment and could not attain equilibrium with solution in the depositional environment. Above 12 m up to 4 m both carbonate and organic fraction exhibit similar values that are closer to the seawater values. This would suggest that the organic in this part equilibrated with the saline water. Above this depth, sediments may have deposited after the estuary was filled and changed into fresh water, $^{87}Sr/^{86}Sr$ in both carbonate and organic show shift towards river water composition. Unlike carbonate and organic leachate fraction, $^{87}Sr/^{86}Sr$ ratios in the Fe-Mn

leachate fraction show a gradual increase upward with minor fluctuations. This exhibits no relation with the $^{87}Sr/^{86}Sr$ values of the residual silicate phase and also do not follow the changes observed for carbonate and organic phase. One possibility is that the increase in $^{87}Sr/^{86}Sr$ value may be related to selective weathering of minerals with more radiogenic value of $^{87}Sr/^{86}Sr$.

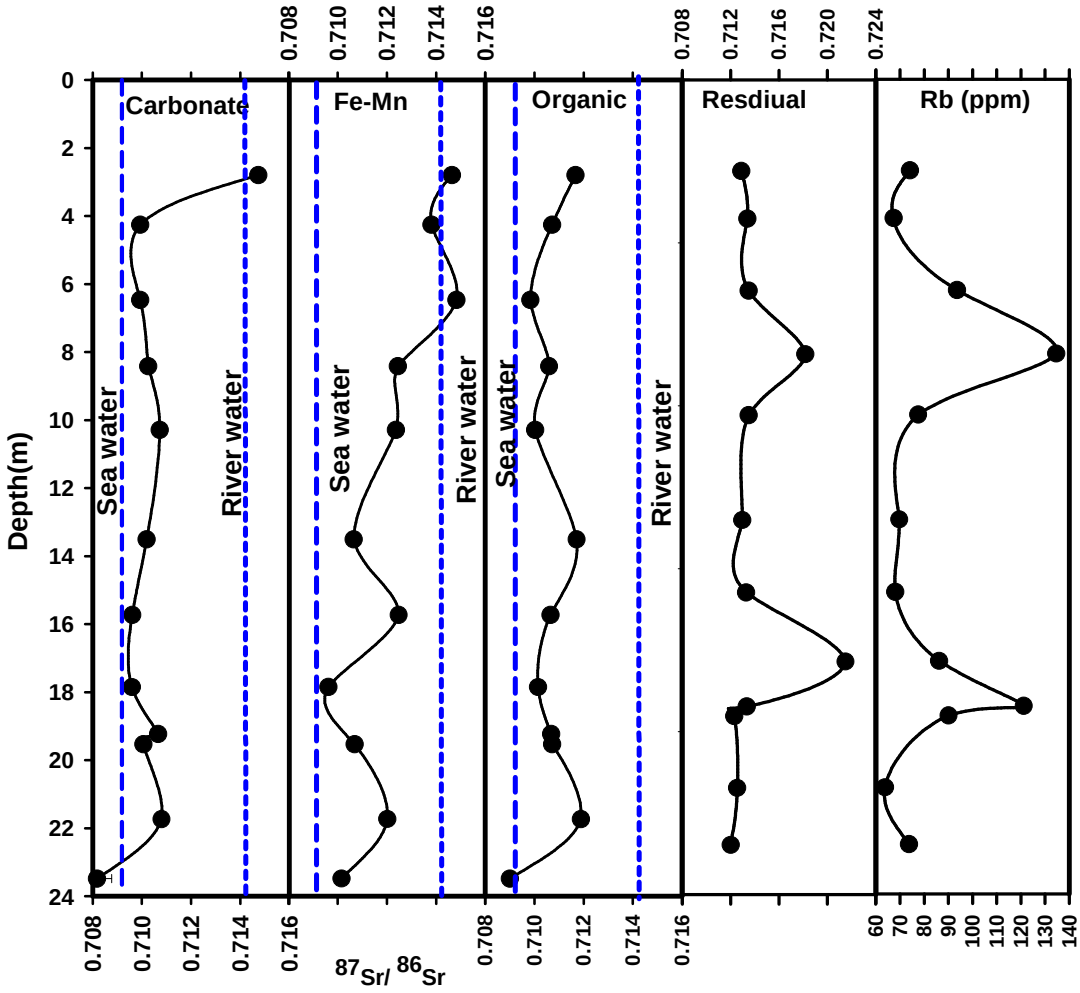

Fig-5.25: The depth wise varation in $^{87}Sr/^{86}Sr$ ratios of exchangeable, carbonate, Fe-Mn and organic phases of the Porayar core sediments. Note that the $^{87}Sr/^{86}Sr$ values in corbonate are closer to sea water compostion compared to Uttrangudi core For comparsion are plotted $^{87}Sr/^{86}Sr$ ratios of residual silicate phase and Rb concentration (in ppm).

Chapter 6

Summary and Conclusions

SUMMARY AND CONCLUSIONS

The Cauvery River originates from the Brahmagiri ranges of Western Ghats in the state of Karnataka and flows for about 800 km before it joins Bay of Bengal along the east coast of south India. For most of it length up to delta the main channel and its tributaries flows through the Archean gneisses of DharwarCraton and Archean to early Proterozoic granulite grade rocks chiefly comprising of charnockite and retrogressed amphibolites grade migmatite gneisses and mylonitic gneisses. In the delta part it is bordered towards north and south west part by Tertiary sedimentary covers.

The River has formed vast fertile delta after bifurcating into several distributaries beyond Tiruchirrapalli where it has deposited thick piles of fluvial and fluvio-marine sediments in response to sea level rise and falls. The Holocene and Pleistocene sediments of present Cauvery River delta has formed by erosion and later deposition over the older sedimentary formations of Cauvery basin deposited during Tertiary and Cretaceous Period in the intra-cratonic rift basins. In an earlier work, the radiocarbon dates obtained on the borehole peat in delta, suggested that the Holocene sediments are 3 m thick about 50 km inland and about 30 m thick near the present shoreline (Sadakata.,1980).

Textural, geochemical and isotopic studies were carried out on the subsurface sediments obtained from the two sediment cores one drilled in the Central east marginal part of the delta located at Porayar, ~2 km inland from the present coast and the other in the southern distal part of the present day delta located at Uttrangudi ~30 km inland. The main objective of the present study includes (1) understanding ofthe spatial and temporal variation in the texture and weathering intensity of sediments in the Cauvery delta and their influence on the chemical composition of the sediments and (2) to determine the spatial and temporal variation in provenance of the sediments using the REE and Sr-Nd isotopic compositions of the sediments and infer the role of climate and relief on the source variability.

On the basis of texture and other physical parameters such as color of the ~30 m core sediments from Uttarangudi location it is inferred that the whole sequence was deposited in fluvial environment and contains channel, levee, flood plain and flood plain

marsh and lake deposits. It is mainly composed of multiple cycles of channel and flood plain sequence deposited mostly in the low energy environment. The radiocarbon and OSL dates obtained on the core indicate a long break in sediment record between the mid Pleistocene and Holocene deposition, which would suggest a period of non-deposition or of erosion during the period of lower sea level. The bottom six units (unit I to VI) from 30.75 m to 7.5 m depth comprise the Pleistocene deposits and the top 3 units i.e. 7 m upward constitute Holocene deposits. Both Pleistocene and Holocene sediments in this core are composed of clayey silt, silty, sandy and silty sand beds and the channel sand at places is underlain by gravely to pebbly sand units. The sediments are at different depths are light brown, dark brown, grayish, greenish gray, grayish brown, grayish black to redin color. Calcretes are present at various depths and the sediments at places are also mottled.

Similarly in the 24m core studied from Porayar location the late Pleistocene sediments are found to unconformably overlie lithified Cretaceous or Tertiary sediments. This indicates erosion of almost all the Pleistocene sediments in this region during the period of lower sea.The presence of foraminifera test in late Pleistocene and Holocene sediments from this location indicate their deposition in an estuarine environment or bay. Except for the bottom sediments below unconformity and the late Pleistocene to early Holocene sediments, that are brown to light yellow in colour, almost the entire top upto 14m depth of the core is dark grey to black in colour. The top 14m is organically rich and contains foraminifera and ostracoda tests in addition to whole or broken macro faunal shells of saline to brackish water affinity. The core is composed of clayey silt, silty clay, sandy silt or silty sand sediments.Calcrete is present only at ~17 m depth otherwise it is absent.

The vertical down core distribution characteristics of major elementsin ~28 m core from the Uttrangudi and 26.5 m core from Porayar location showsignificant temporal variations. The down core variation trend in SiO_2 concentration is observed to follow the trend similar to that exhibited by the sand percentage and opposite to the variation trend of silts. This suggests textural control on its concentration and also suggests that the sand is relatively enriched in quartz. Other elements such as Al, Fe, Ti, Mg and Mn are seen to follow the trend shown by silt and opposite to that of sand. This

would suggest that the minerals holding these elements are mostly concentrated in fines. In Uttrangudi core Na_2O, K_2O and CaO show a weak but positive correlation with SiO_2 and sand %, and negative correlation with Al_2O_3 and silt % in lower part i.e. Unit I to VI, which corresponds to the Pleistocene deposits, whereas in upper part i.e. Unit VII and VIII they exhibit negative correlation with SiO_2 and sand and positive correlation with Al_2O_3 and silt. This may imply that in zone I to VI, i.e. 28 m to ~8 m depth, feldspar is dominantly held in sand fraction, whereas in zone VII and VIII it is predominantly in silt fraction. In Porayar core sediments Na_2O, CaO and to a great extent K_2O show behavior similar to $SiO_2$and sand suggesting that feldspar in these sediments are also mostly hosted in sand i.e. they constitute the coarser fraction.Thus we may conclude that in the studied sediments from both the locations quartz and feldspar form dominant part of sand, whereas the mafic minerals or their weathering product are mainly held in silt and clays. In Uttrangudi core we see abnormal increase in Mn concentration at certain depths which at places are associated with abnormally high concentrations of Ba. The abnormal high concentration of Mn alone may suggest that these horizons have undergone variable degree of Pedogenesis. The depths showing higher concentration of Mn paired with corresponding increase in Ba suggest redox controlled precipitation of Mn in horizons that were initially rich in organic deposits. Mn here may have got mobilized in anoxic environment created below the organic layer and may have moved up with the pore water and got deposited in the oxic environment prevailing above the organic layer. Ba is known to get enriched in organic matter and their higher concentration acts as proxy for organic rich horizons. These horizons are finely laminated and may represent deposition under water in flood plain swamps or lakes. Among the trace elements the similar variation pattern observed in Ba (except where they show abnormal increase) and Sr and their similarity with the variation pattern of Na, Ca and K suggests that these elements are also held in feldspar. The trace elements Ni, Cr and Y correspond to the variation pattern of Al, Fe, Mg, Mn and Ti indicating that these elements are held in mafic and clay minerals.

In log Na_2O/K_2O vs. SiO_2/Al_2O_3 diagram most of the Uttrangudi borehole sediments plot in litharenite and subarkosic field. Few sediments from greater depth plot

in arkosic field suggest that these sediments have lost higher amount of Na i.e. undergone greater degree of plagioclase weathering. Compared to this all the sediments from Porayar location plot in the litharenite field. The plot of sediments in litharenite to subarkosic field indicate that the sediments from both the cores are poorly sorted and are immature. In log SiO_2/Al_2O_3 vs.log Fe_2O_3/K_2O diagram the sediments from Uttrangudi borehole plot in the field of Fe-sandstone and Fe-shale, whereas the Porayar sediments plot below the Uttrangudi sediments in the field of wacke and shale. Higher ratio of FeO/K_2O below 16 m depth in Uttrangudi core is probably because the combined effect of Fe addition due to early digenetic processes, where by Fe may have got added from the solution as indicated by higher mottling seen in sediments from this zone,and higher degree of weathering exhibited by their lower Na and K concentrations.

On comparison with UCC weare able to conclude that the Pleistocene sediments of Uttrangudi are different in their chemistry compared to the Holocene sediments of the same core and the Porayar core. The major difference is in terms of mobile elements. This would suggest that the Pleistocene sediments are more weathered in comparison to Holocene sediments of both locations. This is also indicated bychemical indices, chemical index of alteration (CIA) representing intensity of weathering, which is higher for Pleistocene sediments (70 to 97) from Uttrangudi core in comparison to Holocene sediments from the same core (CIA = 52 to 80) and from Porayar core (CIA = 50-80). The relatively lower weathering of Holocene sediments from both boreholes is also indicated by their overall closeness to the feldspar tie line in the A-CN-K plot in comparison to Pleistocene sediments. This would suggest that during the late Mid-Pleistocene period the climate was more wet and humid in comparison to Holocene period.

In the A-CNK-FMdiagram sediments from the Uttarangudi boreholeexhibit a trend moving away from the CNK end towards the A-FM join. The movement away from CNK & FM indicates mobilization of Ca, Na, K, Fe and Mg in all suites of Uttrangudi sediments and enrichment of Al in finer ones. Unlike this in the plot involving Porayar sediments, we find the trend moving parallel to the CNK-FM line suggesting that the shift in position of plot is due to differing proportion of feldspar and mafic minerals in the

sediments. Thus we may conclude that the chemical variations in Porayar sediments is solely attributed to be process related, whereas in Uttrangudi sediments the trend in addition to physical process of sorting has also been influence by secondary process of weathering and diagenesis.

The potential provenance for the Uttrangudi and Porayar sediments are the rocks of Archean age exposed in the catchment area of the Cauvery River. These include the two major terrains, (i) the northern greenstone granite terrain of Dharwarcraton (DC) consisting of granite Gneisses and minor mafic supracrustal rocks and (ii) the Southern Granulite Terrain (SGT) composed of felsic to intermediate charnockites that are transected by several shear zones. The charnockites in the SGT form high standing hills, whereas the gneisses in Dharwar craton and the shear zones form the low relief areas at different elevations. The bulk composition of the sediments apart from the source also depends on the degree of weathering and later sorting during transportation. During the process of transport and deposition, differential enrichment and depletion of different elements takes place in finer and coarser sediments due to the resultant mineral sorting. Coarser sediments in general are enriched in silica and depleted in other elements particularly Al, Fe, Mg, Mn in comparison to the source due to concentration of mafic minerals in the finer size fraction constituting the finer sediments. As a result the plot among the ratios of above elements particularly the immobile elements and silica shows a wide linear array passing through the plot for the source. In contrast the ratiosof immobile elements tend to retain the ratios in the source and do not show a wider range. Thus the plots among the ratios of immobile elements in sediments help in better constraining of their source. In the present study the plots of Fe/Ti vs Ti/Al in sediments along with the probable source rocks has been used to constrain the source. The plot of sediments in present study show clustering of data points of Pleistocene sediments from Uttrangudi and Holocene sediments from Porayar. Unlike the above two the Holocene sediments from Uttrangudi do not cluster together, but instead form a linear array displaying large variation. This would suggest that the Holocene sediments of the Uttrangudi have received input from differing sources at different times. On comparison with various source lithologies we find that the gneisses of Dharwar Craton separate out

in this diagram and plot away from the sediments from Uttrangudi as well as Porayar sediments. The sediments from Porayar show an overlap with the field of plot of Charnockites and the Gneisses from the transition zone and charnockite from the Cauvery shear zone/Madurai block, Cauvery shear zone, Kodaikanal region and Non garnetiferous charnockite from Nilgiri hills. This would suggest that the SGT rocks have acted as the major source for Porayar sediments. Unlike Porayar, the Pleistocene sediments from Uttrangudi do not show any overlap with the above mentioned catchment lithologies and plot towards lower Fe/Ti and higher Ti/Al end. It is interesting to find that these sediments show overlap with the plots of representative Tertiary rocks exposed west of Uttrangudi location. This would suggest that the source for Uttrangudi was local and it did not receive sediments directly from the upper catchment region during the Pleistocene. Thus to further verify the source we have compared the REE and Sr-Nd isotopic composition of the sediments with that of the rocks exposed in the present catchment region. From our REE results we infer that the source to the sediments have been Charnokitic rocks from high standing hills of Nilgiri and Biligirirangan hills forming part of the Northern Block of the SGT along with and the Kodaikanal-Palanai hill region forming part of the Southern Block of SGT also together known as the Northern Madurai Block (NMB). In addition to above the migmatitic gneiss and charnockite from the NMB also appear to have acted as the source. There is also probability of a local source in form of Tertiary rocks for the Uttrangudi sediments.

We have compared Sr and Nd isotopic composition of the sediments in an attempt to further discriminate the erosion variability among different regions of southern granulite terrain which has been inferred to have acted as the major source for the studied sediments. Thus to assess the erosion distribution of sediments from the granulite terrain we have grouped them into three end members (i) BR hills granulites (BRG) (ii) Nilgiri hills granulite (NHG) and (iii) Shear zones and Madurai block SZ/MB. BRG end member is distinctly different but NRG shows overlap in their $^{87}Sr/^{86}Sr$ values with BRG and of εNd_0 values with SZ/MB end member. The SZ/MB group is distinct from the BRG and NHG group only in their $^{87}Sr/^{86}Sr$ values.

On comparison of the Sr isotopic and εNd_0 values of sediments with above end members groups we find that they have contributed in differing proportion from upper mid Pleistocene to Holocene period. The $^{87}Sr/^{86}Sr$ and εNd_0 of the sediments from Uttrangudi shows five major excursions at depths ~22, ~16, ~5.8, ~4 and ~2 m. The minor positive excursion in both εNd_0 and $^{87}Sr/^{86}Sr$ observed at ~22, ~5.8 and ~2m indicate increased input from the SZ/MB as the rock types from this terrain is characterised by having both high $^{87}Sr/^{86}Sr$ ratio and εNd_0. The prominent excursion at ~16 m depth particularly towards lower εNd_0 indicate towards definite increase in input from the BRG as this terrain is having distinctly lower εNd_0 values. Other negative excursion in $^{87}Sr/^{86}Sr$ and εNd_0 observed at ~4 m depth may also be related to increased input from BRG. The sediment between 6 to 14 m depth show anti relation between Sr and Nd as indicated by increase in εNd_0 value with the concomitant decrease in the $^{87}Sr/^{86}Sr$ values. This relation between $^{87}Sr/^{86}Sr$ and $\varepsilon Nd_0$is observed in the rocks from NHG region suggesting them to have dominantly sourced the sediments for this part. It is observed that the frequency of fluctuation in source of sediments at Uttrangudi site increased during the Holocene period i.e. above ~7 m depth and it also record an increase in input from CSZ/MB block. The sediments from Porayar location show uniform$^{87}Sr/^{86}Sr$ values of ~ 0.713 except for two excursions observed at ~18 m ($^{87}Sr/^{86}Sr$ = 0.72) and 8.3 m ($^{87}Sr/^{86}S$ r=718) depths. In contrast εNd_0 values show larger variations of upto -10 in their εNd_0 values with a range of -34 to -24. The excursions towards higher εNd_0 observed at 19.23, 17.85, 13.5,8.42, 4.26 and 2.8 m depth would suggest increase in input from the SZ/MB domain, whereas excursionsat 23.48, 21.73, 15.73, 10.29 and 6.47m depths suggests increase in input from BRG and NHG terrain. Thus we see that the sediments from Porayar core which represents for most part the Holocene also show frequent changes in the source domain as observed in case of the Holocene sediments from Uttrangudi core. In contrast the fluctuation in source during the Pleistocene is less frequent and the source is observed to fluctuate mainly between NHG and BRG.

From the above discussion we may conclude that the sediment contribution during the Pleistocene period as observed in Uttrangudi core was dominantly from the BRG and NHG domains. The contribution from SZ/MB domain is observed to have

mainly increased towards the late Pleistoceneand continued through the Holocene. In contrast we observe that the contribution from DC has remained minimal for the entire period. Observations made on the basis of REE composition of these sediments also indicate predominantcontribution from SGT and minimal input from the DC. It is inferred in the present study that differences in relief in addition to amount and distribution of rainfall in the year had dominantly controlled the sediment supply from source region. The rainfall distribution pattern indicates that maximum rainfall is received in the Nilgiri hills and the Palani Hills of Madurai block. The annual rainfall in the Shear zone region, BR hills and the Upper catchment region is similar but we observe that in BR hills and the shear zone region the maximum rainfall occurs over a shorter duration. In contrast the rainfall over Mysore Plateau region,formed of gneisses of Dharwar Craton, is slightly less as well it is spread over longer period thus may generate lesser surface runoff. Higher rainfall over shorter period leads to more surface run off leading to greater erosion in contrast to similar or lower rainfall which is distributed over a longer period. In addition the DC has lower relief in comparison to NHG, BRG and MB terrain. Therefore the higher relief in addition to higher rainfall spread over shorter time in the SGT together may have resulted in higher erosion of the SGT rock in comparison to the DC. The temporal variation in input from different parts of the granulite terrain may be due to the local variations in rainfall at different times.

Further study on the Sr isotope composition of the exchangeable phases associated with the sediments indicate temporal and spatial variability in the isotopic composition of ground water. The isotopic composition of the leachate fractions (Carbonate, Fe-Mn and organic phase) that are supposed to act as the proxy for ground water indicate that the ground water during Pleistocene resembled the mix of fresh water (taken as present day River composition) and sea water in equal proportion. In contrast the Sr isotopic composition in Uttrangudi core for the Holocene period shows a shift towards River water composition, whereas the in Porayar sediments it shows greater affinity to sea water composition which is expected as these sediments are inferred to have been deposited in an estuarine environment.

References

Reference

Agemian, H. and Chau, A. S. Y. (1976). "Evaluation of extraction techniques for the determination of metals in aquatic sediments". *The Analyst, v* 101,761-7.

Alappat., L, Tsukamoto., S, Singh., P, Srikanth., D, Ramesh., R and Frechen., M (2010). "Chronology of cauvery delta sediments from shallow Subsurface cores using high-temperature post-ir irsl Dating of feldspar". Geochronometria 37.

Allen, P., Condie, K.C., Narayana, B.L., (1984). "The geochemistry of prograde and retrograde charnockite–gneiss reactions in southern India". *Geochim. Cosmochim. Acta* 49, 323–336.

Amorosi, A., Centineo, M.C., Dinelli, E., Lucchini, F and Tateo, F. (2002). "Geochemical and mineralogical varations as indicators of provenance changes in Late Quaternary deposits of SE Po Plain". *Sedimentary Geology*. *v* 151 Number 3, 1 August 2002 pp 273-292(20)

Anand, R. (2007). "Geochemical and geochronological studies on metavolcanics of the Hutti Schist Belt and granitoids around the schist belts of the Eastern Dharwar Craton". Unpub. Ph.D. Thesis, Pondicherry University, Pondicherry. 111 pp

Anand and Balakrishnan, (2010). "Pb, Sr and Nd isotope systematics of metavolcanic rocks of the Hutti greenstone belt, Eastern Dharwar craton: Constraints on age, duration of volcanism and evolution of mantle sources during Late Archean". *Journal of Asian Earth Sciences*. 39 (2010) 1–11

Anderson, S. P., Blum, J., Brantley, SL., Chadwick, O., Chorover, J., Derry, LA., Drever, J. I., Hering, JG., Kirchner, JW., Kump, LR., Richter, D., White, AF. (2004). "Proposed initiative would study weathering engine". EOS Transactions, vol 85, issue 28. *American earth's Geophysical Union*. pp 265–269.

Armstrong S. C., Sturchio N. C., and Hendry M. J. (1998). "Strontium isotopic evidence on the chemical evolution of pore waters in theMilk River aquifer, Alberta, Canada". *Geochem. Appl* 13, 463–475..

Balachandran, S., Asokan, R., and Sridharan, S. (2006) . "Global surface temperature in relation to northeast monsoon rainfall over Tamil Nadu". *J. Earth Syst. Sci*. 115,349-362.

Balakrishnan, S., Rajamani, V., Hanson, G.N., (1999). "U–Pb ages for Zirconium and Titanite from the Ramagiri areas, southern India: Evidence for accretionary origin of the craton during the Late Archean eastern Dharwar". J. Geol. 107, 69–86.

Balakrishnan, S., Hanson, G.N. and Rajamani., V. (1990). “Pb and Nd isotope constraints on the origin of high Mg and tholeiitic amphibolites, Kolar schist belt, south India”. Contrib. *Mineral. Petrol*. 107, 279–292.

Ball, T.T. and G.L. Farmer, (1998). “Infilling history of a Neoproterozoic intracratonic basin: Nd isotope provenance studies of the Uinta Mountain Group, Western United States”. 87:1-18. *Precambrian Research*

Banerjee P.K., (2000). “Holocene and Late Pleistocene relative sea level fluctuations along the east coast of India”. *Marine Geology*. 167, 243–260.

Banfield, J. F., and Eggleton, R. A. (1989). “Apatite replacement and rare earth mobilisation, fractionation, and fixation during weathering”. *Clays Clay Miner*. 37: 113-127.

Bartlett, J.M., Harris, N.B.W., Hawkesworth, C.J., Santosh, M. (1995). “New isotope constraints on the crustal evolution of South India and Pan-African granulite metamorphism”. *Mem. Geol. Soc*. India 34, 391–397

Bauluz, B., Mayayo, M.J., Fernandez-Nieto, C., Lopez, J.M.G., (2000). “Geochemistry of Precambrian and Paleozoic siliciclastic rocks from the Iberian Range (NE Spain): implications for source-area weathering, sorting, provenance, and tectonic setting”. *Chemical Geology*. 168, 135–150.

Berner RA, Berner EK (1997). “Silicate weathering and climate. In: Ruddiman WF (ed) Tectonic uplift and climate change”. *Plenum*, New York, pp 354–364

Beckinsale, R.D., Drury, S.A, Holt, R.W. (1980). “3.36-Myr old gneisses from the South Indian Craton”. *Nature*. 283, 469–470.

Berner R. A. (1995). “Chemical weathering and its effect on atmospheric CO_2 and climate. In Chemical Weathering Rates of Silicate Minerals”. (ed. A. F. White, S. L. Brantley) Reviews in Mineralogy, Vol. 3 pp.565–583. *Mineralogical Society of America*, Washington D.C.

Bhaskar Rao, Y.J., Chetty, T.R.K., Janardhan, A.S., Gopalan, K. (1996). “Sm-Nd and Rb-Sr ages and p-T- history of the Archean Sittampundi and Bhavani layered meta anorthosite complexes in Cauvery shear zone, South India: evidence for Neoproterozoic reworking of Archean crust”. *Contrib. Mineral. Petrol*. 125, 237-250.

Bhaskar Rao., Y.J, Janardhan., A.S, Vijaya Kumar., T, Narayana., B.L, Dayal., A.M, Taylor., P.N, Chetty., T.R.K. (2003). “Sm–Nd model ages and Rb–Sr isotopic systematics of charnockites and gneisses across the Cauvery shear zone, southern

India implications for the Archaean–Neoproterozoic terrane boundary in the Southern Granulite Terrain". In: Ramakrishnan, M. (Ed.), Tectonics of Southern Granulite Terrain, Kuppam–Palani Geotransect. *Memoirs of the Geological Society of India.* 50, 297–317.

Bhaskar Rao,Y.J., Naha., K Srinivasan.,R and Gopalan., K (1991). "Geology, geochemistry and geochronology of the Archean Peninsular Gneiss around Gorur, Hassan District, Karnataka, India". *Earth Planet Sci*. Vol 100, No 4.

Bhatia, M.R., (1983). "Plate tectonics and geochemical composition of sandstones". *Journal of Geology*. *v* 91, 611-627

Bhatia, M.R., and Crook, K.A.W. (1986). "Trace element characteristics of graywacks and Tectonic setting discrimination of sedimentary basins". *Contribution of Mineralogy and Petrology, v* 92, 181−193

Blum, J. D., and Erel, Y., (1997), "Rb-Sr isotope systematics of a granitic soil chronosequence: The importance of biotite weathering". *Geochimica et Cosmochimica Acta*, v. 61, p. 3193–3204.

Blum J. D. and Erel Y. (2003). "Radiogenic isotopes in weathering and hydrology. In Surface and Ground Water, Weathering, Erosion and Soils" (ed. J. I. Drever). Elsevier Science in Treatise on Geochemistry (eds. K. K. Turekian and H. D. Holland). *v*. 5.

Bluth G.J, Kump LR. (1994). "Lithologic and climatologic controls of river chemistry". *Geochimica Cosmochimica Acta* 58: 2341–2359

Bock, B., McLennan, S.M., Hanson, G.N. (1994). "REE redistribution and its effects on the Nd isotope system in the Austin Glen Member of the Normanskill Formation". New York. *Geochimica et Cosmochimica Acta*. 23, 5245–5253.

Bock, B., Mclennan, S.M. and Hanson, G.N. (1998). "Geochemistry and provenance of the Middle Ordovician Austin Glen Member (Normanskill Formation) and the Taconian Orogeny in New England". *Sedimentology v 45, 635–655*.

Bouhallier, H., Choukroune, P., Ballèvre, M., (1993). "Diapirism, bulk homogeneous shortening and transcurrent shearing in the Archaean Dharwar Craton: the Holenarsipur area, Southern India". *Precambrian Res*. 63, 43–58

Bouhallier, H., Chardon, D. and Choukroune, P. (1995). "Strain patterns in Archaean dome-and-basin stuctures: the Dharwar craton (Karnataka) South India". Earrh Planet. Sci. South India). *Earth Planet. Sci. Lett*. 135, 57-75.Lett. 135, 57-75.

Brandon, A. D. and Meen, J. K. (1995). "Nd isotopic evidence for the position of southernmost Indian terranes within East Gondwana". *Precambrian Res*. 70, 269-280.

Brindley, G.W and Brown, G., (1980). "Crystal structures of clay minerals and their X-ray identification". Monograph no 5 , *Min . Soc. London*, 495p

Bunzl, K., K. R., Schramel, P., Szeles, M., and Winkler, R. (1995). "Speciation of ^{238}U, ^{226}Ra, ^{210}Pb, ^{228}Ra, and stable Pb in the soil near an exhaust ventilating shaft of a uranium mine". *Geoderma v* 67, 45-53.

Bunzl, K. K. R., Schramel, P., Szeles, M., Winkler, R. (1996). "Speciation of ^{238}U, ^{226}Ra, ^{210}Pb, ^{228}Ra, and stable Pb in the soil near an exhaust ventilating shaft of a uranium mine". 67(1-2), 1995, pp 45-53. *International Journal of Rock Mechanics and Mining Science & Geomechanics Abstracts*. *v.* 33, A144. *Geoderma*.

Campos Alvarez, and N.O., Roser B.P (2007)." Geochemistry of black shales from the lower Creataceous Paja Formation, Easteren Cordillera, Colombia: Source weathering , Provenance and tectonic setting". *Journal of South American Earth Science*, 23(4), 271-289.

Casanova, J. and Négrel, Ph., (1995). "Signature isotopique et origine des carbonates des sédiments de la longue séquence carottée du Lac d'Annecy (Haute Savoie)". In: Proceedings of the 16th Regional European Meeting IAS, Aix les Bains 1995, 31pp.

Capo R. C., Stewart B. W., and Chadwick O. A. (1998). "Strontium isotopes as tracers of ecosystem processes: theory and methods".*Geoderma* 82, 197–225.

Casanova, J., Bodénan, F., Négrel, Ph. and Azaroual, M. (1999). "Microbial control on the precipitation of ferrihydrite and carbonate modern deposits from the Cézallier springs (Massif Central, France)". *Sediment. Geol*., 126, 125–hydrothermal 145

Catlos, J. Elizabeth ., Kaan Sayit, Poovalingam Sivasubramanian, and Chandra S. Dubey. (2011). "Geochemical and Geochronological Data from Charnockites and Anorthosites from India's Kodaikanal–Palani Massif, Southern Granulite Terrain". India.

Chadwick B., Ramakrishnan, M. and Viswanatha M.N (1981). "Structural and metamorphic relations between Sargur and Dharwar supracrustal rocks and peninsular Gneiss in central Karnataka". *J.Geol.Soc.India.* 22,557-569.

Chadwick, B., Vasudev, V.N., Krishna Rao, B., Hegde, G.V. (1992). "The Dharwar supergroup: basin development and implications for Late Archean tectonic setting in western India, southern India". In: Glover, J.E., Ho, S. (Eds.), *The Archean:*

Terrains, Processes and Metallogeny, v. 22. University of Western Australia, Publ., pp. 3–15.

Chadwick,B., Vasudev,V.N.,Hedge, G.V. (2000). "The Dharwar craton, southern India ,interpreted as the result of Late Archaean oblique convergence". *Precambrian Res*.99, 91-111.

Chamberlin, T.C., (1899). "An attempt to frame a work ing hypothesis of the cause of glacial periods on an atmospheric basis". *J. Geol*., 7: 545-584.

Chaudhuri, S and Clauer, N (1992). "Sm-Nd isotopes in fine grained clastic sedimentary materials clues to sedimentary processes and recycling growth of continental crust". In Clauer,N and Chaudhuri,S (eds) Isotope Signatures and Sedimentary Records, *Springer* Verlag.

Chetty, T.R.K., Bhaskar Rao, Y.J. and Narayana, B.L. (2003). "A structural cross section along Krishnagiri-Palani Corridor, Southern Granulite Terrain of India". In: M.(Ed.), India. Mem. No. 50, pp. 255-278. *Tectonics of Southern Granulite Terrain*. Geol. SOC. Ramakrishnan.

Choudhary, A.K.. Jain, A.K., Singh, S., Manickavasagam. R.M and Chandra. K. (2011). "Crustal Accretion and Metamorphism of Mesoarchean Granulites in Palghat-Cauvery Shear Zone, Southern India". *Journal Geological Society of India* Vol.77, March 2011, pp.227-238

Cingolani, C.A., Manassero, M and Abre, P (2003). " Composition, Provenance and tectonic setting of Ordovician Silciclastic rocks in the San Rafael Block: Southeren extension of the Precordillera crustal fregment, Argentina". *Journal of South American Earth Sciences Review*, 16(1) IGCP 436 Pacefic Gondwana Margin Special Issue.

Clift, P. D., and J. S. Blusztajn (2005). "Reorganization of the western Himalayan river system after five million years ago". *Nature*, 438, 1001–1003, doi:10.1038/nature04379.

Clift, P. D., et al. (2002). "Nd and Pb isotope variability in the Indus River system; implications for sediment provenance and crustal heterogeneity in the western Himalaya". *Earth Planet. Sci. Lett*., 200, 91–106, doi:10.1016/S0012-821X(02) 00620-9.

Condie, K.C., Dengate, J., and Cullers, R.L (1995). "Behaviour of rare earth elements in a paleoweathering profile on granodiorite in the front range". Colorado, USA, *Geochimca Cosmochimica Acta*. *v* 59, 279-294.

Condie, K.C., Lee, D. and Farmer, L. (2001) “Tectonic setting and provenance of the Neoproterozoic Uinta Mountain and Big Cootonwood groups, northern Utah: constraints from geochemistry, Nd isotopes, and detrital modes”. *Sediment. Geol*., *v*.141-142, pp.443-464.

Condie, K.C. (1993). “Chemical composition and evolution of the upper continental crust: contrasting results from surface samples and shales”. *Chemical Geology* 104, 1–37.

Condie, K.C. (1991). “Another look at rare earth elements in shales”. *Geochim. Cosmochim. Acta*, 55: 2527-2531.

Cox, R., Lowe, D. (1995). “A conceptual review of regional-scale controls on the composition of clastic sediment and the co-evolution of continental blocks and their sedimentary cover”. *Journal of Sedimentary Research* A 65, 1–12.

Cullers, R.L., Berendsen, P. (1998). “The provenance and chemical variation of sandstones associated with the mid- continent rift system”. USA. *Eur. J. Mineral*. *v* 10, 987– 1002.

Cullers, R.L. and Podkovyrov ,V.N. (2000). “ Geochemistry of the Mesoproterozoic Lakhanda shales in southeastern Yakutia, Russia: implications for mineralogical and provenance control, and recycling”. *Precambrian Res*., *v*.104(1-2), pp.77-93.

Cullers, R.L., Barrett, T., Carlson, R., Robinson, B. (1987). “Rare-earth element and mineralogical changes in Holocene soil and stream sediment: a case study in the Wet Mountains, Colorado, USA”. *Chem. Geol*. *v* 63, 275–297.

Cullers, R.L., (1988). “Mineralogical and chemical changes of soil and stream sediment formed by intense weathering of the Danberg granite, Georgia, USA”. *Lithos.* 21, 301–

Cullers RL, Stone J (1991). “Chemical and mineralogical composition of the Pennsylvanian mountain, Colorado, USA (an uplifted continental blocks) to sedimentary rocks from other tectonics environments”. *Lithos* 27:115–131

Cullers, R.L. (2000). “The geochemistry of shales, siltstones, and sandstones of Pennsylvanian–Permian age, Colo- rado, USA: implications for provenance and metamor- phic studies”. *Lithos v* 51, 181–203.

Cullers, R.L.(1994). “The controls on the major and trace element variations of shales, siltstones, and sandstones of Pensylvanian-Perminan age from uplifted continental blocks in Colorado to platform sediment in Kansas, USA”. *Geochimca Cosmochima Acta*. *v* 58, 4955-4972.

D. Srikanth (2012). "Geochemical and Carbon isotope studies on the surface and subsurface sediments of Cauvery Delta, South India".Unpub. Ph.D. Thesis, Pondicherry University, Pondicherry.

DePaolo, D.J. and Wasserburg, G.J., 1976. Nd isotopic variations and petrogenetic models. *Geophys. Res. Lett*., 3: 249-252.

Dessert C., Dupre´ B., Francois L. M., Schott J., Gaillardet J., Chakrapani G. J. and Bajpai S. (2001). "Erosion of Deccan Traps determined by river geochemistry: impact on the. global climate and the $^{87}Sr/^{86}Sr$ ratio of seawater". *Earth Planet. Sci. Lett.* 188, 459–474

Dickinson, W.R., Patchett, P.J., Ferguson, C.A., Suneson, N.H., Gleason, J.D. (2003). "Nd isotopes of Atoka Formation (Pennsylvanian) turbidites displaying anomalous east-flowing paleocurrents in the frontal Ouachita Belt of Oklahoma: implications for regional sediment dispersal". *Journal of Geology,* 111, 733– 740.

Divakar Rao., V. Subba Rao., M.V, Murthy., N.N. (1999). "Granite forming events and their role in crust formation of the Indian shield". *Revista Brasileria de Geociencias* 29(1), 33-40.

Dittrich.,M.B, Reicher., P. W, (2009)."Lake sediments during the transient eutrophication period: Reactive-transport model and identifiability study". *Ecological Modelling*. 220 2751–2769.

Dixon., J.B, Weed., S.B , Kittrick, J.A., Milford,M.H and White., J.l (1977). "*Minerals in soil environments*" . *Soil Sci. Lett*., *v* 248, pp . 426-437.

Drever JI, Zobrist J (1992). "Chemical weathering of silicate rocks as a function of elevation in the southern Swiss Alps". *Geochimica et Cosmochimica Acta* 56:3209–3216

Drury,S.A., Holt, R.W.(1980). "The tectonic framework of the South Indian craton: a reconnaissance involving LANDSAT imagery. *Tectonophysics*" *v* 65, T1-T15.

Duddy, I.R., (1980). "Redistribution and fractionation of rare earth and other elements in a weathering profile".*Chem. Geol*., 30: 363-381.

Dupre´, B., Dessert, C., Oliva, P., Godde´ris, Y., Viers, J., Franc¸ois, L., Millot, R., and Gaillardet, J., (2003). "Rivers, chemical weathering and Earth's climate": Computes rendus Geoscience, v. 335, p. 1141–1160, doi: 10.1016/j.crte.2003.09.015.

Eastin, R., and G Faure. (1970). " Seasonal varation of the solute content and $^{87}Sr/^{86}Sr$ ratio of the Olentangy and Scioto Rivers at Columbs, Ohio". *Ohio J. Sci*, 70, 170-179.

Fagel, N., et al. (2002). "Sources of Labrador Sea sediments since the last glacial maximum inferred from Nd-Pb isotopes". *Geochim. Cosmochim. Acta*, 66(14), 2569–2581,S0016-7037(02)00866-9. doi:10.1016/.

Faure, G., Crocket, J.H. and Hurley, P.M., (1967). "Some aspects of the geochemistry of Sr and Ca in the Hudson Bay and the Great Lakes". *Geochim. Cosmochim. Acta*, 31: 451-461.

Faure G (1986). "Principles of isotope geology". Wiley, New York

Fedo, C.M., Nesbitt, H.W., Young, G.M. (1995). "Unravelling the effects of potassium metasomatism in sedimentary rocks and paleosols, with implications for paleoweathering conditions and provenance". *Geology v* 23, 921–924.

Fedo, C.M., Young, G.M., Nesbitt, H.W., Hanchar, J.M., 1997. "Potassic and sodic metasomatism in the southern province of the Canadian shield: evidence from the Serpent Formation, Huronian Supergroup, Paleoproterozoic Canada". *Precambrian Res*. 84, 17–36.

Fedo, C.M., Eriksson, K.A., Krogstad, E.J. (1996). "Geochemistry of shales from the Archean (~3.0 Ga) Buhwa Greenstone Belt, Zimbabwe: Implications for provenance and source-area weathering". *Geochimica et Cosmochimica Acta v* 60, 1751-1763.

Feng, R. and Kerrich, R. (1990). "Geochemistry of fine-grained clastic sediments in the Archean Abitibi greenstones belt, Canada: implications for provenance and tectonic setting". *Geochim. Cosmochim. Acta*., *v*.54, pp.1061-1081.

Fisher R. S. and Stueber A. M. (1976). "Strontium isotopes in selected streams within the Susquehanna River Basin". *Water Resour. Res*. 12, 1061–1068.

Fleet, A.J., (1984). "Aqueous and sedimentary geochemistry of the rare- earth elements". In: Henderson, P.(ed.), Rare-Earth Element Geochemistry. Elsevier, Amsterdam, 343−373.

Floyd J.D and Stiven, G l. (1991). "Rare Temporary Exposure of the southern Upland Fault Near Abington, Strathclyde". *Scottish journal of Geology, v* 27, 75-80.

Force E. R. and Cannon W. F. (1988). "A depositional model for shallow-marine manganese deposits around black-shale basins". *Econ. Geol*. 83,93-I 17.

Frallick, P.N., Kronberg, B.I., (1997). “Geochemical discrimination of clastic sedimentary rock sources”. *Sedimentary Geology*. 113, 111–124.

Franklyn M. T., McNutt R. H., Kamineni D. C., Gascoyne M., and Frape S. K. (1991) “Groundwater $^{87}Sr/^{86}Sr$ values in the Eye-Dashwa Lakes Pluton, Canada: evidence of Plagioclasewater reactions”. *Chem. Geol*. 86, 111–122.

Gaillardet, J., Dupre´, B., Louvat, P., and Alle`gre, C. J., (1999). “Global silicate weathering and CO2 consumption rates deduced from the chemistry of large rivers” Chemical Geology, v. 159, p. 3–30, doi:10.1016/S0009- 2541(99)00031-5.

Galindo, N. C., Mougin,L., Fakhi, S., Nourreddine, A., Lamghari, A., Hannache, H. (2007). “Distribution of naturally occurring radionuclides (U, Th) in Timahdit black shale” (Morocco). *Journal of Environmental Radioactivity*. 92, 41-54.

Garver, J.I., Royce, P.R., Smick, T.A., (1996). “Chromium and nickel in shale of the Taconic foreland: a case study for the provenance of fine-grained sediments with an ultramafic source”. *Journal of Sedimentary Research* 100, 100–106.

Garzione, C.; Patchett, P.; Ross, G.; and Nelson, J. (1997). “Provenance of Paleozoic sedimentary rocks in the Canadian cordilleran miogeocline: a Nd isotopic study”. *Can. J. Earth Sci*. 34:1603–1618

Ghosh, J.G., De Wit, M.J., Zartman, R.E. (2004). “Age and tectonic evolution of Neoproterozoic ductile shear zones in the southern granulite terrain of India, with implications for Gondwana studies”. *Tectonics* 23,TC3006.

Ghosh, J.G.(1997). “Structural and geochronologic study along parts of Palghat-Cauvery shear zone, South India”. In. R. Cox and L.D.Ashwal (eds.) Proterozoic geology of Res. Group Misc.Pub.No.5, pp.21-22.Madagascar, *Gondwana*.

Gibbs, R. J. (1977). “Transport Phases of Transition Metals in the Amazon and Yukon Rivers”. *The Geological Society of America Bulletin*. 88, 829-843.

Gioia, S.M.C.L. and Pimentel, M.M. (2000). “The Sm-Nd Isotopic Method in the Geochronology Laboratory of the University of Brasília”. *An. Acad. Bras*. Ci. 72, 219–245.

Gleason, J.D., Patchett, P.J., Dickinson, W.R., Ruiz, J., (1995). “Nd isotopic constraints on sediment sources of the Ouachita-Marathon fold belt”. *Geological Society of America* 107, 1192– 1210.

Goldstein, S. J., and S. B. Jacobsen (1987). “The Nd and Sr isotopic systematic of river-water dissolved material: Implications for sources of Nd and Sr in seawater”. *Chem. Geol*., 66, 245– 272.

Goldstein, S. J. & Jacobson, S. B. (1988). “Rare earth elements in river waters”. *Earth Planet. Sci. Lett*. 89, 35-47.

Goldstein, S. L., and R. K. O’Nions (1981), “Nd and Sr isotopicb relationships in pelagic clays and ferromanganese deposits”, *Nature*, 292(5821), 324–327, doi:10.1038/292324a0.

Goldstein, S. J., R. K. O'Nions and P. J. Hamilton. (1984). “A Sm-Nd isotopic study of atmospheric dusts and particulates from major river systems”. *Earth Planet. Sci. Lett*.,*v* 70, 221-236,

Gopalakrishnan, K. (1994). “An overview of southern granulite terrain of Tamil Nadu - constraints in reconstruction of Precambrian assembly of Gondwanaland”. *Gondwana Sym*., Oxford and IBH Publ. Co. Ltd., *v*. 2, pp. 1003-1026.

Gosz J. R., Brookins D. G., and Moore D. I. (1983). Using strontium isotope ratios to estimate inputs to ecosystems. BioScience 33, 23– 30.

Govindaraju, K. (1994). “Compilation of working values and sample description for 383 geostandards”. *Geostandards Newsletter*, 18. 1–158.

GSI miscellaneous publication no 30. 2006.

Gunnel, Y. and Bourgeon, G. (1997). “Soils and climatic geomorphology on the Karnataka plateau, peninsular India”. *Catena* 29, 239-262.

Gunnel, Y., Braucheer, R., Bourles, D., Andre, G., (2007). “Quantitative and qualitatinve insights into bedrock land form erosion on theSouth India craton using cosmogenic nuclides and apatite fission tracks”. *Geological Society of America Bulletin*. 117, 5-6, 576-586.,deoi:10.1130/B25945.1.

Gunnell Y., (1998). “The interaction between geological structure and global tectonics in multistoreyed landscape development: a denudation chronology of the south shield”. *Basic Research, v*10, 281-310.

Gupta, S. K. and K. Y. Chen. (1975). “Partitioning of trace metals in selective chemical fractions of near shore sediments” .*Envi. Lett*., 10: 129-158,

Hamilton P. J., O’Nions R. K., Bridgwater D. and Nutman A. (1983). “Sm/Nd studies of Archean metasediments and metavolcanics from West Greenland and their applications for the Earth’s early history”. *Earth Planet. Sci. Lett*. 62, 263–272.

Hansen, E.C., Newton, R.C. and Janardhan, AS. (1984). “Pressures, temperatures and metamorphism fluid across an unbroken amphbolite to granulite facies transition in southern Karnataka, India. In: Kroner, A., Hanson, G.N. and Goodwin, A.M. (Eds.), Archaean Geochemisuy. The origin and evolution of the Achaean continental crust.” Springer: Berlin-Heidelberg-New York-Tokyo, pp. 161-181.

Harnois L. (1988). “The CIW Index: A new chemical index of weathering”. *Sediment. Geol*. 55.319-322

Harris, N.B.W., Santhosh, M., Taylor, P.N. (1994). “Crustal evolution in South India. Constraints from Nd isotopes”. *J.Geol*.102,139-150.

Hassan, S., Ishiga, H., Roser, B.P., Dozen, K., Naka, T. (1999). “Geo- chemistry of Permian-Triassic shales in the Salt Range, Pakistan: implications for provenance and tectonism at the Gondwana margin”. *Chem. Geol*. 158, 293–314.

Herron, M.M. (1988). “Geochemical Classification of terrigenous sands and shales from core or log data”. *Journal of Sedimentary Petrology* 58 , 820-829.

Hofmann, A., Bolhar, R., Dirks, P., Jelsma, H., (2003). “The geochemistry of Archean shales derived from a mafic volcanic sequence, Belingwe greenstone belt, Zimbabwe: provenance, source area unroofing and submarine versus subaerial weathering”. *Geochim. Cosmochim. Acta* 67, 421–440.

Hofmann, A. (2005). “The geochemistry of sedimentary rocks from the Fig Tree Group, Barberton greenstone belt: implications for tectonic, hydrothermal and surface processes during mid-Archaean times”. *Precambrian Res* 143, 23–49.

Holland H. D. (1984). “The chemical Evolution of the Atmosphere and Oceans”. Princeton University Press.

Holmden, C., Creaser, R. A. and Muehlenbachs, K., (1997).Paleosalinities in ancient brackish water systems determined by 87Sr/86Sr ratios in carbonate fossils: A case study from the Western Canada Sedimentary Basin. *Geochim. Cosmochim.Acta*. 61, 2105–2118.

Holser, W.T. (1997). “Evaluation of the application of rare-earth elements to paleooceanography”. *Palaeogeography Palaeoclimatology Palaeoe- cology* 132, 309–323.

Huntsman-Mapila , P ., Tiercelin, J,J., Benoit,M., Ringrose,S.,Diskin,S., Cotton,J, and Hemond,C. (2009). “Sediment geochemistry and tectonic setting: Applictaion of discrimnatation diagrams to early stages of intracontinental rift evolution, with

examples from the Okavango and Southeren Tanganyika rift basins". *Journal of African Earth Sciences Volume*. 53. Issues 1-2 January 2009, p 33-44.

Hurowitz, J.A. and Mclennan, S.M. (2005). "Geochemistry of Cambro-Ordovician Sedimentary Rocks of the Northeastern United States: Changes in Sediment Sources at onset of Taconian Orogenesis". *Jour. Geol., v.*113, pp.571-587.

Innocent, C., Fagel, N., Hillaire, M.C. (2000). "Sm–Nd isotope system- atics in deep sea sediments: clay-size versus coarser fractions". *Marine Geology* 168, 79–87.

Integrated Hydrological Data Book, (Non-classified River Basin), Central Water Commission, New Delhi, October 2007.

Janardhan, AS., Newton, RC., Hansen, EC. (1982). "The transformation of amphibolite facies gneiss to charnockite in southern Karnataka and northern Tamil Nadu". India. Contrib 79:130–149 *Mineral Petrol*.

Janardhan, AS., Newton, R.C. and Smith, J.V. (1979)." Ancient crustal metamorphism at low PI 1p: charnockite formation at Kabbaldurga, south India". *Nature, v.*278, pp.511-517.

Jaques, A.L., Chappell, B.W., Taylor, S.R., (1983). "Geochemistry of cumulus peridotites and gabbros from the Marum Ophiolite Complex, northern Papua New Guinea". *Contributions to Mineralogy and Petrology* 82, 154–164

Jayananda M and Peucat J J. (1996). "Geochronological framework of southern India". *Gondwana. Res*. Group Mem. 3, 53–75.

Jayananda, M., Chardon, D., Peucat, J.-J., Capdevila, R. (2006). "2.61 Ga potassic granites and crustal reworking in the western Dharwar craton, south India: tectonic, geochronologic and geochemical constraints". *v* 150,1–26. *Precambrian Res*.

Jayananda, M., Kano, T., Peucat, JJ., Channabasappa, S. (2008). "3.35 Ga komatiite volcanism in the western Dharwar craton, southern India: constraints from Nd isotopes and whole-rock geochemistry". *Precambrian Res* 162:160–179.

Jayananda, M., Martin, H., Peucat, J.J. and Mahabaleswar, B. (1995)." Late Archaean crust-mantle interactions: geochemistry of LREE-enriched mantle derived magmas. Example of the Clospet batholith, southern India". *Contrib. Mineral. Petrol. v.*119(2-3), pp.314-329.

Jayananda, M., Moyen, J.F., Martin H., Peucat, J.-J., Auvray B. and Mahabaleswar B. (2000). "Late Archaean (2550-2520 Ma) juvenile magmatism in the Eastern

Dharwar craton, southern India: constraints from geochronology, Nd Sr isotopes and whole rock geochemistry". *Precambrian Res*, 99, 225 254.

Jenne, E.A., (1977). "Trace element sorption by sediments and soils". In: W. Chappell and S.K. Petersen (Editors), Sites and processes. Proc. Symp. Molybdenum in the New York, pp. 42~553.Environment, Vol. 2. Dekker,

John M. M., Balakrishnan S. and Bhadra B. K. (2005). "Contrasting metamorphism across Cauvery Shear Zone, south India". *J. Earth System Science*, 114, No.2, 1-16.

Johnsson, M. J., (1993), "The system controlling the composition of clastic sediments, in processes controlling the composition of clastic sediments: Boulder, Colorado". *Geological Society of America Special Paper* 284, p. 1-19.

Jung, S.J.A., Davies, G.R., Ganssen, G.M., Kroon, D., (2004). "Stepwise Holocene aridi- fication in NE Africa deduced from dust-borne radiogenic isotope records". *Earth and Planetary Science Letters* 221, 27–37.

Kasting, J.F., (1993). "Earth's early atmosphere". *Science* 259, 920–926.

Kessarkar, P.M., Rao, V.P., Ahmad, S.M., Babu, G.A., (2003). "Clay minerals and Sr–Nd isotopes of the sediments along the western margin of India and their implication for sediment provenance". *Marine Geology* 202, 55–69.

Knauth, L.P., Lowe, D.R., (2003). "High Archaean climatic temperatures inferred from oxygen isotope geochemistry of cherts in the 3.5 Ga Swaziland Supergroup, South Africa". *Geological Society of America Bulletin. v* 115, 566–580.

Krogstad, E.J., Hanson, G.N. and Rajamani, V. (1991). "U-Pb ages of zircon and sphene for two gneiss terrains adjacent to the Kolar Schist Belt, south India: evidence for separate crustal evolution histories". *J. Geol. v* 99, 801–816.

Krogstad, E.J., Hanson, G.N. and Rajamani, V.(1995). "Sources of continental magmatism adjacent to the late Archean Kolar Suture Zone, south India: distinct isotopic and elemental signatures of two late Archean magmatic series". *Contrib. Mineral. Petrol., v* 122, 159–173.

Kuhlmann, H., Freudenthal, T., Helmke, P., Meggers, H., (2004). "Reconstruction of local paleoceanography off NWAfrica during the last 40,000 years: influence of local and regional factors on sediment accumulation". *Marine Geology.* 207, 209–224

Kumar, A., Bhaskar Rao, Y.J., Sivaraman, T.V., Gopalan, K. (1996). "Sm–Nd ages of Archaean metavolcanics of the Dharwar craton, South India". *Precambrian Res*. 80, 206–215.

Lahtinen, R., (2000). "Archaean-Proterozoic transition: geochemistry, provenance and tectonic setting of metasedimentary rocks in cen- tral Fennoscandian Shield, Finland". *Precambrian Res*. 104 (3/4), 147–174.

Leleyter L., and Probst J. L. (1999). "A new sequential extraction procedure for the speciation of particulate trace elements in river sediments". *Int. J. Environ. Anal. Chem*. 73, 109–128.

Lerouge. C, Gaucher E.C. , Tournassat C, Negrel P, Crouzet C, Guerrot C, (2010) "Strontium distribution and origins in a natural clayey formation (Callovian-Oxfordian, Paris Basin, France): A new sequential extraction procedure". *Geochimica et Cosmochimica Acta* 74 2926–2942

Lev, S. M Mclennan, S.M., Meyers, W.J and Hanson, G.N (1998). "A Petrographic apporach for evaluating trace element mobility in a black shale". *Journal of sedimentary Research.* 68, 5, 970-980.

Louvat P. and Allegre C.J., (1997): "Present denudation rates on the island of Reunion determined by river geochemistry: Basalt weathering and mass budget between chemical and mechanical erosion", Geochim. Cosmochim. Acta, 61, No. 17, 3645-3669

Lugmair G. W. and Marti K. (1978) "Lunar initial $^{143}Nd/^{144}Nd$: Differ- ential evolution of the lunar crust and mantle". *Earth Planet. Sci. Lett*. 39, 349–357.

Malo, B. A. (1977). "Partial extraction of metals from aquatic sediments". Environmental Science & Technology *v* 11, 277-282.

Marsh, J.S., (1991). "REE fractionation and Ce anomalies in weathered Karoo dolerite". *Chem. Geol*., 90: 189- 194.

McCulloch, M.T and Wasserburg, G.J (1978). "Sm-Nd and Rb-Sr chronology of continental crust formation". *Science . v* 200, 1003-1011.

McDaniel, D.K., McLennan, S.M., Hanson, G.N., (1997). "Provenance of Amazon fan muds: constraints from Nd and Pb isotopes. In: Flood". R.D., Piper, D.J.W., Klaus, vol. 155, pp. 169–176.A.,Peterson, L.C. (Eds.), Proceedings of the Ocean Drilling Program Scientific results.

McLennan, S.M., Hemmings, S., (1992). “Samarium/neodymium elemental and isotopic systematics in sedimentary rocks”. *Geochim. Cosmochim. Acta* 56, 887–898.

Mclennan, S.M. and Taylor, S.R. (1991). “Sedimentary rocks and crustal evolution: tectonic setting and secular trends”. *Jour. Geol*, v.99, pp.1-21.

McLennan, S. M., Taylor, S. R., McCulloch, M. T., and Maynard, J. B. (1990). “Geochemical and Nd-Sr isotopic composition of deep-sea turbidites: crustal evolution and plate tectonic associations”. *Geochimica et Cosmochicmica Acta, v*. 54, p. 2015-2050.

McLennan, S.M., Hemming, S.R., Taylor, S.R., Eriksson, K.A. (1995). “Early Proterozoic crusral evolution: geochemical and Nd–Pb isotopic evidence from metasedimentary rocks, southern North America”. *Geochim. Cosmochim. Acta v* 59, 1153–1177.

McLennan S. M., Nance W.B. and Taylor S.R., (1980). “Rare earth element-thorium correlations in sedimentary rocks, and the composition of the continental crust”. *Geochim.Cosmochim. Acta*. 44, 1833-1839.

McLennan, S.M. (1989). “Rare earth elements in sedimentary rocks: influences of provenance and sedimentary processes”. *Reviews in Mineralogy.* 21, 169-200.

Mclennan, S.M., Hemming, S., Mcdaniel, D.K. and Hanson, G.N. (1993) “Geochemical approaches to sedimentation, provenance, and tectonics. In: M.J. Johnson and A. Basu (Eds.), Processes Controlling the Composition of Clastic Sediments”. *Geol. Soc. Amer*. Spec. Paper, v.284, pp.21-40.

McLennan, S.M., Taylor, S.R. and Eriksson, K.A. (1983). “Geochemistry of Archaean shales from the Pilbara Supergroup, Western Australia”. *Geochim. Cosmochim. Acta*. *v*.47(7), pp.1211-1222.

Meen, J.K., Rogers., J.J.W. and Fullagar, P.D. (1992). “ Lead isotopic compositions of the western Dharwar Craton, southern India: evidence for distinct middle Archean terranes in a late Archean craton” pp. 2455-2470. *Geochim. Cosmochim. Acta,v*. 56,

Meissner B, Deters P, Srikantappa C and Kohler H .(2001). “Geochronological evolution of the Moyar, Bhavani and Palghat shear zones of southern India: Implication of east Gondwana correlations”. *Precamb. Res*. 114 149–175.

Meijerink, A. M. J.(1971). “Reconnaissance Survey of the Quaternary Geology of Cauvery Delta”, *Jour. Geol.Soc.India* 12. pp. 113-124.

Miller, R.G., O'Nions, R.K. (1984). "The provenance and crustal resi- dence ages of British sediments in relation to palaeogeographic reconstructions". *Earth and Planetary Science Letters.* 68, 459–470.

Milodowski, A. E. and Zalasiewicz, J. A. (1991). "Redistribution of rare earth elements during diagenesis of turbidite/hemipelagite mudrock sequences of Llandovery age from central Wales". in Morton, A. C., Todd, S. P., and Haughton, P. D. W., eds., Developments in Sedimentary Provenance Studies: London, Geological Society of London. *Geological Society Special Publication* No. 57, p. 101-124.

Mitra .,D. S and Agarwal.(1981). "Geomorphology and Petroleum Prospects of Cauvery Basin, Tamilnadu, Based on Interpretation of Indian Remote Sensing Satellite (IRS) Data" R P Remote Sensing Laboratory, KDMIPE, ONGC, Dehra Dun - 248 195.

Morton, L. S., Evans, C.V., Harbottle, G., Estes, G.O. (2001). "Pedogenic fractionation and bioavailability of uranium and thorium in naturally radioactive spodosols". *Soil Science Society of America Journal v* 65, 1197-1203.

Mongelli, G. (2004) "Rare-earth elements in Oligo-Miocenic pelitic sediments from Lagonegro basin, southern Apennines, Italy: implications for provenance and source-area weathering. International Journal of Earth Sciences, 93, 612-620.

Mongelli, G., Cullers, R. and Muelheisen, S. (1996). "Geochemistry of Cenozoic shales from the Varicolori Formation, Southern Apennines, Italy: implications for mineralogical, grain size control and provenance". *European Journal of Mineralogy*, 8, 733-754.

Naha K, Srinivasan R and Jayaram S (1993). "Structural relations of charnockites of the Archean Dharwar craton, southern India". *J. Meta. Geol*. 11 889–895

Naha, K. and Srinivasan, R., (1996). "Nature of the Moyar and Bhavani shear zones, with a note on its implication on the tectonics of the southern Indian Precambrian shield". Proc. Ind. Acad. Sci. *Earth and Planet. Sci*, v.105, p.143-189

Naqvi, S.M., Uday Raj, B., Subba Rao, D.V., Manikyamba, C., Nirmal Charan, S., Balaram, V. & Srinivasa Sarma, D. (2002). "Geology and geochemistry of arenite–quartzwacke from the Late Archaean Sandur schist belt—implications for provenance and accretion processes". *Precambrian Res*, 114, 177–197.

Naqvi, S.M., Sawkar, R.H., Subba Rao, D.V., Govil, P.K., Rao, T.G., (1988). "Geology, geochemistry and tectonic setting of Archaean greywacke from Karnataka nucleus, India". *Precambrian Res*. *v* 39, 193–216.

Négrel, Ph., Casanova, J. and Nicoud, G., (1997). “Caractérisation isotopique (O, C, Sr) des flux sédimentaires Quaternaires du bassin versant du lac d’Annecy”. *Bull. Soc. Géol. France*, 168, 243–253.

Nelson, B.K. and D.J. DePaolo, (1988). “Comparison of isotopic and petro- graphic provenance indicators in sediments from Tertiary continental basins of New Mexico”. *Journal of Sedimentary Petrology*. 58:348-357.

Nesbitt, H.W., Young, G.M. (1982). “Early Proterozoic climates and plate motions inferred from major element chemistry of lutites”. *Nature*. 299, 715–717

Nesbitt, H.W., Young, G.M. (1989). “Formation and diagenesis of weathering profiles”. *J. Geol*. 97, 129–147.

Nesbitt, H.W.(1979). “Mobility and fractionation of rare earth elements during weathering of a granodiorite”. *Nature*. v. 279, 206-210.

Nesbitt H. W., Markovics G. and Price R. C. (1980). “Chemical processes affecting alkalis and alkaline earths during continental weathering”. *Geochim. Cosmochim. Acta* .44, 1659–1666.

Nesbitt, H.W., Young, G.M. (1984). “Prediction of some weathering trends of plutonic and volcanic rocks based on thermodynamic and kinetic consideration”. *Geochimica et Cosmochimica Acta.* 48, 1523-1534.

Nesbitt, H.W., Young, G.M., (1996). “Petrogenesis of sediments in the absence of chemical weathering: effects of abrasion and sorting on bulk composition and mineralogy”. *Sedimentology* . 43, 341-358.

Nesse, W.D (2000). “Introduction to Minerology” . Oxford University Press, New York, 442p.

Nutman, A. P.; Chadwick, B.; Ramakrishnan, M.; and Viswanatha, M. N. (1992), SHRIMP U-Pb ages of detri- tal zircon in Sargur supracrustal rocks in western Karnataka, southern India: *Jour. Geol. Soc. India*, *v.* 39, p. 367-374.

Nutmann A P., Chadwick, B., Krishna Rao, B and Vasudev, V N. (1996). “SHRIMP U/Pb zircon ages of acid volcanic rocks in the Chitradurga and Sandur Groups and granites adjacent to the Sandur schist belt, Kanataka”. Y. *Geol. Soc.* India 47 153-164.

O’Nions R. K., Hamilton P. J., and Hooker P. J. (1983). “A Nd isotope investigation of sediments related to crustal development in the British Isles”. *Earth Planet. Sci. Lett*. 63, 229-240.

Pace M. N., Mayes M. A., Jardine P. M., McKay L. D., Yin X. L., Mehlhorn T. L., Liu Q. and Gurleyuk H. (2007). "Transport of Sr2+ and SrEDTA(2) in partially-saturated and sediments". *J. Contam. Hydrol*. 91, 267–287.

Palmer, M. R., and J. M. Edmond (1992). "Controls over the strontium isotope composition of river water". *Geochim. Cosmochim. Acta*, 56, 2099–2111, doi:10.1016/0016-7037(92)90332-D.

Patchett, P.; Roth, M.; Canale, B.; de Freitas, T.; Harrison,J.; Embry, A.; and Ross, G. (1999). "Nd isotopes, geochemistry and constraints on sources of sediments in the Franklinian mobile belt, Arctic Canada. *Geol. Soc. Am. Bull*111:578–589..

Pattanaik, J.K., Balakrishnan S., Bhutani R., Singh P. (2006). "Chemical and Sr isotopic composition of Kaveri, Palar and Ponnaiyar rivers: Significance to weathering of granulites and Granitic geneisses of southern Peninsular India". 93, 523-531. *Current Science.*

Pattanaik . J.K. (2010) . "Sr isotope and geochemical studies on Kaveri, Palar and Ponnaiyar rivers, southern India and 10Be isotope studies on Quaternary sediments of Kaluveli Lake,near Pondicherry". India. Unpub. Ph.D. Thesis, Pondicherry University

Pettijohn, F.J., Potter, P, E., Siever, R., (1972). Sand and Sandstone.Springer-Verlag, New York, 618 pp

Pett-Ridge, J. C., Monastra, V. M., Derry, L. A., and Chadwick, O. A. (2007). "Importance of atmospheric inputs and Fe-oxides in controlling soil uranium budgets and behavior along a Hawaiian chronosequence". *Chemical Geology v* 244, 691-707.

Peucat J. J., Mahabaleswar B. and Jayananda M. (1993) "Age of younger tonalitic magmatism and granulitic metamorphism in the south Indian transition zone (Krishnagiri area): *J. Metamorph. Geol*. 11, 879-888

Peucat J. J., Bouhallier H., Fanning C. M. and Jayananda M. (1995) Age of the Holenarsipur greenstone belt, relationships with the surrounding gneisses (Kamataka, South India). *J. Geol*. 103, 701-710.

Pichamuthu, C.S. (1965) Regional metamorphism and charnockitization in the Mysore state, India. Indian Mineralogist, *v*. 6,pp. 119-126

Plavsa, D., Collins A.S., Foden, J.F., Kropinski, L ., Santosh, M., Chetty, T.R.K. And Clark, C.,(2012). "Delineating crustal domains in Peninsular India: Age and

chemistry of Block orthopyroxene-bearing felsic gneisses in the Madurai" . *Precambrian Res*. 198– 199 (77– 93)

Potter, P.E. (1978). "Petrology and chemistry of modern big river sands". *Journal Geology*. *v* 86, 423–449.

Berner, R.A., and Berner, E.K. (1997). "Silicate weathering and climate, in Rud- diman, W.F., ed., Tectonic uplift and climate change". New York, Plenum Press, p. 353–365.

Radhakrishna B. P. (1993). "Neogene uplift and geomorphic rejuvenation of the India Peninsula". *Curr. Sci*. 64, 787–793.1–53.

Radhakrishna,B.P. (1983). "Archaean granite-greenstone terrain of south Indian shield". In: Naqvi, S.M., Rogers, J.J.W. (Eds.), Precambrian of South India, *v*. 4. *Geological Society of India*, Memoir, pp. 1–46.

Raith, M.M., Srikanthappa,C., Dieter Buhl., Hermann Koehler. (1999). "The Nilgiri Enderbites South India: Nature and Constrains on protolith formation, high grade metamorphism and cooling history". *Pracambrian Res* 98, 129-150.

Raith, M., Srikantappa, C., Ashamanjari, K.G., Spiering, B. (1990). "The granulite terrane of the Nilgiri Hills (Southern India): characterization of high-grade metamorphism". In: vielzeuf, D., Vidal, Ph. (Eds.), Granulites and Crustal Evolution. NATO ASI Series C, Kluwer Academic Publishers, Dordecht, pp. 339-365

Rajamani,.V., Shivkumar, K., Hanson, G. N. and Shirey, S. B. (1985), "Geochemistry and petrogenesis of amphibolites, Kolar schist belt, South India; evidence for komatiitic magma de-rived by low percentages of melting of the mantle": *Jour. Petrol*.,*v* 26, p. 92-123.

Rajesh, H.M. (2012). "A Geochemical Perspective on Charnockite Magmatism in Peninsular India". *Geoscience Frontiers*. 1-16 . doi:10.1016/j.gsf.2012.04.003.

Ramakrishnan, M., (1993). "Tectonic evolution of the granulite terrains of southern India". In: Radhakrishna, B.P. (Ed.), Continental Crust of South India. *Geological Society of India Memoir*, *v*. 25, pp. 35–44.

Raymo ME, Ruddiman WF, Froelich PN. (1988). "Influence of late Cenezoic mountain building on ocean geochemical cycles". *Geology* 16: 649–653.

Revel M., Sinko J.A., and Grousset F.E. (1996). “Strontium and neodymium isotopes as tracers of North Atlantic lithic particles: Paleoclimatic implications”. *Paleoceanography*. *v* 11, 95-113.

Richard, P., Shimizu, N. & Allègre, C.J. (1976). “$^{143}Nd/^{146}Nd$ A Natural Tracer: An Application to Oceanic Basalts”. *Earth Plan. Sci. Lett*. *v* 31, 269–278.

Rigol, A., Roig, M., Vidal, M., Rauret, G. (1999). “Sequential Extractions for the Study of Radiocesium and Radiostrontium Dynamics in Mineral and Organic Soils from Western Europe and Chernobyl Areas”. Environmental Science & Technology *v* 33, 887 - 895

Rollinson, H.R., Windley, B.F., Ramakrishnan, M. (1981). “Contrasting high and intermediate pressures of metamorphism in the Archaean Sargur schists of southern India”. Contrib. *Mineral. Petrol*. 76, 420–429.

Roser, B.P., Korsch, R.J. (1986). “Determination of tectonic setting of sandstone–mudstone suites using SiO_2 content and K_2O/Na_2O ratio”. *J. Geol*. 94, 635–650.

Roser, B.P., Korsch, R.J. (1988). “Provenance signatures of sandstone–mudstone suites determined using discriminant function analysis of major-element data”. *Chemical. Geol*. *v* 67, 119–139.

Roy, P.D., Caballero, M., Lozano, R., Ortega, B., Lozano, S., Jonathan., M.P, Sanchez., J.L, Macias., M.C. (2012) “Provenance of sediments deposited at paleolake San Felipe, western Sonora Desert: Implications to regimes of summer and winter precipitation during last 50 cal kyr BP”. *Journal of Arid Environments* 1-12.

Roy, P.D., Caballero, M., Lozano, R., Ortega, B., Lozano, S., Pi, T., Israde, I., Morton, O. (2010). “Geochemical record of Late quaternary paleoclimate from lacustrine sediments of paleo-lake San Felipe, western Sonora Desert, Mexico”. *Journal of South American Earth Sciences.* 29.

Roy., Moutusi, Martin., B.J, Cherrier., J, Cable J. E,. Smith., C. G. (2010). “Influence of sea level rise on iron diagenesis in an east Florida subterranean estuary” *Geochimica et Cosmochimica Acta*. 74 (2010) 5560–5573.

Ruddiman W.F. (Ed.). (1997). “Tectonic uplift and Climate Change”. Plenum Publishing Corporation, New York, USA, pp. 535.

Rutberg, R. L., Goldstein, S. L., Hemming, S. R. and Anderson, R. F. (2005).” Sr isotope evidence for sources of terrigenous sediments in the southeast Atlantic Ocean: Is there increased available Fe for enhanced glacial productivity”. *Paleoceanography*, *v* 20, PA1018, doi:10.1029/2003PA000999.

Ryan, K.M. and Williams, D.M. (2007). “Testing the reliability of discrimination diagram for determining the tectonic depositional environment of ancient sedimentary basins”. *Chemical. Geol., v*.242, pp.103-125.

Sadakata., N. (1980). “Boring data and fossil pollen analysis in the Cauvery delta, South India”. Chapter 9 In: K. Fujiwara (Ed) Geographical Field Research in South India, 1978, Spl. Pub. No 8, Res. And Sources Unit for Reg. Geogr. University of Hiroshima, 175-179.

Saini, N.K., Mukherjee, P.K., Rathi, M.S., Khanna, P.P. and Purohit, K.K. (1998). “A new geochemical reference sample of granite (DG-H) from Dalhousie, Himachal Himalaya”. *Journal.Geological. Society of India*. *v* 52, 603–606.

Sambasiva Rao, M. (1982). “Morphology and evolution of Moderen Cauvery delta, Tamil Nadu”. India Trans. Inst . *Ind. Geographers* (Pune), 4(1), 67-78.

Santosh, M., Harris, N.B.W., Jackson, D.H. and Mattey, D.P. (1990). “Dehydration and incipient charnockite formatioin: a phase equilibria and fluid inclusion study from South India”. *J. Geol*., v. 98, pp. 915-926

Sastri, V.V., Raiverman, V. (1968), “On the basin study programme of the Cretaceous–Tertiary sediments of the Cauvery Basin”. *Mem. Geol. Soc. India 2*, 143–152.

Sensarma, S., Rajamani, V., Tripathi, J. K. (2008). “Petrography and geochemical characteristics of the sediments of the small River Hemavati, Southern India: Implications for provenance and weathering processes”. *Sedimentary Geology v* 205,111-125.

Shapiro, L., Brannock, W.W. (1962). “Rapid analysis of silicate, carbonate, and phosphate rocks”. United States Geological Survey Bulletin 1144A, 1–56.

Sharma, A., Rajamani, V., 2000a. “Major Element, REE, and Other Trace Element Behavior in Amphibolite Weathering under Semiarid Conditions in southern India”. *The Journal of Geology* 108, 487-496.

Sharma, A., Rajamani, V., 2000b. “Weathering of gneissic rocks in the upper reaches of Cauvery river, south India: implications to neotectonics of the region”. *Chemical Geology v* 166, 203-223.

Sholkovitz, E.R., Elderfield, H., (1988). “Cycling of dissolved rare earth elements in Chesapeake Bay”. *Global Biogeochemical Cycles*, v 2, 157-176.

Singh, P., (2009). “Major, trace and REE geochemistry of the Ganga River sediments: Influence of provenance and sedimentary processes”. *Chemical Geology* 266, 242-255.

Singh, P., Rajamani, V., 2001(a). “Geochemistry of the Kaveri flood plain sediments, Southern India”. *Journal of Sedimentary Research*. 71(1), 50-60.

Singh, P., Rajamani, V., 2001(b). “REE Geochemistry of recent clastic sediments from the Kaveri floodplains, southern India: implication to source area weathering and sedimentary processes”. *Geochimica Cosmochimica Acta* 65, 3093 -3108.

Singh., Pramod, P.P.Mohapatra, Z.A.Malik, S.Doradola, A.H.Laskar, J. Saravanavel ,C.J.Kumanan ,M .G.Yadav ,S ,Balakrishnan , Anupama Krishnamurthy (2013) . “Sea level and coastal changes during the Holocene in the Cauvery River delta, Southern India” . PAGES IV Open Science meeting 2013. Goa.

Srikantappa, C., Santhosh, M., and Yoshida, M., (1996). “The Nilgiri granulites. In: The Archaean and Proterozoic terrain in Southern India within East Gondwana, (Ed.) “ *Gondwana Research Group Memoir*, 3, pp. 185-222.

Srikantappa, C., 2001. Composition and source of deep-crustal fluids and their role in the evolution of charnockitic granulites of southern India. Geol. Surv. of India, Spl. Pub., 55, 15-30.

Stahle, H.J., Raith. M., Hoernes. S. and Delf.A. (1987). “Element mobility during granulite formation at Kabbaldurga, Southern India”. *Journal of Petrology*, *v* 28, part 5, pp, 803-834.

Stallard R. F. and Edmond J. M. (1983) “Geochemistry of the Amazon 2. The influence of geology and the weathering environment on the dissolved load”. *J. Geophys. Res*. 88,9671–9688

Stallard R. F. and Edmon J: M. (1987). “Geochemistry of the Amazon, weathering chemistry and limits to dissolved inputs”. J.Geophys. Res. 92,8293-8302.

Steiger, R. H. and Jäger, E. (1977). “Subcommission on geochronology; convention on the use of decay constants in geochronology and cosmochronology”. *Earth Planet. Sci*. Lett. 36, 359–362.

Stover, R. C., Sommers, L.E., Silviera, D.J., (1976). “Evaluation of metals in waste water sludge”. *Journal of the Water Pollution Control Federation* .48, 2165-2175.

Stueber A. M., Pushkar P., and Hetherington E. A. (1987) “A strontium isotopic study of formation waters from the Illinois Basin, USA”. *Appl. Geochem*. 2, 477–494.

Stueber A. M., Walter L. M., Huston T. J., and Pushkar P. (1993). “Formation waters from Mississippian–Pennsylvanian reservoirs, Illinois Basin, USA: chemical and isotopic constraints on evolution and migration”. *Geochim. Cosmochim. Acta* 57, 763–784

Subramanian, K.S., Selvan, T.A. (2001). “Geology of Tamil Nadu and Pondicherry”. Geological Society of India. Bangalore. pp-192

Swaminath, J., Ramakrishnan, M., (1981). “Early Precambrian supracrustals of southern Karnataka (A) present classification and correlation”. *Memoirs Geological Survey of India v* 112, 23–38.

Swaminath, J., Ramakrishnan, M., Viswanatha, M.N. (1976). “Dharwar stratigraphic model and Karnataka craton evolution”. Rec. Geol. Surv. India *v* 107, 149–175.

Taylor, S.R., McLennan, S.M. (1985). “The Continental Crust: its Composition and Evolution”. Blackwells, Oxford, p. 312.

Taylor, S.R., and McLennan, S.M. (1995). “The geochemical evolution of the continental crust”. *Reviews of Geophysics*, *v*. 33, p. 241–265.

Taylor S. R., McLennan S. M. and McCulloch M. T. (1983).” Geochemistry of loess, continental crustal composition and crustal model ages”. *Geochim. Cosmochim. Acta* 47 (11), 1897–1905.

Taylor P.N., Chadwick B., Moorbath S., Ramakrishnan M. and Viswanatha M. N., (1984). “Petrography, chemistry and isotopic ages of peninsular Gneiss, Dharwar acid Volcanic rocks and the Chitradurga granite with special reference to the late Archean evolution of the Karnatak carton, southern India”. *Precambrian Res*, *v* 23, 349 375

Tessier, A., Campbell, P.G., Bisson, M., (1979). “Sequential extraction procedure for Speciation of Particulate Trace metals”. *Analitica Chemica Acta. v* 51, 844-851

Tomson, J.K., Bhaskar Rao, Y.J., Vijaya Kumar, T., Mallikharjuna Rao, J. (2006). “Charnockite genesis across the Archean–Proterozoic terrane boundary in the South Indian Granulite Terrain, Constraints from major-trace element geochem- istry and Sr–Nd isotopic systematics”. *Gondwana Research* . 10, 115–127

Tomson, J.K., Y.J, Bhaskar Rao., Vijaya Kumar, T. and Choudhary, A.K. (2012). “Geochemistry and neodymium model ages of Precambrian charnockites, Southern Granulite Terrain, India: Constraints on terrain assembly”. *Precambrian Res*. http://dx.doi.org/10.1016/j.precamres.2012.06.014

Toshiaki Tsunogael and M. Santosh .(2003) “Sapphirine and Corundum-bearing Granulites from Karur, Madurai Block, Southern India”. *Gondwana Research* (Gondwana Newsletter Section) *v* 6, No. 4, pp. 925-930.

Trendall, A. F., J. R. de Laeter, D. R. Nelson, and D. Mukhopadhyay (1997a).” A precise U-Pb age for the base of the BIF of the Mulaingiri (1997a), A precise U-Pb age for the craton formation (Bababudan Group, Dharwar Supergroup) of the Karnataka base of the BIF of the Mulaingiri”. *Journal.Geological. Society of India*, 50, 161– 170.

Trendall, A. F., J. R. de Laeter, D. R. Nelson, and Y. J. Bhaskar Rao (1997b). “Further zircon U-Pb age data for the Daginkatte formation, Dharwar Supergroup, Karnataka craton”. *Journal.Geological. Society of India*, *v* 50, 25– 30.

Tripathi, J. K., Rajamani, V., (1999). “Geochemistry of the loessic sediments on Delhi ridge, eastern Thar desert, Rajasthan: implications for exogenic processes”. *Chemical Geology* 155, 265-278

Tripathi, J.K., Rajamani, V., (2007). “Geochemistry and origin of ferruginous nodules in weathered granodoiritic gneisses, Mysore Plateau, Southern India”. *Geochimica et Cosmochimica Acta* .71 (7), 1674–1688

Vaidyanathan R. (1964). “Recognition and correlation of erosion surface in and around the southern Cuddapha basin”. *Journal.Geological. Society of India*, *v* 5, 121 -127.

Valdiya K. S. (1998). “Late Quaternary movements and landscape rejuvenation In southern Karnataka and adjoining Tamil Nadu in southern Indian Shield”.

Viswanatha, M.N., Ramakrishnan, M., 1981. “Bababudan belt”. *Geol.Surv. India Mem*. 112, 91–114

Vonhof, H.B., Wesselingh, F.P. and Ganssen, G.M., (1998). Reconstruction of the Miocene western Amazonian aquatic system using molluscan isotopic signatures. Palaeoclim. Palaeoeco Palaeogeog., 141, 85–93.

Weldeab, S., Emeis, K.C., Hemleben, C., Schulz, H., Vennemann, T.W, (2002). “Sr, Nd isotope composition of Late Pleistocene sapropels and non-sapropel sediments from the Eastern Mediterranean Sea: implication for detrital influx and climatic conditions in the source areas”. *Geochimica et Cosmochimica Acta* 66, 3585–3598.

Wronkiewicz, D.J., Condie, K.C. (1987). “Geochemistry of Archean shales from the Witwatersrand Supergroup, South Africa: source-area weathering and provenance”. *Geochim. Cosmochim. Acta v* 51, 2401–2416.

Wronkiewicz, D. J. and Condie, K. C. (1990). “Geochemistry and mineralogy of sediments from the Ventersdorp and Transvaal Supergroups, South Africa: cratonic evolution during the early Proterozoic”. *Geochim. Cosmochim. Acta* 54, 343–354.

Wronkiewicz, D.J., Condie, K.C. (1989). “Geochemistry and provenance of sediments from the Pongola supergroup, South Africa: evidence for a 3.0 Ga. old continental cra- ton*”*. *Geochim. Cosmochim. Acta* v 53, 1534–1549.

Zimmermann, U. and Bahlburg, H. (2003). “Provenace analysis and tectonic setting of the Ordovican clastic deposits in the southeren Puna Basin NW Argentia”. *Sedimentology, v* 50, 6, p1079-1104

List of Publications

Abstracts in conferences/symposia/volumes:

1. **Malik Zubair Ahmad**, Srikanth, D. and Pramod Singh* (2011) Geochemistry of Late Pleistocene to Late Holocene sediments of two cores from Cauvery delta, Southern India – implications to the provenance, UGC Sponsored National Seminar on "Basins of India, their Resources and Management", Annamalai University, Chidambaram 17-18 February, 2011
2. **Malik Zubair Ahmad ,** S. Balakrishnan and Pramod Singh*. Sr and Nd isotope studies on sediment core samples from Cauvery delta, South India: Evidence for monsoon induced changes in provenance Presented at: "21st V.M. GOLDSCHMIDT" conference 2011, 14th- 19th August, Prague, Czech Republic.
3. PRAMOD SINGH, P.P.Mohapatra, **Z.A.Malik**, S.Doradola, A.H.Laskar, J. Saravanavel ,C.J.Kumanan ,M .G.Yadav ,S ,Balakrishnan , Anupama Krishnamurthy . Sea level and coastal changes during the Holocene in the Cauvery River delta ,Southern India . PAGES IV Open Science meeting 2013. Goa.,
4. **Malik Zubair Ahmad** and Pramod Singh., "Implication of Weathering, Texture and Mineral sorting on sediment geochemistry of Pleistocene- Holocene sediments from Cauvery Delta, South India". National Seminar on Sediments and Sedimentary rocks : Resource potential, depostional processes, Implication and environmental changes. XXIX Convention of Indian association of sedimentologists(IAS-2012) 20-22 December, 2012.